SANDIA REPORT
SAND2018-5909
Unlimited Release
Printed June 2018

DOE/DOT Crude Oil Characterization Research Study, Task 2 Test Report on Evaluating Crude Oil Sampling and Analysis Methods, Revision 1 – Winter Sampling

David Lord, Ray Allen, David Rudeen, Chad Wocken, and Ted Aulich

Prepared by
Sandia National Laboratories
Albuquerque, New Mexico 87185 and Livermore, California 94550

Sandia National Laboratories is a multimission laboratory managed and operated by National Technology and Engineering Solutions of Sandia, LLC, a wholly owned subsidiary of Honeywell International, Inc., for the U.S. Department of Energy's National Nuclear Security Administration under contract DE-NA0003525.

Approved for public release; further dissemination unlimited.

Sandia National Laboratories

Issued by Sandia National Laboratories, operated for the United States Department of Energy by National Technology and Engineering Solutions of Sandia.

NOTICE: This report was prepared as an account of work sponsored by an agency of the United States Government. Neither the United States Government, nor any agency thereof, nor any of their employees, nor any of their contractors, subcontractors, or their employees, make any warranty, express or implied, or assume any legal liability or responsibility for the accuracy, completeness, or usefulness of any information, apparatus, product, or process disclosed, or represent that its use would not infringe privately owned rights. Reference herein to any specific commercial product, process, or service by trade name, trademark, manufacturer, or otherwise, does not necessarily constitute or imply its endorsement, recommendation, or favoring by the United States Government, any agency thereof, or any of their contractors or subcontractors. The views and opinions expressed herein do not necessarily state or reflect those of the United States Government, any agency thereof, or any of their contractors.

Printed in the United States of America. This report has been reproduced directly from the best available copy.

Available to DOE and DOE contractors from
U.S. Department of Energy
Office of Scientific and Technical Information
P.O. Box 62
Oak Ridge, TN 37831

Telephone: (865) 576-8401
Facsimile: (865) 576-5728
E-Mail: reports@osti.gov
Online ordering: http://www.osti.gov/scitech

Available to the public from
U.S. Department of Commerce
National Technical Information Service
5301 Shawnee Rd
Alexandria, VA 22312

Telephone: (800) 553-6847
Facsimile: (703) 605-6900
E-Mail: orders@ntis.gov
Online order: http://www.ntis.gov/search

SAND2018-5909
Unlimited Release
Printed June 2018

DOE/DOT Crude Oil Characterization Research Study, Task 2 Test Report on Evaluating Crude Oil Sampling and Analysis Methods, Revision 1 – Winter Sampling

David Lord
Geotechnology & Engineering Department
Sandia National Laboratories
P.O. Box 5800
Albuquerque, New Mexico 87185-MS0706

Ray Allen
Allen Energy Services, Inc.
Longview, TX 75604

David Rudeen
GRAM, Inc.
Albuquerque, NM 87112

Chad Wocken and Ted Aulich
Energy & Environmental Research Center
University of North Dakota
Grand Forks, ND 58202-9018

Abstract

The Crude Oil Characterization Research Study is designed to evaluate whether crude oils currently transported in North America, including those produced from "tight" formations, exhibit physical or chemical properties that are distinct from conventional crudes, and how these properties associate with combustion hazards that may be realized during transportation and handling. The current report presents results from Task 2, investigating which commercially available methods can accurately and reproducibly collect and analyze crude oils for vapor pressure and composition, including dissolved gases. This issue, Revision 1 – Winter Sampling, incorporates additional seasonal data and compositional analysis results that have become available since publication of a prior report, SAND2017-12482, released in December 2017. Both reports compare performance of commercially available methods to that of a well-established

mobile laboratory system that currently serves as the baseline instrument system for the U.S. Strategic Petroleum Reserve Crude Oil Vapor Pressure Program. The experimental matrix evaluates the performance of selected methods for (i) capturing, transporting, and delivering hydrocarbon fluid samples from the field to the analysis laboratory, coupled with (ii) analyzing for properties related to composition and volatility of the oil, including vapor pressure, gas-oil ratio, and dissolved gases and light hydrocarbons. Several combinations of sample capture and analysis were observed to perform well in both summer and winter sampling environments, though conditions apply that need to be considered carefully for given applications. Methods that perform well from Task 2 will then be utilized in subsequent Task 3 (combustion studies) and Task 4 (compositional analyses of multiple crude types), to be addressed in subsequent reports.

Acknowledgments

This work was jointly funded by the U.S. Department of Energy (US DOE) and U.S. Department of Transportation (US DOT) under the Crude Oil Characterization Research Study. In-kind technical data was also provided from Transport Canada (TC). Additional guidance on technical scope was given by the Crude Oil Research Coordination Steering Committee (CORCSC), comprising US DOE, US DOT, and TC.

Sandia wishes to thank subject matter experts Robert Falkiner, M.Sc. P. Eng, Kesavalu Bagawandoss, Ph.D., J.D., Thomas Hurstell, P.E., and Robbie Lansangan, Ph.D., for providing peer review of the methods, results, and findings presented herein.

Additional thanks are extended to the U.S. Strategic Petroleum Reserve, American Petroleum Institute, Crude Oil Quality Association, Canadian Crude Quality Technical Association, and American Fuel & Petrochemical Manufacturers for facilitating access to crude oil samples collected during this study.

Technical support was also provided by Kirsten Chojnicki and Joe Hogge, Sandia National Laboratories.

Revision History

Revision	Month/Year	Description
Revision 0	November 2017	Original version, SAND 2017-12482, DOE/DOT Crude Oil Characterization Research Study, Task 2 Test Report on Evaluating Crude Oil Sampling and Analysis Methods
Revision 1	June 2018	SAND 2018-5909, adds results of winter sampling and two more analytical methods for crude oil composition.

Page intentionally blank.

Table of Contents

1 Executive Summary 17
1.1 Current Knowledge on Sampling and Analysis Methods 17
1.2 Test Design 18
1.3 Effects of Open vs. Closed Sampling 19
1.4 Comparison of Compositional Analysis Methods 19
1.5 Additional Findings: Effects of Varying Vapor-Liquid Ratio 20
1.6 Sampling/Analysis Methods Selected for Remaining Tasks 21
2 Introduction 23
2.1 Overall Project Objectives 23
2.2 Role of Phase II, Task 2 24
2.3 Project Governance 25
2.4 Scope of Report 25
3 Background 27
3.1 Key Points from Phase I Literature Survey 27
3.2 Guidance from CCQTA Light Ends Memo 28
3.3 Related Study Results 29
3.4 Guidance from ASTM D6377 Standard 30
3.5 Summary Interpretation from Background Reading 31
3.6 Pressurized Compositional Analysis 31
4 Methodology 33
4.1 Sample Acquisition – Summer Samples 33
4.1.1 General Sampling Locations 33
4.1.2 Sample Capture Methods 34
4.2 Sample Acquisition – Winter Samples 42
4.2.1 Sampling Locations and Conditions 43
4.2.2 Sample Collection 43
4.3 Analytical Methods – Summer Samples 47
4.3.1 Crude Oil Vapor Pressure 47
4.3.2 Physical Properties 54
4.3.3 High Temperature PVT Test Cell Experiments 54
4.3.4 Pressurized Compositional Analysis 58
4.4 Analytical Methods – Winter Samples 63
4.4.1 Open BR Sample Transfer 63
4.4.2 Vapor Pressure Analysis, VPCRx(T) 63
4.5 Numerical Analysis 65
4.6 Nomenclature for Experimental Results 66
4.7 Repeatability and Reproducibility 67
5 Experimental Results 69
5.1 Selected Physical Properties – Summer Samples 69
5.1.1 Physical Properties by Sampling Method 69
5.2 Measured Vapor Pressure $VPCR_x(T)$ – ND Bakken Summer Samples 73
5.2.1 General Observations 73
5.2.2 Effects of Sampling Method on VPCRx 76
5.2.3 TVP-95 Vapor Pressure and Gas-Oil Ratio of ND Bakken 78
5.2.4 Homogenity of Sample from Day 1 – Day 3 80

5.2.5 Ambient Fill VPCR Limit at 68°F – Local Atmospheric Pressure Effect 80
5.2.6 Observations with Water Displacement (WD) Method 81
5.2.7 Effects of No Pre-Conditioning on VPCRx(100°F) for x = 1.5, 4.0 81
5.3 Composition – ND Bakken Summer Samples 82
5.3.1 TM2: GPA 2177+ASTM D7900+ASTM D7169 Merge 82
5.3.2 TM3: GOR+ASTM D8003+ASTM D7169 Merge 84
5.3.3 TM4: GPA 2103M+ASTM D2887 Merge 86
5.3.4 TM4a: GPA 2103M+C30+ GC Merge 88
5.3.5 Comparison of Compositions from TM3 and TM4 for ND Bakken 90
5.3.6 Comparison Across Task 2 Compositional Test Methods 91
5.4 Measured Vapor Pressure – TX Eagle Ford Summer Samples 93
5.4.1 General Observations 95
5.4.2 TVP-95 Vapor Pressure and Gas-Oil Ratio of TX Eagle Ford 96
5.4.3 Homogenity of Sample from Day 1 – Day 3 97
5.5 Composition – TX Eagle Ford Summer Samples 97
5.5.1 TM2: GPA 2177+ASTM D7900+ASTM D7169 Data Merge 98
5.5.2 TM3: GOR+ASTM D8003+ASTM D7169 Merge 99
5.5.3 TM4: GPA 2103M+ASTM D2887 Merge 101
5.5.4 TM4a: GPA 2103+C30+ GC Merge 103
5.5.5 Comparisons of TM3 and TM4 Composition for TX Eagle Ford Oil 105
5.5.6 Comparison Across Task 2 Compositional Test Methods 106
5.5.7 Comparison of TM3 Compositions for ND Bakken and TX Eagle Ford Summer Samples 108
5.6 Composition – Wide Boiling Range Data 109
5.6.1 ND Bakken Carbon Number Plots 110
5.6.2 TX Eagle Ford Carbon Number Plots 112
5.7 Selected Physical Properties – Winter Samples 113
5.8 Measured Vapor Pressure – ND Bakken Winter Samples 113
5.9 Composition – ND Bakken Winter Samples 115
5.9.1 TM4: GPA 2103M+ASTM D2887 Merge 115
5.10 Measured Vapor Pressure – TX Eagle Ford Winter Samples 117
5.11 Composition – TX Eagle Ford Winter Samples 118
5.11.1 TM4: GPA 2103M+ASTM D2887 Merge 119
5.12 Summer and Winter Comparisons 121
5.12.1 Selected Physical Properties 121
5.12.2 Measured VPCRx by ASTM D6377 122
5.12.3 Composition 125
5.12.4 EOS Modelled Vapor Pressure 127
5.12.5 Wide Boiling Range Data 128
5.13 EOS Simulations for Bubblepoint Temperature at Sample Collection Point 129
5.14 Simulated Pressure-Volume-Temperature for Heating at V/L = 1.5 131
5.14.1 Implications of TM Differences in EOS Calculations at High Temperature 133
5.15 Manual VPCRx-F(T) by ASTM D7975 133
5.15.1 Manual VPCRx-F Results for ND Bakken – Summer Sample 133
5.15.2 Manual VPCRx-F Results for TX Eagle Ford – Summer Sample 135
6 Discussion 137
6.1 Review of Key Findings 137
6.1.1 Effects of Open vs. Closed Sampling on VPCRx(T) 137

6.1.2 Effects of Open vs. Closed Sampling on Composition 139
6.1.3 Comparison of Pressurized Compositional Methods..... 144
6.1.4 Issues with Reproducibility in VPCR at V/L = 0.02 and 0.05 146
6.1.5 Performance of Commercial Process Simulator Model for Predicting Vapor-Liquid Equilibrium of Test Crudes 147
6.1.6 Conditionally Live Oils 149
6.2 Elaboration on Selected Key Findings 150
6.2.1 VPCRx Discussion 150
6.2.2 Issues around Closed Sampling and Air/Nitrogen 151
6.2.3 Open vs. Closed Sampling for Follow-on Tasks in Current Research Study..... 152
6.3 Additional Topics..... 153
6.3.1 Sweep vs. Single Point Injection..... 153
6.3.2 Issues with Standard Compositional Methods 154
6.3.3 New Purge Method for Manual or Floating Piston Cylinders 154
6.3.4 Shortcomings in Current Standards 154
7 References 157
8 Appendix: Measured D6377 VPCRx and Whole Oil Composition Data 161
Glossary..... 183

Figures

Figure 2-1. Overall conceptual diagram of Crude Oil Characterization Research Study. The focus of the current report, Task 2 Report on Evaluating Crude Oil Sampling & Analysis Methods, is indicated in red text in Phase II above. 24
Figure 2-2. Conceptual diagram of project governance. 25
Figure 3-1. ASTM D6377-14 $VPCR_4$(100°F) vapor pressure data from samples obtained by water displacement cylinder (closed) and bottle (open) sampling. Reproduced with permission from Bagawandoss (2015a). 30
Figure 4-1. Exterior photo of TVP-95 mobile laboratory used in this study. Photo provided with permission from CoreLab. 37
Figure 4-2. Schematic of sampling configuration at Bakken terminal. 37
Figure 4-3. Sampling manifold utilized to facilitate sample collection from operator pipeline. Photo provided with permission from CoreLab. 38
Figure 4-4. Pneumatic booster pump that raises sample to 500 psi prior to injection into TVP-95 trailer. Photo provided with permission from CoreLab. 38
Figure 4-5. Annotated photos illustrate how the "tight-line" crude oil sample is drawn into the pre-conditioning 100°F oven, upper left in photo (a), and into the flash chamber. Crude oil vapors exiting the flash chamber pass through insulated, heat traced lines to a gas flow meter or gas chromatograph, photo (b). Photos provided with permission from CoreLab. 39
Figure 4-6. Representative ASTM D3700 floating piston cylinder. Photo provided with permission from Intertek. 40
Figure 4-7. Representative GPA 2174 water displacement cylinder. Photo by David Lord and reproduced with permission from Intertek. 40
Figure 4-8. Representative ASTM D8009 manual syringe sampling cylinder. Reproduced with permission from Bagawandoss (2015a). 41
Figure 4-9. Representative glass bottle "Boston Round". Photo provided with permission from Intertek. 41
Figure 4-10. Example FPC diagram and connection to crude oil sample source. 45
Figure 4-11. Boston Round sampling methods. From left-to-right: BR1 – tap tube; BR2 – chilled bottle; BR3 – chilled coil and bottle. 46
Figure 4-12. Example of 6377 sample pre-conditioning apparatus comprising an oven that pre-heats the sample (FPC/MPC/WD) to test temperature prior to introduction into the sample chamber. Photos provided with permission from Intertek. 49
Figure 4-13. Photos on left show the 6377 instrument and an inset view of the interior of the conditioning oven (provided with permission from Intertek). Conceptual sketch on right illustrates process to push sample from pressurized cylinder (FPC/MPC/WD) into 6377 sample chamber. 50
Figure 4-14. Photos on left show the 6377 instrument and an inset view of the interior of the conditioning oven (provided with permission from InnoTech Alberta). Conceptual sketch on right illustrates process to push sample from pressurized cylinder (FPC/MPC/WD) into 6377 sample chamber. 51
Figure 4-15. Montage of photo and schematic illustrating how BR samples are introduced into the 6377 instrument using vacuum draw. Photo provided with permission from Intertek.. 52
Figure 4-16. Conceptual diagram of crude oil pressure-temperature test system used in current study. 55

Figure 4-17. Photograph of PVT cell inside clamshell heater, reproduced with permission from University of North Dakota EERC. 56
Figure 4-18. Photograph of valves and instrumentation hookups above the clamshell heater. Left to right: fill valve, needle valve, thermocouple, pressure transducer, pressure relief valve. Photo reproduced with permission from University of North Dakota EERC. 57
Figure 4-19. Schematic of the TVP-95 instrument system used to evaluate bubblepoint pressure, gas-oil ratio, and associated flash gas compositions. 60
Figure 5-1. Bar chart showing average and 2σ VPCRx(68°F) for the ND Bakken oil sorted by V/L and sampling type. 75
Figure 5-2. Bar chart showing average and 2σ VPCRx(100°F) for the ND Bakken oil sorted by V/L and sampling type. 75
Figure 5-3. Bar chart showing average and 2σ VPCRx(122°F) for the ND Bakken oil sorted by V/L and sampling type. 75
Figure 5-4. Expansion curves showing VPCRx(100°F) versus V/L for ND Bakken oil by sampling type. 76
Figure 5-5. Averaged pressure-expansion curves for ND Bakken oil from ASTM D6377 measurements overlaid with TVP-95 BPP and GOR. 79
Figure 5-6. Illustration of effects of BR vacuum draw vs. positive pressure push BRMPC and local atmospheric pressure effects for ND Bakken oil on VPCRx(68°F) measured in Lab 2 and Lab 3. 81
Figure 5-7. Effect of preconditioning on D6377 VPCRx by Lab 2 for ND Bakken oil. 82
Figure 5-8. Bar charts showing mole fraction of components nitrogen (N2) through n-pentane (nC5) as measured by TM2 and compared with TM1 tight-line results for ND Bakken samples. Two replicates for each sample type are shown. 83
Figure 5-9. Pressure-expansion curve and bar chart comparisons of VPCRx(100°F) generated by EOS model from TM2, TM1, and D6377 instrument for ND Bakken samples. 84
Figure 5-10. Bar chart showing mole fraction of components ethane (C2) through n-pentane (nC5) as measured by TM3 and compared with TM1. Sampling type is denoted by bar color. ... 85
Figure 5-11. Pressure-expansion curve and bar chart comparisons of VPCRx(100°F) generated by EOS model from TM3, TM1, and D6377 instrument for ND Bakken samples. 86
Figure 5-12. Bar chart showing mole fraction of components ethane (C2) through n-pentane (nC5) as measured by TM4 and compared with TM1. Sampling type is denoted by bar color. ... 87
Figure 5-13. Pressure-expansion curve and bar chart comparisons of VPCRx(100°F) generated by EOS model from TM4, TM1, and D6377 instrument for ND Bakken samples. 88
Figure 5-14. Bar chart showing mole fraction of components nitrogen (N2) through n-pentane (nC5) as measured by TM4a and compared with TM1 tight-line results for ND Bakken samples. Two replicates for each sample method are shown. 89
Figure 5-15. Pressure-expansion curve and bar chart comparisons of VPCRx(100°F) generated by EOS model from TM4a, TM1, and D6377 instrument for ND Bakken samples. 90
Figure 5-16. Bar chart comparison of composition from TM3 and TM4 for ND Bakken. Components N2–C1 in upper figure and C2–nC5 in lower figure. 91
Figure 5-17. Comparison of averaged measured light ends and fixed gases for each test method - ND Bakken samples. Results for Boston Round samples are outlined in black. 92
Figure 5-18. Comparison of EOS modelled vapor pressures at 100°F for averaged results from each test method – ND Bakken samples. Results for Boston Round samples are outlined in black in top figure and shown with black dash in bottom figure. 93
Figure 5-19. Bar chart showing average and 2σ VPCRx(68°F) for the TX Eagle Ford oil sorted by V/L and sampling type. 94

Figure 5-20. Bar chart showing average and 2σ VPCRx(100°F) for the TX Eagle Ford oil sorted by V/L and sampling type. 94
Figure 5-21. Bar chart showing average and 2σ VPCRx(122°F) for the TX Eagle Ford oil sorted by V/L and sampling type. 95
Figure 5-22. Expansion curves showing VPCRx(100°F) versus V/L for TX Eagle Ford oil by sampling type. 95
Figure 5-23. Averaged pressure-expansion curves for TX Eagle Ford oil from ASTM D6377 measurements overlaid with TVP-95 BPP and GOR. 97
Figure 5-24. Bar chart showing mole fraction of components nitrogen (N2) through n-pentane (nC5) as measured by TM2 and compared with TM1 tight-line results for TX Eagle Ford samples. Two replicates for each sample type are shown. 98
Figure 5-25. Pressure-expansion curve and bar chart comparisons of VPCRx(100°F) generated by EOS model from TM2, TM1, and D6377 instrument for TX Eagle Ford. 99
Figure 5-26. Bar chart showing mole fraction of components ethane (C2) through n-pentane (nC5) as measured by TM3 and compared with TM1 for TX Eagle Ford. Sampling type is denoted by bar color. 100
Figure 5-27. Pressure-expansion curve and bar chart comparisons of VPCRx(100°F) generated by EOS model from TM3, TM1, and D6377 instrument for TX Eagle Ford. 101
Figure 5-28. Bar chart showing mole fraction of components ethane (C2) through n-pentane (nC5) as measured by TM4 and compared with TM1 for TX Eagle Ford samples. Sampling type is denoted by bar color. 102
Figure 5-29. Pressure-expansion curve and bar chart comparison of VPCRx(100°F) generated by EOS model from TM4, TM1, and D6377 instrument for TX Eagle Ford samples. 103
Figure 5-30. Bar chart showing mole fraction of components nitrogen (N2) through n-pentane (nC5) as measured by TM4a and compared with TM1 tight-line results for TX Eagle Ford samples. Two replicates for each sample type are shown. 104
Figure 5-31. Pressure-expansion curve and bar chart comparisons of VPCRx(100°F) generated by EOS model from TM4a, TM1, and D6377 instrument for TX Eagle Ford samples. 105
Figure 5-32. Bar chart comparison of composition for TX Eagle Ford TM3 and TM4 samples. Components N2 – C1 in upper chart and C2 – nC5 in lower. 106
Figure 5-33. Comparison of averaged measured light ends and fixed gases from each test method – TX Eagle Ford samples. Results for Boston Round samples are outlined in black. 107
Figure 5-34. Comparison of EOS modelled vapor pressures at 10 °F for averaged results for each test method – TX Eagle Ford samples. Results for Boston Round samples are outlined in black in top figure and shown with black dash in bottom figure. 108
Figure 5-35. Bar chart comparison of composition from TM3 for ND Bakken and TX Eagle Ford samples (black outline). Components N2 – C1 in upper figure and C2 – nC5 in lower figure. 109
Figure 5-36. Aggregate plot of mole fraction versus carbon number for average ND Bakken summer closed samples for all test methods using both linear (top) and log (bottom) scales. 111
Figure 5-37. Aggregate plot of mole fraction versus carbon number for the TX Eagle Ford summer samples for all test methods using both linear (top) and log(bottom) scales. 112
Figure 5-38. Bar chart and pressure expansion curves of VPCRx(100°F) for the ND Bakken winter oil color coded by sampling type. 114
Figure 5-39. Mole fraction of components nitrogen (N2) through n-pentane (nC5) as measured by TM4 for ND winter samples. Sampling type is denoted by bar color. 116
Figure 5-40. Pressure-expansion curve (top) and bar chart (bottom) comparisons of VPCRx(100°F) generated by EOS model from TM4 compositions for ND Bakken winter samples. 117

Figure 5-41. Bar chart (top) and pressure-expansion curves (bottom) showing VPCRx(100°F) for the TX Eagle Ford winter oil samples sorted by V/L and sampling type. 118
Figure 5-42. Bar charts showing mole fraction of components nitrogen (N2) through n-pentane (nC5) as measured by TM4 for TX Eagle Ford winter samples. Sampling type is denoted by bar color. 119
Figure 5-43. Pressure-expansion curve (top) and bar chart (bottom) comparisons of VPCRx(100°F) generated by EOS model from TM4 compositions for TX Eagle Ford winter samples. Bars color coded by sample type. 120
Figure 5-44. Bar chart showing VPCRx(100°F) vs. V/L for the ND Bakken summer and winter samples. S-CLSD is summer average and 2σ. S-LAB1-FPC is LAB1 D6377 measured. 123
Figure 5-45. Bar chart showing VPCRx(100°F) vs. V/L for the TX Eagle Ford summer and winter samples. Black and gray curves are summer samples, remaining curves are winter samples. S-CLSD is summer average and 2σ . S-LAB1-FPC is LAB1 D6377 measured. ... 124
Figure 5-46. Bar charts showing mole fraction of components nitrogen (N2) through n-pentane (nC5) as measured by TM4 for ND Bakken summer and winter samples. 125
Figure 5-47. Bar charts showing average mole fraction of components nitrogen (N2) through n-pentane (nC5) as measured by TM4 for TX Eagle Ford summer and winter samples. .. 126
Figure 5-48. Comparison of summer and winter EOS estimated VPCRx(100°F) from average TM4 compositions and TM1-TL. Upper plot - ND Bakken; lower plot TX Eagle Ford. 127
Figure 5-49. Aggregate plot of mole fraction (linear scale) versus carbon number for summer and winter ND Bakken samples – linear scale(top) and log scale (bottom). 128
Figure 5-50. Aggregate plot of mole fraction (linear scale) versus carbon number for the TX Eagle Ford summer and winter samples – Linear scale (top) and log scale (bottom). 129
Figure 5-51. Overlay of measured and EOS-simulated PVT for ND Bakken summer crude at starting V/L = 1.5 for T = 50 - 300°C. 132
Figure 5-52. Overlay of measured and EOS-simulated PVT for TX Eagle Ford summer crude at starting V/L = 1.5 for T = 50 - 300°C (ND TM1 data included for reference). 132
Figure 5-53. VPCRx-F by manual tester vs. temperature compared with (a) TVP-95 EOS model and (b) AVG-CLSD D6377 for ND Bakken summer crude. 134
Figure 5-54. VPCRx-F by manual tester vs. temperature compared with (a)TVP-95 EOS model and (b) AVG-CLSD D6377 for TX Eagle Ford summer crude. 136
Figure 6-1. Bar chart showing average and 2σ VPCRx (100°F) for the ND Bakken oil sorted by V/L and sampling type. (This figure is a repeat of Figure 5-2). 137
Figure 6-2. Bar chart showing average and 2σ VPCRx (100°F) for the TX Eagle Ford oil sorted by V/L and sampling type. (This figure is a repeat of Figure 5-20). 138
Figure 6-3. Bar chart showing average ASTM D6377 VPCRx(100F) at V/L = 0.02 to 4.0 for average summer and winter open and closed sampling events at the ND Bakken sampling site (This figure is a repeat of Figure 5-44). 139
Figure 6-4. Bar chart showing average ASTM D6377 VPCRx(100°F) at V/L = 0.02 to 4.0 for average summer and winter open and closed sampling events at the TX Eagle Ford sampling site (This figure is a repeat of Figure 5-45). 139
Figure 6-5. Bar chart comparison of composition from TM3 and TM4 for ND Bakken. Components N2 – C1 in upper figure and C2 – nC5 in lower figure (This figure is a repeat of Figure 5-16). 140
Figure 6-6. Bar chart comparison of composition for TX Eagle Ford TM3 and TM4 samples. Components N2-C1 in upper chart and C2-nC5 in lower (This figure is a repeat of Figure 5-32). 141

Figure 6-7. Bar chart comparison of composition for ND Bakken TM4 samples. Components N2 – C1 in upper figure and C2 – nC5 in lower (This figure is a repeat of Figure 5-46). 142
Figure 6-8. Bar chart comparison of VPCRx(100°F) generated by EOS model from TM4, TM1, and D6377 instrument for TX Eagle Ford samples (This figure is a repeat of Figure 5-29). .. 143
Figure 6-9. Comparison of averaged measured light ends and fixed gases for each test method - ND Bakken samples. Results for Boston Round samples are outlined in black. 144
Figure 6-10. Aggregate plot of mole fraction versus carbon number for average ND Bakken summer closed samples for all test methods. 145
Figure 6-11. Bar chart comparison of VPCRx(100°F) generated by EOS model from TM4, TM1, and D6377 instrument for ND Bakken samples. (This figure is a repeat of Figure 5-13). 148
Figure 6-12. Overlay of measured and EOS-simulated PVT for ND Bakken crude at starting V/L = 1.5 for T = 50 - 300°C (This figure is a repeat of Figure 5-51). 148
Figure 6-13. Pressure-expansion curves for ND Bakken oil generated by EOS for samples containing 1e-4 (FPC), 5e-4 (WD), and 8 e-4(MPC) mole fraction nitrogen. 152
Figure 6-14. Single point injection vs. V/L sweep for D6377 VPCRx at 100°F by LAB3 with ND Bakken oil. 153

Tables

Table 4-1. Test matrix for Task 2 Sampling and Analysis. Color-coding for compositional test methods TM1-TM4 is given below the table. Detail on TM1-TM4 is given in section 4.3.4. 35
Table 4-2. Summary of winter sampling and analytical procedures..... 42
Table 4-3. Temperature and expansion settings for ASTM D6377M VPCRx(T) measurements to be run on samples collected from each sampling method. 47
Table 4-4. Instrument settings setting for "Equilibrium Time" and "Equilibrium dP/dt" required to ensure that the analysis run for each V/L has reached equilibrium conditions. 48
Table 4-5. Laboratory ambient conditions reported for labs 2 and 3 during the 6377 VPCR measurements..... 53
Table 4-6. Allowable concentration ranges for GPA 2103 and GPA 2177. 59
Table 4-7. Component list analyzed by TVP-95. 60
Table 4-8. Temperature and expansion settings for ASTM D6377 VPCRx(T) measurements. 64
Table 4-9. Instrument settings "Equilibrium Time" and "Equilibrium dP/dt" used for all vapor pressure samples..... 64
Table 5-1. Selected physical properties for Bakken and Eagle Ford oil samples. 69
Table 5-2. Relative density at 60, 100 and 122°F (20, 37.8 and 50°C) for Bakken oil samples..... 70
Table 5-3. Relative density at 60, 100 and 122°F (20, 37.8 and 50°C) for Eagle Ford oil samples..... 70
Table 5-4. Mass% total sulfur by sampling method for ND Bakken samples. 71
Table 5-5. Mass% total sulfur by sampling method for TX Eagle Ford samples. 71
Table 5-6. Kinematic viscosity by sampling method for ND Bakken sample. 72
Table 5-7. Kinematic viscosity by sampling method for TX Eagle Ford sample. 72
Table 5-8. IBP by ASTM D86 for ND Bakken and TX Eagle Ford samples..... 73
Table 5-9. Coefficient-of-Variation (C_v) for VPCRx(100°F) for the ND Bakken oil samples, grouped by V/L and sampling method. 74
Table 5-10. Reproducibility Interval for measured VPCRx(100°F) for the ND Bakken oil samples, grouped by V/L and sampling method, compared with R_{std} from ASTM D6377..... 77
Table 5-11. Summary of TVP-95 measurements for ND Bakken crude oil. V/L was calculated from measured GOR, and P denotes separator pressure for GOR test. 79
Table 5-12. Calculated reproducibility interval (psi) for measured VPCRx data at 100°F for TX Eagle Ford oil samples..... 96
Table 5-13. Summary of TVP-95 measurements for TX Eagle Ford crude oil. V/L was calculated from measured GOR, and P denotes separator pressure for GOR test. 96
Table 5-14. Selected physical properties for ND Bakken and TX Eagle Ford oil samples. 113
Table 5-15. Sulfur wt% by ASTM D4294..... 113
Table 5-16. Selected physical properties for ND Bakken and TX Eagle Ford oil samples. W/S is ratio of winter data to summer data. Task 2 summer (2-S); Task 2A winter (2A-W); Ratio winter to summer (W/S). 121
Table 5-17. Sulfur wt% by ASTM D4294..... 121
Table 5-18. EOS estimated temperature for BP pressure equal to local atmospheric pressure..... 130
Table 5-19. Nominal and actual V/L for ASTM D7975 manual testers. 133
Table 6-1. Reproducibility Interval (2.8σ) for measured VPCRx(100°F) for the ND Bakken oil samples, grouped by V/L and sampling method, compared with R_{std} from ASTM D637 (This table is a repeat of Table 5-10). 146

Nomenclature

AES	Allen Energy Services
API	American Petroleum Institute
ASTM	ASTM International (standards organization)
BPP	Bubblepoint pressure (standard condition is 100°F)
BR	"Boston Round" glass bottle
BTEX	Benzene, toluene, ethylbenzene, xylenes
CCQTA	Canadian Crude Quality Technical Association
COQA	Crude Oil Quality Association
DOE	U.S. Department of Energy
DOT	U.S. Department of Transportation
EERC	Energy & Environmental Research Center, University of North Dakota
EOS	Equation of state
FPC	Floating Piston Cylinder
GC	Gas Chromatography
GOR	Gas-Oil volume Ratio
GPA	Gas Processor's Association
MPC	Manual Piston Cylinder
MW	Average Molecular Weight
PSM	Process Simulation Model
RD	Relative Density
r_{std}	Repeatability from ASTM standard (lower case r)
R_{std}	Reproducibility from ASTM standard (upper case R)
SAP	Sampling and Analysis Plan
SNL	Sandia National Laboratories
SPR	Strategic Petroleum Reserve
SRK	Soave-Redlich-Kwong (cubic EOS)
TC	Transport Canada
TM	Test Method
TM1	Separator flash gas analysis and C30+ with numerical merge
TM2	GPA 2177, ASTM D7900, ASTM D7169 with numerical merge
TM3	ASTM D8003-15, GOR flash, ASTM D7169 with numerical merge
TM4	GPA 2103M, physical shrink, ASTM D2887 C7+ with numerical merge
TM4a	GPA 2103M, physical shrink, C30+ GC with numerical merge
TVP	True vapor pressure
V/L	Volume ratio, vapor/liquid
VP	Vapor pressure
VPCRx	Vapor pressure of crude oil at expansion ratio V/L=x, ASTM D6377
WD	Water Displacement Cylinder

1 Executive Summary

This report summarizes findings from the Crude Oil Characterization Research Study[1] Task 2, investigating which commercially available sampling and analysis methods can accurately and reproducibly measure crude oil vapor pressure, light ends, and fixed gas composition and supply adequate property characterization data for follow-on combustion experiments and comparison of multiple crude types at Sandia National Laboratories. Task 2 is one of several tasks outlined in the Crude Oil Characterization Research Study, that as a whole, is designed to investigate whether oils produced from "tight" formations are materially different in their physical, chemical, or combustion properties from oils produced from conventional reservoirs. The combustion tests, in turn, will provide key input data that may be used in determining the level of hazard associated with pool fires and fireballs that can result from accidental release and ignition of crude oil during transport and handling. This Task 2 report addresses the effects of sampling and analysis methods on measurement of selected properties of crude oils, with a focus on vapor pressure, light ends, and fixed gas content. Light ends, in the context of the current work, refer to components of a crude oil with low molecular weight that will readily vaporize at typical ambient conditions where crude oils may be handled in open containers. Light ends would include the familiar short-chain hydrocarbons such as methane, ethane, up through pentane. Fixed gases include nitrogen and carbon dioxide and oxygen that have only minor contribution to overall mass% but can exert significant effects on crude oil vapor pressure. An initial Task 2 report was issued in December 2017 under report number SAND2017-12482. The current report, Revision 1 – Winter Sampling, presents additional data and results taken from the same locations as the first report but under different seasonal conditions. Revision 1 also presents the results from two more compositional analysis methods on the initial Task 2 samples that became available after the initial report was issued. Additional technical reports regarding the Crude Oil Characterization Research Study under subsequent Tasks 3, combustion studies, and 4, property characterization of multiple crude types, are forthcoming. This work is sponsored by the U.S. Department of Energy (DOE), U.S. Department of Transportation (DOT), with in-kind technical data provided by Transport Canada (TC).

1.1 Current Knowledge on Sampling and Analysis Methods

Current knowledge on the effects of sampling methods for vapor pressure of crude oils is documented largely in industry association literature and standards. Fluids in this context are typically divided into one of two categories: "live" oils that are boiling at sampling and/or analysis conditions, and "dead" oils that are not. Live oils require special equipment and protocols that maintain a barrier between the sample and ambient pressure air in order to retain volatile materials. Alternatively, more generic equipment such as glass bottles may be used to collect dead oil. These differing requirements have implications for equipment needs, training, and ultimately costs associated with sample collection. Live fluids should be collected by using piston-cylinder devices (according to relevant industry standards, i.e. ASTM D3700), leveraging high process line pressure to displace the piston and fill the cylinder. Dead fluids are typically drawn into an open bottle from a source tap containing fluid at only slightly higher

[1] Information available at http://energy.gov/fe/articles/crude-oil-characteristics-research

than ambient pressure, displacing air as the bottle fills. It is unclear whether oils that are collected along the supply chain are either live or dead for the purposes of sampling for vapor pressure, and this uncertainty may lead to considerable debate. Results from the limited literature in this area are not clear on exactly what conditions require closed versus open sampling for oils that are not visibly boiling.

The current work recognizes that the distinction of live versus dead oil is coarse, and there is space in between where oils may exhibit volatility below a level that would be conspicuously identified as visible boiling, yet where certain rigor is required to maintain sample integrity. Moreover, such oils require analytical equipment calibrated to a lower range of pressure and dissolved gas content than for traditional live fluids in order to yield reproducible results. The industry has recognized this and is offering new methods and equipment to meet these sampling and analysis needs. This is evidenced in the addition of several new standard methods in the last few years for collecting (ASTM D8009-15 manual piston cylinder) and analyzing crude oils for vapor pressure (ASTM D6377-14, 15, 16 yearly revisions) and pressurized composition (ASTM D8003-15), all of which are employed as part of the current study.

1.2 Test Design

Collecting crude oil samples in the field for vapor pressure testing presents many challenges, as analyses can be very sensitive to small gains or losses in light ends and fixed gas content of the original material. There is a general need to isolate and evaluate the sampling methods to develop a means to reliably deliver a representative sample of oil from the field to the laboratory so that the sample collection method can be eliminated as a potential complication in the vapor pressure analysis. The test design for the current Task 2 effort applied several commercially available field sampling methods at two sampling points in the crude oil supply chain. Sampling methods included "open" methods that allow the sample to have direct contact with the atmosphere during collection and/or transportation, and "closed" methods which contain the sample with a physical barrier and prevent exposure to the atmosphere. One sampling point was at a terminal in North Dakota located between a truck offloading facility and rail loading terminal that handles Bakken production, and a second was located at a terminal in Texas receiving oil from a gathering system just upstream of a refinery that handles Eagle Ford production. Sampling at the North Dakota site occurred at the beginning of September 2016 and again in late March 2017. Sampling at the Texas site occurred in the middle of October 2016 and again in early March 2017. The "summer" crude oils were collected by a commercially available "tight-line" method and compared with industry standard "closed" (floating piston cylinder, manual piston cylinder, water displacement) and "open" (bottle) sampling methods. The "winter" samples collected in March 2017 were captured by open and closed methods.

The samples were tested using a range of commercially available analyses that focused on vapor pressure, light ends, and fixed gases, and also included several physical property measurements commonly used in oil quality determination. The rigor over maintaining the fixed gases and light ends is critical because they have a significant influence on properties important to flammability and overall safety in handling, including vapor pressure, gas-oil ratio, whole oil composition, initial boiling point, and flashpoint. Knowledge of the types and quantity of gases in the oil provides a basis for understanding and furthermore predicting physical properties that are associated with flammability and handling safety.

The "tight-line" system, which brings the analytical equipment to the sampling location in the field and collects and analyzes oil samples through closed, pressurized lines, is considered a "gold standard" of collection and analysis methods and thus served as an experimental baseline against which the other sampling and analysis methods were compared. This system, referred to as the TVP-95, has 20+ years' operating history on the U.S. Strategic Petroleum Reserve (SPR) with technical oversight from Sandia National Laboratories and is calibrated for vapor pressure and dissolved gas concentration in the range that is expected for oils collected from within the North American surface transportation supply chain.

1.3 Effects of Open vs. Closed Sampling

The study generally found that both open and closed industry standard sampling methods yielded comparable results for vapor pressure of crude oil, VPCR, and hydrocarbon content against the tight-line TVP-95 system for the oils that were tested here. It is important to note that the two oils analyzed in this study had most likely been equilibrated to ambient conditions elsewhere in the supply chain before they were sampled, and were not actively boiling or prone to significant losses of light ends and fixed gases at sampling conditions. Moreover, there is no basis in the current work for extending this finding to expect comparable performance of open versus closed sampling to "live" oils that visibly boil when handled in open containers.

Open and closed methods were not, however, equivalent in their ability to deliver adequate single-phase samples to the ASTM D6377 laboratory vapor pressure instrument, especially where low vapor/liquid ratio (V/L < 1) values (headspace vapor volume less than liquid volume) were targeted. Use of open bottles as the direct source of sample into the D6377 instruments led to routinely low VPCR relative to samples introduced from closed cylinders, and more likely reflected local ambient pressure in the laboratory than actual property measurements of the original crude oil samples. The work herein supports the new ASTM D6377-16 requirement that any tests run at vapor/liquid ratio (V/L) < 1 be run from a floating piston (closed) cylinder that can provide sufficient pressure to overcome possible phase separation while the sample is introduced into the vapor pressure test cell.

A winter sampling effort was undertaken to explore whether cold environmental conditions affected the performance of open versus closed sampling for sourcing VPCR and pressurized compositional analyses for oils from the same ND Bakken and TX Eagle Ford locations utilized for summer sampling. Several variants of open sampling with and without bottle chilling were compared with closed sampling, through only one of the four samples, ND Bakken winter, was acquired from a process temperature (48°F) below typical lab ambient (70°F). No significant seasonal effects on open versus closed sampling were observed for collecting VPCRx(100°F) (37.8ºC) samples for either the Bakken or Eagle Ford locations. Pressurized compositional analyses indicated slightly higher methane retention for winter Bakken closed sampling over open methods, however the impacts to VPCRx of this higher methane are small in comparison to the effects of sample-to-sample variance in fixed gas (N2, O2) concentrations observed across the study.

1.4 Comparison of Compositional Analysis Methods

The study also compared commercially available methods for measuring the composition of crude oils to results obtained with the aforementioned TVP-95 system (TM1). The

compositional analyses comprised a range of components from the light dissolved gases, referred to here as fixed gases and light ends, through the middle hydrocarbons that constitute major components of liquid hydrocarbon fuels, up to heavier materials that have carbon number 30 and greater. Four pressurized compositional methods (TM2: GPA 2177 + ASTM D7900 + ASTM D7169 data merge; TM3: ASTM D8003 + GOR + ASTM D7169 data merge; TM4: GPA 2103M + physical shrink + ASTM 2887 data merge; TM4a: GPA 2103M + physical shrink + $C30^+$ GC data merge) were evaluated against the baseline TM1 system in this main report. Three of the four (TM3, 4, 4a) were determined to give results that were of equal value for the purposes of this work and compared well against TVP-95 system (TM1). TM1, 3, 4, and 4a all involved a combination of a vapor-liquid flash for volumetric data coupled with gas chromatography to generate compositional data that were ultimately merged with numerical tools to yield "whole oil" compositions. These whole oil compositions were then passed through a commercial process simulator model commonly used in the oil and gas industry to yield predictions of crude oil vapor pressure and gas-oil ratio that were compared back to the direct physical property measurements made on the same oils. The results of the model predictions overlaid well with the physical property measurements, providing a reasonable level of confidence that the reported compositions as well as the function of the process simulator models were accurate and may be used to predict similar mixtures in the future. While TM2 performance is slightly less desirable than the others relative to the baseline, it has a potential cost advantage over the others (TM1, 3, 4, 4a) as it requires no physical shrink/flash step.

1.5 Additional Findings: Effects of Varying Vapor-Liquid Ratio

The selection of vapor/liquid ratio (V/L) as a measurement point for vapor pressure of crude oil by VPCR has important implications for expected reproducibility of results and sensitivity to small amounts of dissolved gas. This study was unable to generate reproducible measures of VPCR for vapor/liquid ratios V/L = 0.02 and 0.05. Moreover, comparisons between VPCR and the TVP-95 system in the same low V/L range indicated that VPCR was generally higher than the TVP-95, but the effect was dominated by high variability in VPCR measurements. Comparison of VPCR and TVP-95 vapor pressure improved for the higher V/L range 0.5 to 4.0. The authors hypothesize that small amounts of fixed gases such as nitrogen and oxygen were introduced into many of the VPCR oil samples as a function of sampling and handling, and the effects of these gases appeared in the compositional measurements and low vapor-liquid ratio VPCR, but had diminished impact on VPCR as vapor-liquid ratio was increased from 0.5 to 4.0. As such, it was difficult to find a direct measurement point that would provide a reliable estimate for vapor pressure of an oil with a vapor/liquid ratio representative of a loaded railcar, which may be as low as 1%. Reproducibility in VPCR generally improved as V/L was increased to 4.0, largely a result of the fact that VPCR is less sensitive to small variations in gas composition of the sample as V/L increases. The caveat with increasing V/L, however, is that its direct relevance to actual transport container conditions is diminished, as a vapor-liquid ratio of 4:1 is an atypical scenario for a crude oil container in transit. One of the recommendations from this study going forward is to revise some of the industry standard sampling methods to improve their ability to preserve the original sample compositions and prevent contamination by inert gas which has the potential to create very high vapor pressure at low vapor-liquid ratio.

1.6 Sampling/Analysis Methods Selected for Remaining Tasks

The current Sandia plan is to employ closed methods for sample capture for sourcing all vapor pressure, light ends, and fixed gas measurements from this point forward. Both piston cylinder (floating piston or manual depending on source line pressure) and water displacement will be utilized. While the possibility for nitrogen/fixed gas contamination has been observed in closed sampling, its presence can be detected and documented via compositional analysis. Closed sampling also offers a measure of control on light end and fixed gas losses in the event that future sampling encounters oil that has the potential to lose these gases in handling or storage. Also, a revised closed cylinder purging technique to minimize nitrogen contamination from dead volume (internal volume inaccessible to normal purging processes) was developed by the technical team as a result of this work and will be employed moving forward. Regarding compositional analysis, several commercially available methods appear equally suitable from a technical perspective for measuring pressurized composition. Additional factors including cost and availability will influence method selection going forward on Tasks 3 and 4 of this project.

Thus, several different tests for measuring vapor pressure were performed on samples from two "tight" crude oils. As described above, this work has investigated the accuracy of different sampling methods and analytical tests and has determined that certain combinations of collection methods, analytical measurements, and thermodynamic modeling can produce accurate predictions of vapor pressures under conditions that would be seen in the transportation supply chain. Results are presented in greater detail in the main body of the technical report, followed by a discussion of key findings at the end of the main report. Data tables for selected property measurements associated with Task 2 are also included in an Appendix to the main report.

Page intentionally blank.

2 Introduction

This report summarizes findings from the Crude Oil Characterization Research Study Task 2, investigating which commercially available sampling and analysis methods are capable of providing accurate and reproducible measures of crude oil vapor pressure light ends (methane through pentane), and fixed gas composition and provide adequate property characterization data for follow-on combustion experiments and comparison of multiple crude types at Sandia National Laboratories. This work was sponsored by the U.S. Department of Energy and the U.S. Department of Transportation and Transport Canada as part of a more comprehensive project looking at properties of "tight" versus "conventional" oils with an interest in understanding whether crude oil physical and chemical properties, to include presence of light end dissolved gases, have measurable effects on combustion properties in crude oil pool fires and fireballs.

2.1 Overall Project Objectives

The overall objective of the US DOE/DOT Crude Oil Characterization Research Study is to understand and mitigate risks associated with large volume rail transport of crude oil in general and "tight oil" in particular. The project focus is on physical properties of crude oils in the transit system and how these associate with their potential for ignition, combustion, and explosion. A conceptual diagram for the overall project with Phase I, II, III breakout is given in Figure 2-1.

Phase I of the project, problem definition phase, ran from October 2014 – May 2015, and produced a literature survey (Lord, Luketa et al. 2015) as well as a high-level project plan that was subsequently made publicly available through the DOE–FE website[2]. Selected findings from the literature survey are given in the Background section below.

Phase II of the project, crude oil sampling and analysis, was fully staffed starting in October 2015. The Phase II plan comprises 6 main tasks, which underwent some slight modifications from the task titles given in the project plan published in 2015, but retain the same general theme:

- Task 1: Administration and Outreach
- Task 2: Sampling and Analysis Method Evaluation
- Task 3: Combustion Experiments and Modeling
- Task 4: Crude Oil Characterization – Tight vs. Conventional
- Task 5: Large-scale and Rail Car Combustion Testing and Computational Fluid Dynamics (CFD) Modeling
- Task 6: Comprehensive Characterization across Crude Oil Supply Chain

Tasks 1 through 4 in Phase II are current priorities.

[2] See http://energy.gov/fe/articles/crude-oil-characteristics-research

Phase III is envisioned as implementation in which the results are shared and discussed among all stakeholders. The goal is to utilize knowledge gained from the study to inform decisions on industry best practices, standards, and regulations as appropriate.

2.2 Role of Phase II, Task 2

Phase II, Task 2, identified in red in Figure 2-1, seeks to identify crude oil sample collection and analysis (for vapor pressure, light ends, and fixed gas composition) methods most effective in ensuring retention of all (especially the most volatile) components from the point of collection to the point of analysis in the laboratory. The Sandia literature survey from Phase I as well as recent industry papers (Konecnik 2014; Murray 2014; Bagawandoss 2015a) indicate that common practice for sample acquisition and testing is not necessarily a good practice for oils that contain volatile components. The remainder of this document discusses details around sample acquisition and testing to support Phase II Task 2 objectives.

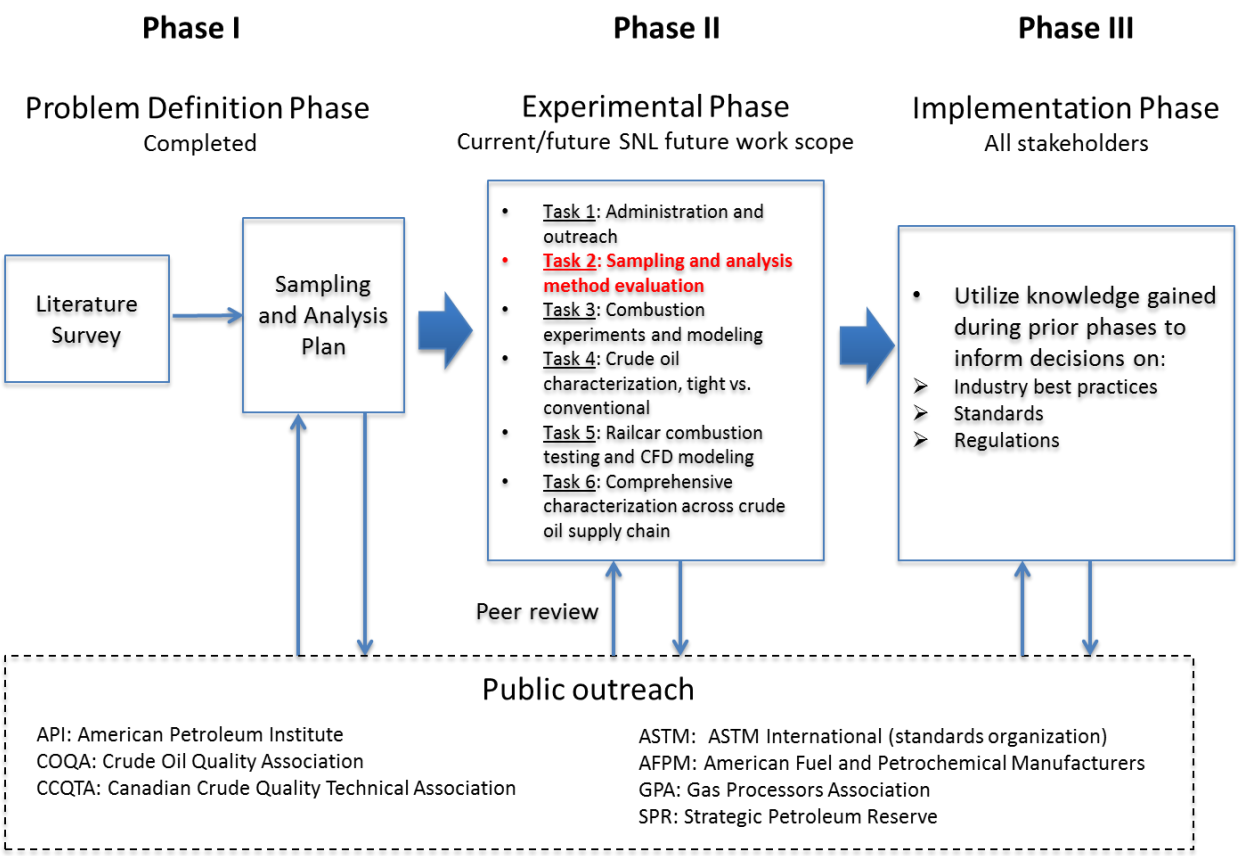

Figure 2-1. Overall conceptual diagram of Crude Oil Characterization Research Study. The focus of the current report, Task 2 Report on Evaluating Crude Oil Sampling & Analysis Methods, is indicated in red text in Phase II above.

2.3 Project Governance

Sandia National Laboratories is lead technical lab on the Crude Oil Characterization Research Study, funded directly by the U.S. Department of Energy and U.S. Department of Transportation. Sandia made arrangements to contract technical services where necessary capabilities were not available in-house. Given the shared interest between the governments of Canada and the United States in crude oil handling and transportation safety, a Crude Oil Research Coordination Steering Committee was formed in order to share emerging information and identify opportunities for research coordination. Administrative participants include the U.S Department of Energy, the U.S. Department of Transportation, and Transport Canada (TC). A conceptual diagram of project governance is given in Figure 2-2.

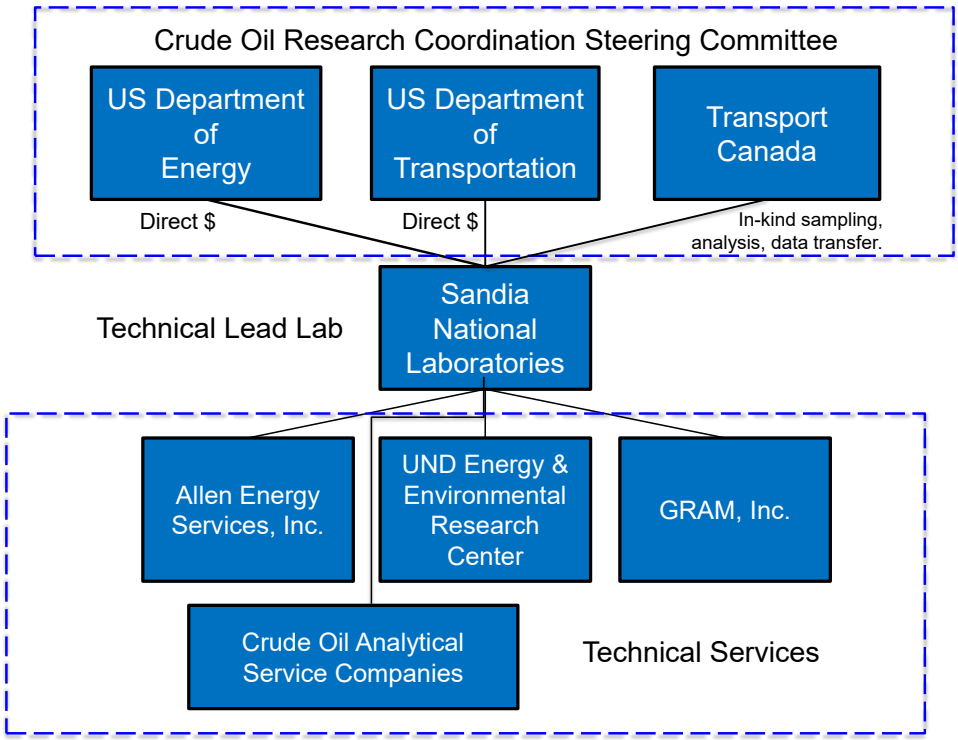

Figure 2-2. Conceptual diagram of project governance.

2.4 Scope of Report

The current report explores the effects of sample capture and analysis methods on selected physical and chemical properties of crude oils, with a focus on parameters that relate to volatility at conditions that are relevant to sample collection, handling, measurement, and transport.

Two crude oil sampling locations were selected for this phase of the study. One sampling point was a terminal that handled Bakken production, and a second was a terminal that handled Eagle Ford production. Sampling methods were varied at each sampling location to include "tight-line" straight to the analytical equipment, "closed" methods where no exposure to atmospheric

pressure was allowed, and finally an “open” method where the sample was allowed to interact with the ambient atmospheric conditions between time of capture and analysis in the laboratory.

Primary analyses included crude oil vapor pressure measured by VPCRx(T) (ASTM 2016c), chemical composition of the oils with focus on light ends and fixed gas content, with composition up to C30+, and selected properties to include relative density, average molecular weight, viscosity, flashpoint, and initial boiling point.

Methods and results associated with aforementioned combustion properties of crude oils will be addressed in separate reports.

3 Background

The issues of capturing and measuring light end and volatile components as part of "whole crude oil" analyses becomes important when properties such as initial boiling point and vapor pressure are considered in testing crude oil for classification for transport (ANSI/API 2014) or for compliance with state-level regulations over crude oil transport (NDIC 2014). Generally speaking, the historical methods of sample capture used in the oilfield for "oil quality" samples allow direct exposure of the hydrocarbon sample to ambient pressure. This opens the possibility of loss of volatile material during sample capture, transportation, storage, and analysis to a degree that may not be widely understood or appreciated. The fact that crude oil vapor pressure sampling and analysis has been treated in many instances as a standard "oil quality" parameter that does not require special handling to prevent light end vapor losses leads to the potential for inconsistent results and associated confusion around the topic of crude oil vapor pressures. These vapor losses can also affect other properties such as initial boiling point, flash point and composition.

Broader understanding around the effects of "open" versus "closed" sampling on compositional and property measurements of crude oils collected from surface storage and transportation facilities has been evolving recently, and is documented through vendor notices (Grabner-Instruments), association notices (CCQTA 2014), reports (CCQTA 2017) and technical presentations (Konecnik 2014; Bagawandoss 2015a; Bagawandoss 2015b) available from industry-specific technical associations such as the Crude Oil Quality Association (COQA) and the Canadian Crude Quality Technical Association (CCQTA), and the American Petroleum Institute (API) (ANSI/API 2014) and government-sponsored technical reports (Prefontaine 2015). Presentation of clear findings on these issues in the broader public peer-reviewed scientific literature has not been realized as yet. The absence of well-publicized scientific comparative studies on this topic indicates a knowledge gap that the current study is trying to help close.

The authors would like to add that there is ample capability and experience within the oil and gas industry to capture and measure complex hydrocarbon fluids containing dissolved gases and furthermore analyze these fluids for vapor pressure, light ends, and fixed gases, but this is largely in the realm of reservoir and production fluid testing. Sampling points for these "live" production fluids, which will readily boil at ambient conditions, are potentially downhole and/or upstream of primary separating and conditioning operations where vapor pressures and associated gas volumes are orders of magnitude higher than what is seen in the surface storage and transportation sector. As such, the methods and equipment designed to handle and analyze these "live" fluids may not have the capabilities to operate effectively or within their calibrated ranges for much lower (though nonzero) vapor pressures and associated gas volumes.

3.1 Key Points from Phase I Literature Survey

In seeking to better understand and mitigate risks associated with frequent and large-volume rail transport of crude oil in general and tight oil in particular, the U.S. Department of Energy (DOE) and U.S. Department of Transportation (DOT) commissioned a review of publicly available crude oil chemical and physical property data and literature related to crude oil potential for ignition, combustion, and explosion. The review was undertaken by Sandia National Laboratories (SNL) in collaboration with Allen Energy Services (AES) and the

University of North Dakota Energy & Environmental Research Center (EERC). A partial list of properties surveyed includes density (expressed as API gravity), vapor pressure, initial boiling point, boiling point distribution, flash point, gas–oil ratio, light ends and dissolved gas composition (including nitrogen, carbon dioxide, hydrogen sulfide, methane, ethane, and propane—and butanes and other volatile liquids), and flash gas composition. Although the review yielded a large database encompassing a wide variety of crude oils and their properties, it also illustrated the difficulty in utilizing available data as the basis for accurately defining and meaningfully comparing crude oils. Reasons for this difficulty include significant variability in:

- Sample collection point – Samples are collected at various points along the crude oil supply chain that extends from well to refinery gate. A partial list of sampling points (listed in supply chain order) includes well head, separator outlet, "heater-treater" outlet, stock tank, rail or pipeline terminal, and rail tanker (at varying points along the route from terminal to refinery gate). Crude oils—especially lighter varieties—may undergo significant changes in key volatility-related properties as they progress along the supply chain.
- Sampling method – Samples are collected using a variety of closed, open, and flow-through methods that vary in effectiveness of capturing 100% of crude oil volatile liquid and dissolved gas constituents. This is especially important in dealing with light crudes, since it means that a given crude sampled at a single supply chain point using a variety of sampling methods could result in a set of samples with significantly different volatility-related properties.
- Analytical method – Samples are analyzed using a variety of methods including those approved by ASTM and other "standard-setting" organizations, modified ASTM methods, and others.

An important outcome of the review was formal recognition of the wide variability in crude oil sample type, sampling method, and analytical method, and acknowledgement that this variability limits the adequacy of the available crude oil property data set as the basis for establishing effective and affordable safe transport guidelines. In recognition of the need for improved understanding of transport-critical crude oil properties, DOE/DOT commissioned SNL to develop a sampling, analysis, and experimental (SAE) plan to accurately characterize tight and conventional crudes based on key chemical and physical properties, and to identify properties that may contribute to increased likelihood and/or severity of combustion events that could arise during handling and transport. A high-level SAE plan was submitted to DOE in April 2015 and was subsequently made publicly available through the DOE–FE website[3].

3.2 Guidance from CCQTA Light Ends Memo

The Canadian Crude Quality Technical Association released a memo in May 2014 (CCQTA 2014) providing guidance on sampling and test methods for determining vapor pressure and light ends content of crude oils.

[3] See http://energy.gov/fe/articles/crude-oil-characteristics-research

The memo made several statements of particular relevance to sampling and analysis applicable to "live" crude:

> *With regards to any reported value for vapor pressure in crude oil, we would consider the data suspect unless the samples were:*
>
> 1. *Sampled in pressurized cylinders (ASTM D3700), or equivalent to prevent the loss of light end components during sampling, transport to laboratory, or handling during analysis.*
> 2. *Introduced into an analyzer under single-phase conditions to mimic the conditions at the time of sampling thus representing the true sample contained within the source.*
> 3. *Not exposed to atmospheric air during sampling, transport or handling operations. Samples in equilibrium with atmospheric air will by definition always have a minimum true vapor pressure (TVP) of barometric pressure. Air exposure can result in incorrectly reported hydrocarbon contributions to measured vapor pressures.*

A distinction between "live" and "dead" crude is important in the context of sampling and measurement. "Live" crude is commonly used to describe an oil contained in a pressurized system that, when brought to normal atmospheric pressure at room temperature, will result in boiling of the sample. "Dead" crude is used to describe oil that when exposed to normal atmospheric pressure at room temperature, will not result in boiling of the sample (CCQTA 2014).

Moreover, the CCQTA memo states:

> *A crude oil shall always be considered "live" until the vapor pressure can be established. Sampling and handling of dead crude oils can usually be done without concern in normal, non-pressurized containers, such as cans and other atmospheric containers.*

This presents a dilemma for those responsible for characterizing a crude oil that undergoes a series of property changes throughout its residence time and physical movement through a supply chain from the point of production (i.e., wellhead) to the point of consumption (i.e., refinery). The material may at one point be "live" (upstream of a gas-liquid separator) and then at another point "dead" (downstream of a gas-liquid separator) and yet another point "live" (heated above prior storage condition) again depending on process history, commingling, and local ambient temperature and pressure.

3.3 Related Study Results

A technical association presentation by Konecnik (2014) indicated that vapor pressure at $VPCR_4$(100°F), of an assortment of crude oils sampled in June 2013 measured routinely higher for samples collected and injected to the 6377 instrument by floating piston cylinder (closed method) than samples obtained by constant volume cylinder and transferred to open bottle method for induction into the 6377 instrument, with differences ranging from ~0.1 to ~5 psi (0.7 to 34 kPa). The author indicated that higher $VPCR_4$ was expected for closed (FPC) sampling, but the largest differences were not expected and unknown factors like machine fouling were likely involved.

Another technical association presentation by Bagawandoss (2015a) yielded similar observed differences for $VPCR_4$(100°F) by ASTM D6377-14 (ASTM 2014d) when comparing samples captured in water-filled spun cylinders (water displacement) and Boston Round bottles. Seven samples were tested and the results are shown in Figure 3-1, where the Cylinder 6377 column

denotes the water displacement samples, and the Bottle 6377 column denotes the bottle samples. All seven cylinder samples measured higher than bottle, and the average difference was reported as 0.796 psi. Sample conditions at time of collection were reported as originating from a pressurized source at 30-180 psig, and 55-62°F (Howe 2016).

Study Data – Cylinder D6377 vs Bottle D6377

Intertek
Valued Quality. Delivered.

Sample ID	Cylinder 6377	Bottle 6377	Difference
Sample 1	10.71 psi	10.51 psi	0.20 psi
Sample 2	11.90	10.34	1.56
Sample 3	10.99	10.21	0.78
Sample 4	10.73	10.12	0.61
Sample 5	10.80	10.21	0.59
Sample 6	10.45	9.22	1.23
Sample 7	10.61	10.01	0.60
Average	10.884	10.088	0.796

- *Water filled Spun Cylinder*
- *Samples for this study were collected on 7 different days*

Figure 3-1. ASTM D6377-14 VPCR$_4$(100°F) vapor pressure data from samples obtained by water displacement cylinder (closed) and bottle (open) sampling. Reproduced with permission from Bagawandoss (2015a).

3.4 Guidance from ASTM D6377 Standard

Industry standards developed by groups of subject-matter experts with a common interest to normalize best practices and make them broadly available to the public are published by organizations such as ASTM, API, and Gas Processors Association (GPA), and are utilized and cited frequently in this work.

ASTM D6377-16, Standard Method for Determination of Vapor Pressure of Crude Oil: VPCRx (Expansion Method) (ASTM 2016c), Section 8 Sampling and Sample Introduction, states the following:

> *The extreme sensitivity of vapor pressure measurements to losses through evaporation and the resulting changes in composition require the utmost precaution and the most meticulous care in the drawing and handling of samples. Sampling of live crude oil shall be performed in accordance with Practice D3700* [Standard Practice for Obtaining LPG Samples Using a Floating Piston Cylinder]. *Sampling in accordance with D4057 shall only be used for dead crude oil and if Practice D3700 is impractical.*

Additionally, ASTM D6377-16, Section 12.1.4 Procedure states:

> *For measurements with V/L ratios < 1, the sample may not be exposed to the atmosphere and shall be contained in a floating piston cylinder. The sample introduction temperature of the measuring chamber shall be equal to the measuring temperature to avoid any influence due to sample expansion.*

3.5 Summary Interpretation from Background Reading

A consistent message from the sources cited here is that sampling method matters when the parent material contains gases in sufficient quantity that losses during collection, transport, handling and analysis in the lab will affect the vapor pressure measured at the benchtop. The dilemma in selecting the most appropriate sample collection method lies in needing to know the properties of the material before the sample is taken, and moreover, how time evolution and processing upstream affect anticipated properties at the sampling point. A conservative approach is to utilize closed or pressurized sampling for sourcing all vapor pressure test samples as this has the best chance of preventing light ends losses. There was no clear information from the aforementioned background sources on comparative performance among available closed/pressurized methods (water displacement vs. floating piston vs. manual piston) or potential for any of these closed methods to introduce errors into the VPCR and/or light ends measurements. Issues of practicality can drive some preference in that the manual piston cylinder (MPC) can draw sample from lower process pressures than the floating piston cylinder (FPC) due to (i) the ability of manual assist to overcome piston seal friction to draw a sample, and (ii) the design of some modern MPC's for a lower pressure rating and thus easier manual use than traditional FPC. The recent (2015) development of a standard method and apparatus for manual piston cylinder sampling, ASTM D8009 (ASTM 2015a), creates opportunity for standardization of closed sampling from low-pressure systems where open tap bottle sampling by ASTM D4057 (ASTM 2012) was widely considered the only option.

3.6 Pressurized Compositional Analysis

Compositional analysis methods for characterizing crude oils are numerous and well-established, though the requirements of the current work are atypical in that a broad range of components are required from the lightest dissolved gases like nitrogen and methane up to stable liquids including C30+. Several prior technical reports (Auers, Couture et al. 2014; Wybenga 2014) on Bakken oils in the context of transportation safety provided data on composition with light ends reported. Analysis methods used there included ASTM D5134 (ASTM 2013b), ITM 6008 (proprietary method), and IP 344 (withdrawn). None of these methods met the current Sandia requirement of utilizing closed, pressurized sample handling and injection along with broad boiling range analysis for all of the required components. This knowledge gap in sampling and compositional analysis was recognized in a literature survey (Lord, Luketa et al. 2015) performed as a precursor to the current study.

Sandia experience with the U.S. Strategic Petroleum Reserve (SPR) Vapor Pressure program brought forward an option to utilize the TVP-95 mobile separator laboratory that was specially designed for measuring vapor pressure, light ends, and fixed gas content in a closed environment for oils that exhibit vapor pressures in the range 10-60 psia at 100°F (69-414 kPa at 37.8°C). Early work at SPR in the 1990's found that commercially available methods for capturing and analyzing crude oil samples from the SPR inventory for vapor pressure, light ends, and fixed gas content did not meet the unique requirements for conditionally stable oils, and were instead geared toward true "live" production fluids. Frustration over inconsistent results with the sample capture and analysis methods available at the time (Lott 1996) led to development of the TVP-95 (Alapati, Sonnier et al. 1997), which has been in use at SPR since the mid-1990's. It's application is described in prior Sandia reports (Hinkebein 2003; Lord and Rudeen 2010). One of the key findings in the early SPR work was that bringing the analytical

laboratory to the sample and tight-lining the sample from the process piping directly into the analytical instrument was an important step toward reducing sampling errors and small loss or gain of gases that exert a meaningful impact on vapor pressure, light ends, and fixed gas analyses but can be very difficult to mitigate. Hence, the "tight-line" sampling is an integral feature of the TVP-95.

One objective of the current study was to locate and test commercially available options for compositional analyses and compare with the TVP-95 system. Sandia engaged with industry groups (API, COQA, CCQTA) and commercial analytical laboratories in order to select several options that are discussed in more detail in the methods section.

4 Methodology

The test matrix for crude oil samples collected and tested in this study is presented in Table 4-1. Recall that a primary independent variable in this phase of the work is sample acquisition method, so the methods are listed row-by-row in the table by common name in column 1 and by applicable standard in column 2. Also note that a second independent variable explored here is the method for determining a "whole oil" composition (light ends and fixed gas included), which typically comprises a mathematical "merge" of results from several analytical steps with support from a numerical tool.

The methodology section of this report is organized into three parts:

(i) Sample acquisition
(ii) Analytical methods
(iii) Numerical analysis

In the following discussions the laboratories performing the sample acquisition and analytical methods reported herein are only identified generically as Lab 1, Lab 2, Lab 3 and Lab 4 to avoid any improper endorsement. Details of specific instrumentation or specific methodology employed by a specific lab are provided where relevant or necessary for proper data interpretation. All involved laboratories provided ATSM D6377 VPCRx data, thus dataset are distinguished by Lab 1, Lab 2 etc. identifiers. Compositional analytical methods are identified distinct from laboratories using a test method (TM) identifier TM1, TM2, TM3, TM4 and TM4a, with each analytical test method clearly delineated in subsequent section of the report. Additional nomenclature details are provided in section 4.6.

4.1 Sample Acquisition – Summer Samples

4.1.1 General Sampling Locations

Samples were acquired from two U.S. locations. One sampling point was in the Bakken production region in North Dakota (ND) at a terminal upstream of a rail loading facility. The second was in the Eagle Ford production region in Texas (TX) at a pipeline terminal upstream of a refinery. Agreements between Sandia National Laboratories and the terminal operators prevent disclosure of specific locations and operator names associated with these sampling events.

Sample acquisition occurred in two coordinated sampling events. The first event occurred at the Bakken terminal in August, 2016. The second event occurred at the Eagle Ford terminal in October, 2016. In both cases, Sandia National Laboratories and contractors assembled at the sampling location and acquired samples over a period of three consecutive calendar days. The TVP-95 mobile laboratory was on-site taking direct line samples for three days. The other contractors acquired spot samples over the first two days. Spot samples were shipped to the fixed laboratories over the next several days for analyses that occurred over the next several months.

4.1.1.1 ND Bakken sampling conditions

Environmental conditions for the ND Bakken sampling were as follows:

- Pipeline oil temperature was reported at 70°F (21°C) during sample collection.
- Mean ambient air temperature over the three-day sampling period was 74°F (23°C) from local airport data.
- Minimum recorded ambient air temperature was 57°F (14°C), and maximum was 89°F (32°C) from local airport data.

4.1.1.2 TX Eagle Ford sampling conditions

Environmental conditions for the TX Eagle Ford sampling were as follows:

- Pipeline oil temperature was reported from 94-98°F (34-37°C) during sample collection.
- Mean ambient air temperature over the three-day sampling period was 77°F (25°C) from local airport data.
- Minimum recorded temperature was 59°F (15°C), and maximum was 94°F (34°C) from local airport data.

4.1.2 Sample Capture Methods

Five sample capture methods were utilized at each sampling location. The primary unique aspect of each of the five different sample types is summarized as follows:

- Tight-line to mobile laboratory – Minimum achievable sample handling at or above original process line pressure in order to convey sample to analytical instruments.
- ASTM D3700 Floating Piston Cylinder – Pressurized sample obtained via displacement of a piston backed by an inert gas or liquid (ASTM 2014a).
- GPA 2174 Water Displacement Cylinder – Pressurized sample obtained via displacement of water (GPA 2014).
- ASTM D8009 Manual Piston Cylinder – Pressurized sample collected using manually operated piston cylinder (ASTM 2015a).
- ASTM D4057 Ambient Pressure Bottle Sampling – Ambient-pressure sample collected using bottom-fill tube to minimize splashing and resultant vapor generation (ASTM 2012).

Table 4-1. Test matrix for Task 2 Sampling and Analysis. Color-coding for compositional test methods TM1-TM4 is given below the table. Detail on TM1-TM4 is given in section 4.3.4.

			Property Measurement								
Sample Technique	**Standard**	**Sample Transfer**	TVP	Compositional Analysis 1	Compositional Analysis 2	Compositional Analysis 3	Avg MW	Relative Density	Viscosity	Flashpoint	IBP
Tight Line to TVP-95 Mobile Laboratory		N/A	Separator shut-in	BPP flash gas GC analysis	GOR flash gas GC analysis	Separator liquid C30+	frz pt dep	ASTM D5002	N/A	N/A	EOS with flash gas
Floating Piston Cylinder	ASTM D3700-14	N/A	ASTM D6377-M	GPA2103-M	GPA2177 + ASTM D7900 + ASTM D7169	ASTM D8003 + ASTM D7169 + GOR flash gas	frz pt dep	ASTM D5002	ASTM D7042	ASTM D56	D86 & GPA 2103
Water Displacement	GPA 2174-14	N/A	ASTM D6377-M	GPA2103-M	GPA2177 + ASTM D7900 + ASTM D7169	ASTM D8003 + ASTM D7169 + GOR flash gas	frz pt dep	ASTM D5002	ASTM D7042	ASTM D56	D86 & GPA 2103
Manual Syringe	ASTM D8009-15	N/A	ASTM D6377-M	GPA2103-M	GPA2177 + ASTM D7900 + ASTM D7169	ASTM D8003 + ASTM D7169 + GOR flash gas	frz pt dep	ASTM D5002	ASTM D7042	ASTM D56	D86 & GPA 2103
Boston Round	ASTM D4057-12	BR to MPC	ASTM D6377-M	GPA2103-M	GPA2177 + ASTM D7900 + ASTM D7169	ASTM D8003 + ASTM D7169 + GOR flash gas	N/A	N/A	N/A	N/A	D86 & GPA 2103
	ASTM D4057-12	BR	ASTM D6377-M	N/A	N/A	N/A	frz pt dep	ASTM D5002	ASTM D7042	ASTM D56	D86 & GPA 2103
Manual Syringe	ASTM D7975-14	N/A	ASTM D7975-14	N/A	N/A	N/A	N/A	N/A	N/A	N/A	N/A

TM1
TM2
TM3
TM4

Note: TM4a added to revision-1 of this report was also based on GPA 2103M, but used different methods from TM4 for heavy-end analysis and numerical merge.

4.1.2.1 Tight-line to mobile laboratory

The use of "tight-line" sampling effectively brings the analytical instrument in close proximity to the sample source in order to eliminate manual handling and minimize, to the extent practical, time and exposure out of the original process environment. The TVP-95 mobile laboratory was selected for this purpose due to its unique capability to collect tight-line samples and quantify vapor pressure, gas-oil ratio, and flash gas composition for oils with vapor pressures from 10-60 psia (70-410 kPa) and gas-oil ratio from 0.2 – 20 scf/bbl (0.036 – 3.6 m^3/m^3). The TVP-95 is the baseline instrument system used to support the U.S. Strategic Petroleum Reserve vapor pressure program and has been in service since 1995 and has an applicable US patent (Alapati, Sonnier et al. 1997). Hardware and software upgrades have been made since 1995, but the basic operating principle has remained the same throughout.

The TVP-95 mobile laboratory shown in Figure 4-1 was positioned within about 50 feet of the sampling location in each sample event, and crude oil was transferred from the pipeline source to the TVP-95 trailer through closed piping (see Figure 4-2). In order to facilitate this, a sampling manifold was attached to the operator's pipeline to allow sampling for both floating piston cylinder (FPC) and closed flowing line to the TVP-95 lab (see Figure 4-2 and Figure 4-3). The oil sample was conveyed through a ½" (12.7 mm) diameter flexible hose rated for 2,000 psi (13.8 MPa) approximately 50 ft. (15m) over the ground to a pneumatic pressure boosting pump staged next to the TVP-95 trailer (see Figure 4-4). Pressure was increased to 500 psi (3.45 MPa) and the oil was conveyed upward several feet through additional ½-inch high-pressure hose to a temperature conditioning oven inside the TVP-95 trailer (see Figure 4-5(a, b)). The oven contains about 1,000 cc volume of ¼-inch tubing in order to give the oil enough residence time to reach the set point temperature of 100°F (37.8°C). Oil was then discharged through tight-line into the main flash chamber at a rate that allowed for constant level control of about 95% liquid, 5% vapor by volume as measured by a float.

Average flowrates through the flash chamber were as follows:

<u>ND Bakken Sample</u>:

- Day 1: (60 cc/min), GOR: 30 cc/min
- Day 2: (70 cc/min for two hours, then 40 cc/min), GOR: 35 cc/min
- Day 3: (60 cc/min), GOR: 25 cc/min

<u>TX Eagle Ford Sample</u>:

- All tests were run at 60cc/min

Compositional samples were collected by closed line off the top of the flash separator for both bubble point and gas-oil ratio tests (see Figure 4-5(b)). All gas sample lines were heat traced and insulated between the flash chamber and the gas chromatograph. Sample draws for the unpressurized C30+ analysis were taken in 60 cc glass jars from the threaded sampling port on the sampling manifold shown in Figure 4-2 and Figure 4-3. Sample draws for the Lab 1 FPC VPCR measurements were taken from the same threaded sampling port on the sampling manifold.

Figure 4-1. Exterior photo of TVP-95 mobile laboratory used in this study. Photo provided with permission from CoreLab.

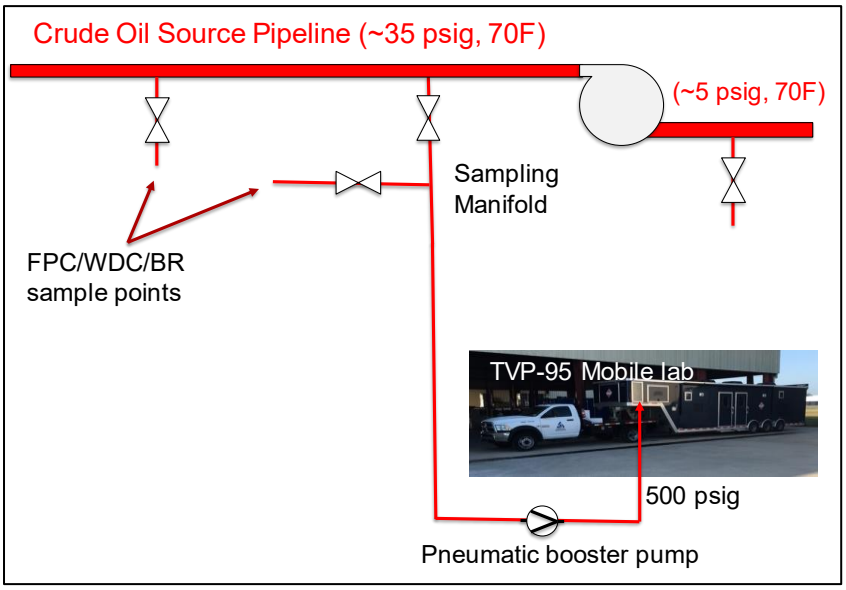

Figure 4-2. Schematic of sampling configuration at Bakken terminal.

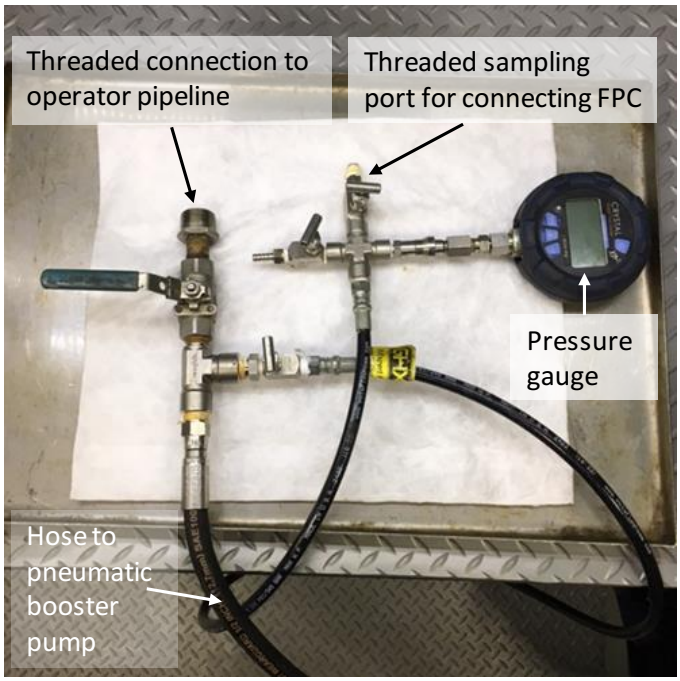

Figure 4-3. Sampling manifold utilized to facilitate sample collection from operator pipeline. Photo provided with permission from CoreLab.

Figure 4-4. Pneumatic booster pump that raises sample to 500 psi prior to injection into TVP-95 trailer. Photo provided with permission from CoreLab.

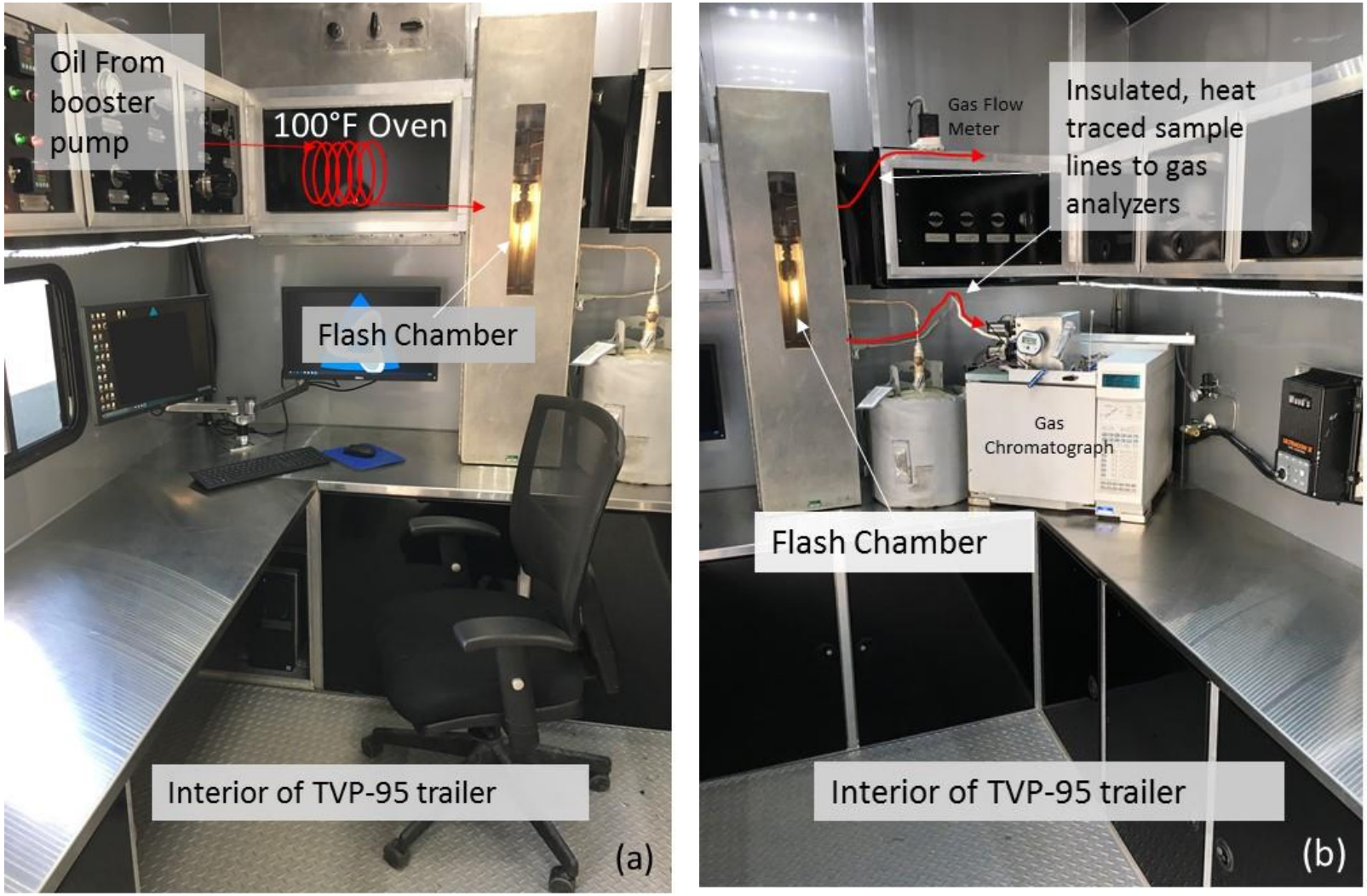

Figure 4-5. Annotated photos illustrate how the "tight-line" crude oil sample is drawn into the pre-conditioning 100°F oven, upper left in photo (a), and into the flash chamber. Crude oil vapors exiting the flash chamber pass through insulated, heat traced lines to a gas flow meter or gas chromatograph, photo (b). Photos provided with permission from CoreLab.

4.1.2.2 Floating Piston Cylinder (FPC)

Floating piston cylinder samples were taken according to ASTM D3700-14 (ASTM 2014a)– "Standard Practice for Obtaining LPG Samples Using a Floating Piston Cylinder" with an example cylinder shown in Figure 4-6. Practice D3700 will yield a pressurized sample filled to 80% of sample container capacity. Labs 1 and 2 in this study backed the piston in FPC samples with ~300 psi (2.1 MPa) nitrogen. Lab 3 backed the piston with a 2:1 water/glycol mix at atmospheric pressure. Maintenance pressure on FPC samples for Lab3 was 300 psig (2.1 MPa).

Figure 4-6. Representative ASTM D3700 floating piston cylinder. Photo provided with permission from Intertek.

4.1.2.3 Water Displacement (WD)

Water displacement samples were taken according to GPA 2174-14 (GPA 2014) – "Obtaining Liquid Hydrocarbon Samples for Analysis by Gas Chromatography." Sample collection was performed using the Water Displacement Method-Partial Displacement, section 5.3 resulting in a cylinder 80% filled with hydrocarbon sample and 20% vapor space. Lab 2 utilized tap water while Lab 3 utilized distilled water as displacement fluid. A representative water displacement cylinder is shown in Figure 4-7.

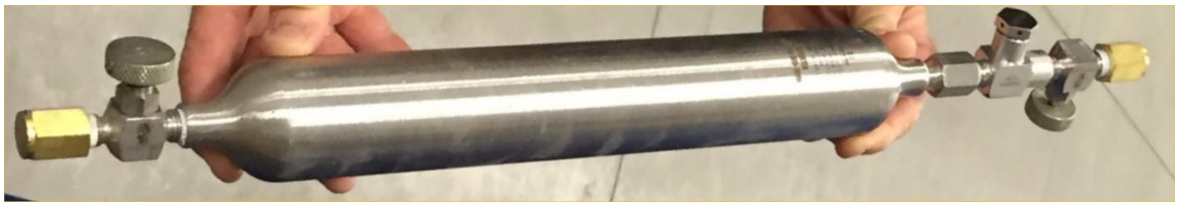

Figure 4-7. Representative GPA 2174 water displacement cylinder. Photo by David Lord and reproduced with permission from Intertek.

4.1.2.4 Manual Piston Cylinder (MPC)

Manual displacement cylinder samples were taken according to ASTM D8009–15 (ASTM 2015a) – "Standard Practice for Manual Piston Cylinder Sampling for Volatile Crude Oils, Condensates, and Liquid Petroleum Products." This method offers the option of manual piston movement by mechanical means (see Figure 4-8) rather than by differential pressure as in ASTM D3700. The method can be used for samples having vapor pressures of up to 44 psia nominal (300 kPa) at 122°F (50°C), but is especially useful in situations where sampling point pressure may be insufficient to overcome the pressure seal-driven friction associated with some FPCs. The method can be used to yield a pressurized sample filled to 80% of container capacity. Lab 2 used 300 psi nitrogen (2.1 MPa) as a pre-charge fluid (D8009-15, procedure B), and upon completion of

sampling, used the same for transportation and storage. Lab 3 used ASTM D8009-15 procedure A, without pre-charge gas. Lab 3 then used 75 psi (520 kPa) nitrogen to maintain pressure during sample conditioning and handling.

Figure 4-8. Representative ASTM D8009 manual syringe sampling cylinder. Reproduced with permission from Bagawandoss (2015a).

4.1.2.5 Boston Round open bottle sampling (BR)

Open bottle samples were taken according to ASTM D4057-12 (ASTM 2012) – "Standard Practice for Manual Sampling of Petroleum and Petroleum Products." This specification describes a wide variety of devices, systems, and methods that can be used to acquire petroleum samples. In particular, it includes discussion on the use of glass bottles (section 6.2: Boston Rounds) along with a delivery tube (section 7.7.1) that extends to the sample container bottom to permit filling of the sample from the bottom up. An example photo of a crude oil sample obtained for this study stored in a glass bottle in the laboratory is shown in Figure 4-9. Glass bottles were generally filled to 80% liquid with 20% vapor space above. No specific temperature controls were implemented during sample collection, transportation, or storage in the laboratory.

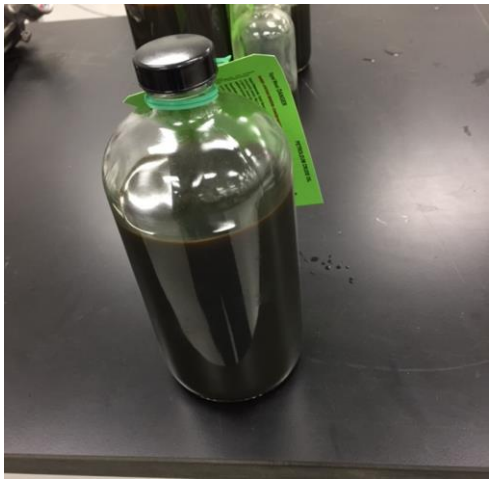

Figure 4-9. Representative glass bottle "Boston Round". Photo provided with permission from Intertek.

4.1.2.6 Sample transfer from BR to MPC (BRMPC) or FPC (BRFPC)

In order to facilitate laboratory testing that requires pressurized sample injection, some of the BR samples were transferred to manual piston cylinders in the laboratory. Lab 2 placed the BR bottles into an ice bath to chill to ~32°F (0°C), before drawing into a manual syringe drive cylinder through 1/8-inch tubing. Such samples are labeled "BRMPC" or "BRFPC" in this report depending on whether the final container was an MPC (BRMPC) or FPC (BRFPC). Lab 3 transferred bottle samples to MPC at ambient lab temperature.

4.2 Sample Acquisition – Winter Samples

Winter samples were taken in addition to summer to evaluate the potential for seasonal differences in the performance of open vs. closed sampling for supplying crude oil VPCR and pressurized compositional measurements. Crude oils conditioned and sampled at colder temperatures have the potential to retain more light ends and fixed gases than oils conditioned at warmer temperatures. In turn, winter samples then handled in open and unpressurized systems and warmed during handing and analysis have the potential to lose more volatiles than samples obtained in warm ambient or completely closed sampling conditions.

The winter sampling event consisted of collecting and analyzing crude oil samples in a similar fashion to previous Task 2 efforts, with some exceptions. First, the field samples were collected while ambient temperatures were below laboratory temperatures, nominally less than 68°F. Multiple open and closed sampling methods were used to provide data indicating how sample handling techniques, specifically chilled sample collection, impact retention of light ends. The TVP-95 system was not used for winter sampling. Samples were collected from the same Texas and North Dakota locations used previously.

Analytical methods used for this winter sampling task were focused on providing comparative data related to vapor pressure, sulfur, and compositional analysis. Table 4-2 summarizes the sampling procedures and analytical methods used for this winter sampling event. The sampling procedures incorporated lessons learned in the Task 2 summer sampling in attempt to minimize introduction of N2 in the sampling train by incorporating a revised MPC purging procedure discussed below.

Table 4-2. Summary of winter sampling and analytical procedures

Acronym	Sample Technique	Standard	Sample Transfer	Property Measurement		
				Vapor Pressure	Compositional Analysis	Sulfur*
FPC	Floating Piston Cylinder	ASTMD3700	N/A	TX	TX, ND	–
MPC	Manual Piston Cylinder	ASTM D8009	N/A	ND	–	ND
WD	Water Displacement	GPA 2174	N/A	TX	–	TX, ND
BR1	Open Bottle, ambient temperature	ASTM D4057	None	ND	–	ND
BR1MPC	Open Bottle, ambient temperature	ASTM D4057	BR to MPC	TX, ND	TX, ND	–
BR2MPC	Open Bottle, chilled bottle	ASTM D4057-M	BR to MPC	TX, ND	TX, ND	TX, ND
BR3MPC	Open Bottle, chilled line and bottle	ASTM D5842-14 Section 7.2.2.1	BR to MPC	TX, ND	TX, ND	TX, ND

ND – Bakken; TX – Eagle Ford.
*No sample transfer (BR to MPC) was needed for sulfur measurements.

4.2.1 Sampling Locations and Conditions

4.2.1.1 ND Bakken sampling conditions

Winter sampling of North Dakota Bakken crude oil occurred on March 23, 2017 at the same location utilized for summer sampling.

- Pipeline oil temperature was reported at 48°F (9°C) during sample collection and average line pressure was 138 psig (952 kPa).
- Mean ambient air temperature for sampling day was ~40°F (4°C) from local airport data.
- Minimum recorded ambient air temperature was 30°F (-1°C), and maximum was 50°F (10°C) from local airport data.

4.2.1.2 TX Eagle Ford sampling conditions

Winter sampling of Texas Eagle Ford crude oil occurred on March 2, 2017 at the same pipeline terminal used for summer sampling.

- Pipeline oil temperature was reported from 94-97°F (34-36°C) during sample collection and line pressure was 15-65 psig (103-448 kPa).
- Mean ambient air temperature for sampling day was ~60°F (16°C) from local airport data.
- Minimum recorded temperature was 49°F (9°C), and maximum was 70°F (21°C) from local airport data.

4.2.2 Sample Collection

Samples were collected using both open and closed methods, to include selected industry standards and slight variants as described below.

4.2.2.1 ASTM D3700 Floating Piston Cylinder

Floating piston cylinder (FPC) samples were taken according to ASTM D3700-14 (ASTM 2014a) – "Standard Practice for Obtaining LPG Samples Using a Floating Piston Cylinder", similar to samples collected during previous Task 2 activities. For the winter sampling portion of the study, the FPC method was used exclusively for sourcing the pressurized compositional analyses.

The rinse method described in 4.2.2.2.1 was not used on the FPC samples.

4.2.2.2 ASTM D8009 Manual Piston Cylinder

Manual piston cylinder (MPC) samples were taken according to ASTM D8009-15 (ASTM 2015a) – "Standard Practice for Manual Piston Cylinder Sampling for Volatile Crude Oils, Condensates, and Liquid Petroleum Products," Sampling Procedure B, Manual Piston Cylinder with Pre-Charge Gas.

Additionally, a purge method (summarized directly below) was implemented for MPC samples in an effort to minimize the volume of air trapped within fittings of the cylinder that can have a significant impact on accurate vapor pressure methods.

Due to the timing of the development of this purge method, it was applied to the ND Bakken winter sampling only. It was not applied to the TX Eagle Ford winter sampling. This did not appear to influence the measured composition and vapor pressure results from the MPC samples outside of the variance in the data.

4.2.2.2.1 MPC crude oil sampling with cylinder purge

It appeared from Task 2 summer analyses conducted prior to the winter work that inadvertent introduction of N2/air into the closed sampling cylinders, either due to trapped N2/air in cylinders, fittings, valves, etc. can contribute significantly to measured VPCR's at low V/L's. Based upon this observation a new procedure was incorporated into the Task 2A sampling plan for sampling with MPCs consisting of multiple purges of the sample through the sample lines, valves, and cylinder to attempt to fully purge any potential dead spaces in the system of any gases. Version 03-Mar-2017 of the procedure, developed by Ray Allen, Allen Energy Services and Robert Falkiner, CCQTA, is detailed below.

Description

Due to spurious low quantities of air (N2/O2) in some FPC and MPC crude samples, the following purge procedure is recommended to purge any air from sample lines, inlet/purge/pressure safety valves and sample chamber prior to obtaining the final representative sample.

The purge procedure is specific to each vendor design of FPC/MPC depending upon the location and orientation of the valves. The cylinder will be oriented and/or oscillated during the purge procedure to maximize the removal of air from the sample system.

This detailed procedure for a Welker FPC/MPC models CP-SI or CP-SY is as follows (refer to Figure 4-10):

1. Connect sample manifold valve (6) to product source valve, open product source valve, manifold valve (6) and purge thru hose end valve (1), until approximately 5 line volumes have been purged.
2. Close hose end valve (1).
3. Connect hose end valve (1) to cylinder product inlet valve (3).
4. Open sample inlet valve (3) and pull in approximately 20-100 ml of sample, by either reduction of backpressure by opening precharge valve (5) and, if required, pulling piston handle. Once partial fill complete block in precharge valve (5) and if pull handle required mechanically lock in handle position.
5. With cylinder in the horizontal position and purge valve (4) positioned at the 12 o'clock position, ensure purge line to collection vessel is installed prior to opening purge valve (4). During cylinder purge observe sample pressure gauge, being careful to maintain sample pressure to a minimum of 5 psi (34 kPa) above of product vapor pressure.
6. While purging raise the sample inlet end of the cylinder from horizontal to vertical position multiple times to insure all trapped gases are removed from cylinder dead volumes.

7. Purge cylinder until 5-10 times the initial sample fill has been purged through the system. At end of the purge push piston back to the zero(bottom) position, by either increasing piston backside pressure or pushing handle, to remove all sample from cylinder under sample pressure to insure fresh sample introduced.
8. Once purge complete close purge valve (4).
9. Fill cylinder with sample to proper sample volume.

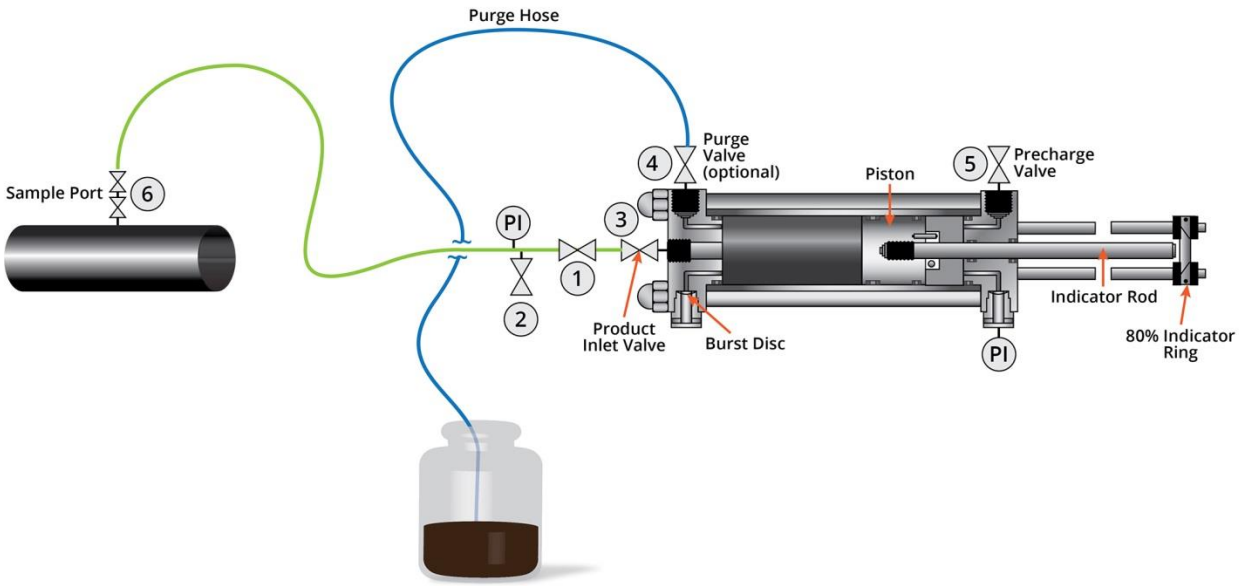

Figure 4-10. Example FPC diagram and connection to crude oil sample source.

4.2.2.3 GPA 2174 Water Displacement Cylinders

Samples using water displacement cylinders (WD) were collected according to GPA 2174-14 (GPA 2014) – "Obtaining Liquid Hydrocarbon Samples for Analysis by Gas Chromatography", similar to samples collected during previous Task 2 activities. Attempts to create 20% outage were unsuccessful due to insufficient sample vapor pressure under the given conditions to displace the water. Sample cylinders were placed in an ice-filled cooler for transport to the analytical laboratory. Samples collected by WD were generally held on retain and only analyzed for selected cases.

4.2.2.4 Open Bottles

Open bottle samples were collected using three levels of rigor to observe whether light ends losses would be affected by chilling the sample and associated apparatus. The three variants are depicted graphically in Figure 4-11, and denoted BR1, BR2, and BR3.

4.2.2.4.1 ASTM D4057 Open Bottle Sampling using a Delivery Tube

Open bottle samples were taken according to ASTM D4057 (ASTM 2012) "Standard Practice for Manual Sampling of Petroleum and Petroleum Products" Section 6.1 *Glass Bottles* and Section 7.7.1 *Tank Tap Sampling* utilizing a tube that provides sample delivery to the bottom of the bottle.

Similar to samples collected during previous Task 2 work, samples were collected in open jars at ambient temperature and stored at ambient temperature in the laboratory.

4.2.2.4.2 ASTM D4057-M Using a Delivery Tube into a Chilled Open Bottle

Open bottle samples were also taken according to ASTM D4057 (same as above) but with a modification using chilled glass bottles (See Figure 4-11b). Sample bottles were placed in a cooler with ice the day prior to sampling and remained on ice until delivery to the laboratory. Samples were then stored in a laboratory refrigerator.

4.2.2.4.3 ASTM D5842-14 section 7.2.2.1 (c), using a tube chiller assembly and delivery tube into a chilled bottle

Open bottle samples were also obtained using ASTM D5842-14 (ASTM 2014b) "Standard Practice for Sampling and handling of Fuels for Volatility Measurement," Section 7.2.2.1, using a chilled sample line and chilled sample bottle. This sampling procedure includes the use of a coil of copper tubing immersed in an ice filled cooler. Oil exiting the source pipeline sample port traveled through the chilled copper tubing and into a sample bottle. The sample bottle was immersed in ice during the filling process. Filled sample bottles were capped and placed in an ice filled cooler for transport to the laboratory. Samples were then stored in a laboratory refrigerator.

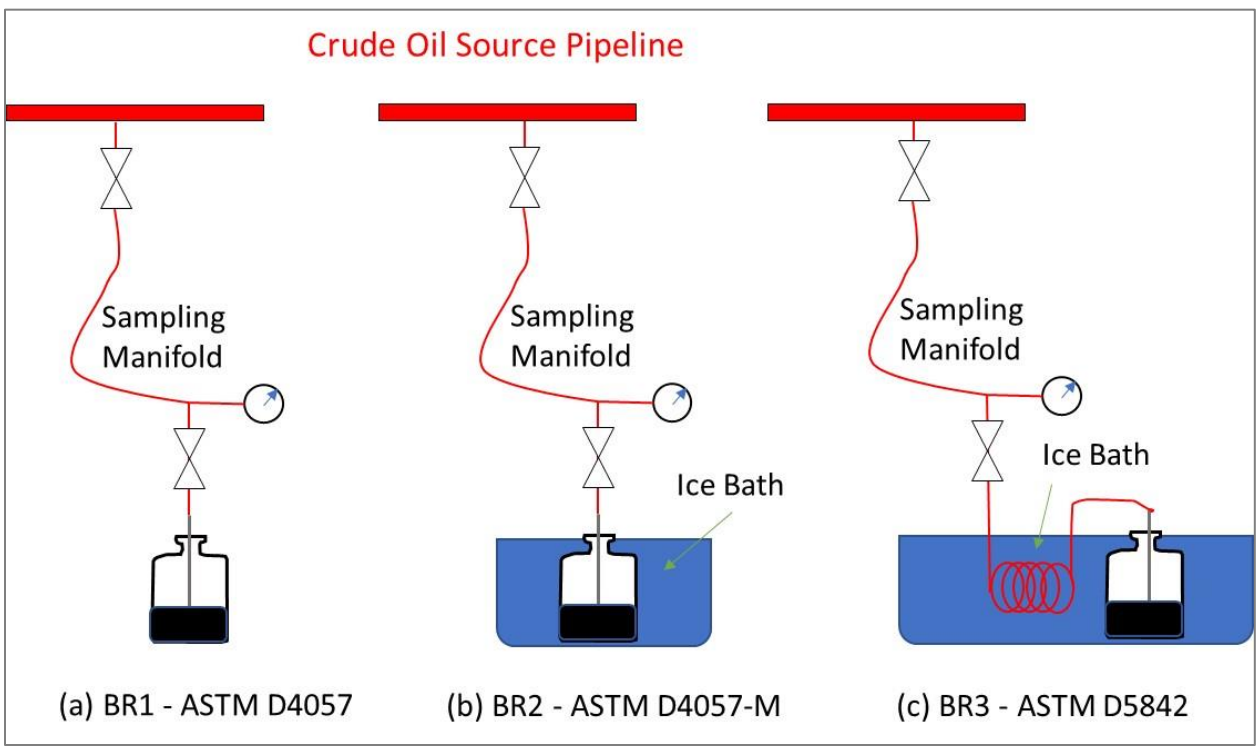

Figure 4-11. Boston Round sampling methods. From left-to-right: BR1 – tap tube; BR2 – chilled bottle; BR3 – chilled coil and bottle.

4.3 Analytical Methods – Summer Samples

Analytical methods include testing for vapor pressure, gas-oil ratio, oil composition, and selected physical properties.

4.3.1 Crude Oil Vapor Pressure

Samples were analyzed for vapor pressure using three basic methods:

(i) Flash separator using the TVP-95 mobile laboratory with two operating modes:

a. Closed vapor space yields bubblepoint pressure (BPP) at selected temperature.

b. Flowing vapor stream yields gas-oil ratio (GOR) at local atmospheric pressure and selected temperature.

(ii) VPCRx(T) via ASTM D6377-16, Standard Test Method for Determination of Vapor Pressure of Crude Oil: VPCRx(Expansion Method) (ASTM 2016c).

(iii) VPCRx-F(Tm°C) via ASTM D7975-14, Standard Test Method for Determination of Vapor Pressure of Crude Oil: VPCRx-F(Tm°C) (Manual Expansion Field Method) (ASTM 2014c).

4.3.1.1 Flash separator method (TVP-95)

The TVP-95 mobile laboratory employs a single-stage flash separator process that can be run in either vapor shut-in mode or vapor flow-through mode. The shut-in mode simulates a condition near equilibrium bubblepoint for a liquid, and the instrument is designed and calibrated to measure bubblepoint pressure for crude oils that exhibit vapor pressure in the range 10-60 psia (70-410 kPa).

In addition, the flash separator can be run in vapor flow-through mode in order to provide a measure of gas-oil ratio (GOR) from 0.2 – 20 scf/bbl (0.036 – 3.6 m^3/m^3). Test conditions were set to T = 100°F (37.8°C) and local atmospheric pressure at the test site. The TVP-95 test report indicated that the ND Bakken GOR tests were run at 14.0 psia (97 kPa), and the TX Eagle Ford tests were run at 14.7 psia (101 kPa).

4.3.1.2 VPCRx(T) method

Labs were instructed to follow the D6377-16M method with a modification to sample conditioning as noted below. Vapor pressure "curves" were to be developed by running a series of pressure-expansion points on oil from each of the four sample collection methods. The selected temperature and expansion points are given in Table 4-3. Each sample was analyzed at least twice.

Table 4-3. Temperature and expansion settings for ASTM D6377M VPCRx(T) measurements to be run on samples collected from each sampling method.

Temperature		Expansion Ratio (x)					
(°F)	(°C)	V/L	V/L	V/L	V/L	V/L	V/L
68	20	0.02	0.05	0.2	0.5	1.5	4.0
100	37.8	0.02	0.05	0.2	0.5	1.5	4.0
122	50	0.02	0.05	0.2	0.5	1.5	4.0

Samples must be allowed to reach an effective equilibrium for each expansion point, with D6377 instrument settings given in Table 4-4.

Table 4-4. Instrument settings setting for "Equilibrium Time" and "Equilibrium dP/dt" required to ensure that the analysis run for each V/L has reached equilibrium conditions.

V/L	Minimum Equilibration Time (sec)	Equilibration dP/dt (kPa/min)
0.02	1800	0.21
0.05	1200	0.21
0.20	900	0.14
0.50	600	0.14
1.5	500	0.14
4.0	300	0.14

The "M" modifier on the ASTM D6377M test method relates specifically to the equilibrium criteria above in Table 4-4 and the temperature conditioning of the test fluid. Sandia National Laboratories requires that the test fluid be pre-conditioned to the test temperature PRIOR TO PRESSURIZED INJECTION into the sample chamber in the 6377 device. This is done in order to prevent liquid thermal expansion effects from further pressurizing the cell before the expansion sequence starts, leading to erroneously high pressure values for low V/L.

4.3.1.3 Sample conditioning

The baseline ASTM D6377-16 method, section 8.3.1, reads "Transfer the sample at room temperature but at least 5°C above the pour point of the sample from the container into the measuring chamber." This indicates that the sample is heated from room temperature to test temperature while inside the sample chamber.

All labs were instructed to run a modified ASTM D6377-16 method by which they pre-conditioned crude oil samples to test temperature prior to introduction into the test cell, independent of V/L. The concern for pre-conditioning was raised in the developmental stages of this work as Sandia was offered access to DOT/PHMSA data that contained many high outlier $VPCR_{0.02}$(122°F) for oil samples that were introduced into the VPCR sample chamber at room temperature, sealed, and heated to test temperature (consistent with ASTM D6377-14, -15, and -16). The rationale for this was that thermal expansion of the hydrocarbon liquid induced by heating from room temperature to 100 or 122 °F (37.8 or 50°C) would likely create a pressure spike in the fixed-volume measuring chamber and result in an artificially high pressure and possibly liquid-lock the cell at the low (0.02, 0.05) V/L conditions. This is consistent with the concern about sample expansion stated within ASTM D6377-16, section 12.1.4. Note the BR samples were not pre-conditioned, rather handled as described in section 4.3.1.5 below.

A variant on the pre-conditioning requirement was run for a select group of samples in which the lab was instructed to adhere to the D6377-16 standard with no pre-conditioning just as it would for routine production runs for a typical client. Both Bakken and Eagle Ford samples were run from FPC, MPC, and WD cylinders at T = 100°F (37.8°C), V/L = 1.5 and 4.0. Note also that the

smaller V/L points explored in other parts of this study (0.02, 0.05, 0.2, 0.5) were not run in this mode because the D6377-16 standard states in section 12.1.4

> *For measurements with V/L ratios < 1, the sample may not be exposed to the atmosphere and shall be contained in a floating piston cylinder. The sample introduction temperature of the measuring chamber shall be equal to the measuring temperature to avoid any influence due to sample expansion.*

Figure 4-12 illustrates one representative configuration used in this study to pre-condition the 6377 samples. The closed sample cylinder (FPC/MPC/WD) was housed in a pre-conditioning chamber (lab oven) and heated to test temperature. The 6377 VPCR instrument can be seen on the left, located immediately next to the oven so that the sample tubing leaving the oven passes directly into the instrument housing, minimizing potential for temperature loss.

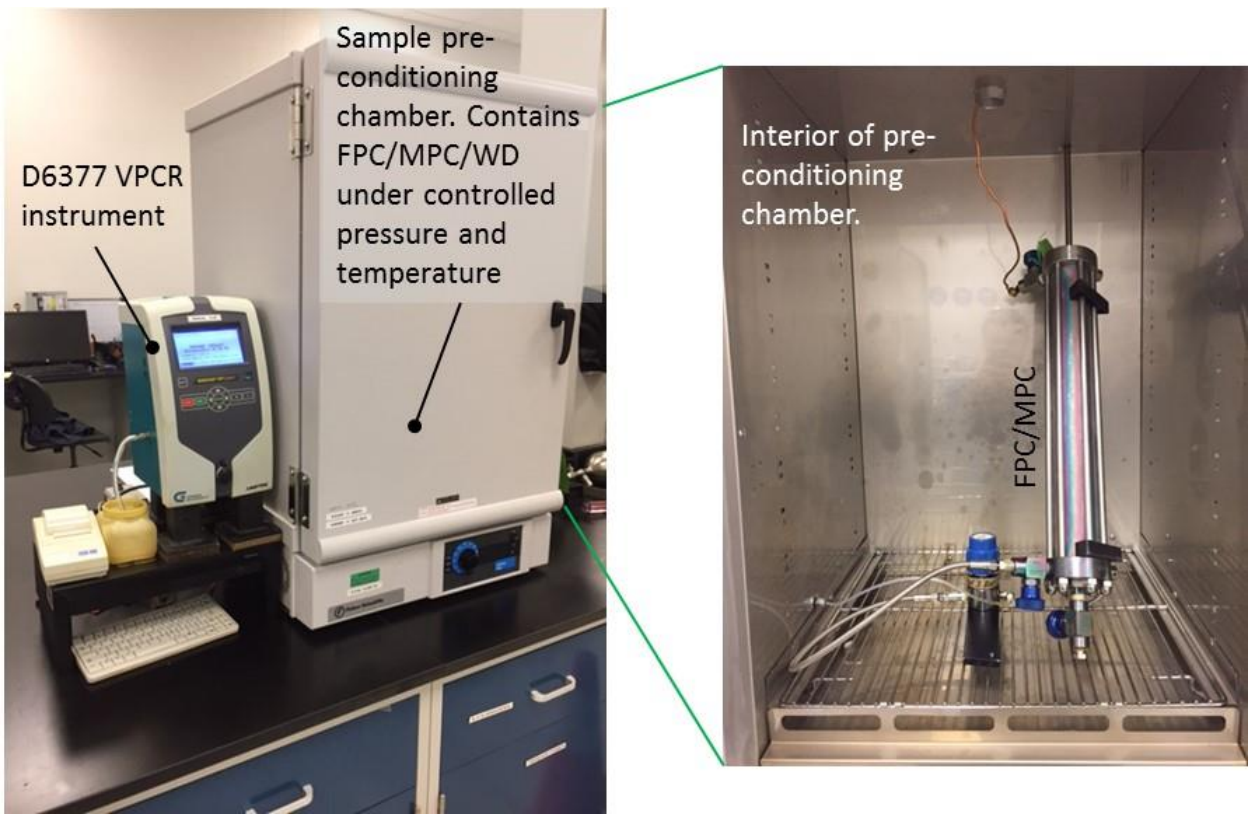

Figure 4-12. Example of 6377 sample pre-conditioning apparatus comprising an oven that pre-heats the sample (FPC/MPC/WD) to test temperature prior to introduction into the sample chamber. Photos provided with permission from Intertek.

4.3.1.4 Pressurized sample introduction into VPCR instrument

There are several important differences to note in how the crude oil samples were introduced into the VPCR instruments and how the sample was conditioned in the process. All closed methods (FPC, MPC, WD, and BRMPC) were introduced under positive gauge pressure using a pressure source of inert gas from the laboratory. The open BR method relied on a vacuum draw of sample from the benchtop to the sample chamber in the instrument.

Figure 4-13 is a montage of photo and schematic illustrating how the FPC/MPC/WD cylinders are introduced into the 6377 sample chamber using back-pressure from a lab gas source in Lab 2. An important feature of this system is that the sample is always maintained above its bubblepoint pressure from the cylinder all the way into the 6377 sample chamber. As such, it is never subject to two-phase separation during sample chamber loading. The general guideline in this work was to maintain about 45-60 psia (310-410 kPa) pressure between the regulator and the 6377 instrument. Note BRMPC cylinders were handled by these protocols as well. Note this configuration assumes that bubblepoint pressures for the crudes are below 60 psia (410 kPa) at the highest temperature in the test environment.

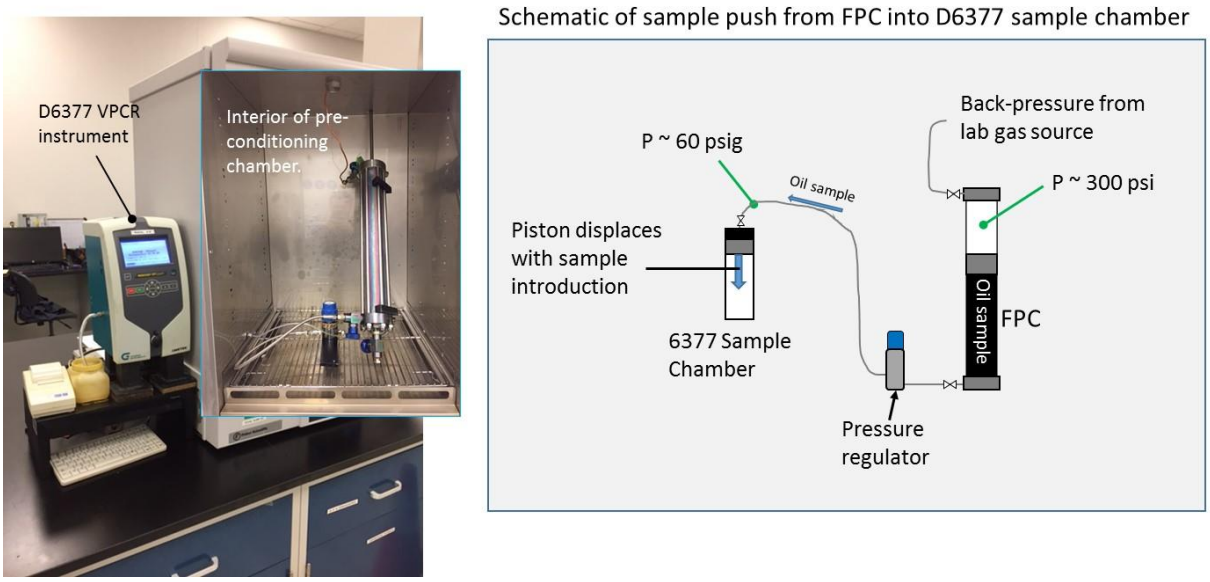

Figure 4-13. Photos on left show the 6377 instrument and an inset view of the interior of the conditioning oven (provided with permission from Intertek). Conceptual sketch on right illustrates process to push sample from pressurized cylinder (FPC/MPC/WD) into 6377 sample chamber.

The Lab 3 configuration is slightly different and illustrated in Figure 4-14. Their procedure is as follows:

- The cylinder is pressurized to 75 psig (520 kPa) and the pressure on the cylinder is controlled by a gas drive which is connected to the pre-charge end of the cylinder. The valve on the sample side is closed.
- A Blue M laboratory oven is used to equilibrate the sample to the measurement temperature.
- The valve on the sample side of the cylinder is opened and the sample is displaced through the sample line into the 6377 instrument.
- Poly tubing connects the cylinder to the VP unit and is insulated both inside and outside of the oven.

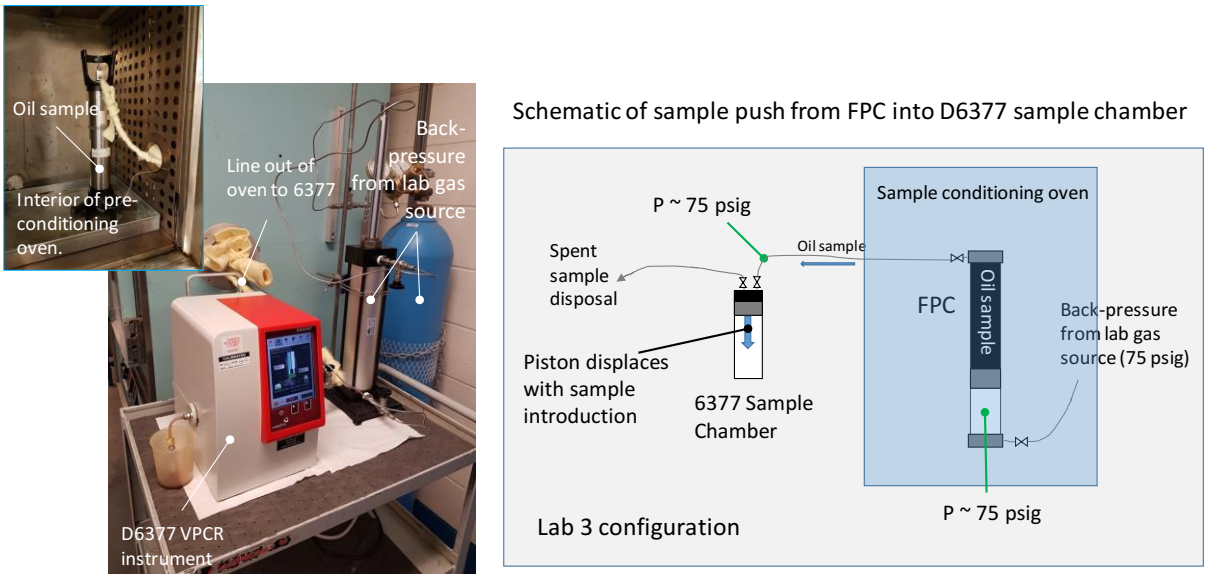

Figure 4-14. Photos on left show the 6377 instrument and an inset view of the interior of the conditioning oven (provided with permission from InnoTech Alberta). Conceptual sketch on right illustrates process to push sample from pressurized cylinder (FPC/MPC/WD) into 6377 sample chamber.

4.3.1.5 Unpressurized sample introduction into VPCR instrument

Pre-conditioning BR samples by heating them to 100 and 122°F (37.8 and 50°C) just like the closed samples was precluded due to safety concerns caused by volatilization of the light gases in an unpressurized bottle on the benchtop. Labs were instructed to run the BR samples just as they do for production runs under ASTM D6377-16, hence maintain the bottle at room temperature on the benchtop. Figure 4-15 is a montage of photo and schematic showing how the BR samples were introduced into the 6377 sample chamber using a vacuum draw. Recall a pressure difference is required to overcome elevation differences and friction loss in order move a fluid from one location to another. Since the vapor space inside the BR sample is maintained at local atmospheric pressure (denoted P = 1 atm in figure), the pressure differential necessary to move the liquid sample from the bottle to the sample chamber is provided by displacing the piston in the 6377 instrument to create a vacuum (denoted P < 1 atm in figure), at which point the oil sample is drawn through a piece of tubing and into the 6377 instrument. One of the risks of this procedure is that the sample may flash inside the tubing or sample chamber, creating an initial condition in the chamber of a 2-phase fluid (V/L > 0) when the operating assumption is that the starting condition is V/L = 0. When the instrument is then operated at low V/L, this can create a significant potential for error in reported VPCRx. While the pressure measurement may be technically accurate, the V/L reported with that pressure may be misrepresented due to errors in starting V and L. For large V/L (=4), this effect becomes reduced or irrelevant because the relative error in reported V/L diminishes significantly with V/L > 1.

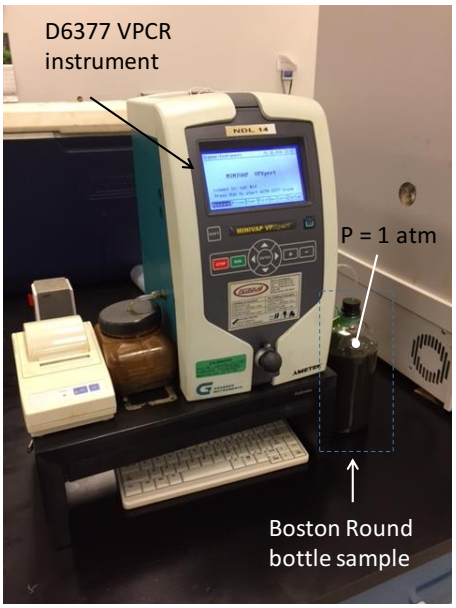

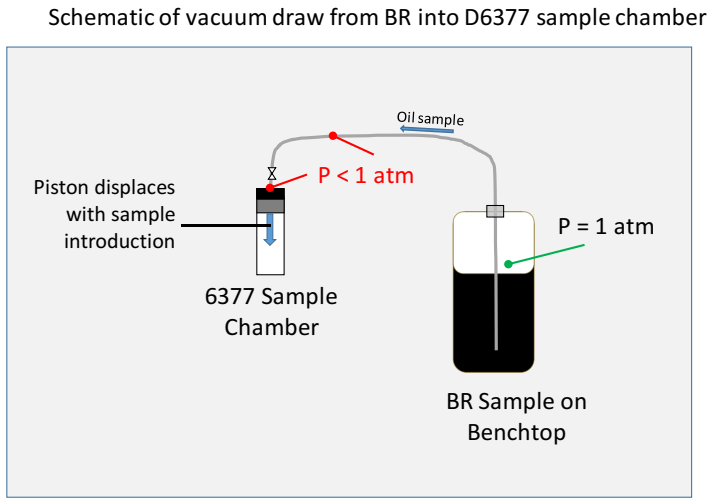

Figure 4-15. Montage of photo and schematic illustrating how BR samples are introduced into the 6377 instrument using vacuum draw. Photo provided with permission from Intertek.

The reader should be reminded that ASTM D6377-16 section 12.1.4, reads "For measurements with V/L ratios < 1, the sample may not be exposed to the atmosphere and shall be contained in a floating piston cylinder. The sample introduction temperature of the measuring chamber shall be equal to the measuring temperature to avoid and influence due to sample expansion." Note that running BR samples straight from the bottle at V/L < 1 represents a departure from section 12.1.4 methods. The BRMPC transfer, however, allows for the sample collected in BR to be run under pressure as shown in Figure 4-13. Both BR and BRMPC sample transfer options were explored in this study.

4.3.1.6 Additional sample handling notes

Regarding BR sample handling on the benchtop, both Labs 2 and 3 reported gently rolling the BR sample to ensure a homogeneous sample prior to inserting a rubber stopper with the sample draw tubing passing through (see Figure 4-15 above for illustration).

Labs 2 and 3 provided the following data shown in Table 4-5 on laboratory ambient conditions pertinent to the VPCR testing results reported in Sections 5.2 and 5.4.

Table 4-5. Laboratory ambient conditions reported for labs 2 and 3 during the 6377 VPCR measurements.

Lab 2						
Date	Sample Source	Comments	Temperature	Pressure	Temperature	Pressure
		6377	[deg F]	[psia]	[deg C]	[kPa]
10/4/2016	ND	Ambeint fill/measure	68	14.5	20	100
10/5/2016	ND	Ambient fill/100F & 122F measure	68	14.6	20	101
10/20/2016	TX	Ambient fill/measure & 100F measure	68	14.9	20	103
10/21/2016	TX	Ambeint fill/122F measure	68	14.7	20	101
Lab 3						
Date	Sample Source	Comments	Temperature	Pressure	Temperature	Pressure
		6377	[deg F]	[psia]	[deg C]	[kPa]
10/18/2016	ND	VPCRx data	72.5	13.5	22.5	93.34
10/19/2016	ND	VPCRx data	72.0	13.6	22.2	94.03
10/20/2016	ND	VPCRx data	71.8	13.5	22.1	92.92
10/21/2016	ND	VPCRx data	71.8	13.5	22.1	93.25
10/24/2016	ND	VPCRx data	71.8	13.6	22.1	93.86
10/25/2016	ND/TX	VPCRx data	72.5	13.5	22.5	93.37
10/26/2016	ND/TX	VPCRx data	71.8	13.6	22.1	93.65
11/1/2016	ND/TX	VPCRx data	71.4	13.4	21.9	92.71
11/2/2006	ND/TX	VPCRx data	68.7	13.5	20.4	93.24
11/16/2016	ND/TX	VPCRx data	71.6	13.5	22	92.84
11/17/2016	ND/TX	VPCRx data	72.3	13.7	22.4	94.27

4.3.1.7 Manual vapor pressure by ASTM D7975

The manual vapor pressure tester method was applied on each sampling day for the ND Bakken and TX Eagle Ford sampling events. The instrument takes a vapor pressure measurement (VPCRx-F(T)) on a liquid sample in the field at a known (though not necessarily controlled) temperature by use of a hand-operated piston-cylinder device. Two nominal expansion ratios were tested in this work, namely V/L = 0.25 and 4.0. These V/L values bound the suitability range of the ASTM D7975 standard and are specifically addressed in the calibration process and repeatability discussion. Reported temperature for each VPCRx–F(T) measurement was obtained with a handheld infrared temperature gun focused on the outer shell of the test cylinder. The 7975 sampler is connected to the crude source through a flexible sampling hose, and the vapor pressure is measured in the sampling cylinder without further transfer. As such, the method is effectively "tight-line" and not subject to the set of handling variables that are introduced when a sample is disconnected from the source line, transported to the lab, stored, and then re-connected to the analytical equipment.

Lab 3 ran a set of comparison D6377 runs at nominal V/L = 0.25 at 86°F (30°C) on closed capture spot samples for close comparison with the D7975 runs. Two replicate samples were captured for each of the 4 sample types.

Cylinder dead volume calculations per section 10 of ASTM D7975 were applied to each manual test instrument, and V/L values that appear in section 5.15 represent the calibrated V/L.

4.3.2 Physical Properties

Selected physical properties were measured for samples obtained by each sampling method as follows:

- Average molecular weight (MW) by freezing point depression
- Relative density (RD) at 60, 100, 122°F by ASTM D5002-13, Standard Test Method for Density and Relative Density of Crude Oils by Digital Density Analyzer (ASTM 2013a)
- Kinematic Viscosity by ASTM D7042, Standard Test Method for Dynamic Viscosity and Density of Liquids by Stabinger Viscometer (and the Calculation of Kinematic Viscosity) (ASTM 2014e) at 68 and 100°F (20 and 37.8°C)
- Flashpoint by ASTM D56-16a, Standard Method for Flash Point by Tag Closed Cup Tester (ASTM 2016e)
- Initial boiling point by ASTM D86, Standard Test Method for Distillation of Petroleum Products and Liquid Fuels at Atmospheric Pressure (ASTM 2016d)
- Sulfur weight % by ASTM D4294 Standard Test Method for Sulfur in Petroleum and Petroleum products by Energy Dispersive X-Ray Fluorescence Spectrometry (ASTM 2016f)

Measurements for basic physical properties were generally taken in duplicate and these successive runs were compared with repeatability standards associated with the published method. If the repeatability standard was met, an average for the duplicate measurements was reported.

4.3.2.1 Calculated IBP

Wispinski, Prefontaine et al. (Wispinski, Prefontaine et al. 2016) defines two distinct methods for estimating initial boiling point (IBP) – by distillation (ASTM D86) and by gas chromatography (ASTM D7169). In ASTM D86 distillation (ASTM 2016d), IBP is the corrected temperature at the instant the first drop of condensate falls from the condenser tube. ASTM D7169-16 (ASTM 2016a) is a standard test method for boiling point distribution by high temperature gas chromatography. It defines IBP as the temperature corresponding to an accumulated 0.5% of the total area of the eluted sample. For this study, a calculated IBP was determined from merged (discrete) whole oil carbon number reports provided by each participating lab using a method similar to the D7169 definition. Mass% for hydrocarbons C1 –Cn was summed until the cumulative mass exceeded 0.5%. IBP was the boiling temperature for the corresponding hydrocarbon.

4.3.3 High Temperature PVT Test Cell Experiments

Pressure-volume-temperature (PVT) data for the crude oils were required in order to supply rupture disc specifications for upcoming crude oil fireball tests that will be addressed in a future report. Specifically, vapor pressure for a closed crude oil system starting with 40% liquid, 60% vapor (by volume with no air) at ambient temperature (68°F, 20°C) was needed for a temperature range from ambient up to 662°F (350°C).

A laboratory-scale PVT test system was configured as illustrated in Figure 4-16. The pressure vessel was a stainless steel cylinder rated to 2750 psig (19.0 MPa) at 752°F (400°C). Operating conditions extended up to 1500 psig (10.3 MPa) and 752°F (400°C). A water/fuel inlet was located

at the top of the cylinder, and a drain was located at the bottom of the cylinder. A 2000 psig (13.8 MPa) pressure relief valve was connected near the top of the cylinder. The pressure vessel was housed inside a heater capable of reaching at least 752°F (400°C).

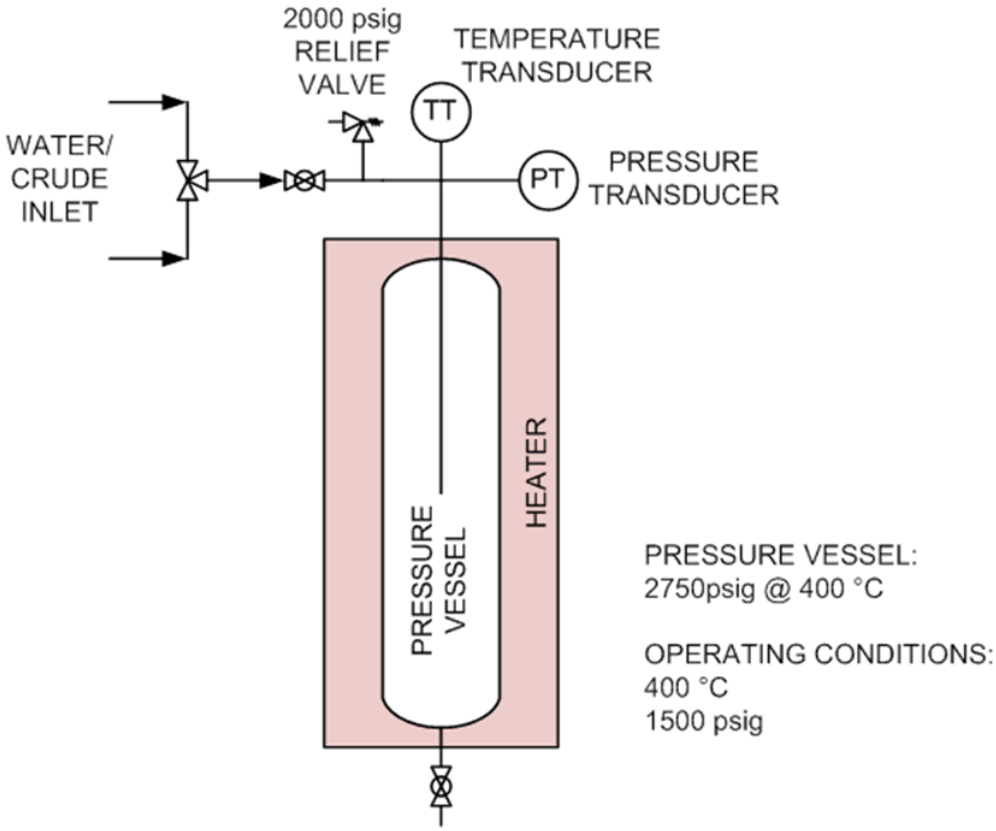

Figure 4-16. Conceptual diagram of crude oil pressure-temperature test system used in current study.

A photograph of the test system is presented in Figure 4-17 showing the test cell inside the clamshell heater. Another photograph showing the valves and instrumentation hookups is presented in Figure 4-18.

Figure 4-17. Photograph of PVT cell inside clamshell heater, reproduced with permission from University of North Dakota EERC.

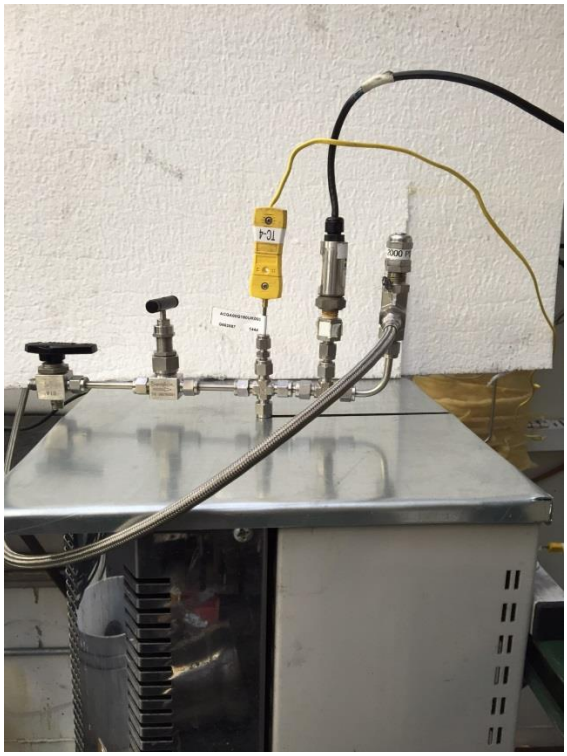

Figure 4-18. Photograph of valves and instrumentation hookups above the clamshell heater. Left to right: fill valve, needle valve, thermocouple, pressure transducer, pressure relief valve. Photo reproduced with permission from University of North Dakota EERC.

4.3.3.1 Sample introduction

The test requires that only a fixed mass of fuel (liquid + vapor) occupy the PVT cell volume at all times during the test. Fill procedure therefore used a water displacement method designed after industry standard GPA 2174 "Obtaining Liquid Hydrocarbon Samples for Analysis by Gas Chromatography," section 5.3 "Partial Water Displacement" (GPA 2014), with slight modifications. The cell was initially filled with water which was displaced out the bottom drain, drawing in liquid fuel to 40% of the cell by volume. Water was then completely drained from the cell leaving 60% volume occupied by fuel vapor on top of the 40% liquid volume of fuel.

4.3.3.2 Heating cycle

Once the PVT cell was shut in with 40% liquid, 60% vapor by volume, the temperature was increased from 75°F (24°C) to 572°F (300°C) over a period of about 8 hours. Cooling back to 30°C was then allowed over a time period of about 17 hours. Pressure and temperature were monitored throughout the entire period and reported at 15-second increments.

4.3.4 Pressurized Compositional Analysis

Samples were analyzed for composition using commercially available methods for the purposes of (i) defining a whole oil composition that can be compared directly with other oils and (ii) serving as input to equation of state models for simulating physical properties, most importantly for simulating vapor-liquid equilibrium conditions that can be compared with measured VPCRx(T) for the same source material and pressure-temperature curves at a fixed mass and V/L.

Determining the composition of crude oil requires an understanding of the complexity of the source material, the intended use of the compositional data obtained, and the capabilities, limitations, and costs of the analytical methods that are available in the marketplace. During the market survey stage of this work, it became apparent that the analytical basis for generating a whole oil composition suitable for use in this study would actually require a combination of several methods with a numerical merge step that could ultimately be packaged as a commercial product. The basic reason for multiple steps is that the light gases with low boiling temperatures require different analytical methods and handling than the heavier components with higher boiling temperatures. In many cases, the physical properties of materials on one end of the boiling point spectrum were incompatible with the analytical instruments designed for the other, and physical separation of the parent material was required to prevent the incompatible material from contacting the sensitive equipment. In the end, the data are re-constructed to create a "whole oil" that can be used to model behavior pressure-volume temperature behavior and associated physical properties.

Methods utilized in this study included:

(i) TM1(BPP): Bubblepoint pressure flash gas measurement, unpressurized C30+ measurement, and recombination to whole oil (section 4.3.4.2).

(ii) TM1(GOR): Gas-oil ratio (at 100°F and local atmospheric pressure) single stage flash gas measurement, unpressurized C30+ measurement, and recombination to whole oil (section 4.3.4.3).

(iii) TM2: Pressurized GPA 2177 GC, unpressurized ASTM D7900, and ASTM D7169 with numerical merge (section 4.3.4.4).

(iv) TM3: Gas-oil ratio single-stage flash gas measurement, pressurized ASTM D8003, unpressurized ASTM D7169 with numerical recombination to whole oil (section 4.3.4.5).

(v) TM4: Pressurized GPA 2103M with physical shrink and unpressurized ASTM D2887M with numerical recombination to whole oil (section 4.3.4.6).

(vi) TM4a: Pressurized GPA 2103M with physical shrink and C7+ analysis by unpressurized C30+ GC method. This implementation of GPA 2103 uses a different heavy-end analysis and numerical merge than TM4 (section 4.3.4.7).

4.3.4.1 Listing of standard methods utilized for compositional analyses in the current work

- ASTM D2887-16a, Standard Test Method for Boiling Range Distribution of Petroleum Fractions by Gas Chromatography ASTM (2016b)
- ASTM D8003-15, Standard Test Method for Determination of Light Hydrocarbons and Cut Point Intervals in Live Crude Oil and Condensates by Gas Chromatography (ASTM 2015b)

- ASTM D7169-11, Standard Test Method for Boiling Point Distribution of Samples with Residues Such as Crude Oils and Atmospheric and Vacuum Residues by High Temperature Gas Chromatography (ASTM 2011)
- ASTM D7900, Standard Test Method for Determination of Light Hydrocarbons in Stabilized Crude Oils by Gas Chromatography (ASTM 2013c)
- GPA 2103-03, Tentative Method for the Analysis of Natural Gas Condensate Mixtures Containing Nitrogen and Carbon Dioxide by Gas Chromatography (GPA 2003)
- GPA 2177-13, Analysis of Natural Gas Liquid Mixtures Containing Nitrogen and Carbon Dioxide by Gas Chromatography (GPA 2013)

Some comments on applicable ranges of the two above mentioned pressurized GPA methods are warranted. Both are capable of measuring the same set of compositions that are of interest in the current work, but their applicable concentration ranges vary significantly (see Table 4-6). GPA 2177 is designed for analysis of natural gas liquids and cannot handle C7+ concentration greater than 5 mole%, which precludes all of the whole oils to be analyzed in this study. The closely-related GPA 2103 is designed for natural gas condensate mixtures, which implies potentially much more C7+, up to 80% as indicated in the allowable ranges given in the standard, and is better suited for the current work. The two methods are linked in that the 2103 utilizes the 2177 for its pressurized N2, CO2, and C1-C6 GC analysis, and then performs a distillation and physical property measurements to ultimately quantify the C7+ in the whole oil. The 2103 utilizes a pre-cut column to separate the C7+ from the lighter components. N2, CO2, and C1-nC6 are sent to an analytical column while the C7+ is sent to vent. The C7+ fraction is determined separately by physically measuring its volume.

Table 4-6. Allowable concentration ranges for GPA 2103 and GPA 2177.

Components	Concentration Ranges Allowed (mole%)	
	GPA 2103	GPA 2177
Nitrogen	0.01 – 5.0	0.01 – 5.0
Carbon Dioxide	0.01 – 5.0	0.01 – 5.0
Methane	0.01 – 40.0	0.01 – 5.0
Ethane	0.01 – 15.0	0.01 – 95.0
Propane	0.01 – 15.0	0.01 – 100.0
Iso-butane	0.01 – 15.0	0.01 – 100.0
n-Butane and 2,2-Dimethylpropane	0.01 – 15.0	0.01 – 100.0
Iso-pentane	0.01 – 15.0	0.01 – 15.0
n-pentane	0.01 – 15.0	0.01 – 15.0
2,2-Dimethylbutane, 2,3-Dimethylbutane, and 2-Methylpentane, 3-Methylpentane, Cyclopentane, n-Hexane	0.01 – 50.0	0.01 – 15.0
Heptanes and heavier	5.0 – 80.0	0.01 – 5.0

4.3.4.2 TM1(BPP): Bubblepoint pressure flash gas analysis with C30+ and numerical recombination

The bubblepoint pressure flash gas analysis utilizes the TVP-95 single-stage flash separator (Alapati, Sonnier et al. 1997) as described previously in 4.1.2.1 to create a vapor bubble and a liquid stream near equilibrium conditions at a set point temperature of T = 100°F (37.8°C). A schematic is shown in Figure 4-19. Note that a measurement at the incipient bubblepoint requires collection and analysis of an infinitely small volume of saturated vapor in equilibrium with a liquid, which is not practical from an analytical perspective. The TVP-95 creates a practical alternative by forming a mL-scale vapor space in a liter-scale separator through which many unit volumes of fresh crude oil is passed until a steady vapor pressure is observed while maintaining constant feed rate and liquid-vapor level control. Once this steady pressure has been observed for about an hour, a vapor sample is drawn from the top of the separator and passed through heat-traced lines to the GC for analysis, which yields mole% for the 26 components listed in Table 4-7 .

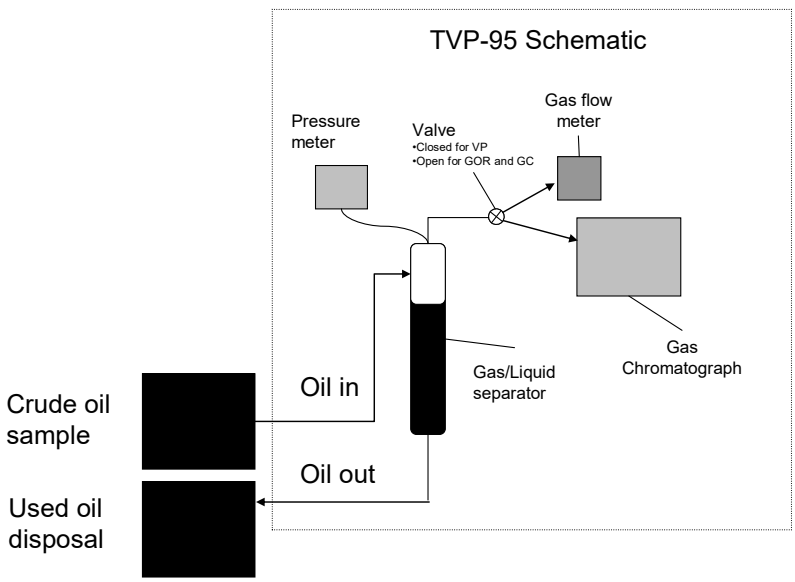

Figure 4-19. Schematic of the TVP-95 instrument system used to evaluate bubblepoint pressure, gas-oil ratio, and associated flash gas compositions.

Table 4-7. Component list analyzed by TVP-95.

Nitrogen	N-Butane	Methylcyclohexane
Carbon Dioxide	Iso-Pentane	Toluene
Argon	N-Pentane	Iso-Octane
Oxygen	Iso-Hexanes	Octanes
Hydrogen Sulfide	N-Hexane	Ethyl Benzene
Methane	Methylcyclopentane	Xylenes
Ethane	Benzene	Nonanes
Propane	Cyclohexane	Decane Plus
Iso-Butane	Heptanes	

The compositional data listed in Table 4-7 are then processed by an in-house equation of state model, the Sandia EOS Solver, along with inputs including separator pressure, vapor-liquid ratio (= 0 for bubblepoint), flash temperature, average MW and RD for the oil. The Sandia Solver uses a successive substitution routine that adjusts a C8+ hypo group mole% and re-normalizes the light ends and fixed gas mole% to ultimately yield a whole oil composition that exhibits the bubblepoint pressure observed in the TVP-95 flash separator. Applications of the Sandia EOS Solver to the US Strategic Petroleum Reserve program are given in several public reports (Lott 1996; Hinkebein 2003; Lord and Rudeen 2010).

An additional unpressurized compositional analysis is run on source to build the heavy ends profile for components with carbon numbers above C9. The material for this sample is collected in a glass jar at atmospheric conditions (see reference to this step in section 4.1.2.1 above) from a sampling port on the feed line going into the TVP-95 separator. This material is therefore assumed stabilized with the local atmospheric conditions and processed by a combination of unpressurized gas chromatography by ASTM D7900 and ASTM D7169 with modifications. The operator considers the modifications proprietary so additional procedural details are unavailable.

4.3.4.3 TM1(GOR): GOR flash gas analysis with C30+ and numerical recombination

The gas-oil ratio (GOR) flash gas analysis utilizes the TVP-95 flash separator operated in a steady-state flowing mode for both liquid and vapor, with temperature set at 100°F and pressure set to local atmospheric. Flowrate and residence time in the separator were designed to provide a near-equilibrium condition for oils typically tested at the Strategic Petroleum Reserve (gas-oil ratio at T = 100°F and P = 14.7 psia from 0.2 – 20 scf/bbl (0.036 – 3.6 m^3/m^3)). Vapor and liquid volumetric flow rates are monitored, and once steady conditions have been observed for about an hour, a 5-minute average V/L flowrate is captured and a vapor sample is drawn from the top of the separator and passed through heat-traced lines to the GC for analysis, which yields mole% for the 26 components listed in Table 4-7.

The unpressurized C30+ analysis described above for TM1(BPP) is applied in the same manner for TM1(GOR).

4.3.4.4 TM2: GPA 2177, ASTM D7900, ASTM D7169 with numerical data merge

This test methodology combines three gas chromatograph runs with a numerical data merge to yield a single carbon number report. The method utilizes a pressurized GPA 2177 to capture the light gases through C6, then utilizes an unpressurized ASTM D7169 for a wide boiling point range analysis up to 1330°F (720°C) corresponding to about C100, and adds a second unpressurized GC run via ASTM D7900 to add resolution to the C4-C8 range where interferences in the D7169 may give unreliable separation. The process entails the following:

- Pressurized gas chromatographic (GC) analysis of N2, CO2, C1-C6 components using GPA 2177-13
- Unpressurized GC analysis of C2-C9 using ASTM D7900
- Unpressurized GC analysis of ~C5-C100 using ASTM D7169. For the current application, carbon numbers C30 and above are lumped into a single C30+ hypo group.
- Numerical data merge for a carbon number report
- Associated RD, MW will result from EOS calculation using whole oil model

4.3.4.5 TM3: ASTM D8003-15 with GOR flash and ASTM D7169 analysis

This test methodology combines three gas chromatograph runs with a numerical data merge to yield a single carbon number report. The method utilized atmospheric GOR flash to capture the light gases through C9, then utilizes a pressurized ASTM D8003 for C1-C25+ and adds an unpressurized ASTM D7169 for a wide boiling range analysis up to 1330°F (720°C) to about C100. The ASTM D8003 and D7169 data sets are merged at C9, eliminating the bias of D7169 in the light boiling component composition. To produce a whole oil composition from N2 to C25+, the flashed gas composition from the GOR analysis is merged with ASTM D8003 and ASTM D7169 results.

The process entails the following:

- Pressurized gas chromatographic (GC) analysis of the GOR flashed gas, CO, CO2, H2S, He, H2, O2, N2 and C1-C9
- Pressurized GC analysis of C1-C24 using ASTM D8300
- Unpressurized GC analysis of ~C5-C100 using ASTM D7169. For the current application, carbon numbers C25 and above is lumped into a single C25+ hypo group.
- Numerical data merge for a carbon number report (N2 – C30+)

4.3.4.6 TM4: GPA 2103M with physical shrink and ASTM D2887 C7+ analysis

This test methodology combines gas chromatography with physical property analysis and numerical recombination to yield a whole oil with components to include combined N2 andO2, CO2, carbon number, and major isomers from C1-C29 with a lumped C30+. The process entails several analytical steps as follows:

- Pressurized gas chromatographic (GC) analysis of combined N2 and O2, CO2, C1-C5 components using GPA 2177-13.
- Physical liquid volume measurement of C6+ fraction by combination of physical shrink experiment on whole oil at controlled temperature and lab atmospheric pressure followed by an ASTM D2001 distillation to T = 107°F. Subsequent modified ASTM D86 distillation to provide C6-C10 fraction at T = 385°F and C11+ residual
- Physical property measurements of stabilized C6+, C6-C10, and C11+ fractions for average MW by freezing point depression and RD by ASTM D5002-13
- Unpressurized GC analyses of the C6-C10 (by flame ionization detector) by GPA 2186-M and C6+ fractions (by flame ionization detector) by ASTM D2887M
- Numerical data merge using GC and physical properties data to a single whole oil carbon number (N2 – C30+) report with computed total MW and RD

4.3.4.7 TM4a: GPA 2103M with physical shrink and C7+ analysis by unpressurized C30+ GC analysis

This test methodology combines gas chromatography with physical property analysis and numerical recombination to yield a whole oil with components to include N2, CO2, carbon number, and major isomers from C1-C29 with a lumped C30+. This implementation of GPA 2103M utilizes unpressurized physical separation processes for the C7+ components that are distinct from TM4, and is therefore referred to as TM4a.

The process entails several analytical steps as follows:

- Pressurized gas chromatographic (GC) analysis of N2, CO2, C1-C6 components using GPA 2177-13
- Physical liquid volume measurement of C7+ fraction by combination of physical shrink experiment on whole oil at controlled temperature and lab atmospheric pressure followed by distillation to T = 180°F. (using ASTM D1160)
- Physical property measurements of stabilized C7+, for average MW by freezing point depression and RD by ASTM D4052
- Analyses of the C7+ by unpressurized C30+ GC method (different method than TM4).
- Numerical data merge using GC and physical properties data to a single whole oil carbon number (N2 - C30+) report with computed total MW and RD (different method than TM4).

4.4 Analytical Methods – Winter Samples

Samples collected within the winter sampling event were analyzed for vapor pressure, sulfur (ASTM D4294) , and composition.

4.4.1 Open BR Sample Transfer

Open bottle samples collected by ASTM D4057 at ambient temperature were handled in two ways:

- BR1: Samples were not transferred to an MPC for VPCR analysis, nor were they kept refrigerated. These samples were maintained at ambient conditions and introduced to the vapor pressure instrument by vacuum induction.
- BR*n*MPC: Samples were transferred to an MPC to facilitate positive pressure sample push into the VPCR analyzer.

Open bottle samples collected by BR2 or BR3 chilled methods (and some by BR1 for compositional analysis) were transferred to a manual piston cylinder (MPC) for pressurized injection into analytical devices. BR2 and BR3 samples were kept refrigerated up to the point they were transferred into the MPC. The combined BR sampling and MPC sample transfer techniques will be identified in the remainder of the report as BR1MPC, BR2MPC and BR3MPC. BR1 will be used for the atmospheric drawn BR.

4.4.2 Vapor Pressure Analysis, VPCRx(T)

Vapor pressure measurements were performed using ASTM D6377-16M (ASTM 2016c) and included a series of pressure-expansion points at T = 100°F (37.8°C). All samples injected into the 6377 instrument from MPC were analyzed for vapor pressure using the temperature and expansion points summarized in Table 4-8. The open bottle samples collected by ASTM D4057 at ambient conditions (BR1) without further sample transfer were only analyzed at V/L = 1.5 and 4.0 (consistent with guidance in ASTM D6377-16, section 12.1.4).

Table 4-8. Temperature and expansion settings for ASTM D6377 VPCRx(T) measurements.

Temperature		Expansion Ratio (x)					
(°F)	(°C)	V/L	V/L	V/L	V/L	V/L	V/L
100	37.8	0.05	0.1	0.2	0.5	1.5[1]	4.0[1]

[1] Vapor Pressure test conditions for D4057 open bottle (BR1), ambient temperature samples.

All samples collected by MPC and chilled open bottle methods were pre-conditioned to the test temperature prior to pressurized injection into the vapor pressure analyzer. The sample container, injection tubing, and all associated tubing and fittings were maintained at the test temperature. The sample injection temperature of the vapor pressure analyzer was set to the same temperature as the measurement temperature to prevent liquid thermal expansion within the analyzer and erroneously high vapor pressure readings. For D4057 ambient temperature open bottle samples, no pre-conditioning was performed.

The vapor pressure instrument settings for equilibration time and rate of change were configured according to the parameters listed in Table 4-9. These equilibration time and rate-of-change settings were informed by the study authors' field experience using a 6377 instrument on oils at the US Strategic Petroleum Reserve. The objective of these settings is to assure that the pressure transients associated with instrument operation settle out and the recorded pressure is representative of thermodynamic equilibrium at set point V/L and temperature. The "M" modifier on the ASTM D6377 test method refers specifically to the equilibrium criteria described in Table 4-9 and the temperature conditioning of the test fluid as described for summer samples. All 6377 VPCR measurements were performed in duplicate as successive runs, and reported as separate values to Sandia.

Table 4-9. Instrument settings "Equilibrium Time" and "Equilibrium dP/dt" used for all vapor pressure samples.

V/L	Minimum Equilibration Time (sec)	Equilibration dP/dt (kPa/min)
0.05	1200	0.2
0.10	1000	0.2
0.20	900	0.2
0.50	600	0.15
1.5	500	0.1
4.0	300	0.1

4.4.2.1 Pressurized Compositional Analysis

Compositional analysis conducted on winter samples was performed by GPA-2103M (GPA 2003) with physical shrink and unpressurized ASTM D2887-M (ASTM 2016b) with numerical recombination to whole oil. This method is identified at Test Method 4 (TM4). All compositional

analyses were sourced from ASTM D3700 FPC's. The source oil was transferred directly from the process line into the 3700 cylinder. As such, no transfer step was required in the lab.

4.5 Numerical Analysis

A commercially available, EOS based process simulation model (PSM) was used to generate EOS estimates of pressure- expansion curves (P vs. V/L) and P vs. T curves for a 40% filled closed tank (V/L=1.5) using whole oil composition data provided by each of the laboratories. EOS predicted expansion curves were compared to measured VPCRx data in order to validate EOS modeling in general and more specifically to evaluate the consistency between measured compositional and measured VPCRx data for a given oil. The P vs. T at V/L=1.5 predictions support combustion tests performed by SNL.

PSM - EOS modeling details include the following:

- Merged mole% component lists provided by TM2, 3 and 4 were used as is – no surrogates were generated and component breakdown was different for each lab.
- For TM1, the TVP-95 based whole oil (N2-C8+) and the separate C30+ analysis were merged by Sandia.
- The lab performing TM4a did not provide a merged mole% component list. They did, however, provide intermediate results for the GPA-2177 light-end, physical shrink and C30+ GC heavy-end analyses. Data from these analyses were merged by Sandia.
- C8 – C30+ hypo components were modeled using normal nC8-nC30 surrogates
- Soave Redlich Kwong (SRK) cubic EOS
- Default SRK binary interaction coefficients, BICs which are parameters within the EOS that "weight" the interaction between component pairs. BICs are used to improve the predictive capability of an EOS.
- Default component properties

The expansion curve model consisted of a series of streams with known vapor volume fraction, *vf*, corresponding to V/L = (0, 0.02, 0.05, 0.2, 0.5, 1.5, 4.0) and controlled by a PSM spreadsheet. The process works as follows:

- Initiate the process with stream 1 by inputting the whole oil composition, setting the temperature $T(1)$ = (68, 100 or 122°F) and setting the vapor mole fraction, $nf(1) = 0$
- The PSM-EOS returns BPP and initial oil density, $\rho(1)$
- For Stream $i = 2$ to n: $T(i) = T(1)$
- Since mass is fixed and volume (vf) is known, $\rho(i) = \rho(1) /(1+vf(i))$
- $nf(i)$ is adjusted until $\rho(\text{PSM-EOS}) = \rho(i)$
- PSM-EOS returns pressure, $P(vf(\text{i}))$

Note that the PSM model is a flowing system where mass, volume and moles are expressed as rates and assumes steady state flow and phase equilibrium.

P vs. *T* for a fixed mass/volume system was modelled similarly, except system density is fixed and temperature is varied by stream. Stream 1 initial vapor volume fraction, $vf(1)$, is set by user which establishes the fixed system density, ρ (1). For streams 2 to n, $nf(i)$ is adjusted to generate the target density at the specified temperature and the PSM-EOS returns the corresponding pressure.

4.6 Nomenclature for Experimental Results

Nomenclature for identifying VPCRx samples and analyses was developed as follows.

A sample ID is designated based on the following information:

- Analysis laboratory
- Crude origin
- Sample type
- Temperature
- Replicate

An example VPCRx sample ID is given below.

Example: LAB1-ND-FPC-68F-1

Laboratory-	Crude-	Sample-	Temperature-	Replicate
LAB1	ND	FPC	68F	1
LAB2	TX	MPC	100F	2
LAB3		WD	122F	3
LAB4		BR		4
		BRMPC		A
		FPC		EOS
		BPP		
		GOR		

Where acronyms are defined as follows:

ND	– North Dakota Bakken
TX	– Texas Eagle Ford
FPC	– Line filled floating piston cylinder
MPC	– Manual piston cylinder
WD	– Water displacement cylinder
BR	– Boston Round
BRMPC/BRFPC	– Boston Round transferred into MPC or manually transferred to FPC
BPP	– Lab 1 TVP-95 bubble point pressure test
GOR	– Lab 1 TVP-95 GOR test

Replicate Notes:

The replicate field has different meaning for different labs and data.

For Lab 1, the replicate field is used to denote sampling day. As such, 1 = day 1; 2 = day 2, etc.

For Lab 2, 1 and 2 generally indicate runs on separate aliquots of fluid from the same sample cylinder

For Lab 3 replicates 1 and 2 are single aliquots of fluid subjected to several V/L tests before ejection of sample; 3 and 4 represent a single aliquot at each V/L.

Two special suffix are also used – "A" for average (of replicates for example) and EOS for PSM-EOS estimates.

The following are used for compositional data:

TM1-TL – Tight-line to TVP-95 BPP and GOR tests (sections 4.3.4.2 and 4.3.4.3)

TM2 – GPA 2177, ASTM D7900 and ASTM D7169 (section 4.3.4.4)

TM3 – ASTM 8003-15 GOR, ASTM D7169 merge (Section 4.3.4.5)

TM4 – GPA 2103M, ASTM D2887 (section 4.3.4.6)

TM4a – GPA 2103M, C30+ unpressurized GC (section 4.3.4.7)

Summer/Winter Nomenclature:

S- and W- prefixes are used in data/curve labels to identify data from the original Task 2 Summer sampling and the Task 2A Winter sampling, respectively.

4.7 Repeatability and Reproducibility

"Repeatability" and "reproducibility" are useful terms employed later in this report describing laboratory test results. The following definitions appear in current ASTM standards:

<u>*Repeatability (r)*</u> – The difference between successive test results obtained by the same operator with the same apparatus under constant operating conditions on identical test material would, in the long run, in the normal and correct operation of the test method, exceed the values calculated as per the following equations only one case in twenty.

<u>*Reproducibility (R)*</u> – The difference between two single and independent results obtained by different operators working in different laboratories on identical material would, in the long run, in the normal and correct operation of the test method, exceed the following values only one case in twenty.

Values for each *r* and *R* depend upon a number of factors including the specifics of the test method, options within the test method, and concentration range of a measured parameter.

In ASTM Standardization News May/June 2009 Ullman offered some clarification on the calculation and interpretation of repeatability and reproducibility (Ullman 2009). The value of *r*, called the *repeatability interval* is found by multiplying the repeatability standard deviation by 2.8.

It is similar to the statistical estimate of 95% confidence interval for the difference between two readings. Similarly for the *R*, the *reproducibility interval*, which is the reproducibility standard deviation times 2.8. These assume that the data are normally distributed; that we are comparing only two independent reading and when the difference is greater than the interval there is only a 5% chance that is actually due to random chance, or conversely there is a 95% chance that it is due process differences.

In this report the following terminology will be used:

r_{std} and R_{std} – repeatability and reproducibility provided by the ASTM standard for the property under consideration.

2.8σ(property) – 2.8 times the standard deviation of the set of measured properties across labs for a given sample type or across sample types (not true reproducibility, but used here as a measure for sampling differences), used for comparison with R_{std}.

5 Experimental Results

5.1 Selected Physical Properties – Summer Samples

Selected physical properties data are shown in Table 5-1 for the Bakken and Eagle Ford summer samples collected in this study. Both oils are considered light (≥ 33°API), sweet (< 1 mass% total sulfur) crudes by API guidelines (API 2011). Kinematic viscosity for both oils is similar (2.0-3.4 mm^2/s) over the temperature range tested, and comparable to reference values for light sweet crudes that were offered to Sandia from producer data in the Bakken and Eagle Ford regions. All measured flashpoints were < 50°F (10°C). Initial boiling points by D86 distillation were similar between oils at 84 and 89 °F.

Table 5-1. Selected physical properties for Bakken and Eagle Ford oil samples.

Property	Method	Acronym	Units	ND Bakken		TX Eagle Ford	
				average	stdev	average	stdev
Relative Density at 60°F (15.6°C)	ASTM D5002	RD	-	0.8142	0.0016	0.7955	0.0039
API gravity at 60°F (15.6°C)	ASTM D5002	°API	°API	42.3	–	46.4	–
Total Sulfur	ASTM D4294	S	mass%	0.0863	0.0064	0.1147	0.0250
Avg Molecular Weight	Frz. pt. dep.	MW	g/mole	168.9	3.7	178.4	1.8
Kinematic Viscosity at 68°F (20°C)	ASTM D7042	ν_{20}	mm^2/s	2.726	0.121	3.449	0.394
Kinematic Viscosity at 100°F (37.8°C)	ASTM D7042	$\nu_{37.8}$	mm^2/s	2.085	0.124	2.552	0.098
Flashpoint	ASTM D56	FP	°F	< 50	–	< 50	–
Initial Boiling Point	ASTM D86	IBP	°F	84.1	0.8	89.4	1.6

5.1.1 Physical Properties by Sampling Method

Selected physical properties were examined according to sampling method and compared back to the overall sample mean, standard deviation, and reproducibility. Generally speaking, systematic dependencies on sampling method were not observed for the properties tested here.

5.1.1.1 Relative density by ASTM D5002

Results for relative density of crude by ASTM D5002 are summarized in Table 5-2 and Table 5-3 for the ND Bakken and TX Eagle Ford summer samples taken in this study, respectively. Average values across all sampling types are given for each temperature. Relative density decreases slightly with temperature rise due to liquid thermal expansion as expected. One exception to this is observed for the FPC sample at T = 122°F (50°C), for which RD increased relative to the colder measurement points, the reason for which is unclear. A complicating factor in the unpressurized ASTM D5002 method is that volatiles may be lost from the liquid phase with heating, so a slight distillation causing an increase in RD of the remaining liquid is likely taking effect at the same time the liquid is heated. The net effect may be competing thermal expansion decreasing RD with

distillation increasing RD. In any event, scanning across sampling methods, differences associated with method were very small and not deemed significant.

Table 5-2. Relative density at 60, 100 and 122°F (20, 37.8 and 50°C) for Bakken oil samples.

Bakken	Relative Density @60°F (20°C)	Relative Density @100°F (37.8°C)	Relative Density @122°F (50°C)
FPC	0.8145	0.8111	0.8163
MPC	0.8136	0.8129	0.8103
WD	0.8124	0.8072	0.8055
BR	0.8167	0.8112	0.8097
Avg	0.8143	0.8106	0.8105
R_{std}	0.0034	0.0033	0.0033

$R_{std} = 0.00412X$

Table 5-3. Relative density at 60, 100 and 122°F (20, 37.8 and 50°C) for Eagle Ford oil samples.

Eagle Ford	Relative Density @60°F (20°C)	Relative Density @100°F (37.8°C)	Relative Density @122°F (50°C)
FPC	0.7954	0.7785	0.7704
MPC	0.7953	0.7809	0.7747
WD	0.7999	0.7796	0.7722
BR	0.7975	0.7816	0.7765
BRMPC	0.8053	0.7831	0.7761
Avg	0.7990	0.7805	0.7733
Rstd	0.0033	0.0032	0.0032

$R_{std} = 0.00412X$

5.1.1.2 Mass% total sulfur by ASTM D4294

Mass% total sulfur (S) as determined from samples captured by five methods is shown in Table 5-4 for the ND Bakken sample, and in Table 5-5 for the TX Eagle Ford sample. In every instance measured here for the Bakken and Eagle Ford samples, mass% total sulfur falls well below the API 1% delineation point for sweet vs. sour (API 2011).

Measurements across methods were further compared against each other and the reproducibility (R_{std}) formula cited in ASTM D4294-16. The ND Bakken samples exhibited an average S = 0.086 % with 2.8σ = 0.018 %. This uncertainty band is slightly higher than the expected R at 0.015% but comparable enough to say that the performance observed in this study was consistent with that expected for the method. Upon reviewing the data in Table 5-4 for the ND Bakken samples, no significant dependency of S upon sampling method was observed.

The TX Eagle Ford samples shown in Table 5-5 exhibited an average S = 0.115 % with 2.8σ = 0.070 %, about 4x the expected R at 0.018%. The open samples BR and BRMPC exhibited higher

values for S (~0.14%) than any of the closed samples (0.09-0.1%) at a difference level that exceeds R = 0.018%. This suggests that sampling method (open vs. closed) may have a measurable influence on the measured S, though the finding is not consistent across the Bakken vs. Eagle Ford oils, nor it is significant enough to yield any difference in sweet vs. sour designation. The ASTM D4294-16 method Section 11: *Sampling* identifies Practice D4057 as appropriate for manual sample capture for sulfur testing, implying open sampling is acceptable. An additional statement in ASTM D4294-16 method Section 1.4 states, "*Volatile samples (such as high vapor pressure gasolines or light hydrocarbons) may not meet the stated precision because of selective loss of light materials during the analysis*." Between the two samples analyzed in this study, the single Bakken sample exhibited a higher vapor pressure than the single Eagle Ford sample, but showed no sensitivity in S measurement to open versus closed sampling.

Table 5-4. Mass% total sulfur by sampling method for ND Bakken samples.

Sample	D4294 Sulfur Mass%
FPC	0.0934
MPC	0.0874
WD	0.0758
BR	0.0867
BRMPC	0.0885
Avg	0.0863
R_{std}	0.015

$R_{std} = (1.9182\ ((X\ 10000)^{0.6446}))/10000$

Table 5-5. Mass% total sulfur by sampling method for TX Eagle Ford samples.

Sample	D4294 Sulfur Mass%
FPC	0.0862
MPC	0.1071
WD	0.0986
BR	0.1401
BRMPC	0.1415
Avg	0.115
R_{std}	0.018

$R_{std} = (1.9182\ ((X\ 10000)^{0.6446}))/10000$

5.1.1.3 Viscosity by ASTM D7042

Kinematic viscosity is reported in Table 5-6 for the ND Bakken and Table 5-7 for the TX Eagle Ford samples, listed by sampling type and temperature. Note dynamic viscosity may be computed

by dividing kinematic viscosity by density of the liquid. There was no consistent trending associated with open vs. closed sampling.

Table 5-6. Kinematic viscosity by sampling method for ND Bakken sample.

Bakken	D7042 Viscosity @68°F(20°C), mm^2/s	D7042 Viscosity @100°F(37.8°C), mm^2/s
FPC	2.7096	2.2178
MPC	2.6469	1.9578
WD	2.6944	2.1943
BR	2.6417	2.0955
BRMPC	2.9363	1.9619
Avg	2.7258	2.0855
R_{std}	0.016	0.012

R_{std} = 0.00584 X @ 40 °C

Table 5-7. Kinematic viscosity by sampling method for TX Eagle Ford sample.

Eagle Ford	D7042 Viscosity @68°F(20°C), mm^2/s	D7042 Viscosity @100°F(37.8°C), mm^2/s
FPC	3.2093	2.4617
MPC	3.1460	2.4787
WD	3.1826	2.5029
BR	3.6594	2.6535
BRMPC	4.0467	2.6635
Avg	3.4488	2.5521
R_{std}	0.020	0.015

5.1.1.4 Flashpoint by ASTM D56

Every instance of flashpoint measured in this study for both the ND Bakken and TX Eagle Ford oils, independent of sampling method, measured at < 50°F (10°C).

5.1.1.5 Initial boiling point (IBP)

A summary of IBP as determined by ASTM D86 distillation is given in Table 5-8. IBP temperatures all fall between 80-90 °F (27-32 °C). An alternative means to determine IBP via calculating the 0.5% mass eluted from gas chromatographic method was also determined and every instance of *calculated* IBP in this study for both the ND Bakken and TX Eagle Ford whole oils, independent of sampling method, measured at -44°F (-42°C). IBP by D86 distillation is subject to significant losses of light ends and fixed gases and is more accurately categorized as a process to find the lowest temperature at which re-condensation is observed.

Table 5-8. IBP by ASTM D86 for ND Bakken and TX Eagle Ford samples.

Sample	IBP, °F	
	ND-Bakken	TX Eagle Ford
FPC	83.2	90.6
MPC	85.1	90.0
WD	84.5	89.9
BR	83.6	87.1
Avg	84.1	89.4

5.2 Measured Vapor Pressure $VPCR_x(T)$ – ND Bakken Summer Samples

Average and 2σ values for VPCRx(T) are shown for the range of V/L values tested on the ND Bakken samples for three analysis temperatures 68, 100, and 122°F (20, 37.8, 50°C) in Figure 5-1 through Figure 5-3. The height of each colored bar represents the sample mean, and the error bars represent the 2σ associated with the sample set. The color of each bar represents a sampling method (FPC, MPC, etc.). VPCR samples were collected by three laboratories in the coordinated sampling event and analyzed by four laboratories. Each of the three collecting labs analyzed the samples that they collected, and one collecting lab sent samples to a fourth independent lab for analysis.

5.2.1 General Observations

A general feature seen in Figure 5-1 through Figure 5-3 and throughout this study is that VPCRx (with T = constant) increases as V/L decreases from 4.0 to 0.02, consistent with expectations for a crude oil that contains a range of components with different boiling points. Another general feature is that the variability in measured VPCR as quantified by the 2σ value (error bars), increases significantly as V/L decreases. This can also be illustrated by tabulating the coefficient-of-variation $C_v = 2\sigma/\text{mean}$ for each V/L and sampling method, as shown in Table 5-9. C_v increases notably, especially for closed methods, as V/L decreases. The FPC exhibits the highest C_v at low V/L, with MPC, WD, and BRMPC to a lesser degree in that order. The open BR stands apart from the rest in that it exhibits an effectively constant C_v (~0.14) across the entire V/L range tested. This does not necessarily imply that the BR method yields equally valid results at all V/L. Rather, there may be factors associated with the sample handling and induction into the 6377 instrument that help to bound the 2σ for this sampling type. This is discussed in more detail later in the report.

Table 5-9. Coefficient-of-Variation (C_v) for VPCRx(100°F) for the ND Bakken oil samples, grouped by V/L and sampling method.

Sample	V/L					
	0.02	0.05	0.2	0.5	1.5	4.0
LAB1-FPC*	-	0.05	0.03	0.02	0.00	0.00
Closed**	0.43	0.29	0.25	0.15	0.07	0.08
FPC	0.61	0.48	0.43	0.24	0.09	0.11
MPC	0.20	0.22	0.11	0.14	0.07	0.09
WD	0.15	0.09	0.08	0.05	0.03	0.06
BR	0.14	0.15	0.13	0.13	0.14	0.13
BRMPC	0.09	0.09	0.09	0.06	0.03	0.05

*Day-to-day variability for LAB1-FPC.

**Combines results from FPC, MPC, and WD sampling methods into one C_v.

The high 2σ values seen above are driven largely by a number of anomalously high VPCR values that are not normally distributed about the mean, and those are observed for the FPC samples more than in any other sampling method. The 6377 tests are not configured to allow for a direct compositional analysis of the same material that was introduced into the VPCR cell. As such, there is no direct analysis available to test for the exact reason why a given sample returned a high (or low) VPCR relative to others that were similarly sampled. Generally speaking, several cylinders are used to obtain spot samples in back-to-back succession from the sample source and handled using the same procedures. VPCR data shown here and some of the compositional data that are shown later in this report suggest that there are some high outlier cylinders that may be associated with notably more nitrogen/air that was seen on average from spot samples or in the "tight-line" sampling.

An alternate means to present the same data is shown in an overlay of expansion curves in Figure 5-4, where the x-axis is scaled to V/L. This provides physical significance to the x-axis, indicating that the VPCR increases more steeply as V/L decreases.

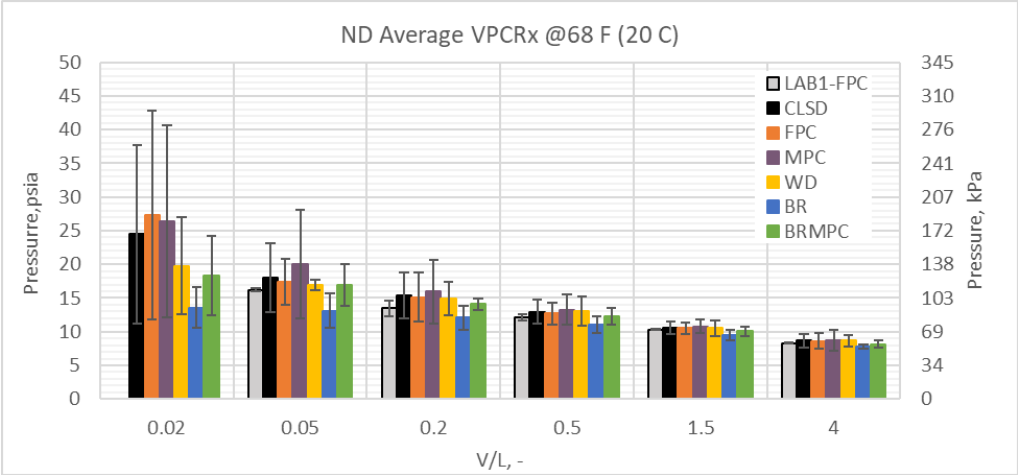

Figure 5-1. Bar chart showing average and 2σ VPCRx(68°F) for the ND Bakken oil sorted by V/L and sampling type.

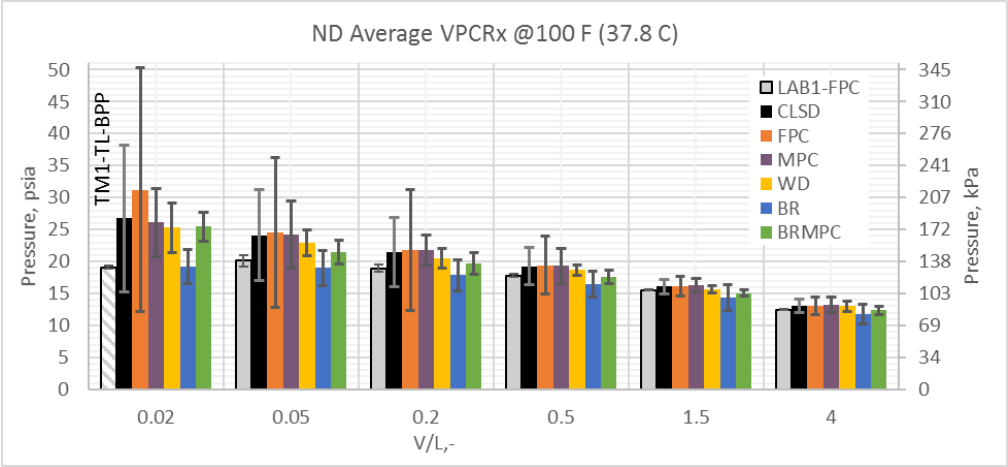

Figure 5-2. Bar chart showing average and 2σ VPCRx(100°F) for the ND Bakken oil sorted by V/L and sampling type.

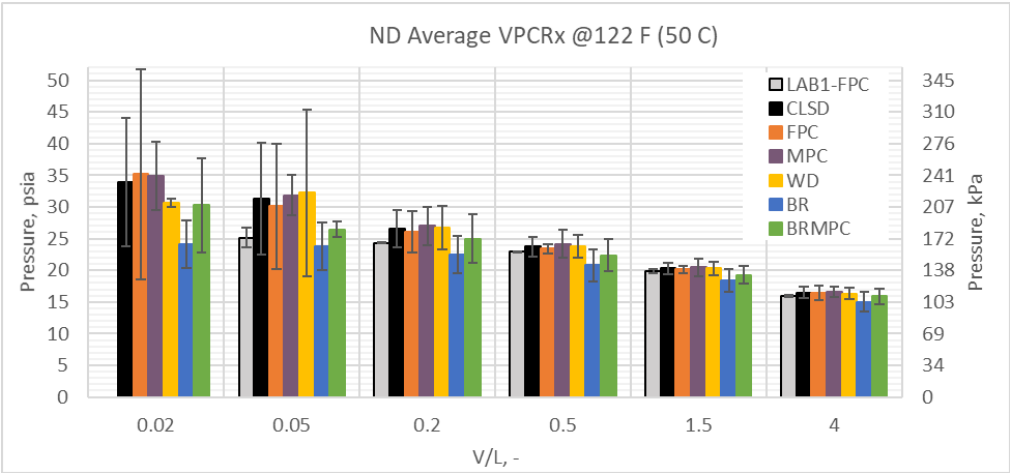

Figure 5-3. Bar chart showing average and 2σ VPCRx(122°F) for the ND Bakken oil sorted by V/L and sampling type.

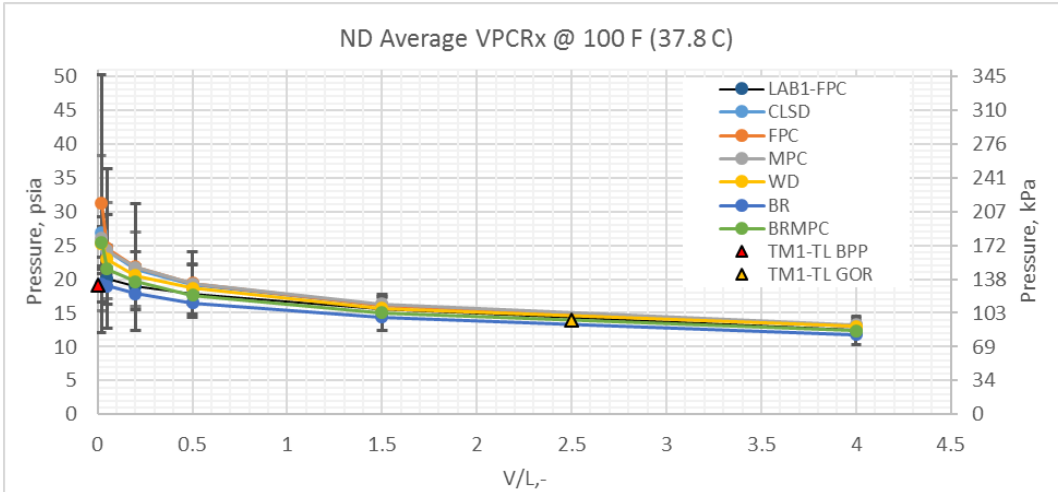

Figure 5-4. Expansion curves showing VPCRx(100°F) versus V/L for ND Bakken oil by sampling type.

5.2.2 Effects of Sampling Method on VPCRx

Effects of sampling method on VPCRx appear to depend in part on the V/L of interest. No significant sensitivity was revealed at high V/L, but increasing sensitivity was seen as V/L was reduced to 0.02. The authors caution that this observation is only applicable to the current samples that were stable at sampling conditions, and would in all likelihood not hold if the sample was a "live" crude that was prone to lose light ends and fixed gas due to active boiling at sampling or handling conditions prior to analysis. In the case of live crude, open vs. closed sampling method effects would likely extend to high V/L.

5.2.2.1 High V/L, x = 4.0 and 1.5

The highest V/L (x = 4) considered here showed no significant dependence on sampling method for the ND Bakken sample tested here. Similar performance was observed at V/L = 1.5. These conclusions stem from the observation that the 2σ error bars for all methods tested here overlap for x = 4.0 and 1.5.

5.2.2.2 Low V/L, x = 0.02 and 0.05

High variability in the x = 0.02 and 0.05 measurements shown in Figure 5-1 through Figure 5-3 make it difficult to establish whether the values reflect accurate property measurements of the base materials or artifacts of the sampling and/or analysis methodologies. Observed 2σ at x = 0.02 ranged from ~19 psi for the FPC to around 2-5 psi for the other capture methods, and was reduced slightly at x = 0.05, but when normalized by the mean values by converting to C_v, uncertainties were of the same magnitude at both V/L values.

Some discussion of the stated reproducibility (R_{std}) in the D6377 standard and the observed reproducibility interval of the current test data (2.8σ) may be useful here to understand how the magnitude of variances observed in this work compare to the expected performance of the standard method. When evaluating a pair of measurements on the same source material in the normal and correct execution of the test method, there is only a 5% chance that a difference greater than R_{std} is due to random chance, and not a difference in test method (Ullman 2009). While the current

VPCR data are not presented in a run-by-run manner to facilitate reader inspection, the authors can confirm instances of measurement pairs differing by more than R_{std} are common in this dataset. A more robust comparison may be implemented by reviewing Table 5-10, which shows the computed reproducibility intervals for the current data and compares those to the expected R_{std} published in the standard. Note that the current study examined many more V/L and temperature conditions than are covered by the published R_{std}, but the end members (V/L = 0.02, 4.0) are covered at T = 100°F and should provide a basis for comparison. The bottom rows show R_{std} for selected conditions of V/L = 0.02 and 4.0 for closed and open sampling. Compare these with the reproducibility intervals shown above for the various sampling types. In nearly every case observed, the 2.8σ is notably larger than the R_{std} for the associated V/L and sampling method. This implies that simple random chance is not the likely driver for the differences that Sandia is seeing, and differences in test method are a more likely explanation. Sandia is assuming that the parent crude oil sample material was reasonably homogeneous coming out of a given sampling location, as supported by the stable performance of the TVP-95 on-site at each sampling event. Test method from sample acquisition forward includes all the details of sample cylinder purge process and potential entrapment of gases that could affect the sample, any and all connections and disconnections to equipment in the field or in the lab, and details of sample introduction into the test equipment at the laboratory.

Table 5-10. Reproducibility Interval for measured VPCRx(100°F) for the ND Bakken oil samples, grouped by V/L and sampling method, compared with R_{std} from ASTM D6377.

ND Sample	V/L					
	0.02	0.05	0.2	0.5	1.5	4.0
LAB1-FPC*	0.40	1.27	0.83	0.42	0.08	0.08
Closed**	16.06	9.96	7.64	4.11	1.62	1.50
FPC	26.71	16.51	13.16	6.40	2.15	1.93
MPC	7.38	7.38	3.27	3.82	1.53	1.67
WD	5.45	2.93	2.22	1.22	0.74	1.18
BR	3.70	3.88	3.35	2.89	2.79	2.15
BRMPC	3.16	2.61	2.38	1.41	0.64	0.92
R_{std} FPC	2.94	–	–	–	–	0.62
R_{std} Nonpress.	–	–	–	–	–	0.76

*Day-to-day variability for LAB1-FPC

**Reproducibility across FPC, MPC, and WD closed sampling methods

The authors acknowledge that the above discussion on R_{std} vs. 2.8σ makes a statement that test method matters for VPCRx, which appears contradictory to the general conclusion made above in section 5.2.2.1 that VPCRx is insensitive to sampling method at V/L = 4.0 and 1.5. It is critical to understand that vapor pressure measurements are very sensitive to small sample-to-sample differences in gas content, and any process in the test method that adds or removes gases from the sample will introduce significant effects on vapor pressure, especially at V/L < 1.0. Sampling method is really only a subset of the test method – one component of a series of steps. As such, it

is plausible have a situation where results do not appear very sensitive to sampling method, but do ultimately show a strong dependence on overall test method.

Higher vapor pressures from a sample set are not necessarily a more accurate representation of the base material, as entrainment of gases from pressurized sources during sample acquisition, handling, and analysis may actually introduce small amounts of gas. Those are typically fixed gases that can have a significant effect on VPCR at small V/L with diminishing impact as V/L increases. This issue is discussed again in the compositional analysis sections 5.3 and 5.5 of this report.

Low V/L is inherently more sensitive to sample handling and inherent system tolerances than high V/L. As such, it is expected that low V/L will show lower repeatability and reproducibility than high V/L. Simply compare, in Table 5-10, the published R_{std} for FPC = 2.94 psi (20.3 kPa) for V/L = 0.02 with R_{std} = 0.62 psi (4.26 kPa) for V/L = 4. Factors such as loss of small amounts of light ends and fixed gases from the parent sample or entrainment of air or inert gas from sample handling will reveal themselves at the very low V/L, but will be nearly invisible at V/L = 4. Moreover, small uncertainty in 6377 piston sample chamber position inherent to the system can affect the true V/L by several orders of magnitude more at V/L = 0.02 than at 4.0.

The one sampling method that did appear to distinguish itself at low V/L was the BR open bottles with systematically lower VPCR than MPC and BRMPC for V/L = 0.02 and a trend of the same but to a lesser degree as V/L increases. Alternatively, when the BR samples (open capture in the field) were transferred into a MPC in the lab prior to introduction into the test cell (BRMPC) and pushed into the 6377 cell under positive gauge pressure, VPCRx at low V/L was maintained reasonably high and was comparable to all other closed methods. This observation suggests that the means of introducing the sample into the test cell was more influential on the measured VPCR than the original open capture process for these samples.

This pattern of observing low VPCR at low V/L in BR samples is evident across all three temperatures by reviewing Figure 5-1 through Figure 5-3. The authors hypothesize that these features were likely a result of the ambient fill method inherent to the BR method where the 6377 VPCR test cell was filled by vacuum draw (see the Methodology chapter for a detailed description). As the test cell was closed upon completion of fill, the pressure was fixed at a starting value of local ambient pressure or below. This is simply a function of ambient pressure in the laboratory and not a material property of the original sample. Recall ASTM D6377-16 section 12.1.4 instructs not to source VPCR measurements at V/L < 1 from BR samples, rather to use FPC. The data presented here indicate that working in this V/L range from BR samples may lead to inaccurate and/or inconsistent results. This effect is discussed further in section 5.2.5.

5.2.3 TVP-95 Vapor Pressure and Gas-Oil Ratio of ND Bakken

The TVP-95 mobile laboratory returned a vapor pressure near bubblepoint pressure (BPP) conditions at T = 100°F, and gas-oil ratio (GOR) with associated V/L at separator pressure (P) and T = 100°F as shown in Table 5-11. BPP and GOR values were stable on days 1 and 2, though the GOR was reduced on day 3. The operators noted a change in system pressure required to maintain flowrates on day 3 which may be correlated to a change in oil properties that is reflected in the lower GOR on day 3 than on days 1 and 2. BPP and GOR values shown below are also overlaid in Figure 5-4. The fact that the BPP and GOR values from the TVP-95 fall within the band of measurements from the D6377 method indicate reasonable agreement between analytical methods.

Table 5-11. Summary of TVP-95 measurements for ND Bakken crude oil. V/L was calculated from measured GOR, and P denotes separator pressure for GOR test.

Sample	BPP, psia	GOR, scf/bbl	V/L, –	P, psia
Day 1	19.0	12.4	2.5	14.0
Day 2	19.2	12.8	2.5	14.1
Day 3	19.2	9.7	2.0	13.7

The bubblepoint pressure (BPP) of a multicomponent liquid cannot be directly measured, but it can be inferred from where an extrapolation of the the pressure-V/L curve crosses the Y-axis at V/L = 0. BPP can also be inferred from the TVP-95 separator pressure when run with a small vapor headpsace that is closed to the atmosphere. A graphic showing the TVP-95 BPP overlaid with expansion curves for measured VPCRx(100°F) for the ND Bakken oil is shown in Figure 5-5. The TVP-95 BPP appears to sit at the lower end of measured values collected here. Discussion later in this report looks into the compositional differences that are associated with these vapor pressure differences. All of the curves converge as V/L increases to within about 1 psi.

There are several possible reasons why the TVP-95 BPP is lower than other measures:

- The tight-line process delivers a materially different sample to the separator chamber than any of the other sample capture methods.
- The fundamental property that the TVP-95 measures is a vapor pressure close to, but not technically equivalent to, the bubblepoint pressure. The vapor space in the TVP-95 is small relative to the liquid, but the effective V/L is greater than 0.
- The flowing TVP-95 configuration does not allow all of the vapor in the separator to contact all of the liquid that passed through and come to a true thermodynamic equilibrium.

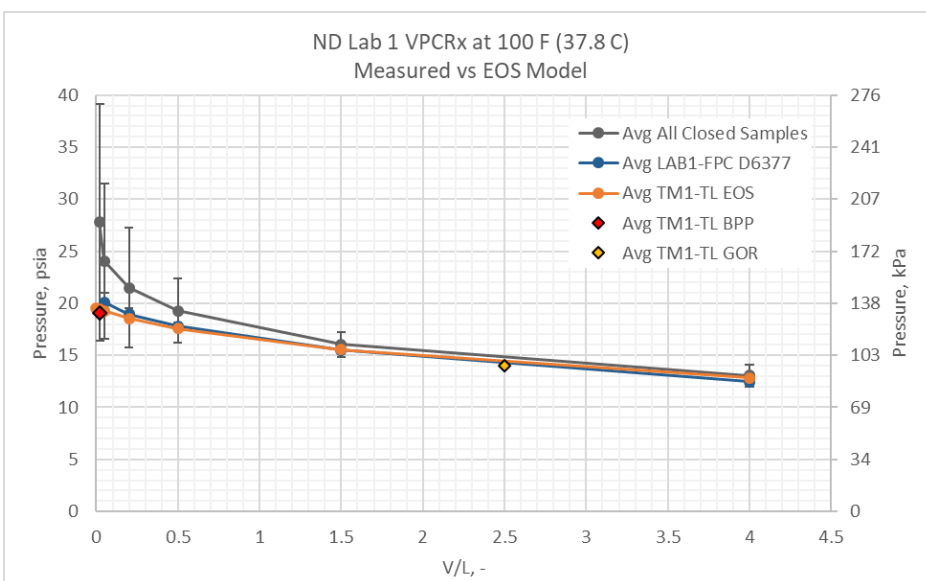

Figure 5-5. Averaged pressure-expansion curves for ND Bakken oil from ASTM D6377 measurements overlaid with TVP-95 BPP and GOR.

5.2.4 Homogenity of Sample from Day 1 – Day 3

The TVP-95 crew was on-site all three sampling days and ran separator tests as well as VPCR tests on all three days. The first two sampling days saw high repeatbility, and a slight downturn in VPCR was observed on Day 3. The TVP-95 operators also noted that the oil appeared to be getting heavier on day 3 than on the prior two days due to increased regulated pressure required to maintain flowrates the same as days 1 and 2. Recall all spot samples that were analyzed in the fixed labs were taken on days 1 and 2.

5.2.5 Ambient Fill VPCR Limit at 68°F – Local Atmospheric Pressure Effect

Some additional discussion is provided here pertaining to ambient fill effects from open bottles into the 6377 instrument. VPCRx(68°F) data obtained for BR and BRMPC sampling methods for the ND Bakken sample are re-plotted in Figure 5-6 relative to local atmospheric pressures in the two labs where they were processed in order to provide context. Lab 2 results are shown on the left half of the figure, and Lab 3 results are shown on the right half of the figure. Local atmospheric pressure was reported at 14.5 psia (100 kPa) in Lab 2 and 13.5 psia (93 kPa) in Lab 3 (reference Table 4-5) and both pressure levels are marked by red dashed lines in Figure 5-6. Plotting in this mannner highlights the differences in BR vs. BRMPC effects on VPCR. For both labs, note that VPCR for the BR never exceeds the red dashed line at atmospheric pressure, while VPCR for the BRMPC does for the lower V/L's. The authors believe that ambient fill VPCR is thus bounded by local atmospheric pressure, while true vapor pressure of the parent material may be significantly higher, as indicated by the BRMPC results.

Another observation here is that Lab 3 VPCRx(68°F) is routinely lower than for Lab 2 at every V/L, and there are at least two plausible explanations based on sample handling and local ambient conditions. First, Lab 3 reported a lower local atmospheric pressure than Lab 2 during handling and testing. As such, any procedure that exposed the subject crude oil to ambient pressure created potential for differential (albeit unintentional) conditioning of the oil to a vapor pressure of 14.5 psia (100 kPa) in Lab 2 and 13.5 psia (93 kPa) in Lab 3. This would likely reveal itself in subsequent VPCR testing, as it did in Figure 5-6. Also add that Lab 2 chilled all the BRMPC samples to 32°F prior to transfer from BR to MPC, while Lab 3 transferred at ambient temperature. This would tend to preserve more light ends and inroganic gases in the Lab 2 samples and maintain higher VPCR for the BRMPC relative to Lab 2, again visible in Figure 5-6 upon close inspection.

All of these observations reinforce the requirement for the utmost rigor in sample handling for vapor pressure measurements, as the source material in both of these labs was oil from the same pipeline source but looked measurably different according to sampling method and analysis location.

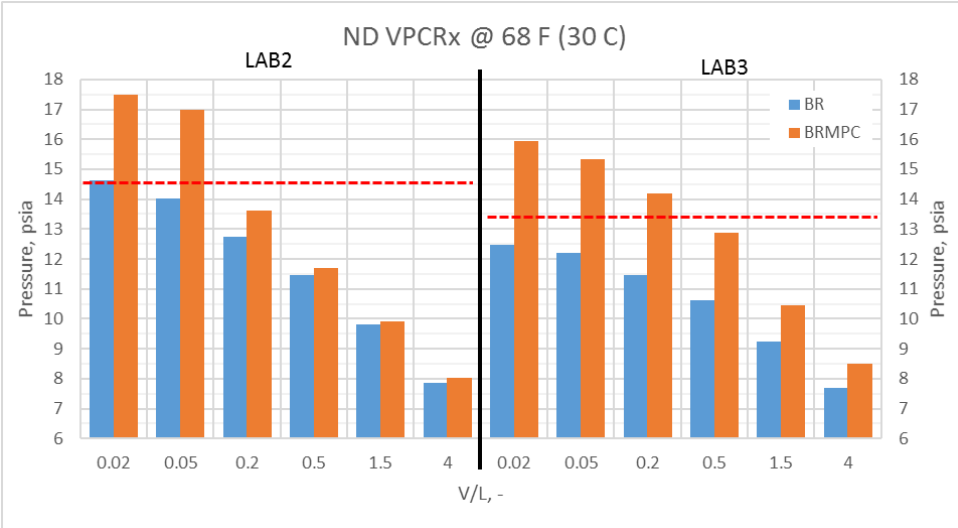

Note: Each bar is average of 2 replicates.

Figure 5-6. Illustration of effects of BR vacuum draw vs. positive pressure push BRMPC and local atmospheric pressure effects for ND Bakken oil on VPCRx(68°F) measured in Lab 2 and Lab 3.

5.2.6 Observations with Water Displacement (WD) Method

There was an isolated incident of $VPCR_{0.05}$(68°F) of a WD sample increasing by 10 psi (69 kPa) from before and after exposure to water used as a push fluid in lab operations. Analysis of that same push water in the D6377 instrument indicated that it had VPCR orders of magnitude higher than expected for pure water, and that it was likely saturated with helium gas since it was previously stored under helium at ~1000 psi (6.9 MPa). A workaround that was used moving forward was to couple the WD cylinder with an FPC that starts filled with unpressurized water connected directly to the WD cylinder and then uses house gas to pressurize the gas side of the FPC eliminating the concern of contaminating the hydrocarbon test sample.

5.2.7 Effects of No Pre-Conditioning on VPCRx(100°F) for x = 1.5, 4.0

All VPCR results for closed sampling methods reported elsewhere in this report utilized a temperature pre-conditioning protocol referenced in 4.3.1.3. One variant to this was explored where the lab ran as dictated by the ASTM D6377 standard by drawing the test fluid at lab ambient temperature, sealing the test cell, and heating to 100°F (37.8°C), which is effectively a "no pre-conditioning" case. Results are provided in Figure 5-7 showing side-by-side VPCRx data for pre-conditioning (no outline bars), and no pre-conditioning (black outline bars) at V/L = 1.5 and 4.0. Little effect of the temperature conditioning is observed for these cases. Greater effects would be expected for smaller V/L, but the 2016 version of the D6377 standard requires pre-conditioning for all V/L < 1 to mitigate possible liquid thermal expansion errors, so that low V/L case was not explored any further.

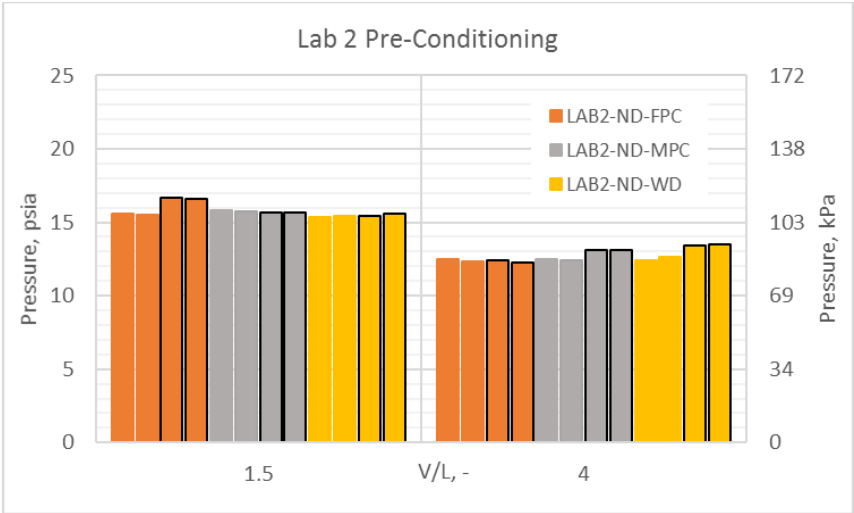

Note: 2 replicates: 1st pair, no outline - pre-conditioned; 2nd pair, black outline no pre-conditioning.

Figure 5-7. Effect of preconditioning on D6377 VPCRx by Lab 2 for ND Bakken oil.

5.3 Composition – ND Bakken Summer Samples

Compositional results from TM2, TM3, TM4 and TM4a for components N2 (ethane) through nC5 (n-pentane) mole fraction are compared against the baseline TM1-TL (TVP-95 system) on a component-by-component basis in following subsections. TM1-TL is fed exclusively by tight-line from the source pipeline to the instrument system and thus should show the least air contamination and light end loss. It is important to recognize that while the magnitude of the mole fraction for components N2-C1 is very small, the pure-component vapor pressures are very large, and as such, can have a large influence on the net vapor pressure of the whole oil, especially at low V/L. Higher carbon numbers (>C5) were measured and reported for each test method, but they have a negligible effect on vapor pressure at 100°F, and are addressed in a later section of the report. In addition to compositional results, EOS performance using the compositions is compared with average measured D6377 VPCR for all sample capture methods. In general, hydrocarbon contents compare well with no distinction evident across sampling method or analysis method on the hydrocarbon basis. However, several of the spot samples showed high nitrogen content and current hypothesis is that this phenomenon is attributable to a sample acquisition or handling step and is likely not a feature of the parent sample material collected from process line on-site in ND. The pressurized analysis for TM2, 3, 4, and 4a requires that the BR sample is transferred to an MPC, so all BR appear as BRMPC.

5.3.1 TM2: GPA 2177+ASTM D7900+ASTM D7169 Merge

5.3.1.1 Measured Light Ends and Fixed Gases

Whole oil composition for N2 through nC5 mole fraction determined by TM2 is compared to TM1–TL baseline using bar charts in Figure 5-8 for ND Bakken sampling methods. Sampling method is denoted by color. Two analytical runs were obtained by TM2 for each sample type and both are shown in the figure. Some notable differences in mole fraction between sampling types are observed for C1-nC5 with the TM2 C1 fraction for closed samples significantly higher than

TM1-TL, and for the BRMPC which is a factor of two low. For C2-nC5, all sample results are lower than TM1-TL with the MPC being consistently the lowest. All sample methods, however, yielded effectively the same whole oil composition.

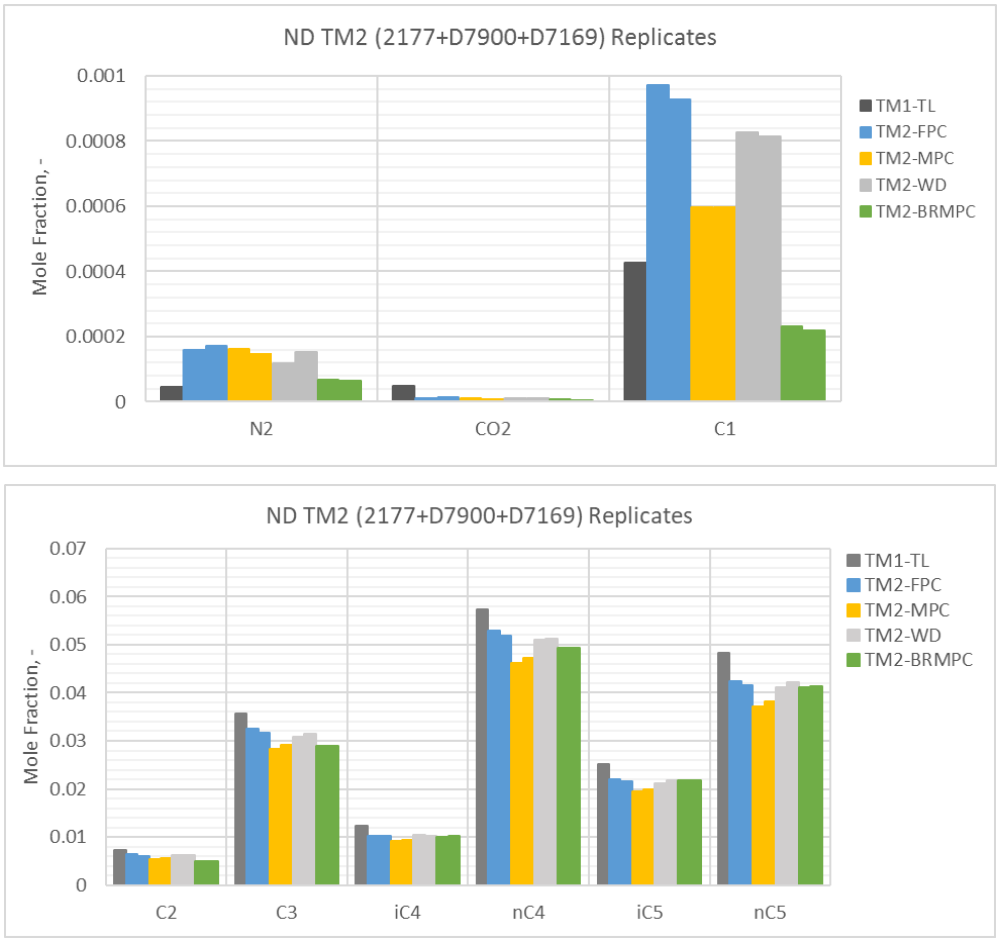

Figure 5-8. Bar charts showing mole fraction of components nitrogen (N2) through n-pentane (nC5) as measured by TM2 and compared with TM1 tight-line results for ND Bakken samples. Two replicates for each sample type are shown.

5.3.1.2 Calculated vapor pressure from TM2 composition

EOS model estimates of VPCRx(100°F) were generated using the compositional data acquired from TM2 and are compared with averaged VPCRx(100°F) data from ASTM D6377 measurements described in section 5.2. The results are presented in pressure-expansion curve and bar chart formats in Figure 5-9. A representative TM1 pressure-expansion curve is included with dashed lines connecting EOS-simulated pressure-expansion points. All TM2 expansion curves fall below the TM1 tight-line with the FPC replicates consistently the highest and BRMPC consistently the lowest. The difference between BRMPC and FPC at low V/L correlates with the measured C1 content because (for this test method) N2 was low for all sample types. In spite of C1 content being high relative to TM1 for all closed samples, the low C2 – nC5 content resulted in a downward shift in the expansion curve for V/L > 0.2.

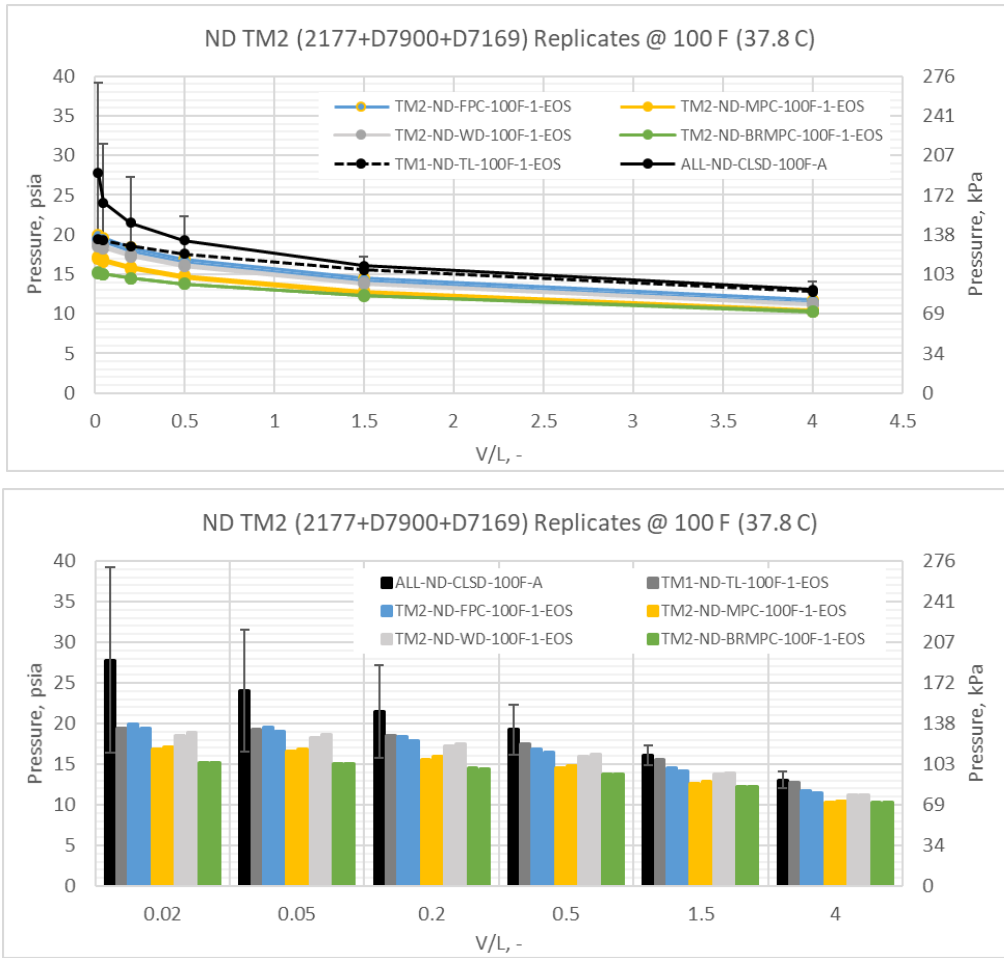

Figure 5-9. Pressure-expansion curve and bar chart comparisons of VPCRx(100°F) generated by EOS model from TM2, TM1, and D6377 instrument for ND Bakken samples.

5.3.2 TM3: GOR+ASTM D8003+ASTM D7169 Merge

5.3.2.1 Measured light ends and fixed gases

Whole oil composition for N2 through nC5 mole fraction as determined by TM3 is compared to TM1-TL in Figure 5-10. Sampling method is denoted by color. Two analytical runs were obtained by TM3 for each sample type, and are shown as separate bars of the same color.

Notable differences in mole fraction between sampling types are observed for N2 and O2 and C1. Moving up to C2 through nC5, no significant differences were observed by test method or sampling method. All sample methods yielded effectively the same hydrocarbon content.

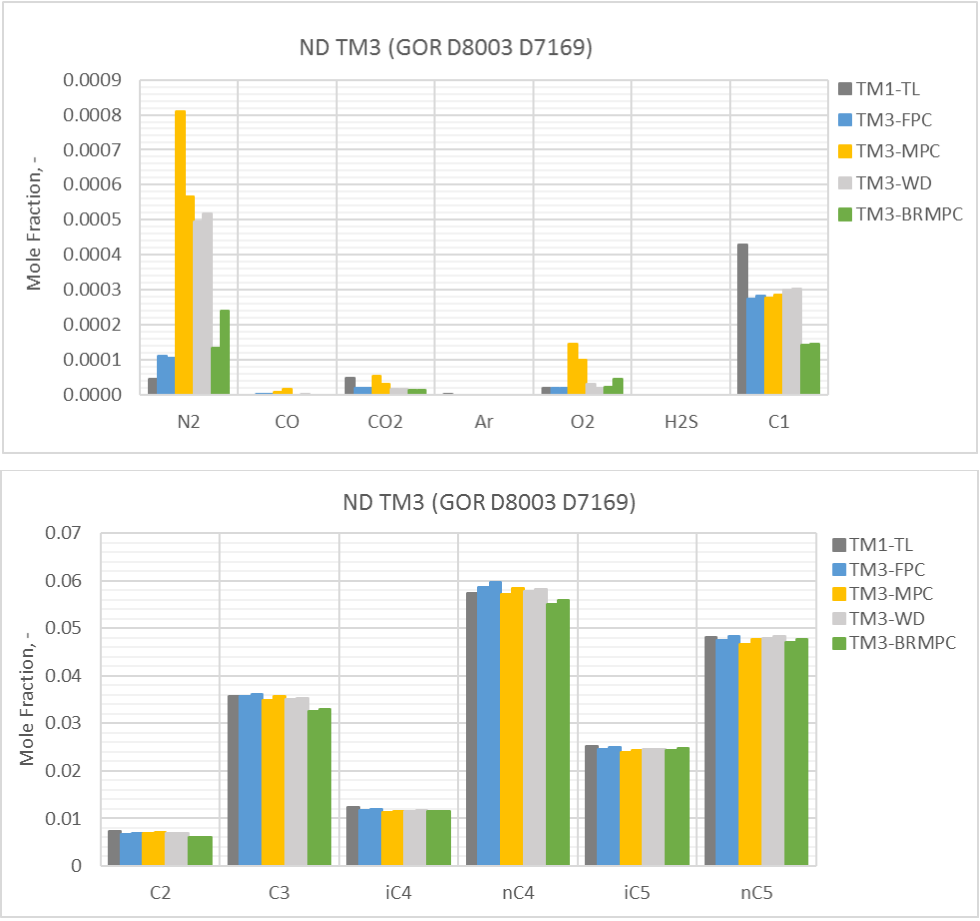

Figure 5-10. Bar chart showing mole fraction of components ethane (C2) through n-pentane (nC5) as measured by TM3 and compared with TM1. Sampling type is denoted by bar color.

5.3.2.2 Calculated vapor pressure from TM3 composition

EOS model estimates of VPCRx(100°F) were generated using the compositional data acquired from TM3 and compared with averaged VPCRx(100°F) data generated from ASTM D6377 measurements described above in section 5.2. The results are presented in pressure-expansion curve and bar chart formats in Figure 5-11. A representative TM1 pressure-expansion curve is shown in Figure 5-11 with dashed lines connecting EOS-simulated pressure-expansion points. All of the TM3 pressure-expansion curves fell into a band around the TM1 results. The BR samples yielded the low-end vapor pressures, while the MPC samples yielded the high end. FPC and WD fell in the middle. Results from all approaches agreed within about 2 psi for $VPCR_4$(100°F). Some divergence was observed as V/L approached 0.02, with the low end around 17 psi and the high end at 25 psi. These differences were driven largely by sample-to-sample variances in N2, O2, and C1 that can be seen in Figure 5-10 above. Key observations include:

i. Variability in EOS-calculated VPCR by sampling method is greatest at low V/L where differences in the lightest gas components have the greatest impact

ii. EOS-calculated VPCR is generally lower than direct-measured at all V/L's shown, though the margin is small and typically within several psi, and becomes insignificant at V/L = 4.

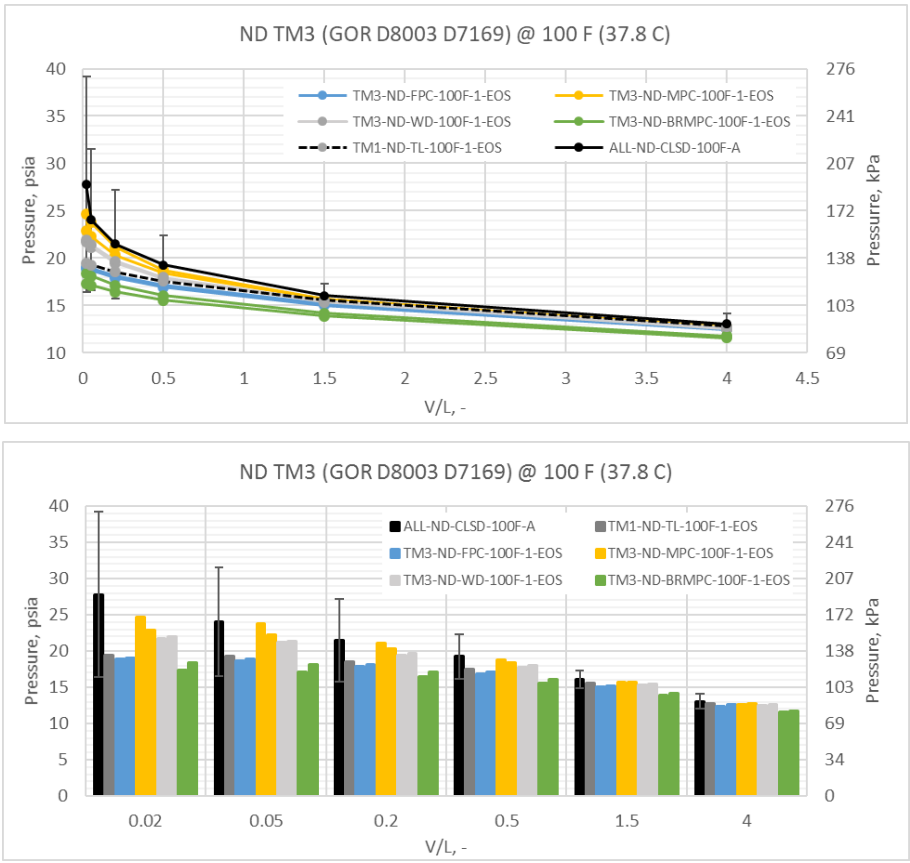

Figure 5-11. Pressure-expansion curve and bar chart comparisons of VPCRx(100°F) generated by EOS model from TM3, TM1, and D6377 instrument for ND Bakken samples.

5.3.3 TM4: GPA 2103M+ASTM D2887 Merge

Whole oil composition for N2 through nC5 mole fraction as determined by TM4 is compared to TM1-TL in Figure 5-12 for the ND Bakken sample. Sampling method is denoted by color. The pressurized analysis for TM4 requires that the BR sample is transferred to an MPC, so all BR appear as BRMPC. A single analytical run was obtained by TM4 for each sample type. TM4 does not analyze for O2 independently, rather it elutes with N2 so that the N2 peak represents the sum of N2 and O2 in the sample.

Notable differences in mole fraction between sampling types are observed for N2 and possibly CO2. For C2 through nC5 in Figure 5-12, no significant differences were observed by test method or sampling method, and methods yielded effectively the same compositions in this carbon number range.

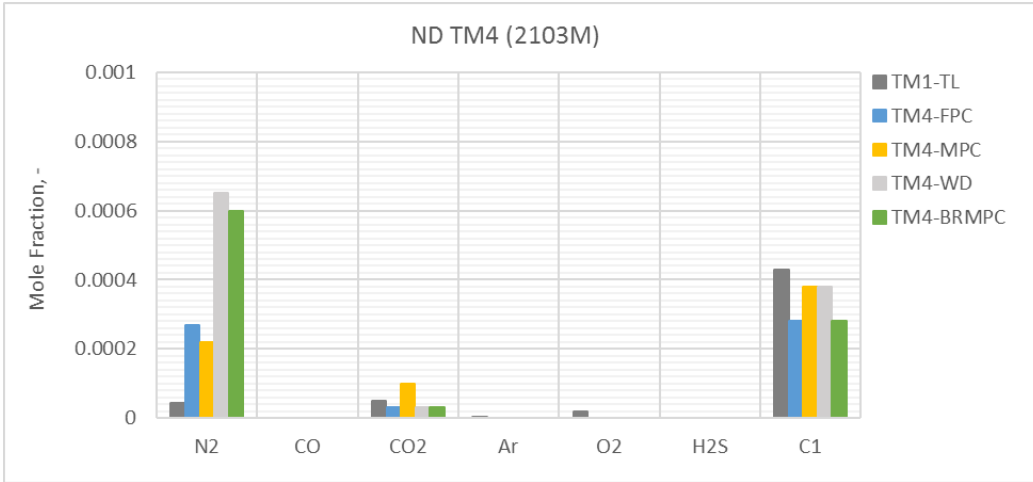

N2 is N2 +O2 for TM4

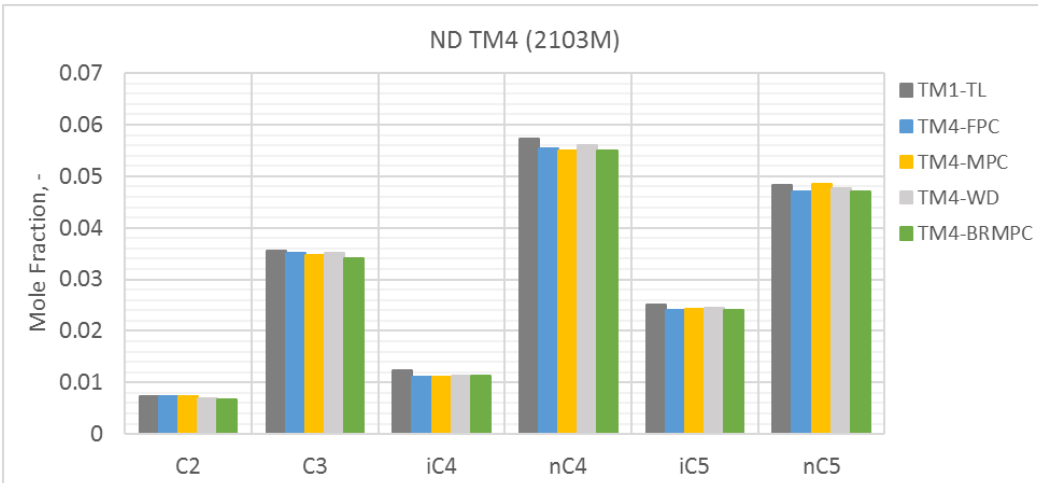

Figure 5-12. Bar chart showing mole fraction of components ethane (C2) through n-pentane (nC5) as measured by TM4 and compared with TM1. Sampling type is denoted by bar color.

5.3.3.1 Calculated vapor pressure from TM4 composition

EOS model estimates of VPCRx(100°F) were generated using the compositional data generated from TM4 and compared with averaged VPCRx(100°F) data (ALL-ND-CLSD-100F-A) generated from ASTM D6377 measurements described above in section 5.2. The results are presented in pressure-expansion curve and bar chart format in Figure 5-13.

A representative TM1 pressure-expansion curve is shown in Figure 5-13 with dashed lines connecting EOS-simulated pressure-expansion points. The TM4 pressure-expansion curves generally fell into a band on top of or between the average measured VPCR for all cosed samples and the TM1 results. Results from all approaches agreed within about 2 psi for VPCR between 0.5 and 4. Slight divergence was observed as V/L approached 0.02, with the low end around 20 psi and the high end at 23 psi. These differences were driven largely by sample-to-sample variances in N2 that can be seen in Figure 5-12 above.

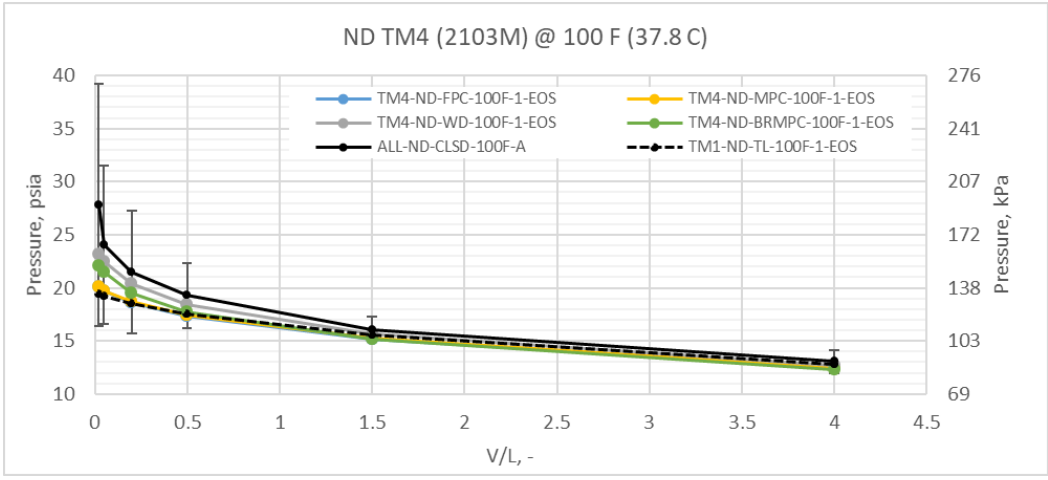

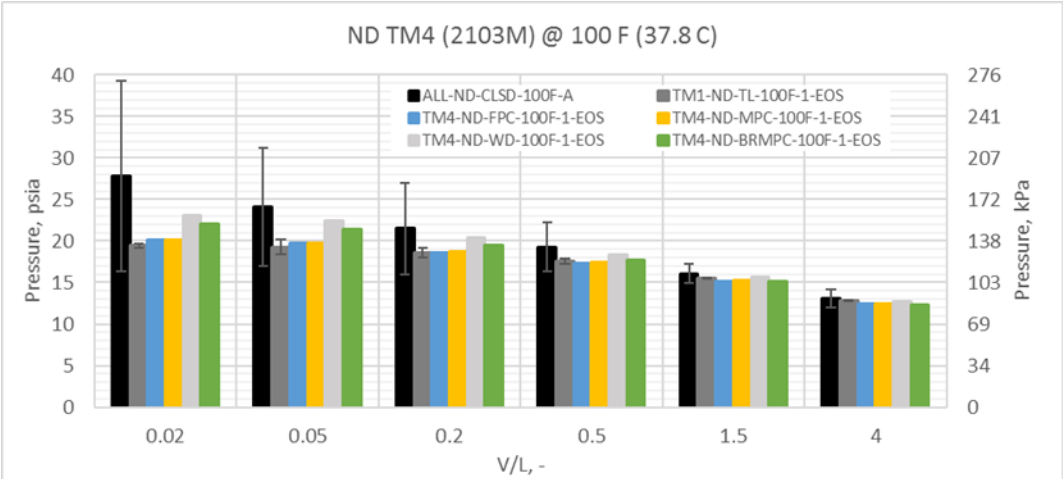

Figure 5-13. Pressure-expansion curve and bar chart comparisons of VPCRx(100°F) generated by EOS model from TM4, TM1, and D6377 instrument for ND Bakken samples.

5.3.4 TM4a: GPA 2103M+C30+ GC Merge

5.3.4.1 Measured Light Ends and Fixed Gases

Whole oil composition for N2 through nC5 mole fraction as determined by TM4a is compared to TM1–TL baseline using bar charts in Figure 5-14 for ND Bakken sampling methods. Sampling method is denoted by color. Two analytical runs were obtained by TM4a for each sample type and both are shown in the figure. All sample results are similar to TM1-TL with exception of the MPC N2 which is a factor of 3-4 high and the BRMPC C1 which is a factor of 2-4 low. The BRMPC is also consistently the lowest for C2-nC5, but only slightly. All methods yielded effectively the same hydrocarbon content, except for the BRMPC C1 (low outlier).

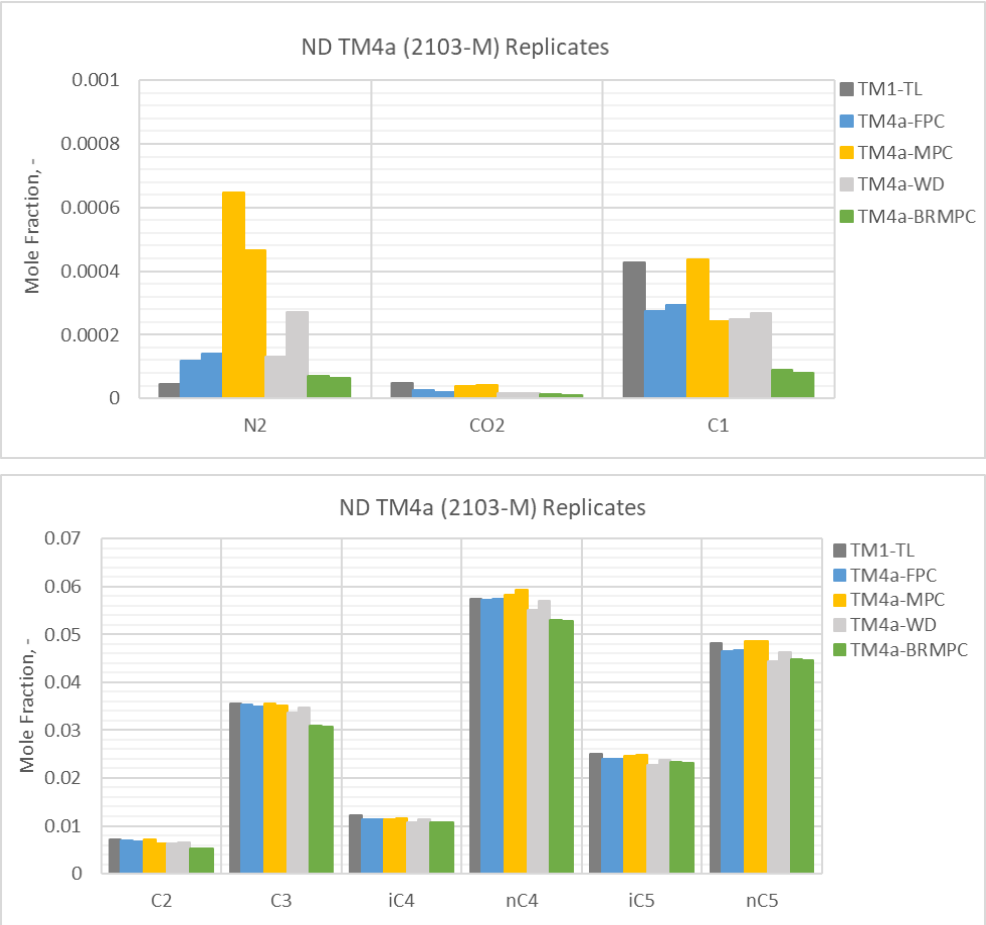

Figure 5-14. Bar chart showing mole fraction of components nitrogen (N2) through n-pentane (nC5) as measured by TM4a and compared with TM1 tight-line results for ND Bakken samples. Two replicates for each sample method are shown.

5.3.4.2 Calculated vapor pressure from TM4a composition

EOS model estimates of VPCRx(100°F) were generated using the compositional data generated from TM4a and compared with averaged VPCRx(100°F) data generated from ASTM D6377 measurements described above in section 5.2. A representative TM1-TL pressure-expansion curve is also shown in the figure. The results are presented in pressure-expansion curve and bar chart format in Figure 5-15. The FPC replicates show some spread (~3 psi) at low V/L and fall between the average closed and TM1 and converge for V/L >1 due to the FPC N2 and C1 content and variability shown in the compositions charts in Figure 5-14. The remaining sample types are either at or below TM1 with BRMPCs, again, being the lowest. The behavior correlates directly to C1-nC5 content being at or below the corresponding TM1 content, with BRMPC C1 content being significantly lower.

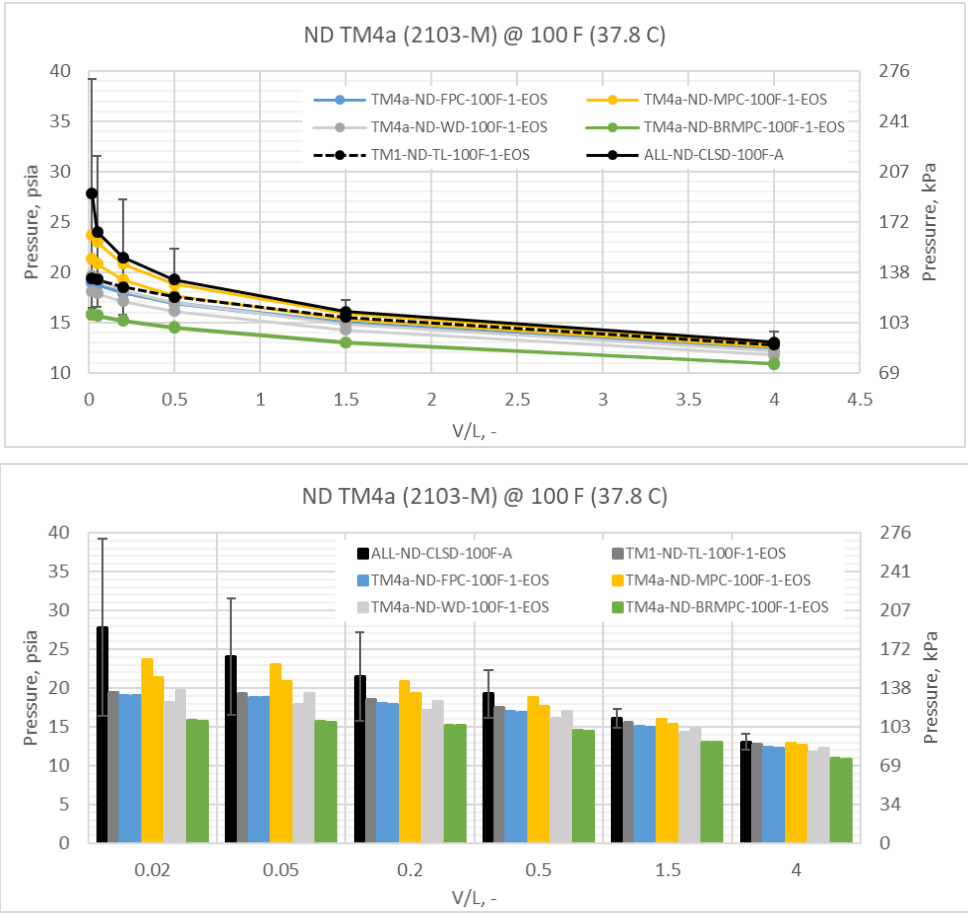

Figure 5-15. Pressure-expansion curve and bar chart comparisons of VPCRx(100°F) generated by EOS model from TM4a, TM1, and D6377 instrument for ND Bakken samples.

5.3.5 Comparison of Compositions from TM3 and TM4 for ND Bakken

Whole oil composition for N2 through nC5 mole fraction as determined by both TM3 and TM4 are compared for all sample types in Figure 5-16 bar charts for the ND Bakken samples. Sampling method is denoted by color; TM4 results are differentiated by black outline and only the first replicate for TM3 results is shown for clarity. TM1-TL results are also included in the charts.

Notable differences in mole fraction are observed between TM3 and TM4 for N2, however the differences are dominated more by sample-to-sample differences than lab-to-lab. On average, TM4 may show slightly higher N2 content, though the reader is reminded that N2 for TM4 reflects the sum of O2 and N2 eluted in the test method. For C1, TM3 and TM4 show similar mole fraction content, except TM3-BRMPC which is significantly lower.

Moving to C2 (ethane) through nC5 (N-Pentane) presented in the lower chart of Figure 5-16, no significant differences were observed by test method or sampling method. All methods yielded effectively the same compositions.

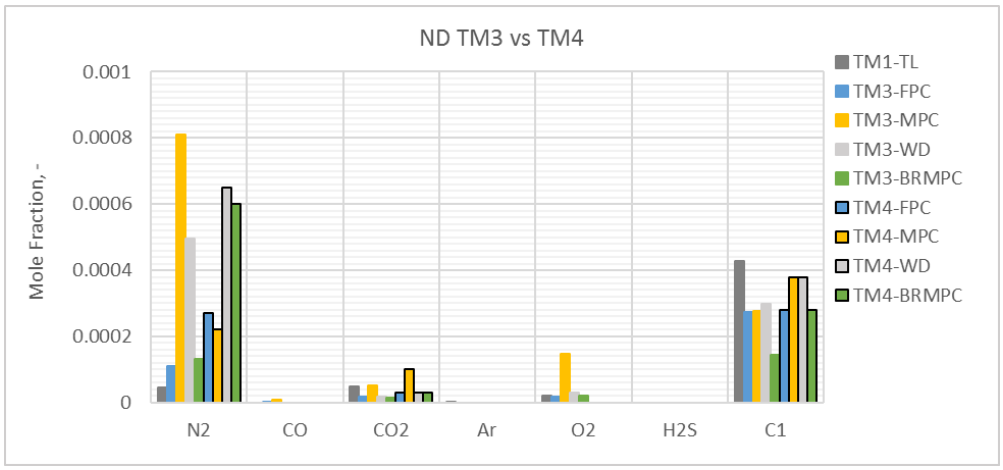

Note: N2 for TM4 is N2+O2.

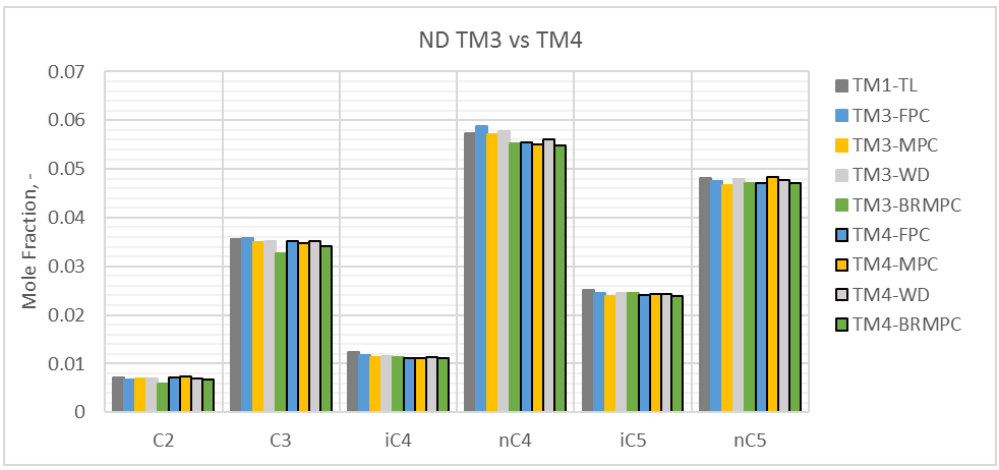

Note: TM4 data outlined in black. Only replicate 1 for TM3 is shown.

Figure 5-16. Bar chart comparison of composition from TM3 and TM4 for ND Bakken. Components N2–C1 in upper figure and C2–nC5 in lower figure.

5.3.6 Comparison Across Task 2 Compositional Test Methods

5.3.6.1 Measured light ends and fixed gases

Light ends and fixed gas compositions measured by all test methods for ND Bakken samples are compared using bar charts provided in Figure 5-17. Mole fractions of each component were averaged across all closed sample methods and replicates and averaged across all open BR samples and replicates for each test method. In the figure, the first four bars after TM1-TL are closed sample results and the last four bars (outlined in black) are open BR sample results. N2 mole fractions are small, but high relative to TM1-TL (dark gray) and vary by an order-of-magnitude (5e-5 to 6e-4) which can significantly impact vapor pressure at low V/L. C1 mole fractions are low relative to the TM1-TL baseline (except for TM2-CLSD) and vary by up to a factor of 4 with open BR samples consistently lower than closed. TM4 was the only BR method that was chilled during sample transfer to MPC prior to compositional analysis, which may have helped better maintain the C1 level between open and closed than TM 2, 3, and 4a. Results for components C2 – nC5 from all test methods are very similar, with TM2 (blue) consistently showing the lowest mole fraction for both closed and open samples.

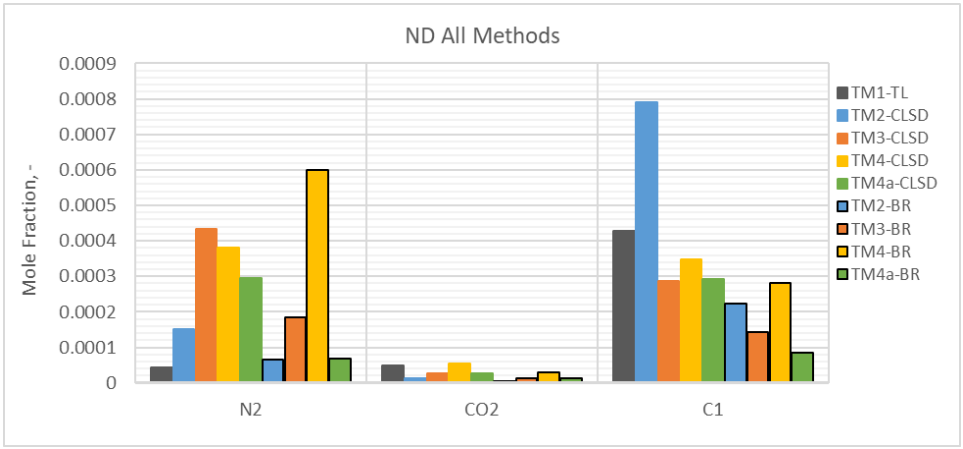

Note: N2 for TM4 is N2+O2

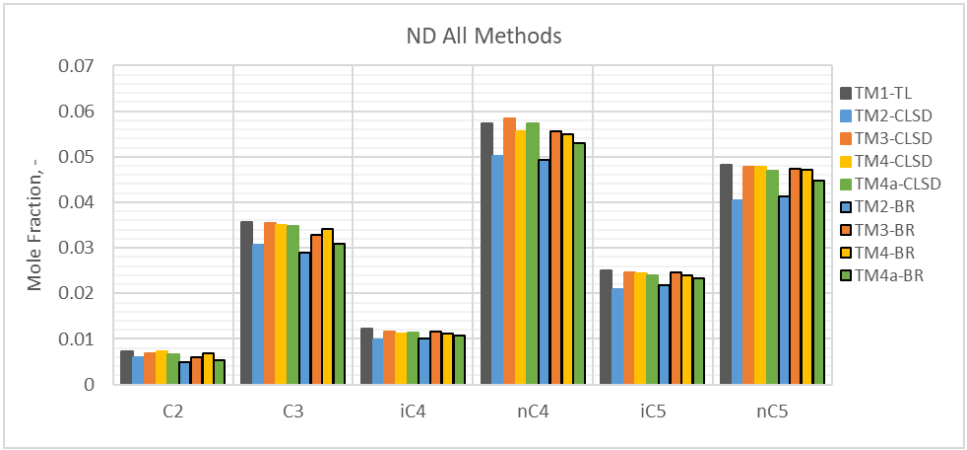

Figure 5-17. Comparison of averaged measured light ends and fixed gases for each test method - ND Bakken samples. Results for Boston Round samples are outlined in black.

5.3.6.2 EOS modelled vapor pressure

EOS modelled vapor pressure-expansion data at 100°F (37.8°C) for all test methods are compared in Figure 5-18. Also included in the figure are average measured VPCRx for closed sampling method (AVG-CLSD-Meas) and the baseline LAB1 measured VPCRx using FPC sampling (LAB1-FPC-Meas). EOS VP results for open BR samples are outlined in black in the bar charts and shown as black dashed lines in the curve plots. For both open and closed sampling methods EOS VP results are low and variable relative to the average measured for all test methods, but consistent with all previous results, in that variability diminishes as V/L increases. However, EOS VP results for closed samples fall within the 2σ bounds of the AVG-CLSD-Meas. For open sample methods, EOS VP results for all test method except TM4 are below the 2σ lower bound. EOS VP results for TM2 are consistently the lowest for both the closed and open sample methods and TM4a open BR results are also consistently low.

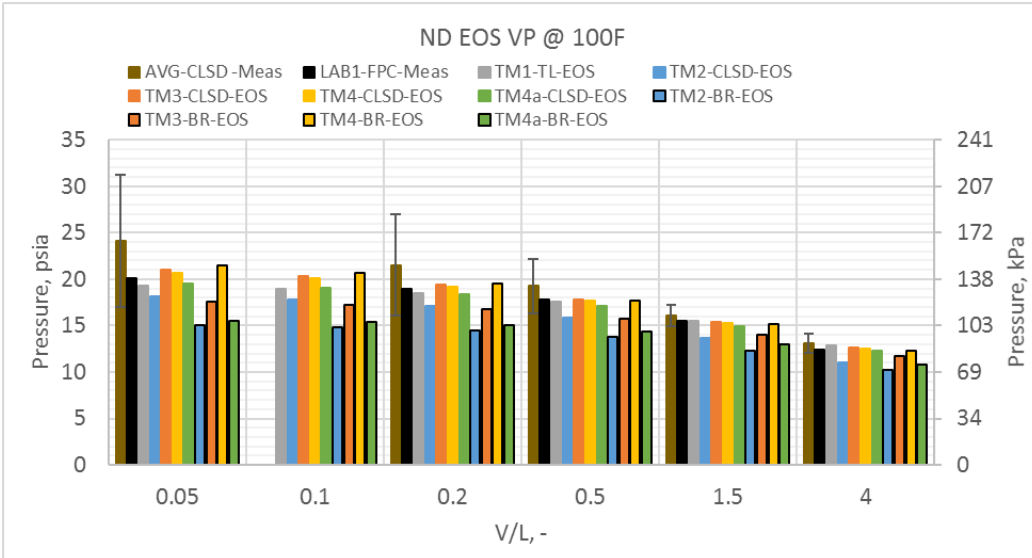

Note: first two bars are measured data, remainder are EOS estimated.

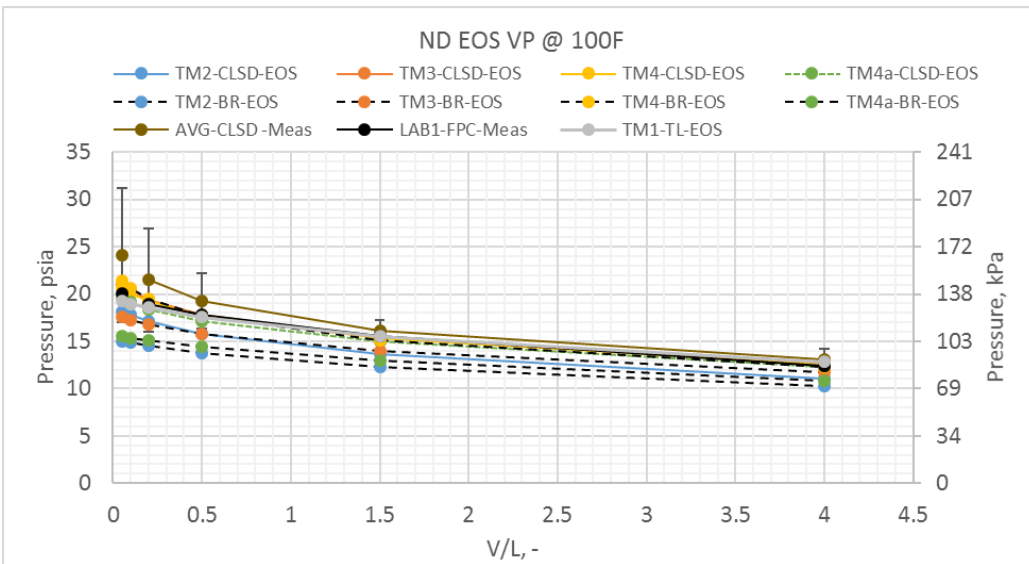

Figure 5-18. Comparison of EOS modelled vapor pressures at 100°F for averaged results from each test method – ND Bakken samples. Results for Boston Round samples are outlined in black in top figure and shown with black dash in bottom figure.

5.4 Measured Vapor Pressure – TX Eagle Ford Summer Samples

Vapor pressures for the TX Eagle Ford samples are shown for three analysis temperatures 68, 100, and 122 °F (20, 37.8, 50 °C) in Figure 5-19 through Figure 5-21. The height of each colored bar represents the sample mean, and the error bars represent the 2σ associated with the sample set. The color of each bar represents a sampling type (FPC, MPC, etc.). VPCR samples in Figure 5-19 through Figure 5-21 were collected by three laboratories in the coordinated sampling event and analyzed by the same test methods.

Relative to the ND Bakken sample, the TX Eagle Ford sample exhibited lower vapor pressure at all temperatures and V/L points. The likely reason for this is related to the process temperatures for both oils, with TX oil collected at ~96°F (36°C) line conditions and ND oil collected at ~70°F (21°C) line conditions. Source oil in both supply chains was exposed to atmospheric pressure upstream of the sampling point. Provided both came into pressure equilibrium with local atmosphere upstream/prior to the Sandia sample event, the warmer TX oil ended up with lower gas content than the ND oil. As such, the TX oil had lower vapor pressure at reference conditions than the ND oil. Detailed information on process or handling upstream of the sampling points was unavailable. It is known that both locations were downstream of truck offloading points and contained commingled production from a number of wells.

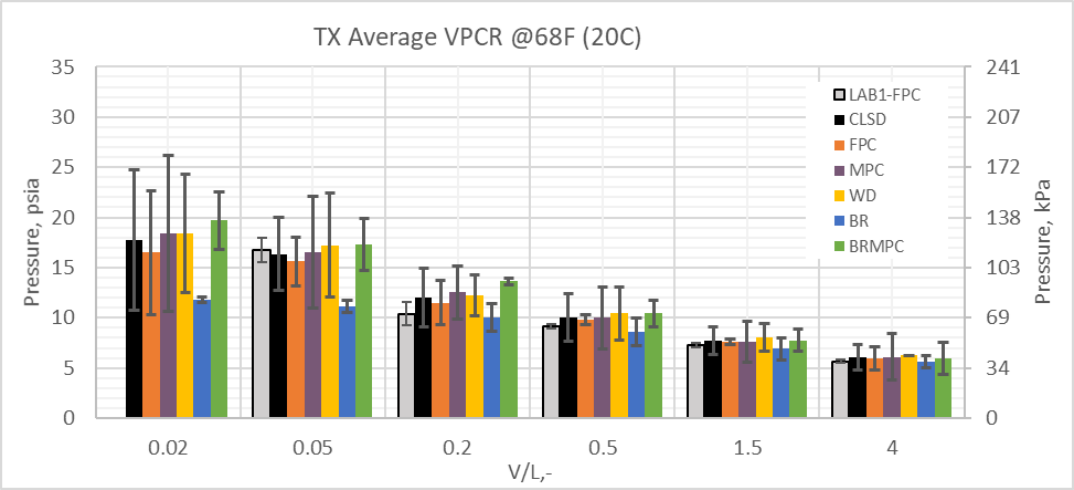

Figure 5-19. Bar chart showing average and 2σ VPCRx(68°F) for the TX Eagle Ford oil sorted by V/L and sampling type.

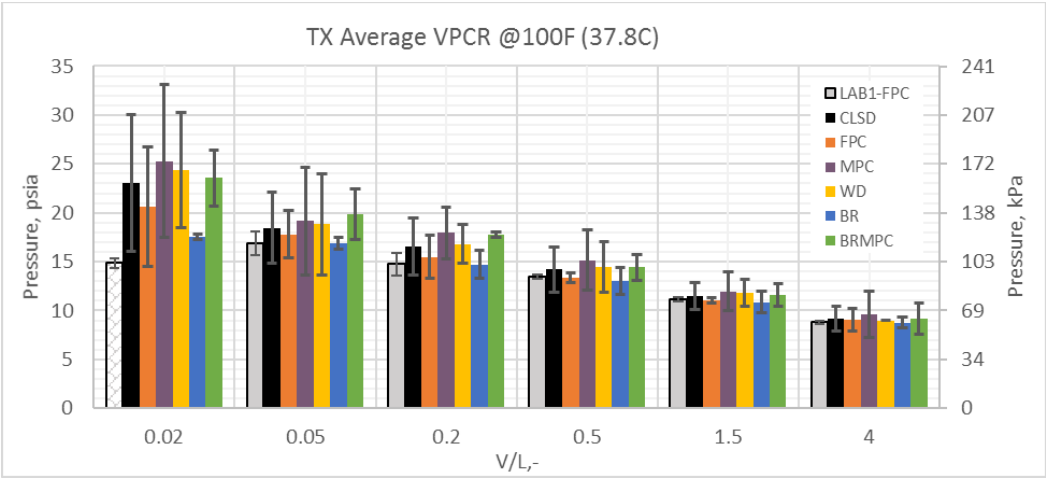

Figure 5-20. Bar chart showing average and 2σ VPCRx(100°F) for the TX Eagle Ford oil sorted by V/L and sampling type.

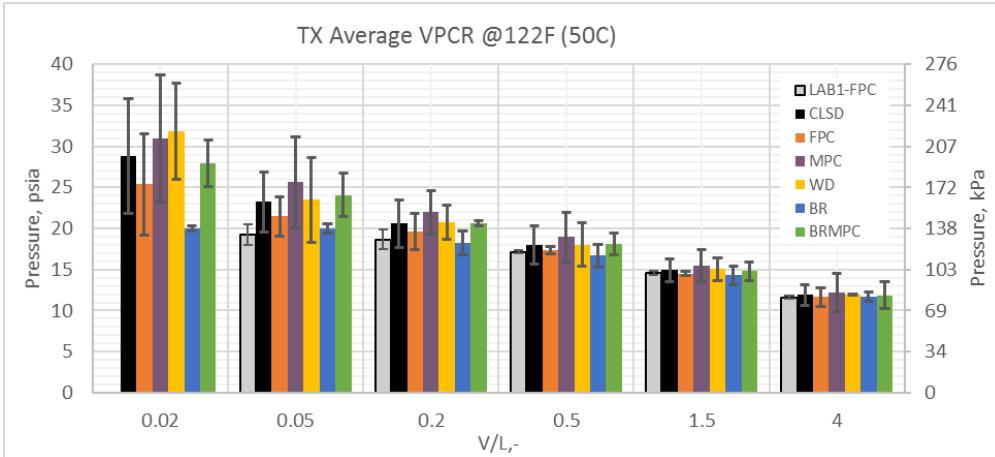

Figure 5-21. Bar chart showing average and 2σ VPCRx(122°F) for the TX Eagle Ford oil sorted by V/L and sampling type.

An alternate means to present the same VPCRx data is shown in an overlay of expansion curves in Figure 5-22, where the x-axis is scaled to V/L. This provides physical significance to the x-axis, indicating that the VPCR increases more steeply as V/L decreases. Obvious in the figure is the spread at low V/L and the convergence as V/L increases.

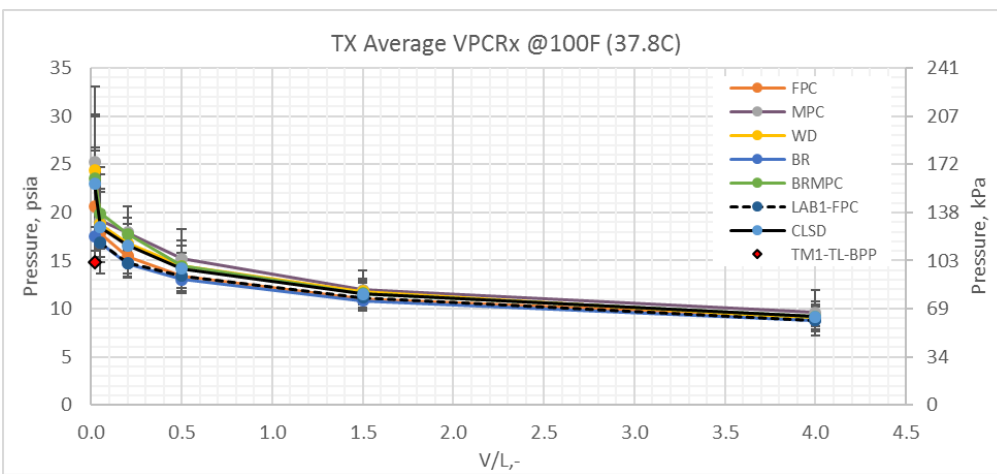

Figure 5-22. Expansion curves showing VPCRx(100°F) versus V/L for TX Eagle Ford oil by sampling type.

5.4.1 General Observations

Similar to what was observed for the ND Bakken sample, VPCRx was relatively insensitive to sampling method, though there was a possible exception at low V/L: BR samples. The magnitude of the calculated R= 2.8 σ(VPCRx) for low V/L indicates that there was notable variability among measurements, and at a magnitude larger than expected based on published R_{std} = 2.94 psi (20.3 kPa) for V/L = 0.02 in FPCs (see Table 5-12). This level of uncertainty makes it difficult to place high confidence in the differences seen between specific sampling methods. Nonetheless, an interesting observation that stands for the TX Eagle Ford as well as for the ND Bakken is that the BR samples exhibit a mean $VPCR_{0.02}$ lower than the closely related BRMPC. As a reminder, the

only difference between these samples is that the BRMPC samples were transferred to closed cylinders in the lab and pushed into the 6377 instrument under positive gauge pressure while BR samples were drawn into the 6377 instrument under slight vacuum. The fact that BRMPC samples behaved more like the other closed sampling methods than the BR indicates that the sample introduction into the VPCR instrument is driving the differences in results rather than losses of volatiles during the sample capture in the field. Comments from section 5.2.2.2 on ambient fill method for BR samples would apply here as well.

Table 5-12. Calculated reproducibility interval (psi) for measured VPCRx data at 100°F for TX Eagle Ford oil samples.

TX Sample	V/L					
	0.02	0.05	0.2	0.5	1.5	4
LAB1-FPC*	0.72	1.72	1.61	0.29	0.30	0.23
Closed**	9.76	5.08	4.07	3.28	1.90	1.81
FPC	8.56	3.39	3.10	0.63	0.41	1.60
MPC	10.91	7.73	3.72	4.29	2.79	3.27
WD	8.23	7.23	2.84	3.65	1.90	0.04
BR	0.40	0.84	1.97	1.91	1.55	0.81
BRMPC	3.97	3.64	0.44	1.86	1.59	2.24
R_{std}-FPC	2.94	–	–	–	–	0.62
R_{std} Nonpress	–	–	–	–	–	0.76

*Day to day variability for LAB1-FPC

**Reproducibility across FPC, MPC, and WD closed sampling methods

5.4.2 TVP-95 Vapor Pressure and Gas-Oil Ratio of TX Eagle Ford

The TVP-95 mobile laboratory returned a vapor pressure near bubblepoint pressure (BPP) conditions at T=100°F, and gas-oil ratio (GOR) with associated V/L at separator pressure (P) and =100°F as shown in Table 5-13. BPP and GOR values were stable on all three days. Note the BPP T=100°F was very close to atmospheric pressure with a low measured GOR and V/L (at low end of detection limit). This appears to be a "weathered" or "dead" oil that has previously equilibrated with the local atmospheric pressure.

Table 5-13. Summary of TVP-95 measurements for TX Eagle Ford crude oil. V/L was calculated from measured GOR, and P denotes separator pressure for GOR test.

	BPP	GOR	V/L	P
	[psia]	[scf/bbl]	[-]	[psia]
Day 1	14.6	0.2	0.04	14.6
Day 2	15.1	0.2	0.04	14.7
Day 3	14.9	0.1	0.03	14.7

A graphic showing the TVP-95 BPP overlaid with expansion curves for measured VPCRx(100°F) for the TX Eagle Ford oil is shown in Figure 5-23. The TVP-95 BPP appears to sit at the lower end of measured values collected here. Discussion later in this report looks into the compositional differences that are associated with these vapor pressure differences. All of the curves converge as V/L increases to within about 1 psi (7 kPa). The possible reasons why the TVP-95 BPP is lower than other measures was discussed in section 5.2.3.

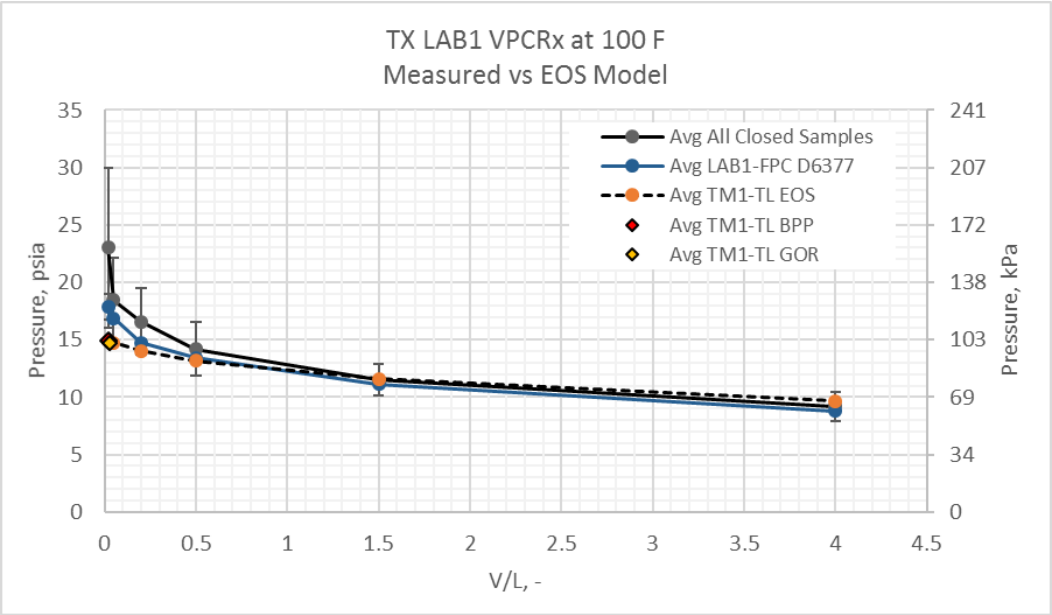

Figure 5-23. Averaged pressure-expansion curves for TX Eagle Ford oil from ASTM D6377 measurements overlaid with TVP-95 BPP and GOR.

5.4.3 Homogenity of Sample from Day 1 – Day 3

The TVP-95 was on-site all three sampling days and ran separator tests as well as VPCR tests on all three days. All three sampling days saw high repeatability. Recall all spot samples analyzed offsite were taken on Days 1 and 2.

5.5 Composition – TX Eagle Ford Summer Samples

Compositional results from TM2, TM3, TM4 and TM4a are compared below against the baseline TM1-TL (TVP-95 system) on a component-by-component basis for N2 – nC5. Higher carbon numbers were measured and reported, but they have a negligible effect on vapor pressure at 100°F, and are addressed in a later section of the report. In addition, EOS performance using the same compositions is compared with average measured D6377 VPCR for closed sample capture methods. In general, hydrocarbon contents compare well with no distinction evident across sampling method or analysis method on the hydrocarbon basis. As seen for ND Bakken, several of the spot samples showed high nitrogen content and the current hypothesis is that this phenomenon is attributable to a sample acquisition or handling step and is likely not a feature of the parent sample material collected from process line on-site in TX.

5.5.1 TM2: GPA 2177+ASTM D7900+ASTM D7169 Data Merge

5.5.1.1 Measured Light Ends and Fixed Gases

Whole oil composition for N2 through nC5 mole fraction as determined by TM2 is compared to TM1–TL baseline using bar charts in Figure 5-24 for TX Eagle Ford sampling methods. Sampling method is denoted by color. Two analytical runs were obtained by TM2 for each sample type and both area shown in the figure. Some notable differences in mole fraction between sampling types are observed for C1-nC5. Unlike ND, all sample C1 results are high relative to TM1-TL with the BRMPC being the lowest and closest to TM1-TL. For components C2-nC5 only the WD sample showed results similar to the TM1-TL. The FPC, MPC and BRMPC samples were self-consistent but lower than the TM1–TL.

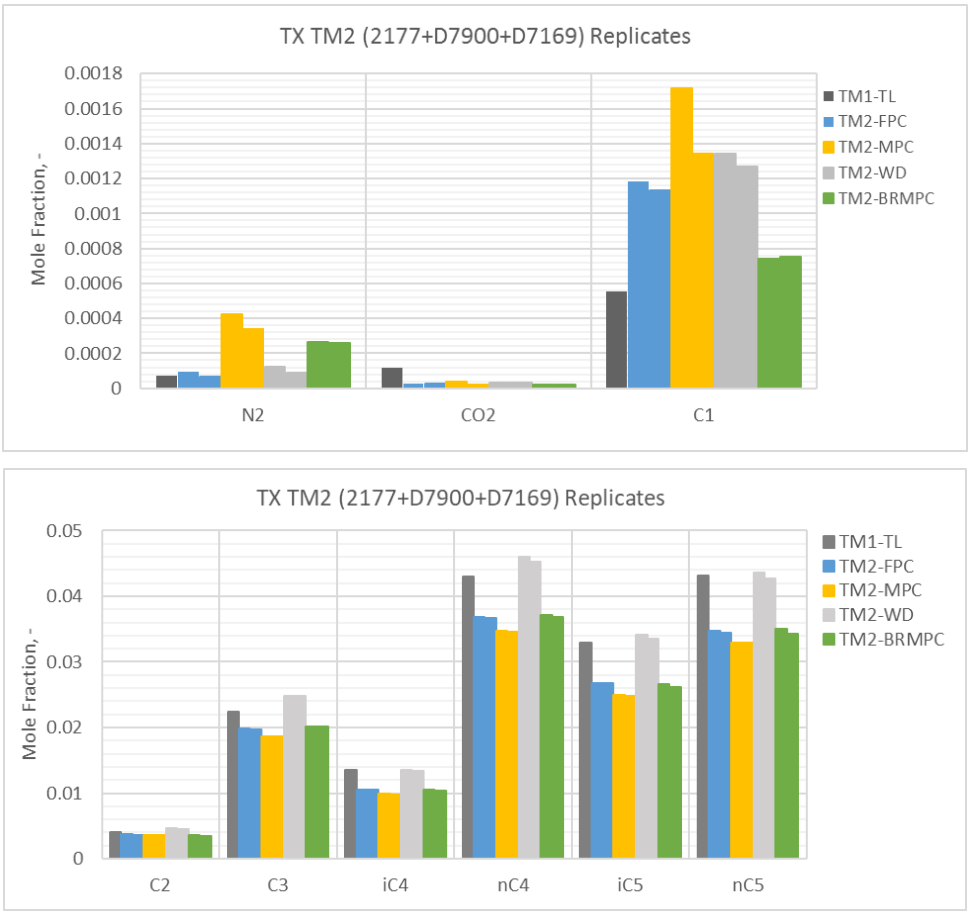

Figure 5-24. Bar chart showing mole fraction of components nitrogen (N2) through n-pentane (nC5) as measured by TM2 and compared with TM1 tight-line results for TX Eagle Ford samples. Two replicates for each sample type are shown.

5.5.1.2 Calculated vapor pressure from TM2 composition

EOS model estimates of VPCRx at 100°F were generated using the compositional data acquired from TM2 and compared with averaged ASTM D6377 measured VPCRx(100°F) data described previously in section 5.4. The results are presented in pressure-expansion curve and bar chart

formats in Figure 5-25. The TM2 EOS-generated VPCRx(100°F) generally fall between the TM1-TL baseline and the average for all closed methods at low V/L and vary about 4 psi. At large V/L, EOS-VP scatter tightly around same baselines with the WD sample consistently being the highest and BRMPC being the lowest.

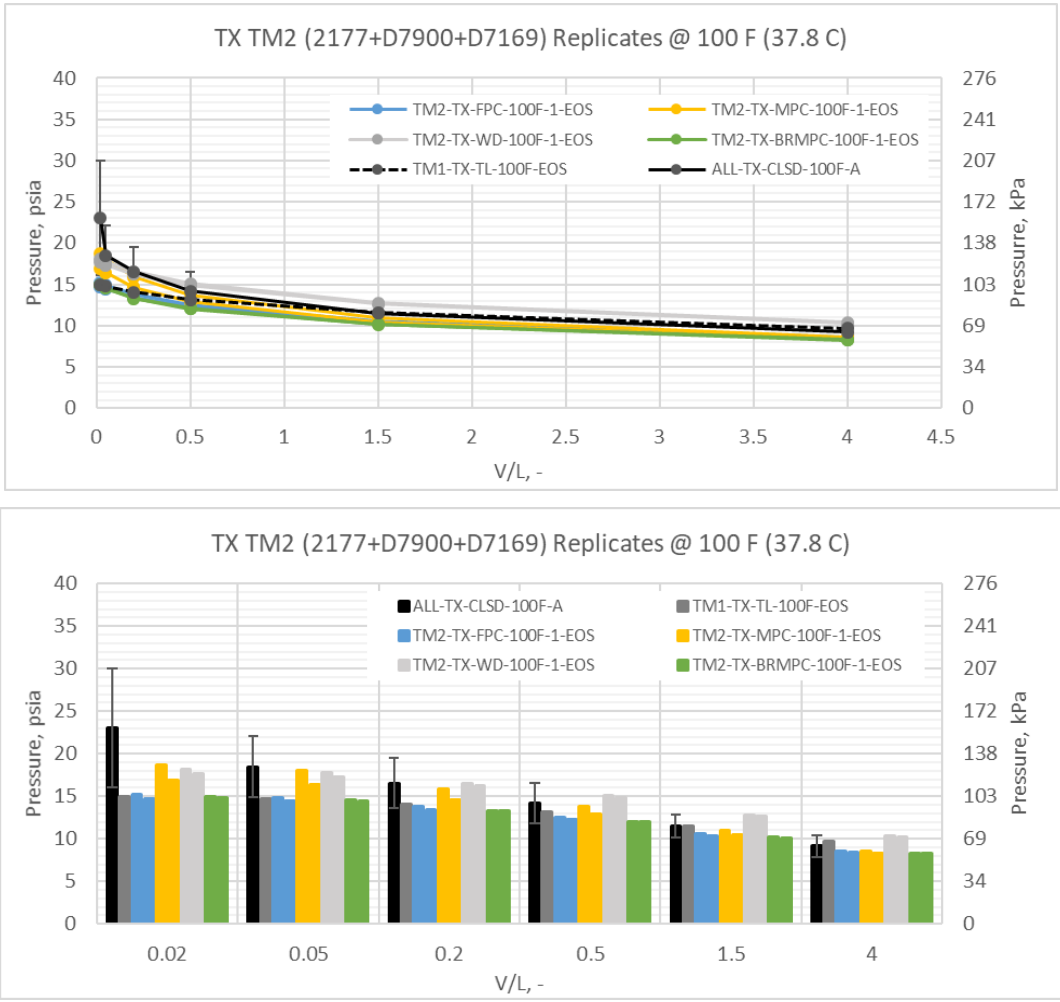

Figure 5-25. Pressure-expansion curve and bar chart comparisons of VPCRx(100°F) generated by EOS model from TM2, TM1, and D6377 instrument for TX Eagle Ford.

5.5.2 TM3: GOR+ASTM D8003+ASTM D7169 Merge

5.5.2.1 Measured light ends and fixed gases

Whole oil composition for N2 through nC5 mole fraction as determined by TM3 is compared to TM1-TL in Figure 5-26. Sampling method is denoted by color. The pressurized analysis for TM3 requires that the BR sample is transferred to an MPC, so all BR appear as BRMPC. Two analytical runs were obtained by TM3 for each sample type, and are shown as separate bars of the same color. All spot sampling methods show higher nitrogen than the TM1 tight-line. WD and BRMPC show the highest nitrogen among these. For the most part, the light hydrocarbons methane through n-pentane are effectively the same for all sampling methods.

Figure 5-26. Bar chart showing mole fraction of components ethane (C2) through n-pentane (nC5) as measured by TM3 and compared with TM1 for TX Eagle Ford. Sampling type is denoted by bar color.

5.5.2.2 Calculated vapor pressure from TM3 composition

EOS model estimates of VPCRx(100°F) were generated using the compositional data acquired from TM3 and compared with averaged VPCRx(100°F) data generated from ASTM D6377 measurements described previously in section 5.4. The results are presented in pressure-expansion curve and bar chart formats in Figure 5-27. TM3 EOS-generated VPs generally fall between the TM1-TL baseline and the average for all closed methods at all V/L considered here.

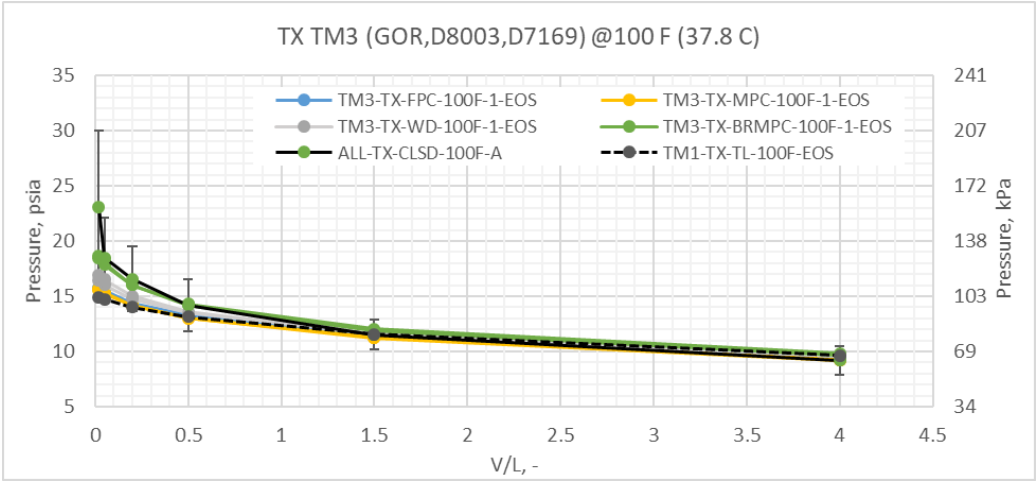

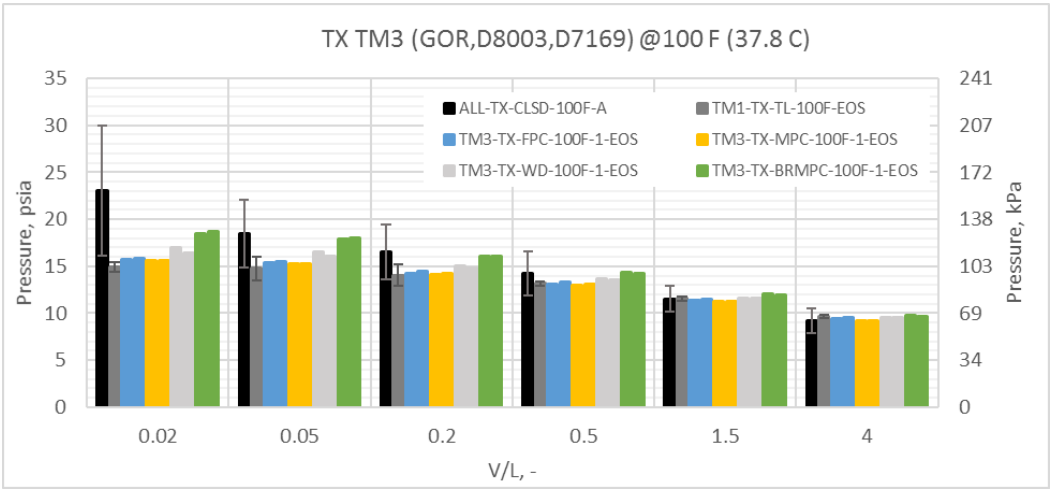

Figure 5-27. Pressure-expansion curve and bar chart comparisons of VPCRx(100°F) generated by EOS model from TM3, TM1, and D6377 instrument for TX Eagle Ford.

5.5.3 TM4: GPA 2103M+ASTM D2887 Merge

TM4 was applied to the TX Eagle Ford samples for MPC, WD, and BRMPC samples. FPC samples were not available for TM4 analysis. TM4 does not analyze for O2 independently, rather it elutes with N2 so that the N2 peak represents the sum of N2 and O2 in the sample.

5.5.3.1 Measured light ends and fixed gases

Whole oil composition for N2 through nC5 mole fraction as determined by TM4 is compared to TM1-TL in Figure 5-28. Sampling method is denoted by color. The pressurized analysis for TM4 requires that the BR sample is transferred to an MPC, so all BR appear as BRMPC. Similar to what was observed in TM3, higher N2 is observed in TM4 over the TM1-TL baseline for spot samples, though the sampling type showing higher N2 has shifted more conspicuously to WD and BRMPC in this case. The C2 through nC5 groups showed consistent behavior across all sampling methods in Figure 5-28.

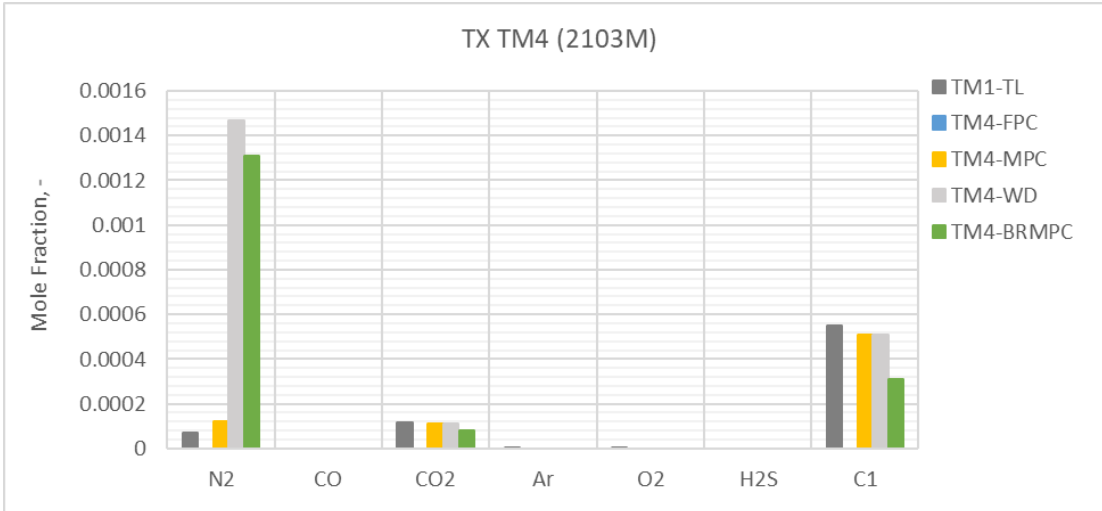

Note: TM4-FPC not available. N2 is N2+O2 for TM4

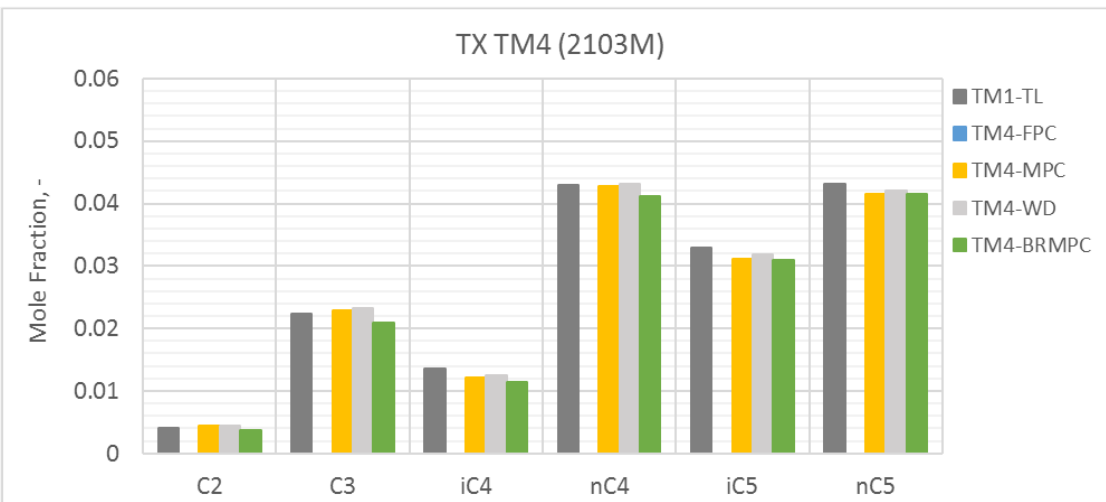

Note: TM4-FPC not available.

Figure 5-28. Bar chart showing mole fraction of components ethane (C2) through n-pentane (nC5) as measured by TM4 and compared with TM1 for TX Eagle Ford samples. Sampling type is denoted by bar color.

5.5.3.2 Calculated vapor pressure from TM4 composition

EOS model estimates of VPCRx(100°F) were generated using the compositional data acquired from TM4 and compared with averaged VPCRx(100°F) data generated from ASTM D6377 measurements described previously in section 5.4. The results are presented in pressure-expansion curve and bar chart format in Figure 5-29. The MPC EOS-VPs fell right on top of the TM1-TL generated curve, while EOS-VP results from the WD and BRMPC were both higher than the VPCRx(100°F) data generated from ASTM D6377 measurements. This is consistent with the high N2 measured and shown in Figure 5-28. VPCR from all of the sampling methods effectively converge ate V/L = 4, which is consistent with showing the same hydrocarbon content.

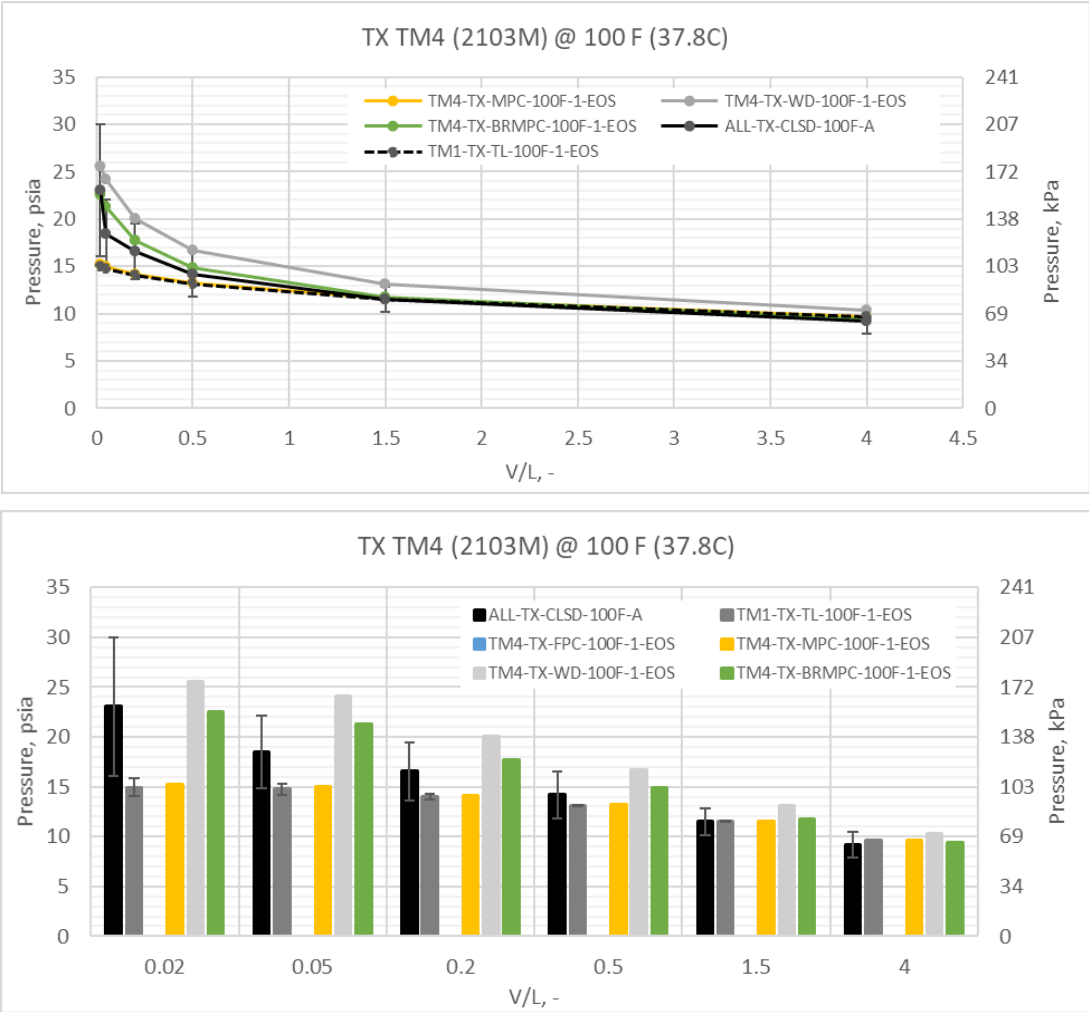

Note: TM4-FPC not available

Figure 5-29. Pressure-expansion curve and bar chart comparison of VPCRx(100°F) generated by EOS model from TM4, TM1, and D6377 instrument for TX Eagle Ford samples.

5.5.4 TM4a: GPA 2103+C30+ GC Merge

5.5.4.1 Measured Light Ends and Fixed Gases

Whole oil composition for N2 through nC5 mole fraction as determined by TM4a is compared to TM1–TL baseline, using bar charts in Figure 5-30 for TX Eagle Ford sampling methods. Sampling method is denoted by color. Two analytical runs were obtained by TM4a for each sample type and both are shown in the figure. All sample results are similar to TM1-TL with exception of the MPC N2 (similar to ND) which is a factor of ~5 high and the BRMPC C1 which is a factor of ~2 low. The BRMPC is also consistently the lowest for C2-nC5, but only slightly. All methods yielded effectively the same hydrocarbon content.

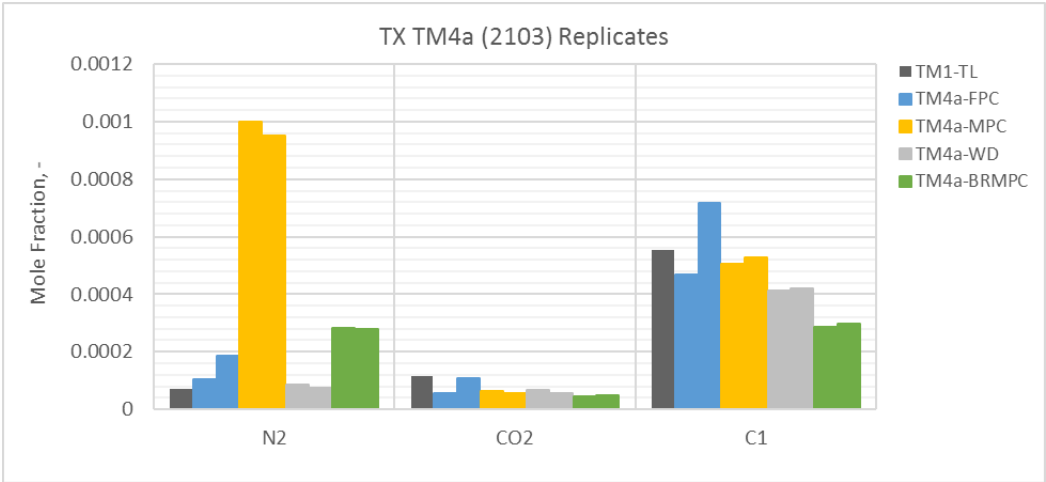

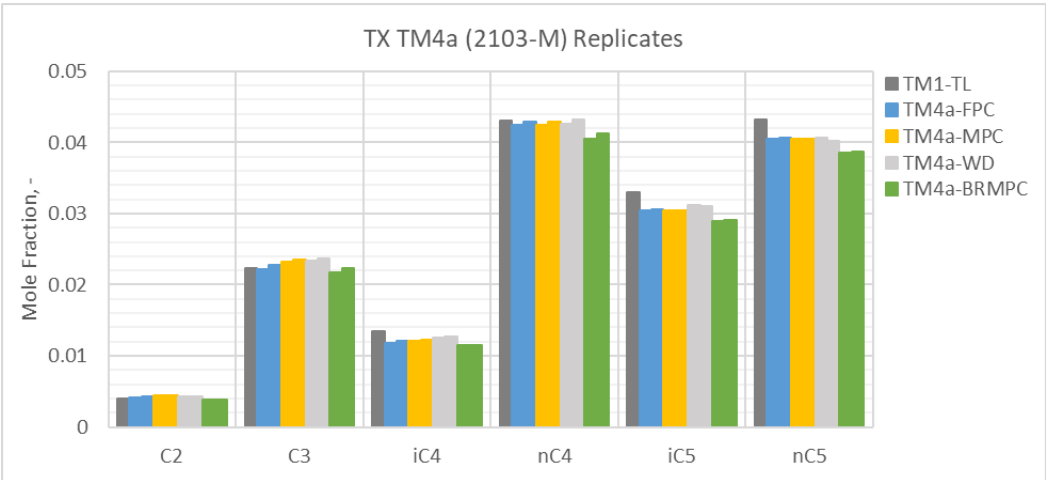

Figure 5-30. Bar chart showing mole fraction of components nitrogen (N2) through n-pentane (nC5) as measured by TM4a and compared with TM1 tight-line results for TX Eagle Ford samples. Two replicates for each sample type are shown.

5.5.4.2 Calculated vapor pressure from TM4a composition

EOS model estimates of VPCRx at 100°F were generated using the compositional data acquired from TM4a and compared with averaged ASTM D6377 measured VPCRx(100°F) data described previously in section 5.4. The results are presented in pressure-expansion curve and bar chart formats in Figure 5-31. All cases except the MPC fell tightly scattered around the TM1- EOS generated curve, while EOS-generated VP results from the MPC were higher than the averaged measured data. This is consistent with the high measured N2 shown in Figure 5-30. EOS-VP and measured VPCR data from all of the sampling methods effectively converge at V/L = 4, which is consistent with showing the same hydrocarbon content.

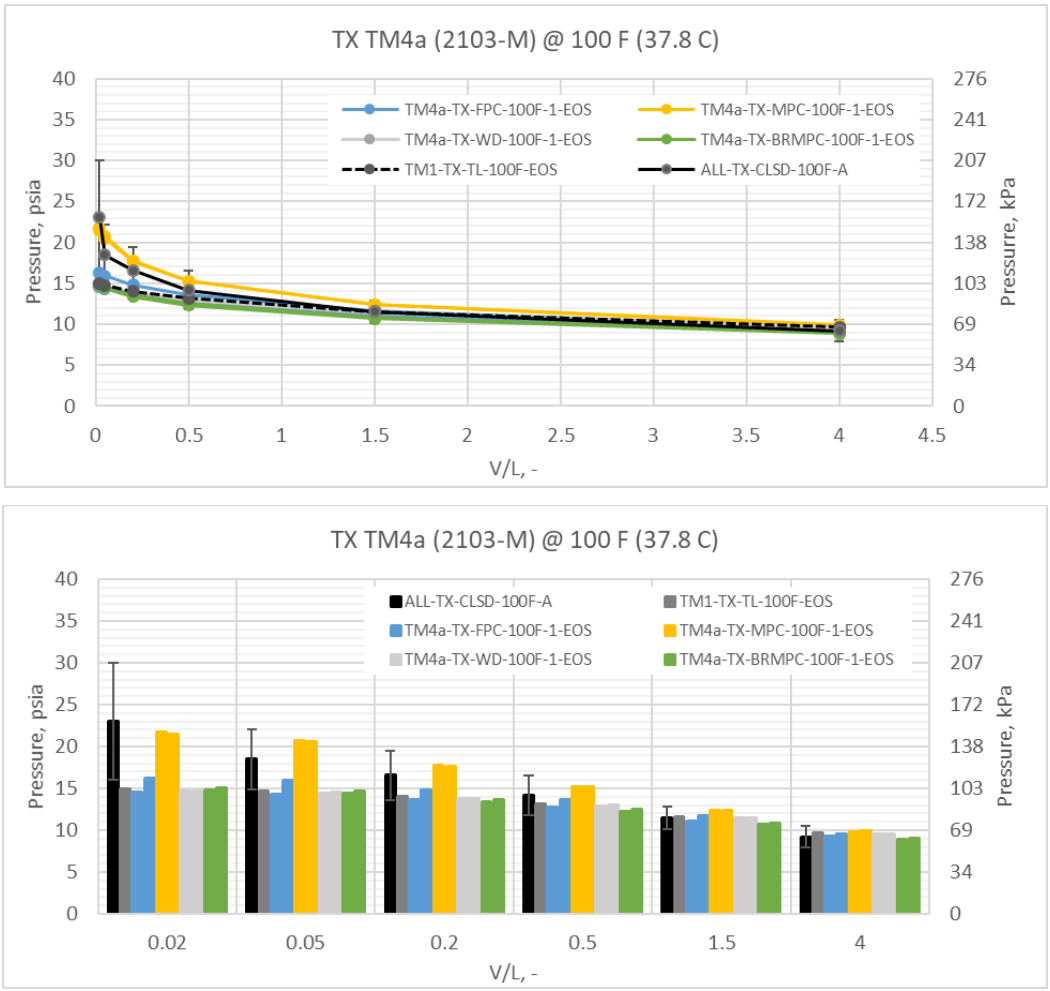

Figure 5-31. Pressure-expansion curve and bar chart comparisons of VPCRx(100°F) generated by EOS model from TM4a, TM1, and D6377 instrument for TX Eagle Ford samples.

5.5.5 Comparisons of TM3 and TM4 Composition for TX Eagle Ford Oil.

Whole oil composition for N2 through nC5 mole fraction as determined by both TM3 and TM4 are compared for all sample types in Figure 5-32 bar charts for the TX Eagle Ford samples. Sampling method is denoted by color; TM4 results are differentiated by black outline; and only the first replicate for TM3 results is shown for clarity. TM1-TL results are also included in the charts for reference.

Notable differences in mole fraction are observed between TM3 and TM4 for N2, again the differences are dominated more by sample-to-sample differences than lab-to-lab except for TM4 WD and BRMPC. On average, TM4 shows slightly higher N2 content. Though, the reader is reminded that N2 for TM4 reflects the sum of O2 and N2 eluted in the test method. For C1, TM3 and TM4 show similar mole content, except TM4-BRMPC is significantly lower. For mid-range hydrocarbons C2 (ethane) through nC5 (n-pentane) presented in the lower chart of Figure 5-32, no significant differences were observed by test method or sampling method. All methods yielded effectively the same hydrocarbon content.

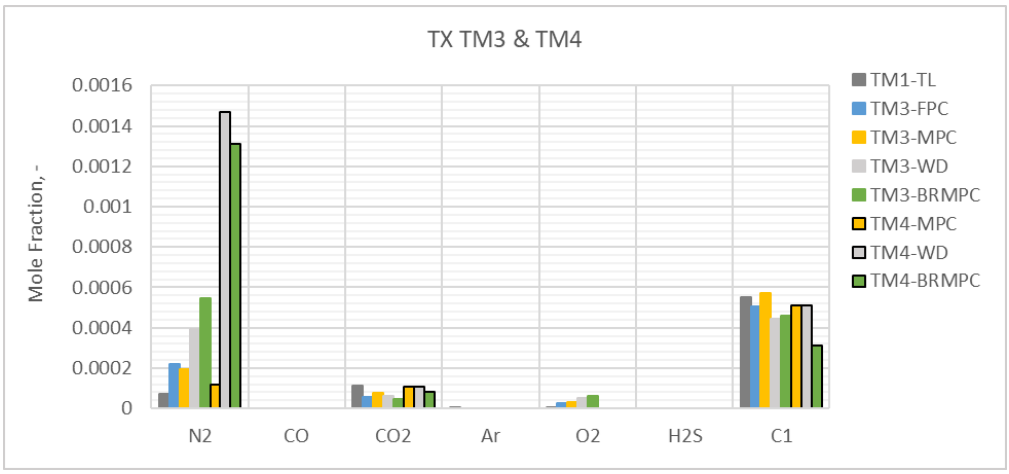

N2 is N2+O2 for TM4

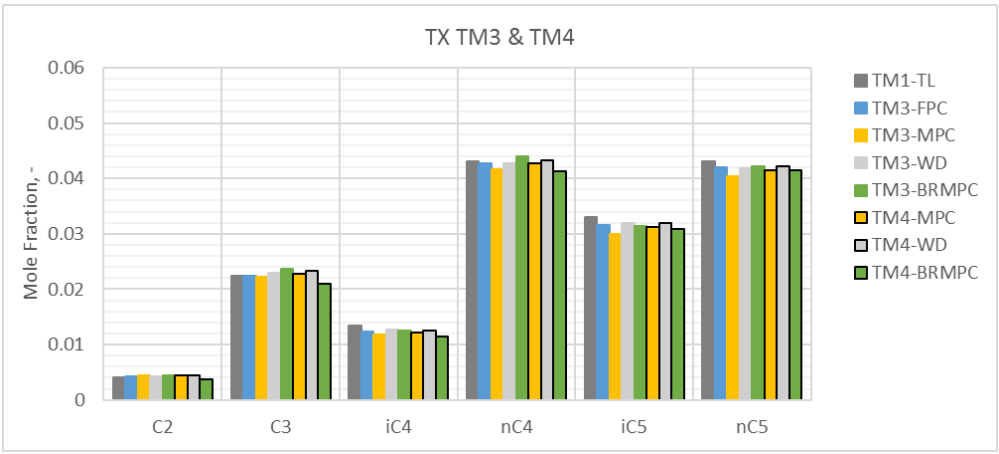

Note: TM4-FPC not available. Only replicate 1 for TM3 is shown. TM4 data outlined in black.

Figure 5-32. Bar chart comparison of composition for TX Eagle Ford TM3 and TM4 samples. Components N2 – C1 in upper chart and C2 – nC5 in lower.

5.5.6 Comparison Across Task 2 Compositional Test Methods

5.5.6.1 Measured light ends and fixed gases

Light ends and fixed gas compositions measured by all test methods are compared using bar charts provided in Figure 5-33 for TX Eagle Ford sampling methods. Mole fractions of each component were averaged across all closed sample methods and replicates and averaged across all open BR samples and replicates for each test method. In the figure, the four bars after TM1-TL are closed sample results and the last four bars (outlined in black) are open BR sample results. N2 mole fractions are small, but high relative to TM1-TL (dark gray) and vary by an order-of-magnitude (1e-4 to 1.3e-3). C1 mole fractions for closed samples are similar to TM1-TL except for TM2 which is a factor of 2 higher. Open BR sample results for C1 are low relative to the TM1-TL baseline and lower than closed sample results, except (again) for TM2 which is high. Results for components C2 – nC5 from all test methods are similar, with TM2 (blue), as for ND, consistently showing the lowest mole fraction for both closed and open samples.

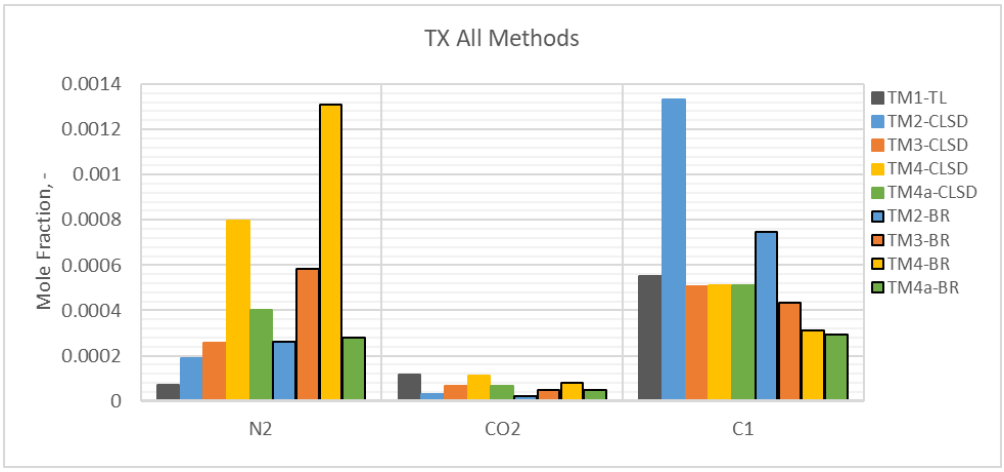

N2 is N2+O2 for TM4

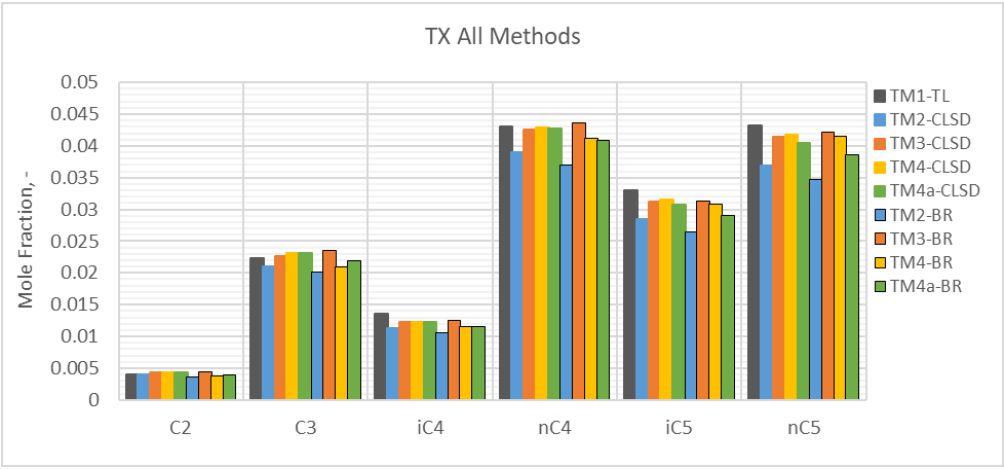

Figure 5-33. Comparison of averaged measured light ends and fixed gases from each test method – TX Eagle Ford samples. Results for Boston Round samples are outlined in black.

5.5.6.2 EOS modelled vapor pressure

EOS modelled vapor pressure expansion data for all test methods are compared two ways in Figure 5-34 – bar charts (upper plot) and as VP vs. V/L curve plots (lower plot) for TX Eagle Ford sampling methods. Also included in the figure are average measured VPCRx for closed sampling method (AVG-CLSD-Meas) and the LAB1 baseline using FPC sampling (LAB1-FPC-Meas). EOS VP results for open BR samples are outlined in black in the bar charts and shown as black dashed lines in the curve plots. EOS results for both open and closed sampling methods are low and variable relative to the average measured for all test methods, except TM4 open and closed which are consistently high. These results are consistent with previous results in that variability diminishes as V/L increases. Also, all EOS results for closed samples fall within the 2σ bounds of AVG-CLSD-Meas and are similar to the LAB1 measured baseline. For open sampling methods, EOS VP results for both TM2 and TM4a are consistently low.

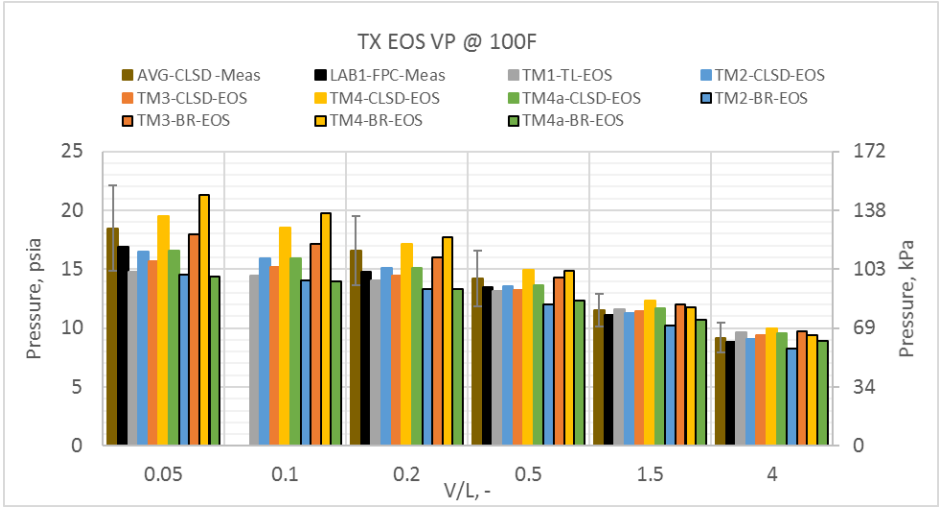

Note: first two bars are measured data, remainder are EOS estimated.

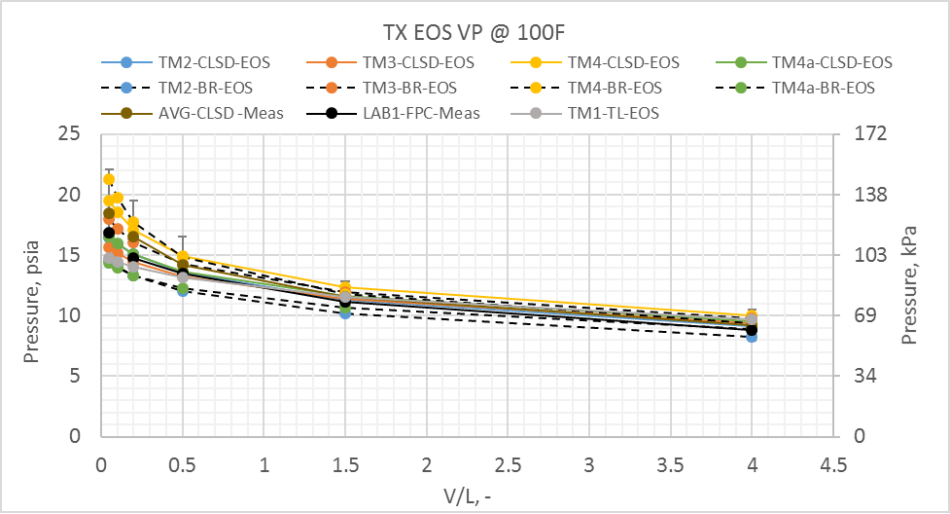

Figure 5-34. Comparison of EOS modelled vapor pressures at 10 °F for averaged results for each test method – TX Eagle Ford samples. Results for Boston Round samples are outlined in black in top figure and shown with black dash in bottom figure.

5.5.7 Comparison of TM3 Compositions for ND Bakken and TX Eagle Ford Summer Samples

Whole oil composition for N2 through nC5 mole fraction as determined by TM3 for ND Bakken and TX Eagle Ford are compared Figure 5-35 bar charts. Sampling method is denoted by color; TX Eagle Ford results are differentiated by black outline; and only the first replicate is shown for clarity. TM1 results (dark gray) are also included in the charts for reference. Wide variances are observed for N2 in Figure 5-35, but dominated more by sample-to-sample differences than by production source. Taking an average across sampling methods, TX and ND show similar N2 content. For C1, TX shows consistently higher mole content than ND. For mid-range HCs C2 (ethane) through nC5 (n-pentane) presented in the lower chart of Figure 5-35, additional differences were observed between locations – mole fraction for C3, nC4 and nC5 were up to 1.5% higher for the ND Bakken oil, which supports the higher BPP and GOR measurements for that oil.

This is an instructive case that reminds the reader that observed equilibrium vapor pressure and gas-oil ratio of a crude oil results from a weighted sum across relevant volatile components rather than from a single component. As such, the presence of more C1 measured in the TX Eagle Ford samples shown in Figure 5-35 does not necessarily drive the BPP and GOR higher than observed in the ND Bakken. On the contrary, the presence of higher C2, C3, and nC4 all together in ND Bakken actually shift the BPP and GOR (@100°F) higher than the TX Eagle Ford sampled in this work.

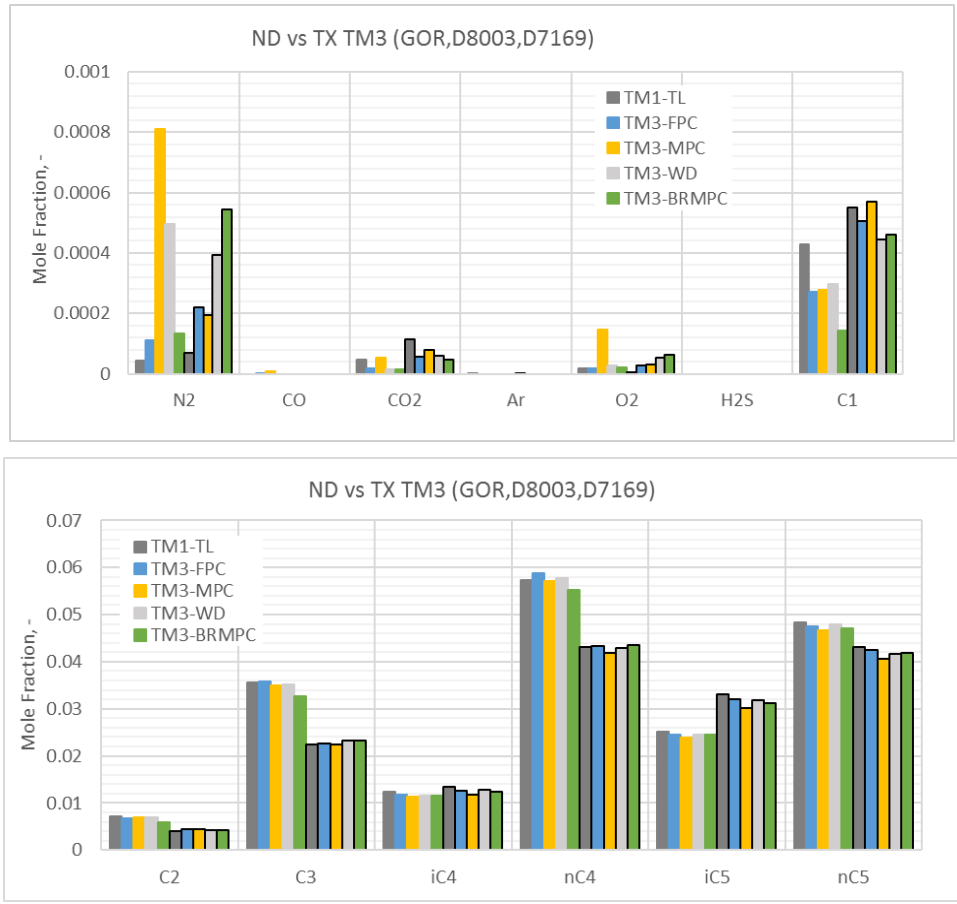

Note: only replicate 1 is shown. TX-TM3 data outlined in black.

Figure 5-35. Bar chart comparison of composition from TM3 for ND Bakken and TX Eagle Ford samples (black outline). Components N2 – C1 in upper figure and C2 – nC5 in lower figure.

5.6 Composition – Wide Boiling Range Data

Compositional data for all five test methods (TM1, TM2, TM3, TM4 and TM4a) were transmitted to Sandia in carbon number reports. The light ends and fixed gas results were presented above in sections 5.3 and 5.5. The middle and heavier hydrocarbons were also reported, though each laboratory had its own specific numerical merge process and groupings of isomers, BTEX, etc. As such, direct comparison by carbon number grouping, especially for C6-C9, was more difficult than for the light hydrocarbons. It is important to emphasize that the compositional data from each lab

was imported into the PSM basis environment in such a way that minimal interpretation by Sandia was required in order to preserve the original data, and mass% vs. boiling range data were maintained as reported to the extent possible. Graphics are shown below which compare the carbon number reports in a visual format, though carbon number groupings in the C6-C10 range do not necessarily imply a single boiling point for each grouping in the PSM. For the comparisons in this section the average of all closed sampling methods for each compositional test method is used.

5.6.1 ND Bakken Carbon Number Plots

Starting with Figure 5-36 upper plot, the light components that drive the vapor pressure at ambient temperature barely show at the current linear scale. The mole fractions visibly increase from C2 to a peak at C8 around mole fraction 0.10-0.12 and then decrease in a tapering fashion monotonically with carbon number. Differences in the lightest gases through C3 are nearly indistinguishable by simple visual inspection of sampling method or compositional analysis method. Visible differences start to appear for C4-C9, though some of this effect is driven by individual labs' methods for grouping these components. All test methods show a range of responses for C7 and C8 from 0.08 to 0.12 mole fraction with TM4 (but not TM4a) showing slightly higher mole fractions for C7-C9. Recall that a simple C8-C30+ merge was performed by Sandia for TM1 and a C7-C30+ merge was performed for TM4a. Heavy ends generally overlay well for C10 and up. The effect of lumping heavy ends into a C25+ versus a C30+ group can be seen at the right end of the carbon number axis, where TM2 and 3 terminates with a C25+ hypo group and TM4 and 4a terminates with a C30+ hypo group. Lumping into a single hypo group effectively integrates under all of the higher carbon numbers and places them into a single group.

The lower plot in the figure uses a log scale for mole fraction, which highlights small differences in the light ends and fixed gases. Because vapor pressure around ambient temperature is so strongly driven by the individual component vapor pressures of the lightest components, this format is actually more useful to interpreting where meaningful differences may be seen. Note the highest N2 mole fraction appears for TM3-MPC, which also returns the highest EOS-calculated VPCR at low V/L (see Figure 5-11). The VPCRx(100°F) observed at larger V/L from 1.5 to 4.0 is driven more by the C2-C4 components, which fall close together in mole fraction and thus support the convergence of the expansion curves in this V/L range (see Figure 5-11, Figure 5-13, Figure 5-27).

Implications on EOS simulations of PVT behavior at higher temperature are addressed in section 5.13.

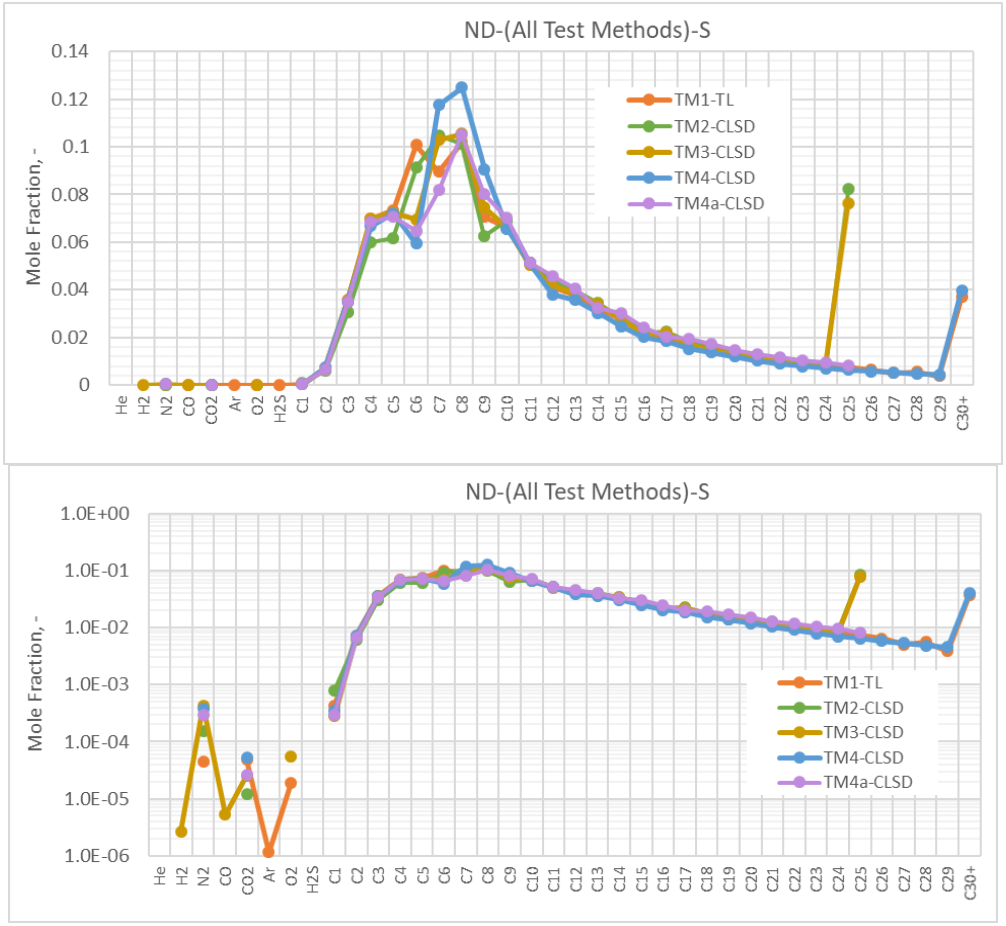

N2 for TM4 is N2+O2

Figure 5-36. Aggregate plot of mole fraction versus carbon number for average ND Bakken summer closed samples for all test methods using both linear (top) and log (bottom) scales.

5.6.2 TX Eagle Ford Carbon Number Plots

Average closed-sample carbon number plots for the TX Eagle Ford test methods are shown in linear and log scales (Figure 5-37). Linearly scaled data is shown in the upper plot, log-scaled in the lower. Similar to what was observed for the ND Bakken, the mole fractions for dissolved gases are all very low, but then concentration visibly increases from C2 to a peak at C8 around mole fraction 0.10-0.12 and then decreases in a tapering fashion monotonically with carbon number. Note that simple numerical merges were also performed by Sandia for TX Eagle Ford TM1 an TM4a.

Light ends and fixed gases are indistinguishable at the linear-scale shown here but segregate at the log-scale in a way that helps identify N2 levels that drive differences in vapor pressure at T = 100°F and low V/L. The middle carbon numbers C6-C10 vary among methods as they did for the ND oil with TM4 (but not TM4a) showing slightly higher mole fractions for C7-C9 and lowest above C9. Recall that a simple C7-C30+ merge was performed by SNL for TM4a. The small differences over C10-C19 are immaterial for calculating vapor pressure at low temperature. Implications on EOS simulations of PVT behavior at higher temperature are addressed in section 5.13.

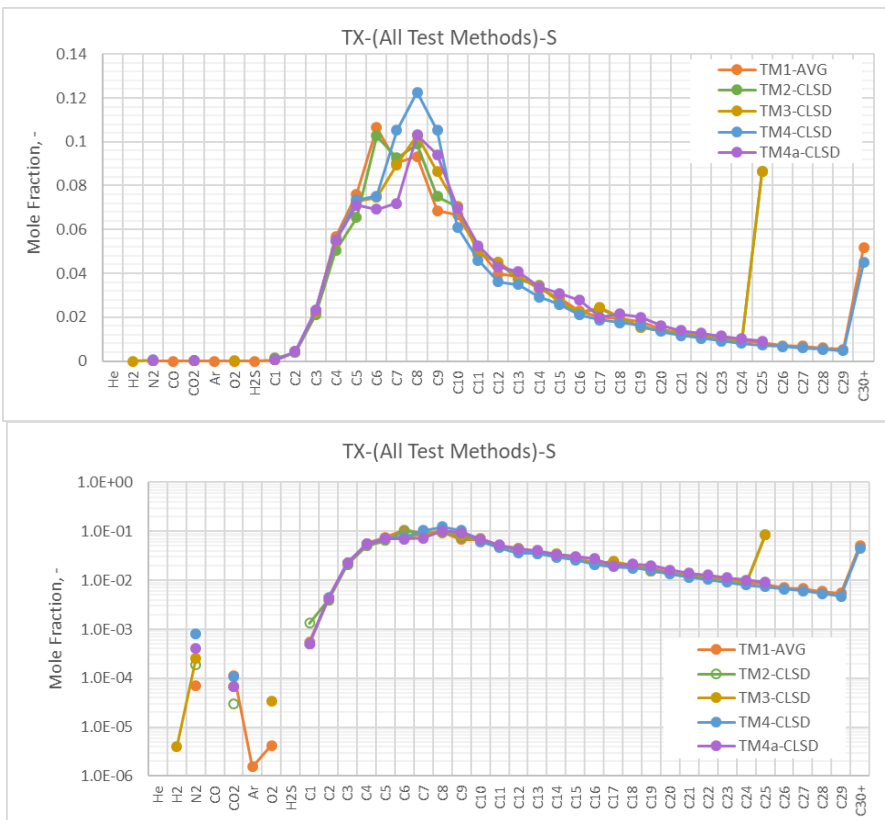

For TM4 N2 is N2+O2

Figure 5-37. Aggregate plot of mole fraction versus carbon number for the TX Eagle Ford summer samples for all test methods using both linear (top) and log(bottom) scales.

5.7 Selected Physical Properties – Winter Samples

Selected physical properties data for the ND Bakken and TX Eagle Ford winter samples collected in this study are shown in Table 5-14. Both oils are considered light (≥ 33°API) crudes by API guidelines (API 2011), with the ND Bakken only marginally lighter.

Table 5-15 provides sulfur weight % by ASTM D4294 for multiple winter samples. All samples tested here would be considered "sweet," with total sulfur well below the 1.0 mass% designation suggested by API (API 2011). No significant differences in total sulfur are observed when comparing open (BR) vs. closed (MPC, WD) sampling. ND Bakken MPC is about 5-9% lower than other Bakken measurements.

Table 5-14. Selected physical properties for ND Bakken and TX Eagle Ford oil samples.

TM4 2103M Property	ND Bakken	TX Eagle Ford
	2A-W	2A-W
Relative Density at 60°F	0.7997	0.7932
API Gravity at 60°F	45.44	46.88
Molecular Weight	154.76	166.55

Table 5-15. Sulfur wt% by ASTM D4294.

Sample Method	ND Bakken, wt%	TX Eagle Ford, wt%
BR1 - D4057	0.0848	-
BR2 - D4057M	0.0871	0.1397
BR3 - D5842	0.0866	0.1457
MPC - D8009	0.0796	-
WD - GPA2174	0.0843	0.1297
Winter Open Avg	0.0862	0.1427

5.8 Measured Vapor Pressure – ND Bakken Winter Samples

Figure 5-38 shows a bar chart and pressure-expansion curve summaries of measured VPCRx(100°F) (37.8°C) for winter samples of ND Bakken. Bars are grouped by vapor/liquid ratio, V/L, from 0.05 to 4.0. and are color-coded by winter sampling method (W-MPC, W-BR1MPC, W-BR2MPC, W-BR3MPC, W-BR1). Two replicates are shown.

The samples fall into ever tighter bands as V/L approaches 4.0 with all sampling types give generally the same results. This was also observed for the summer samples as discussed in sections

5.2 and 5.4, where both open and closed industry standard sampling methods yielded samples of nearly equivalent vapor pressure, provided certain conditions for sampling and analysis were met.

Also consistent with summer samples is the large variability in the VPCR data at low V/L, which continues to suggest that there are some outlier spot samples that may be associated with notably more nitrogen/air than was seen in TM1-TL sampling.

The purple W-BR1 data shown in Figure 5-38 for V/L = 1.5 and 4.0 are ambient BR samples that were drawn into the D6377 device out of the bottle using the standard procedure via vacuum draw (no chilling or MPC). Results at these V/L are essentially identical to the modified samples BR1MPC, BR2MPC and BR3MPC. The D6377 standard does not recommend this procedure for V/L< 1. VPCR for the three BR-MPC winter samples show differences decreasing to almost zero at V/L=4.

An alternate means to present the same data is shown in an overlay of pressure-expansion curves in the lower chart of Figure 5-38, where the x-axis is scaled to V/L. This provides physical significance to the x-axis, indicating that the VPCR increases more steeply as V/L decreases. The figure emphasizes the differences at low V/L and convergence as V/L increases.

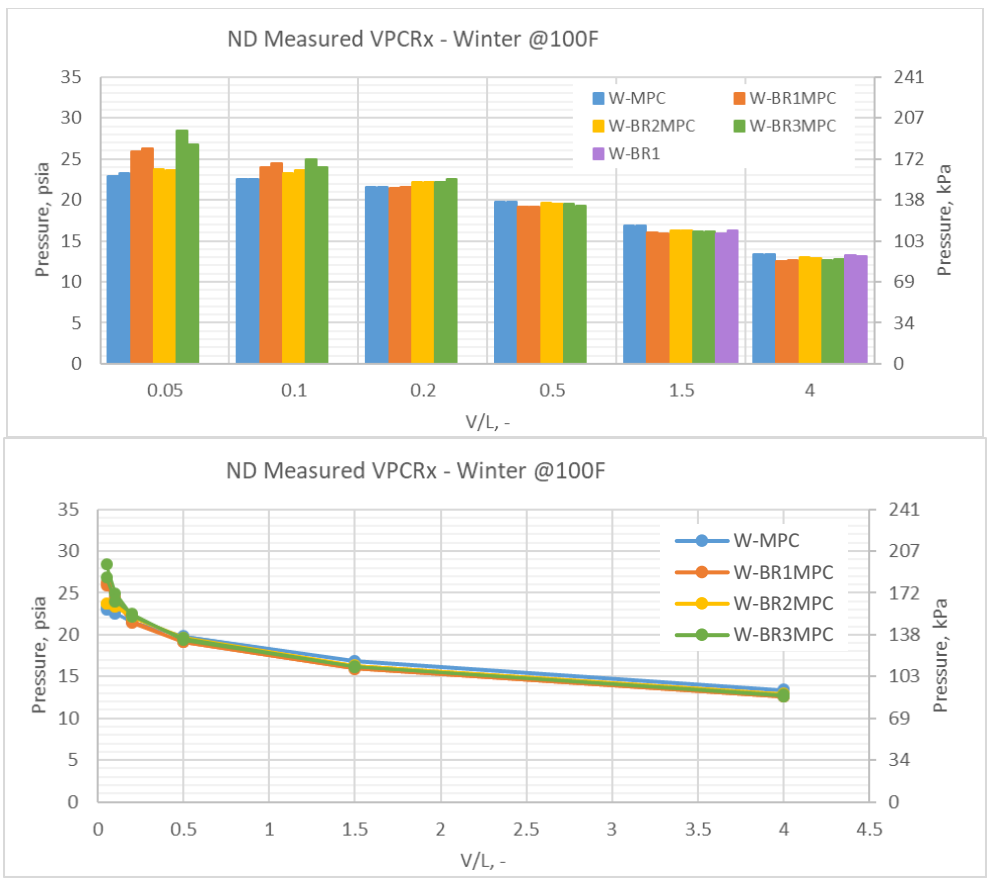

Figure 5-38. Bar chart and pressure expansion curves of VPCRx(100°F) for the ND Bakken winter oil color coded by sampling type.

5.9 Composition – ND Bakken Winter Samples

Compositional data were only obtained by TM4 (GPA 2103M) for ND Bakken winter samples. No baseline TM1-TL analyses were performed. Results are compared below by sampling method. In addition, EOS performance using the same compositions is compared with measured D6377 VPCRx(100°F) (37.8°C) data. As with summer samples, hydrocarbon content generally compares well, with no strong distinction evident across sampling method on the hydrocarbon basis. Methane (C1) is an exception to this, though the net effect is lost when looking at measured or EOS-simulated vapor pressure. A close review of the C2-C5 data indicate that the closed FPC method also tends to retain slightly more of these light ends that the open methods, though this effect is not apparent in the direct VPCR measurements (see Figure 5-38) These small differences may fall within the inherent uncertainty in VPCR and compositional measurement methods. Several of the spot samples showed high N2 content, and current hypothesis is that this phenomenon is attributable to a sample acquisition or handling step and is likely not a feature of the parent sample material collected from process line on-site in ND.

5.9.1 TM4: GPA 2103M+ASTM D2887 Merge

5.9.1.1 Measured light ends and fixed gases

Whole oil composition for open and closed winter samples for N2 through nC5 mole fraction as determined by TM4 is shown in Figure 5-39 for the ND Bakken samples. Sampling method is denoted by color. A single analytical run was obtained by TM4 for each sample type. TM4 does not analyze for O2 independently, rather it elutes with N2 so that the N2 peak represents the sum of N2 and O2 in the sample.

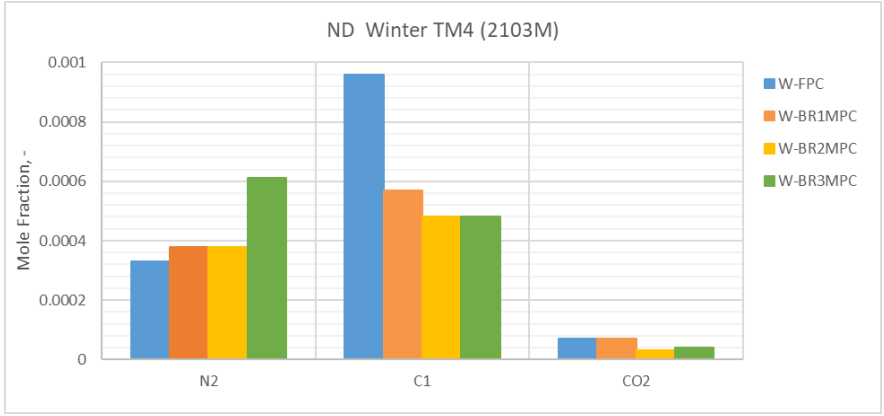

N2 is N2+O2

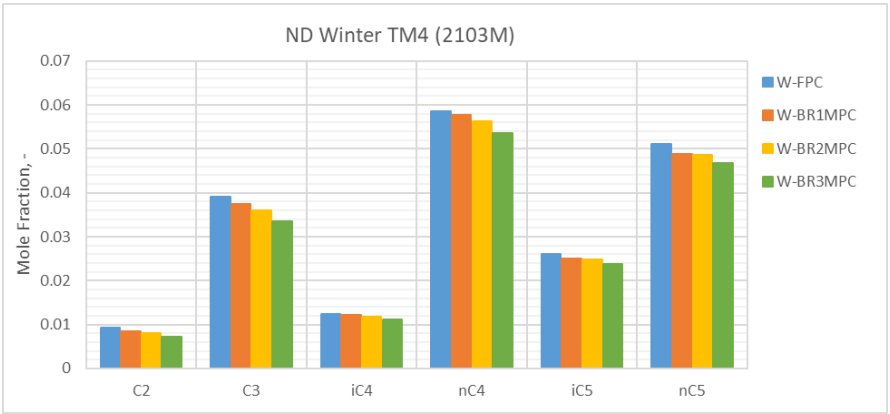

Figure 5-39. Mole fraction of components nitrogen (N2) through n-pentane (nC5) as measured by TM4 for ND winter samples. Sampling type is denoted by bar color.

Mole fraction data in Figure 5-39 are generally consistent across all samples with slightly high values of N2 for the W-BRMPC and C1 for the W-FPC visible in the upper plot. This variability is not unusual for light-end data in this study given that open samples are exposed to air and greater relative retention of light gases is expected in closed samples. For C2 (ethane) through nC5 (n-pentane), no significant differences were observed by test method or sampling method, though W-FPC appears to yield mole fractions consistently a little higher than the open methods. There appears to be a small decreasing mole fraction trend across the three BR samples, though this is difficult to substantiate because BR1MPC through BR3MPC used increasing rigor to retain light ends, which should lead to the opposite trend, if any. Moreover, the VPCR direct measurements did not show any systematic effects of sampling type in the winter data. Summary observations here are that all of the winter sampling methods yielded effectively the same compositions, excepting some subtle losses of C1 in open vs. closed.

5.9.1.2 EOS Calculated Vapor Pressure from TM4 Composition

EOS model estimates of VPCRx(100°F) were generated using the compositional data from TM4 for all ND Bakken winter samples and are compared with the W-MPC D6377 measured VPCRx. The results are presented in pressure-expansion curve (top) and bar chart (bottom) formats in Figure 5-40.

The EOS-simulated ND Bakken winter pressure-expansion are shown in Figure 5-40 (upper), The pressure-expansion curves fall into a tight band bounded on top by the FPC-EOS result, which had the highest C1-nC5 content. Results from all approaches agreed within a ~3 psi. The differences were driven largely by sample-to-sample variances in C1-nC5 content that can be seen in Figure 5-39 above and thus the shift across all V/L.

While the FPC forms the upper bound on the VPCR Figure 5-40, its closed-sampling equivalent MPC for directly-measured VPCRx(100°F) shown in Figure 5-38 does not similarly form an upper bound or stand out from the other methods across the V/L range tested. The reason for this difference is unclear.

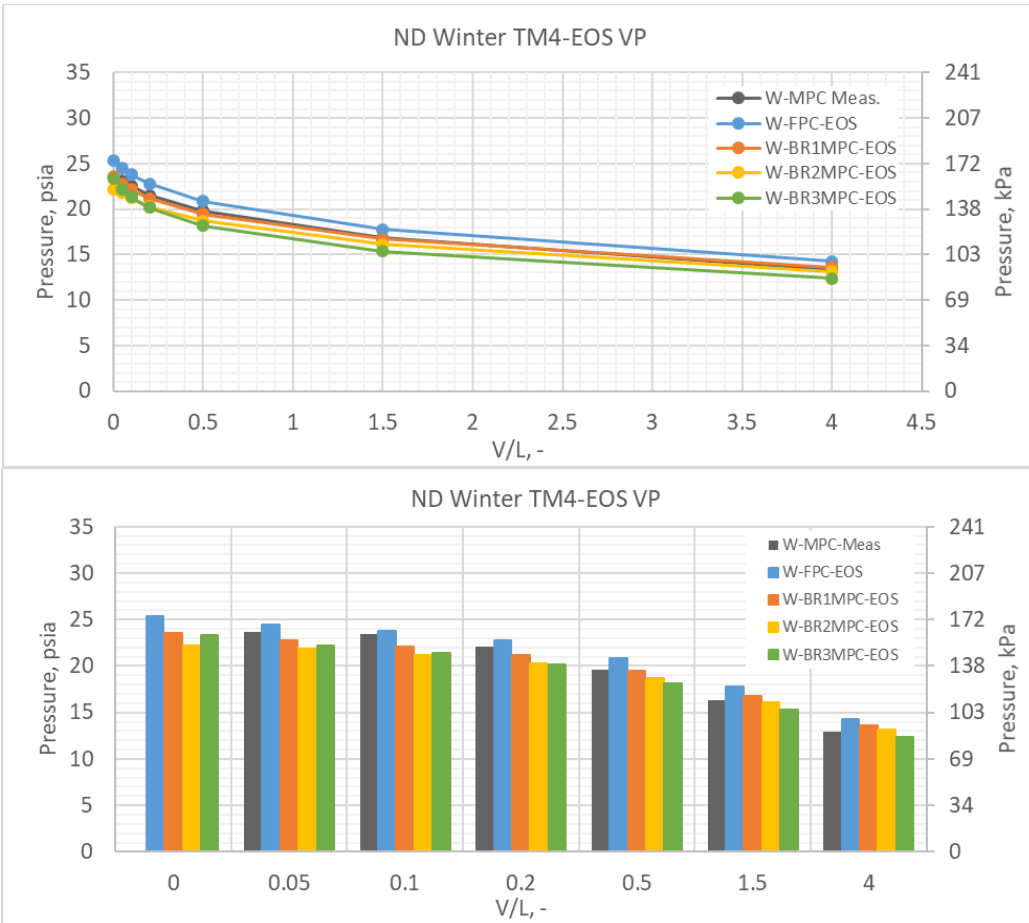

Figure 5-40. Pressure-expansion curve (top) and bar chart (bottom) comparisons of VPCRx(100°F) generated by EOS model from TM4 compositions for ND Bakken winter samples.

5.10 Measured Vapor Pressure – TX Eagle Ford Winter Samples

Measured VPCRx (100°F) (37.8°C) for the TX Eagle Ford winter samples are shown in Figure 5-41. The color of each bar represents a sampling type (FPC, WD, etc.). Similar to what was observed for the ND Bakken sample, TX Eagle Ford VPCRx was relatively insensitive to sampling

method and results collapsed to tighter bands as V/L increased. Pressure-expansion-curves are bounded on the low side at small V/L by the BR1MPC data and on the high side by BR3MPC.

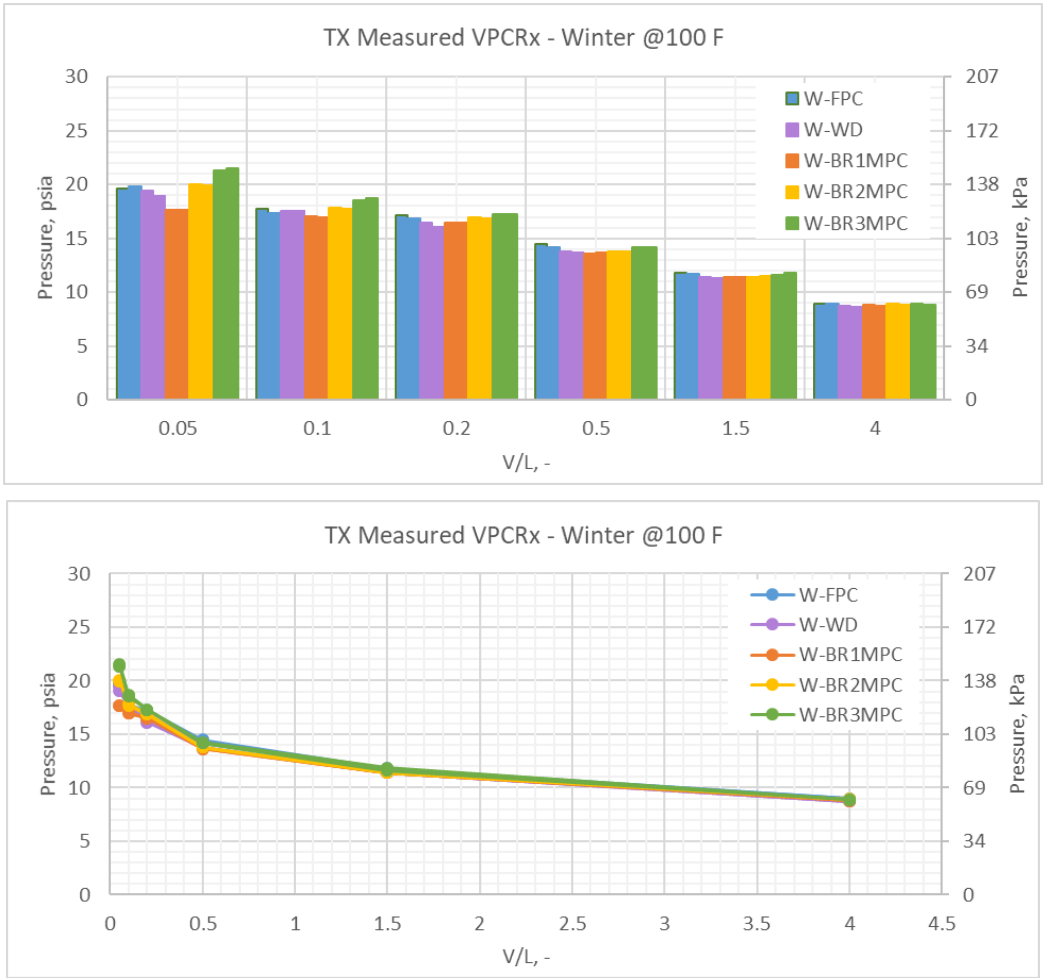

Figure 5-41. Bar chart (top) and pressure-expansion curves (bottom) showing VPCRx(100°F) for the TX Eagle Ford winter oil samples sorted by V/L and sampling type.

5.11 Composition – TX Eagle Ford Winter Samples

Compositional data were only obtained by TM4 (GPA 2103M) for TX Eagle Ford winter samples. Results from TM4 are compared below on a component-by-component basis for components N2-nC5. In addition, EOS performance using the same compositions is compared with average measured D6377 VPCR for the two closed sample capture methods (FPC, WD). Generally, hydrocarbon contents compare well with no strong distinction evident across sampling method or analysis method on the hydrocarbon basis. Spot samples showed variability in N2 content and current hypothesis is that this phenomenon is attributable to a sample acquisition or handling step and is likely not a feature of the parent sample material collected from process line on-site in TX.

5.11.1 TM4: GPA 2103M+ASTM D2887 Merge

TM4 was applied to the TX Eagle Ford samples for a FPC and the three BRMPC sample techniques. Recall TM4 does not analyze for O2 independently, rather it elutes with N2 so that the N2 peak represents the sum of N2 and O2 in the sample.

5.11.1.1 Measured light ends and fixed gases

TX Eagle Ford whole oil composition for N2 through nC5 mole fraction as determined by TM4 for winter samples is provided in Figure 5-42 bar charts. Sampling method is denoted by color. Similar to what was observed throughout this study, high N2 is observed in some spot sampling. This observation generally holds for both oil sources (ND Bakken, TX Eagle Ford), both seasons, and all spot sampling methods. C1 for W-FPC is higher than for all three W-BR methods, and this is also consistent with observations across the study that the closed methods appear to retain more C1 than open. The C2 through nC5 groups showed consistent behavior across all sampling methods.

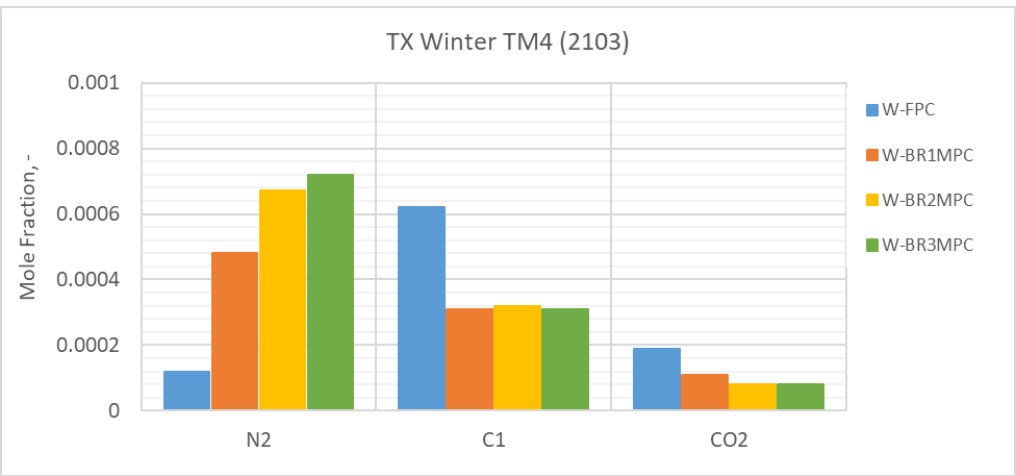

N2 is N2+O2

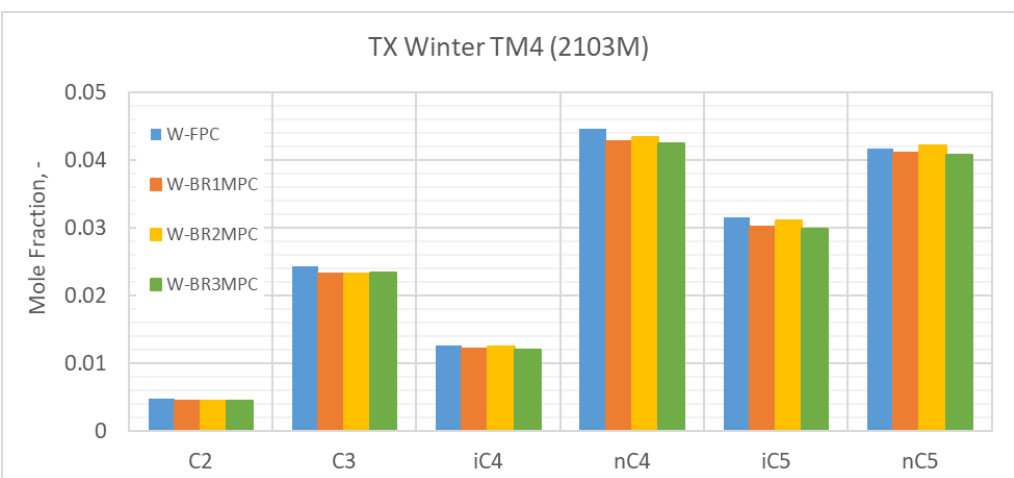

Figure 5-42. Bar charts showing mole fraction of components nitrogen (N2) through n-pentane (nC5) as measured by TM4 for TX Eagle Ford winter samples. Sampling type is denoted by bar color.

5.11.1.2 EOS Calculated Vapor Pressure from TM4 Composition

EOS model estimates of VPCRx(100°F) were generated using the compositional data from TM4 for all TX Eagle Ford winter samples and compared with measured D6377 VPCRx for the FPC sample capture method (the only closed sample). The results are presented in pressure-expansion curve and bar chart formats in Figure 5-43. EOS VP from all of the sampling methods effectively converge for V/L > 1, which is consistent with showing virtually identical hydrocarbon content (as opposed to ND winter data) with N2 content affecting VP at V/L < 1 where there is a 1:1 correspondence.

It is noteworthy that the FPC-EOS sample shown in Figure 5-43 forms a lower bound on VPCR where V/L < 0.5, in spite of the fact that it showed the highest C1 content in Figure 5-42. This highlights the effect of the relatively low N2 concentration found in the FPC-EOS sample. This is more evidence that the low V/L behavior is strongly influenced by sample-to-sample variations in fixed gases that may be introduced by sample handling. However,the influence dimishes and EOS-VP converges for V/L > 0.5. Generally, the EOS-VP expansion curves are flatter than measured, that is, 1-4 psi low at small V/L and 1 psi high at large V/L.

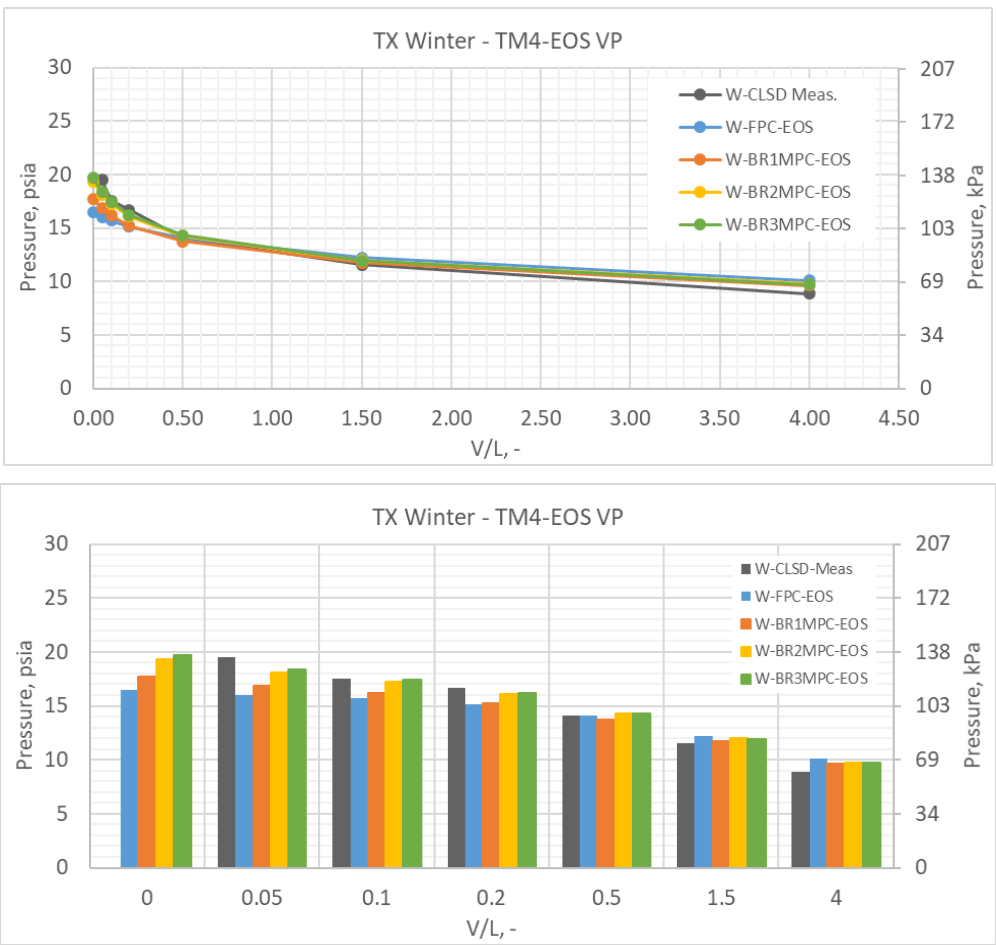

Figure 5-43. Pressure-expansion curve (top) and bar chart (bottom) comparisons of VPCRx(100°F) generated by EOS model from TM4 compositions for TX Eagle Ford winter samples. Bars color coded by sample type.

5.12 Summer and Winter Comparisons

A simple evaluation of the seasonal differences in the crude oils and the performance of the open and closed sampling methods is given below. Observations presented above indicate that sampling performance was not strongly seasonal. This suggests that the winter and summer oils from a given location may be similar in overall properties and composition – or at least similar enough to allow sampling performance to remain comparable across seasons. Data comparisons consist of averaged selected physical properties, VPCRx(100°F) and averaged TM4 compositional test method results for a limited set of closed sample methods and several open samples methods.

5.12.1 Selected Physical Properties

Selected physical properties data are compared in Table 5-16 for the ND Bakken and TX Eagle Ford samples collected in this study, denoted as 2A-W for winter samples and 2-S for summer samples. Also shown are the ratios of winter values to summer values (W/S). Both oils are considered light (≥33°API) crudes by API guidelines (API 2011), with the ND Bakken only marginally lighter. The W/S ratio indicates no significant difference between the summer and winter properties.

Table 5-16. Selected physical properties for ND Bakken and TX Eagle Ford oil samples. W/S is ratio of winter data to summer data. Task 2 summer (2-S); Task 2A winter (2A-W); Ratio winter to summer (W/S).

TM4 2103M Property	ND Bakken			TX Eagle Ford		
	2A-W	2-S	Ratio W/S	2A-W	2-S	Ratio W/S
Relative Density at 60°F	0.7997	0.8011	0.9983	0.7932	0.7899	1.0043
API Gravity at 60°F	45.44	45.12	1.01	46.88	47.64	0.98
Molecular Weight	154.76	151.83	1.02	166.55	165.10	1.01

Table 5-17 provides sulfur weight% by ASTM D4294 for average summer and winter values. All samples tested here would be considered "sweet," with total sulfur well below the 1.0 mass% designation suggested by API (API 2011). Slightly more difference in sulfur content is seen between summer and winter for TX Eagle Ford than for ND Bakken.

Table 5-17. Sulfur wt% by ASTM D4294.

Sample	ND Bakken, wt%	TX Eagle Ford, wt%
Winter Avg	0.0845	0.1384
Summer Avg	0.0863	0.1147

5.12.2 Measured VPCRx by ASTM D6377

5.12.2.1 ND Bakken measured VPCRx

Figure 5-44 provides a bar chart and pressure-expansion curve comparisons of average measured VPCRx(100°F) (37.8°C) for summer and winter samples of ND Bakken. Bars are grouped by vapor/liquid ratio, V/L, from 0.05 to 4.0. The first three bars (shades of gray) are averaged summer results the remaining bars are winter results. S-LAB1-FPC is the LAB1 summer sample; S-CLSD is the average of all closed summer samples; S-BRMPC is the average summer BRMPC. The height of each bar represents the sample mean VPCR, and the error bars represent the 2σ associated with the summer closed sample set. The remaining bars are color-coded by average winter sampling method – W-MPC (only closed method used for VPCRx) and W-BRMPC.

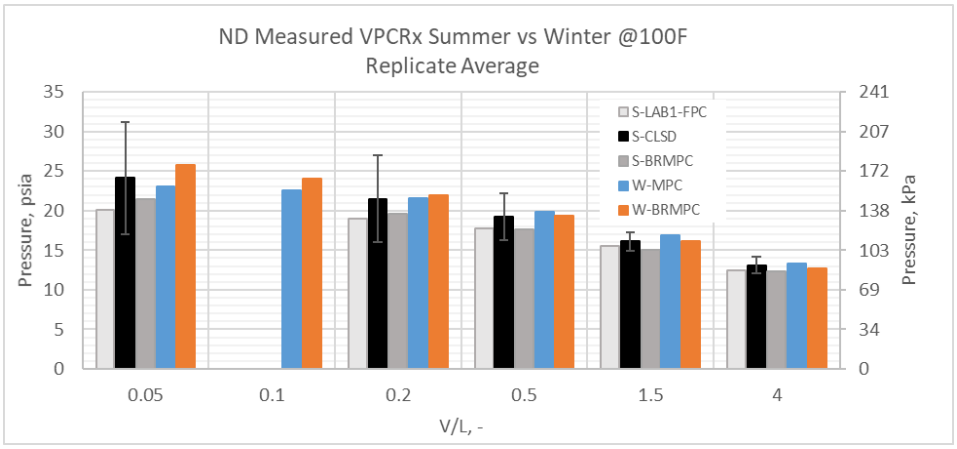

Note: First three bars are summer samples, remainder are winter. VPCR data was not collected at V/L= 0.1 for summer samples.

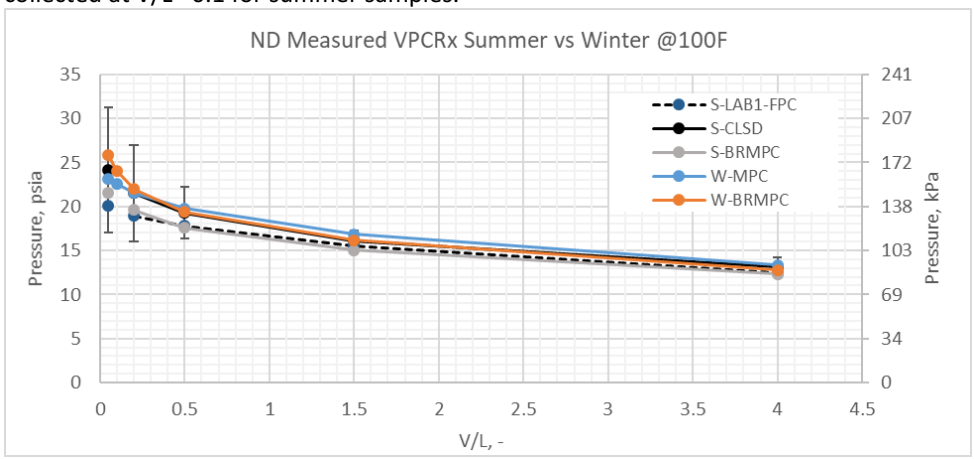

Figure 5-44. Bar chart showing VPCRx(100°F) vs. V/L for the ND Bakken summer and winter samples. S-CLSD is summer average and 2σ. S-LAB1-FPC is LAB1 D6377 measured.

When reviewing any particular V/L, all mean VPCRx(100°F), independent of sampling type or season, fall within the 2σ error bars for closed summer sampling. Error bars decrease in magnitude as V/L increases, and the samples similarly fall into ever tighter bands as V/L approaches 4.0. All sampling types in a given season give generally the same results. This was also observed for the summer samples, where both open and closed industry standard sampling methods yielded samples of nearly equivalent vapor pressure, provided certain conditions for sampling and analysis were met.

VPCR for the winter samples appear slightly higher (though within 2σ error bars) than the corresponding summer samples at all V/L with the difference decreasing to almost zero at V/L=4. The presence of slightly higher VPCR for winter samples would be expected as equilibration at open tanks upstream of the sampling point would lead to slightly higher VPCR oil in cold conditions than in warm conditions.

5.12.2.2 TX Eagle Ford measured VPCRx

Average measured VPCRx for the TX Eagle Ford winter samples (W-CLSD and W-BRMPC) are shown at T = 100°F (37.8°C) in Figure 5-45 and compared to summer VPCRx results for LAB1-FPC, average closed summer samples (S-CLSD) and average BRMPC. TX Eagle Ford VPCRx was relatively insensitive to sampling method and results collapsed to tighter bands as V/L increased. No seasonal trend in winter versus summer VPCR for the TX oil is observed.

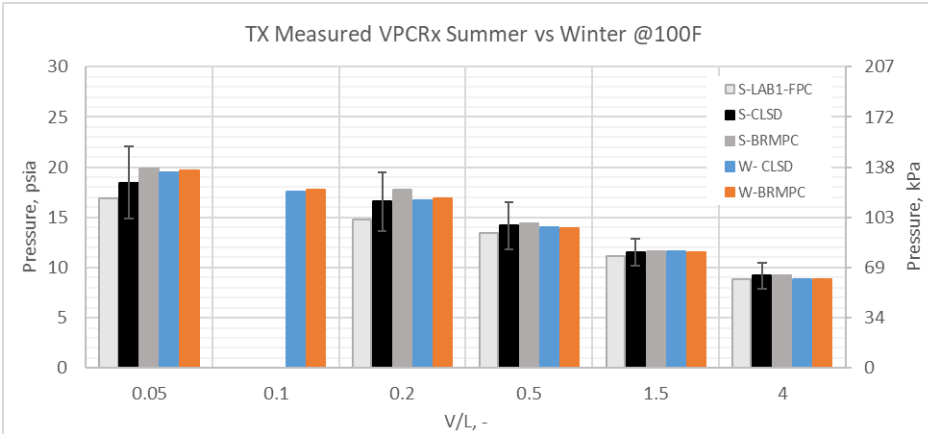

Note: First three bars are summer samples, remainder are winter. VPCR data was not collected at V/L= 0.1 for summer samples.

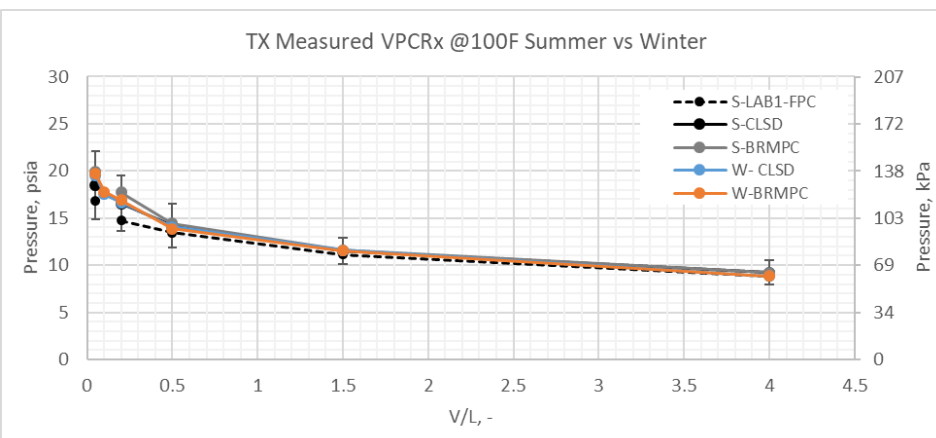

Figure 5-45. Bar chart showing VPCRx(100°F) vs. V/L for the TX Eagle Ford summer and winter samples. Black and gray curves are summer samples, remaining curves are winter samples. S-CLSD is summer average and 2σ . S-LAB1-FPC is LAB1 D6377 measured.

5.12.3 Composition

5.12.3.1 ND Bakken Measured light ends and fixed gases

Average whole oil compositions covering N2 through nC5 as determined by TM4 (2103M) for ND Bakken summer and winter, open and closed samples are compared using bar charts in Figure 5-46. The first three bars (shades of gray) are averaged summer results, the remaining bars are winter. Note that an FPC was the only closed winter sample method. Consistent with previous data, high, apparently random, variability in mole fraction across closed sampling types are observed for N2 and C1. All N2 values are similar but considerably higher than the summer TM1–TL with summer and winter BRMPC being the two largest. C1 content is variable with BRMPCs seasonally the smallest and C1 content for both winter samples are larger than their corresponding summer sample. For C2 through nC5, winter samples are slightly higher than corresponding summer sample but not in any practical sense. The open vs. closed and summer to winter differences are expected and consistent with the VPCRx results in Figure 5-44.

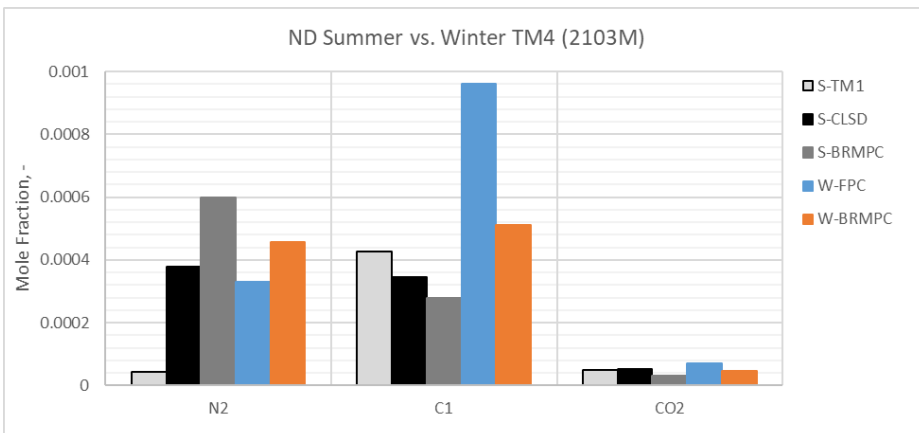

N2 is N2+O2 for TM4 results

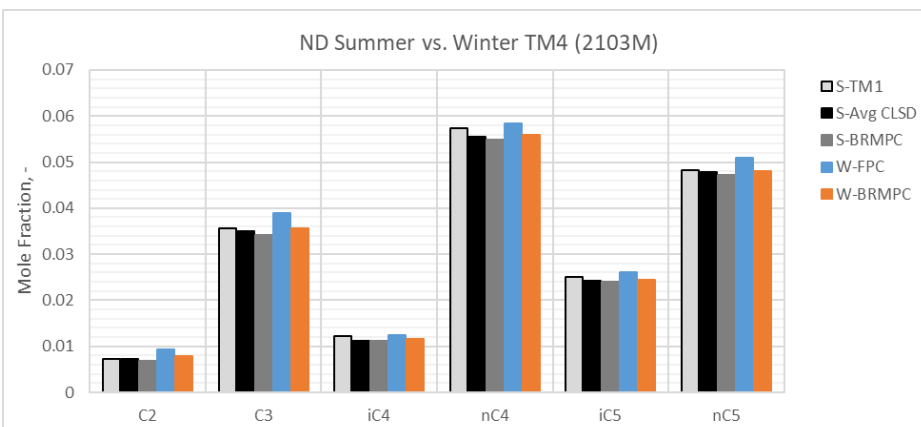

Note: First three bars are summer samples, remainder are winter.

Figure 5-46. Bar charts showing mole fraction of components nitrogen (N2) through n-pentane (nC5) as measured by TM4 for ND Bakken summer and winter samples.

5.12.3.2 TX Eagle Ford measured light ends and fixed gases

Average whole oil compositions covering N2 through nC5 as determined by TM4 for TX Eagle Ford summer and winter, open and closed samples are compared using bar charts in Figure 5-47. The first three bars (shades of gray) are averaged summer results the remaining bars are winter. Note that an FPC was the only winter closed sample method. The seasonal observations on TX Eagle Ford are essentially the same as for ND Bakken: N2 and C1 variability; N2 content higher in open samples; C1 higher in closed samples; C2-C5 content similar across all samples with winter values slighlty larger than corresponding summer values. However, summer to winter C1 content is more similar than it was for ND Bakken.

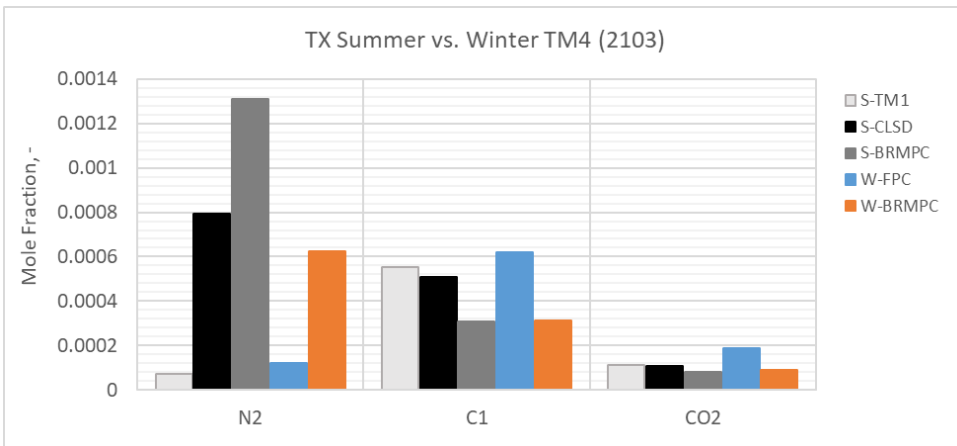

N2 is N2+O2

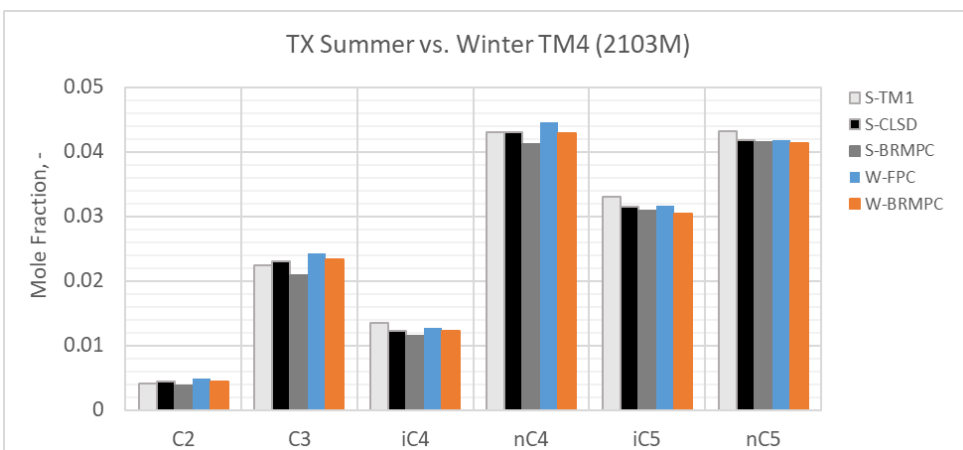

Note: First three bars are summer samples, remainder are winter.

Figure 5-47. Bar charts showing average mole fraction of components nitrogen (N2) through n-pentane (nC5) as measured by TM4 for TX Eagle Ford summer and winter samples.

5.12.4 EOS Modelled Vapor Pressure

Comparisons of summer and winter EOS modelled VPCRx(100°F) from average TM4 compositions are provided for ND Bakken and TX Eagle Ford crude oils in Figure 5-49. Open and closed samples were averaged separately and the winter closed sampling only consisted of an FPC. Also, shown are the summer TM1-TL baseline EOS results. Looking at the ND Bakken results in the upper plot, the W-FPC is shifted high across all V/L indicative of high C1 – nC5 content (refer to Figure 5-46). The remaining curves show spread at low V/L due to variability in N2 and C1 but converge at higher V/L due similar C2-C5 content. The TX Eagle Ford results (lower plot) show significant spread at low V/L that correlates directly with the N2 mole fraction and converge tightly for V/L >1 because of the similarity in C1-nC5 content. (See Figure 5-47). In both ND and TX results the S-TM1-TL baseline was the lower bound due to its very low N2 mole fraction.

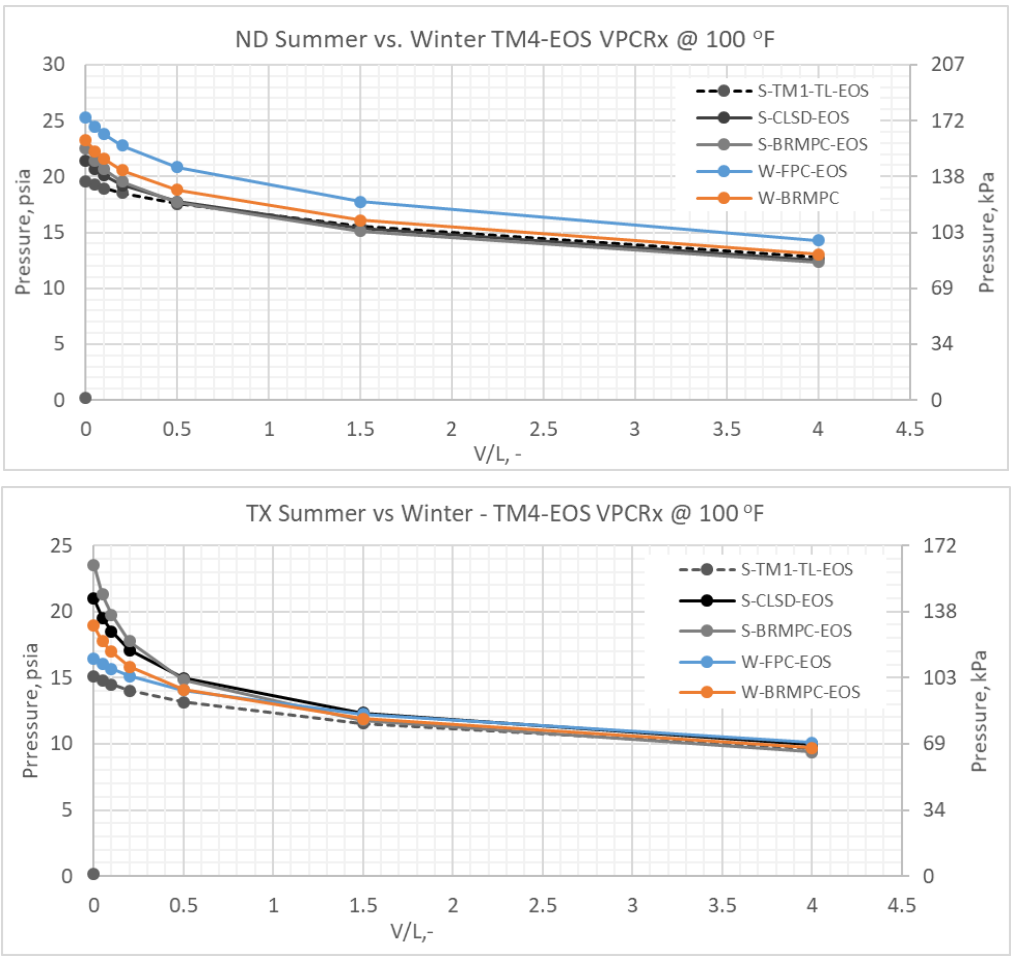

Figure 5-48. Comparison of summer and winter EOS estimated VPCRx(100°F) from average TM4 compositions and TM1-TL. Upper plot - ND Bakken; lower plot TX Eagle Ford.

5.12.5 Wide Boiling Range Data

Carbon number plots for summer and winter samples of ND Bakken and TX Eagle Ford crude oils using TM4 are compared in Figure 5-49 and Figure 5-50, respectively. Linearly scaled data is shown in the upper plot, log-scaled in the lower plot of each figure. Averaged data are used in the figures, where, W-FPC was the only winter closed sample type; W-BRMPC is the average of three BRMPC sample types; and S-TM4-CLSD is the average of all available closed summer sample data from TM4. Winter carbon number curves are very similar to summer data previously discussed in section 5.6 for both ND and TX oils, with small differences in very light-ends evident at the log scale and for C4-C11 using linear scale. The results indicate the summer and winter oils are for all practical purposes the same.

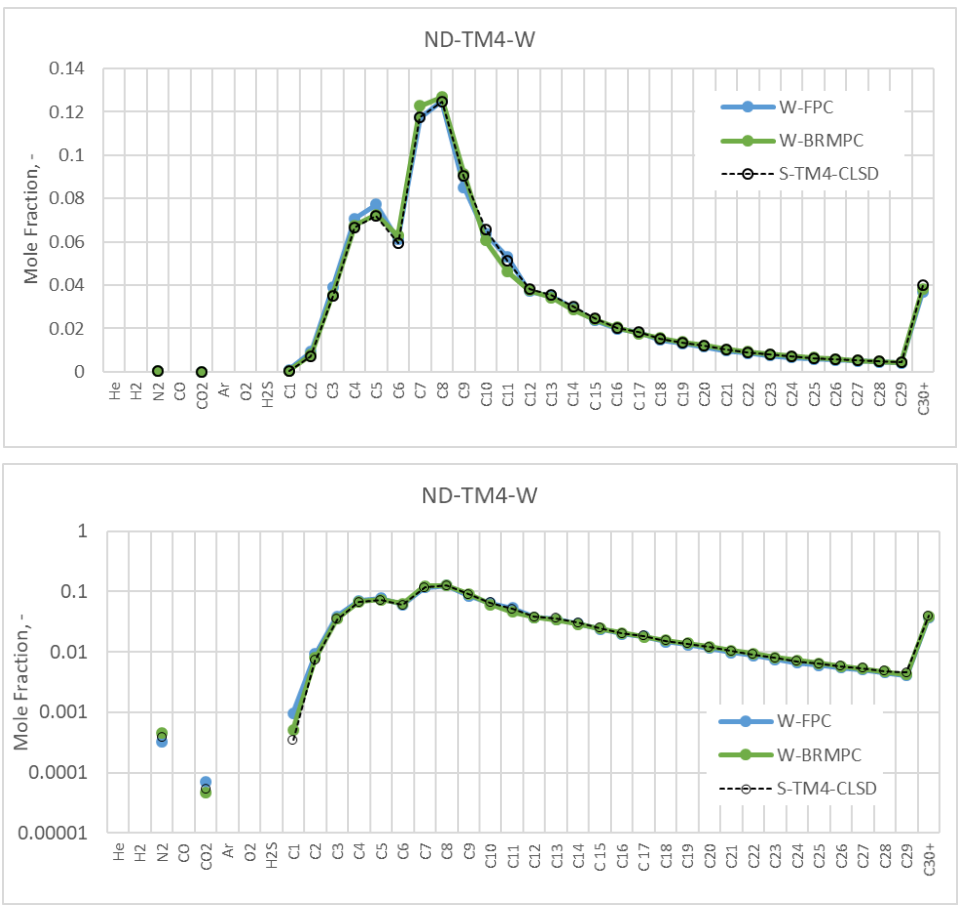

N2 is N2+O2

Figure 5-49. Aggregate plot of mole fraction (linear scale) versus carbon number for summer and winter ND Bakken samples – linear scale(top) and log scale (bottom).

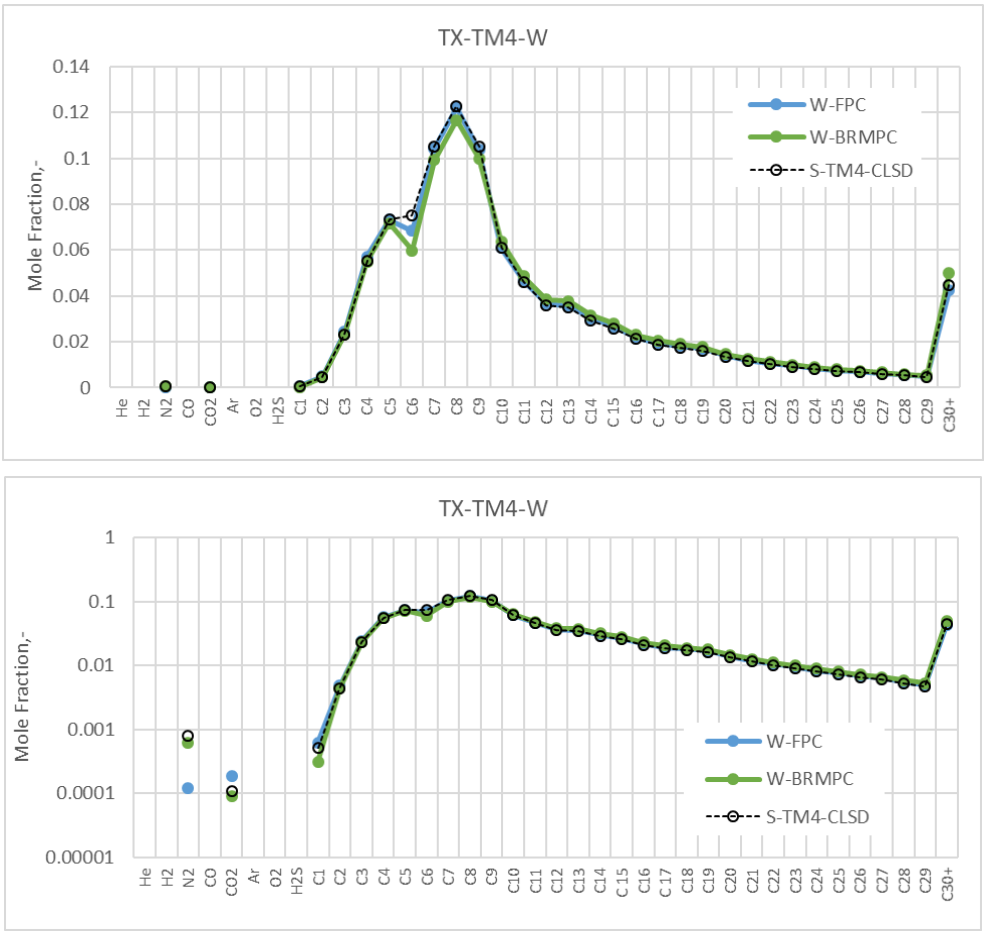

N2 is N2+O2

Figure 5-50. Aggregate plot of mole fraction (linear scale) versus carbon number for the TX Eagle Ford summer and winter samples – Linear scale (top) and log scale (bottom).

5.13 EOS Simulations for Bubblepoint Temperature at Sample Collection Point

The EOS model was used to estimate the temperature at which each oil stream (ND summer, winter; TX summer, winter) was equilibrated with local ambient pressure (bubblepoint temperature), and these computed values were compared to the observed feed stream temperatures. While ambient air temperature is expected to differ from the liquid temperature and exert some influence on the equilibrium flash process, when reducing the current comparison to a single value, the liquid temperature is likely more important than the air temperature. The level of agreement between the simulated and measured temperatures provide a measure of fidelity of the compositional data, the EOS model, and also a measure of consistency among the reported sampling conditions and fluid properties ultimately measured in the lab.

Table 5-18 shows a comparison of EOS-estimated bubblepoint temperature and line temperatures at the sampling points for the oils collected in this study. The local atmospheric pressure (Local P_{atm}) at the collection sites in ND and TX are shown in the top row of the table. For summer samples, the line temperature was measured by the sampling technician at 70°F in ND, and 96°F

in TX. EOS-predicted bubblepoint temperatures are shown for selected sampling methods in the rows immediately below. The TVP-95 (TM1-TL-EOS) returned a bubblepoint temperature of 71°F, and TM-4 piston cylinders returned bubblepoint temperature of 65°F, both of which compare well to the observed line T = 70°F. TM4-BRMPC for ND summer samples returned bubblepoint temperature of 48°F, which is notably lower than expected. Upon a closer look, the TM4-BRMPC samples contained higher N2 than the TVP-95 or other MPC samples, and this had the effect of creating a fluid that exhibits a lower bubblepoint temperature than those with the same hydrocarbon base but lower nitrogen. A simple numerical exercise that removed half of the nitrogen from the ND summer BRMPC samples to bring them in line with the other MPC samples taken in ND returns a bubblepoint temperature of 65°F, which agrees well with the others. TX summer samples exhibited a similar pattern, where TM1-TL and TM4-M/FPC samples returned bubblepoint temperatures very close to the 96°F measured at the sampling point, while BRMPC's showed bubblepoint temperature < 30°F but exhibited an order of magnitude more nitrogen than TM1 or the MPC methods.

Winter sampling shown in the lower half of Table 5-18 exhibited a parallel downward shift in line temperature and calculated bubblepoint temperature as expected. The ND TM4-FPC value returned a low bubblepoint temperature of 39°F, but a look back at the compositional data in Table 5-18 indicates that the FPC sample C1 was nearly double all of the other C1 measurements for other sampling methods. If ND TM4-C1 is reduced by 50%, the resulting calculated bubblepoint temperature is 48°F, matching well with observed line temperature. The calculated bubblepoint temperatures (89, 85°F) for the Texas winter samples compared well with observed (91°F).

Table 5-18. EOS estimated temperature for BP pressure equal to local atmospheric pressure.

	Temperature, °F		Comments
	ND	TX	
Local P_{atm}, psia	14	14.6	
Summer			
Line Temperature	70	96	As reported by sampling technician
TM1-TL + EOS	71	97	–
TM4 + EOS	65	95	ND-FPC; TX-MPC
TM4-BRMPC + EOS	48	<30	High N2
Winter			
Line Temperature	48	91	–
TM4-FPC + EOS	39	89	ND - High C1
TM4-BR1MPC + EOS	47	85	–

The bubblepoint temperature analysis demonstrated here provides an additional test for consistency of compositional results with sampling conditions, and readily flags outliers in fixed gas and C1 composition.

5.14 Simulated Pressure-Volume-Temperature for Heating at V/L = 1.5

A special case for determining the PVT relationship at a higher temperature range was implemented here in order to support upcoming crude oil combustion tests. A vessel filled with oil to V/L = 1.5 at ambient temperature was heated to 572°F (300°C) while pressure was monitored. Laboratory measurements are compared with EOS model results in Figure 5-51 for the ND Bakken summer samples and in Figure 5-52 for the TX Eagle Ford samples. In both cases, measured versus modeled agree well up to 392°F (200°C), but then the model starts to deviate high above 392°F (200°C). For the ND Bakken, the model over-predicts pressure by about 10-20% relative to the lab measurements above 392°F (200°C). For the TX Eagle Ford, the model over-predicts pressure by about 25-35% relative to the lab measurements above 200°C. Both oils show an inflection point in the measured data at 392°F (200°C) that initiate the deviation from the EOS model result. The boiling point of pure water at 120 psia (827 kPa) is about 342°F (172°C), which coincides with the inflection point on both plots, so water phase behavior may be involved, but the cause of the deviation is not clearly understood.

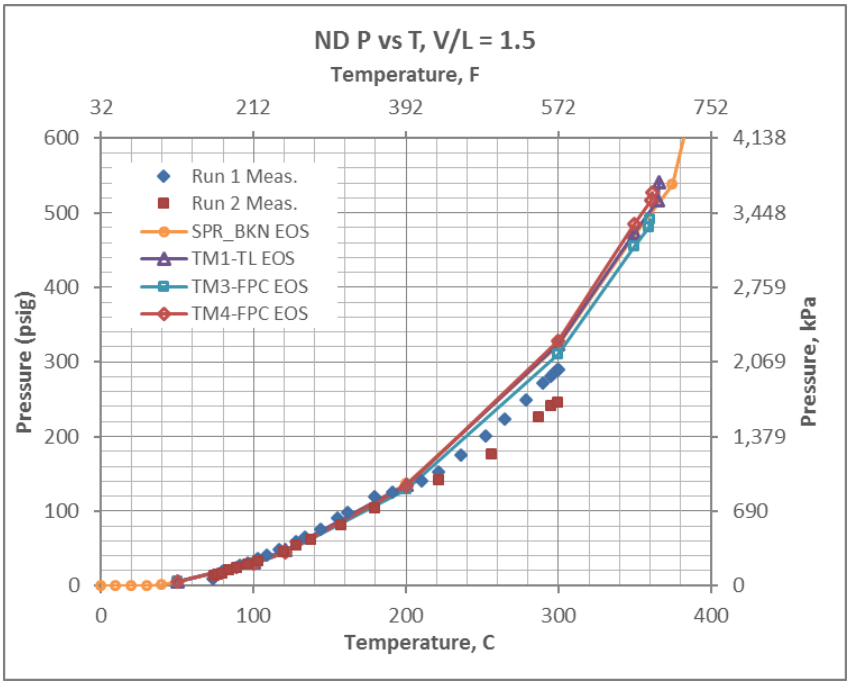

Figure 5-51. Overlay of measured and EOS-simulated PVT for ND Bakken summer crude at starting V/L = 1.5 for T = 50 - 300°C.

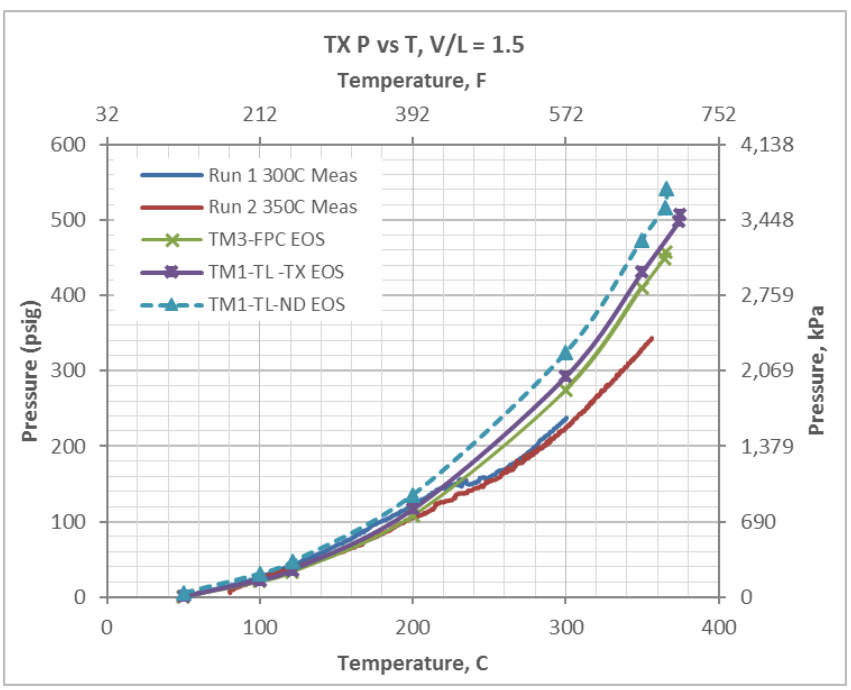

Figure 5-52. Overlay of measured and EOS-simulated PVT for TX Eagle Ford summer crude at starting V/L = 1.5 for T = 50 - 300°C (ND TM1 data included for reference).

5.14.1 Implications of TM Differences in EOS Calculations at High Temperature

Re-examining the PVT figures above (Figure 5-51 and Figure 5-52) for effects of compositional test method (TM1, TM3, TM4) indicates nearly indiscernible differences (< 10%) in EOS-calculated pressure at temperature from 50-300°C based on the TM. Intended use of these calculations was for mechanical design of test vessels where a safety factor of 1.5 to yield was used for the tank shell and a 20% tolerance for burst disc design was needed. As such, adding 50% over the already slightly higher model predictions for pressure was conservative for the vessel design, and choice of TM1, 3, or 4 to supply the compositional data for the EOS calculations was therefore not critical.

5.15 Manual VPCRx-F(T) by ASTM D7975

Vapor pressures acquired by the manual tester method (ASTM D7975) are compared with ASTM D6377 measurements and with the TVP-95 EOS model expansions in this section of the report. Recall the manual vapor pressure tester operates in the field and in this application takes measurements at a temperature that is monitored but not controlled. Temperatures can vary from measurement to measurement and differ from the temperatures specified for the VPCRx testing discussed above (68,100 and 122°F). Also, because of dead space in the filling system and errors in the volume guides the actual V/L ratios differ from the nominal design ratios of 0.25:1 and 4:1. The actual ratios, corrected using the calibration procedure specified in ASTM D7975, are provided in Table 5-19.

Table 5-19. Nominal and actual V/L for ASTM D7975 manual testers.

Nominal	Lab 1	Lab 3
0.25	0.24	0.24
4.0	3.04	2.86

5.15.1 Manual VPCRx-F Results for ND Bakken – Summer Sample

Manual VPCR-F data for ND Bakken oil are plotted as pressure vs. temperature and compared to data interpolated from the TM1-TL EOS and AVG-CLSD ASTM D6377 data in Figure 5-53(a) and (b), respectively. Also, shown in these figures are a series of D6377 measurements (green dots) taken at V/L=0.25 and T=86°F by LAB3. This data range from 14 to 18 psi and span the TM1 V/L=0.24 line. The data represents 2 replicates for each of the 4 sampling methods and are consistent with VPCR results discussed above. Also, shown in the figures are the $VPCR_4$ (nominal) corrected to 100°F (37.8°C) using CCQTA nomographs (CCQTA 2016).

The manual VPCR-F data presented in Figure 37(a) are from both labs and cover two distinct temperature ranges. The data compare reasonably well with the linear interpolated EOS data from TM1 at both V/Ls, nominally V/L's of 0.24 and 3. Differences between VPCR-F and EOS data are on the order of 1 psi (6.9 kPa).

The manual VPCR-F data are repeated in Figure 5-53(b) but are compared with the average closed-sample D6377 results (AVG-CLSD). Recall that the TM1-EOS and AVG-CLSD data tended to

bound the EOS results for most test and sample methods. Comparisons to AVG-CLSD at V/L~3 are very good. However, at V/L=0.24 VPCR-F's are several psi lower than the AVG –CLSD, likely reflecting reduced N2 in the manual VPCR tester. The reduction in N2 for the manual tester is due to the multiple purge cycles called out in the D7975 procedure for sampling. The procedure prescribes a minimum of three (3) full cylinder volume purges prior to final sampling and testing.

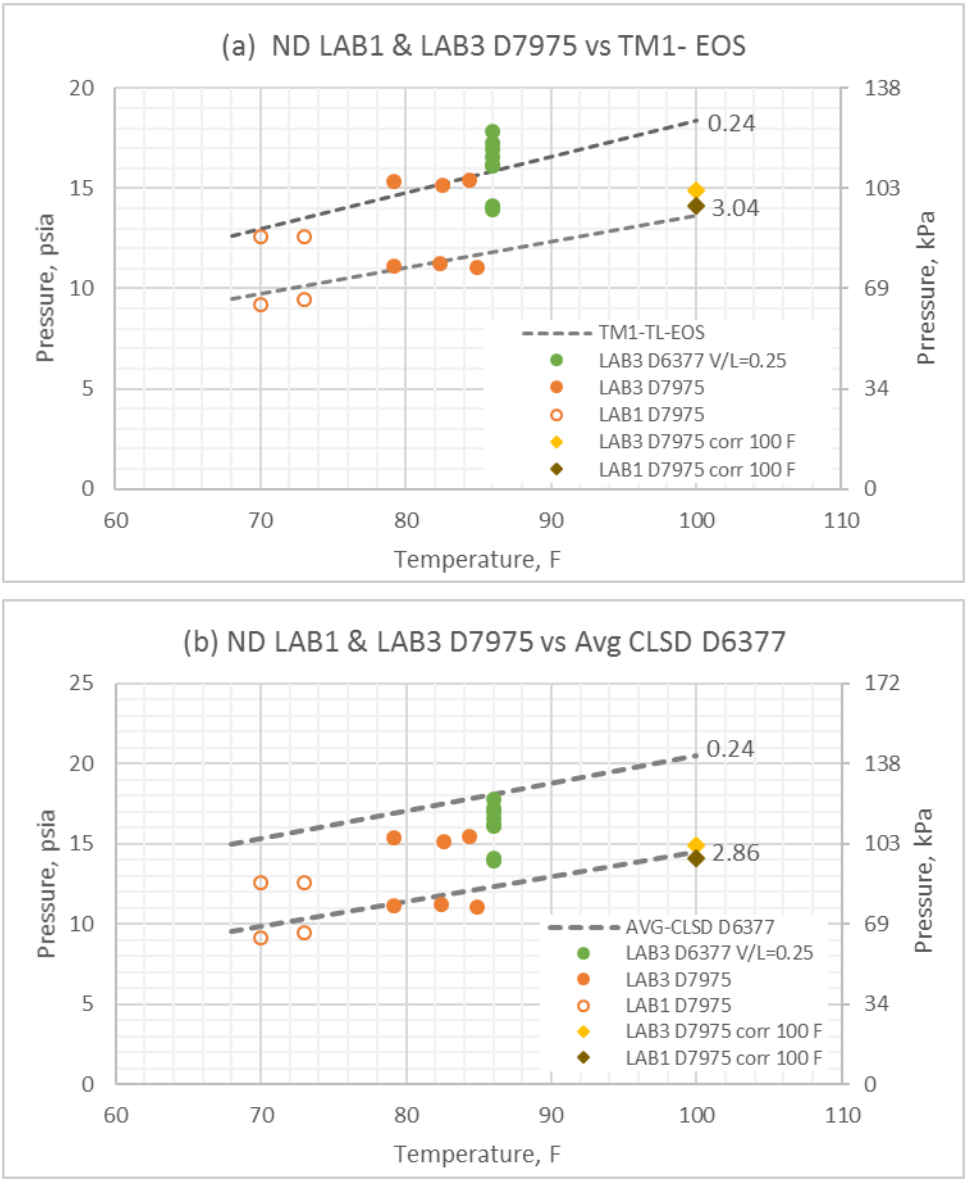

Figure 5-53. VPCRx-F by manual tester vs. temperature compared with (a) TVP-95 EOS model and (b) AVG-CLSD D6377 for ND Bakken summer crude.

5.15.2 Manual VPCRx-F Results for TX Eagle Ford – Summer Sample

As with the ND Bakken, manual VPCRx-F data were obtained for the TX Eagle Ford and the same comparisons were made of the VPCRx-F versus the TM1-EOS and average-closed-data and are presented in Figure 5-54(a) and (b) below.

The TX Eagle Ford data when compared to the TM1-EOS provide a close fit at measurement temperatures near the oil sample temperature of 90-96°F, and as the measurement temperature drops the deviation from the TM1-EOS curves increases. This deviation may be a result of not allowing the oil and vapor to temperature equilibrate with ambient. The oil sample temperature was 90-96°F, ambient temperature ranged from 66-79°F. The manual cylinder is uninsulated. The temperature of the cylinder was measured using an IR gun type thermometer. If the temperature measurement is made in the liquid area of the cylinder this may not represent the vapor space temperature, as the vapor has a much lower heat capacity and will be cooled more quickly. This cooling will result in condensing of the vapor and producing a lower pressure in the cylinder. As measured temperatures increase the deviation from the TM1-EOS decrease.

The TX Eagle Ford compared to the average closed-sample D6377 results (AVG-CLSD) we see a result similar to the ND Bakken. Little impact to the V/L~3 comparisons but the V/L=0.24 results are again significantly lower than the AVG-CLSD results.

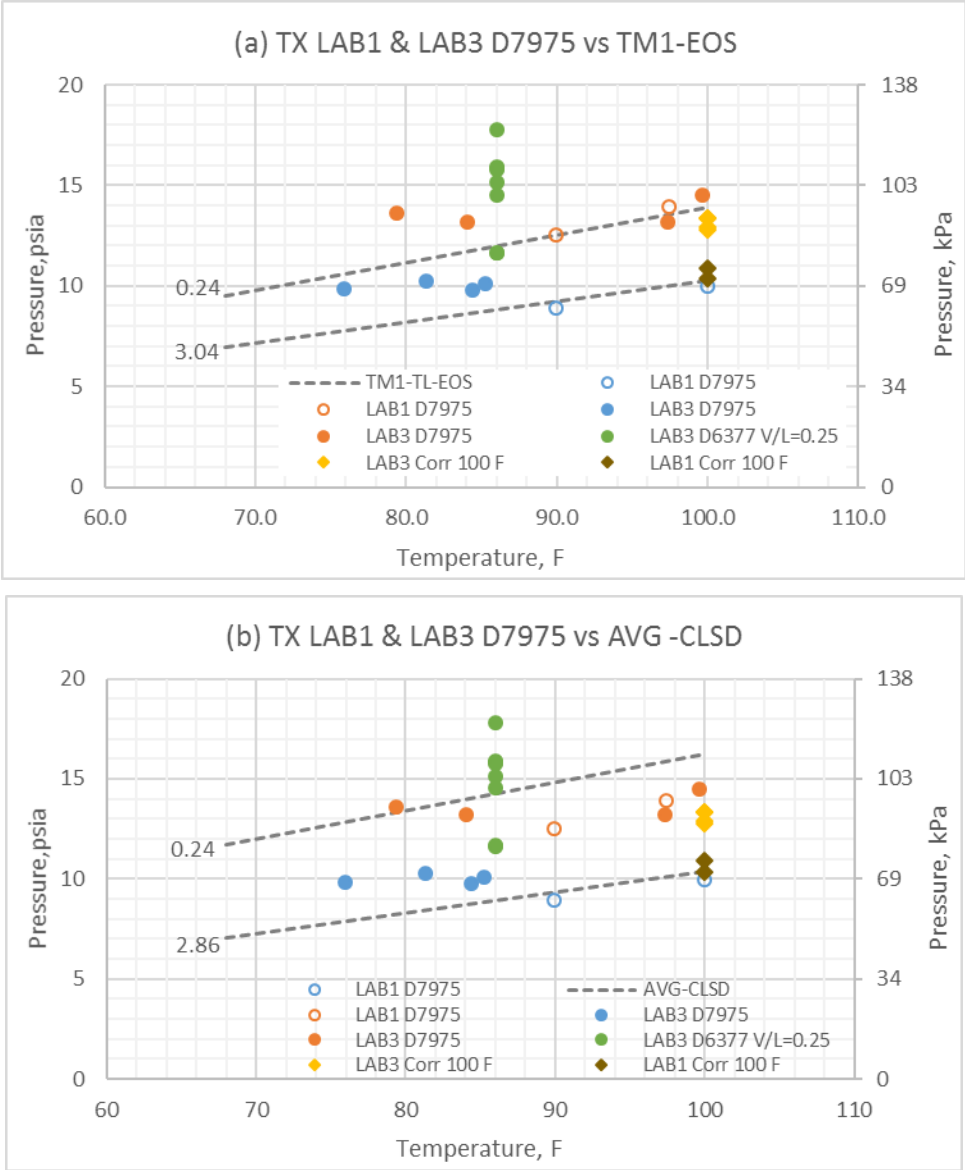

Figure 5-54. VPCRx-F by manual tester vs. temperature compared with (a)TVP-95 EOS model and (b) AVG-CLSD D6377 for TX Eagle Ford summer crude.

6 Discussion

6.1 Review of Key Findings

6.1.1 Effects of Open vs. Closed Sampling on VPCRx(T)

The study found that for certain situations, both open and closed industry standard sampling methods yielded samples for laboratory analysis that returned nearly equivalent vapor pressure and hydrocarbon content, which also compared well against the tight-line TVP-95 system, though a number of conditions applied. It is first important to recognize that the oils collected in this study had most likely been exposed to atmospheric storage conditions in the supply chain upstream of the sampling points, so that they were not actively boiling "live" oils at sampling conditions. Note that only one of the four samples across oils and seasons, ND Bakken winter, was acquired from a process temperature (48°F) below typical lab ambient (70°F). Since only one valid comparison could be made using low process temperature, conclusions stemming from the VPCRx and composition results are limited.

For vapor pressure VPCRx(T) at high vapor/liquid ratio (V/L = 1.5, 4.0), there were no significant differences in VPCR as a function of sampling type. This changed, however, as V/L was decreased below 1.5, where the open BR samples showed lower VPCR than the other methods. The current report presents the case in section 5.2.5 that operating the ASTM D6377 instrument by using vacuum draw from an ambient pressure BR bottle will return VPCR measurements bounded on the upper end by local atmospheric pressure in the lab while true vapor pressure of the parent material may be significantly higher. Regarding VPCR measurements at V/L < 1, the reader should note that ASTM D6377-16 requires that the sample be contained in a FPC. Data from the current study support this requirement; the BR samples show lower VPCRx(100°F) than the other sampling methods for V/L = 0.02–0.5. These points are illustrated for VPCRx(100°F) measurements in Figure 6-1 (ND) and Figure 6-2 (TX), which were presented earlier in this report, but are reproduced here for clarity relative to the discussion of key findings.

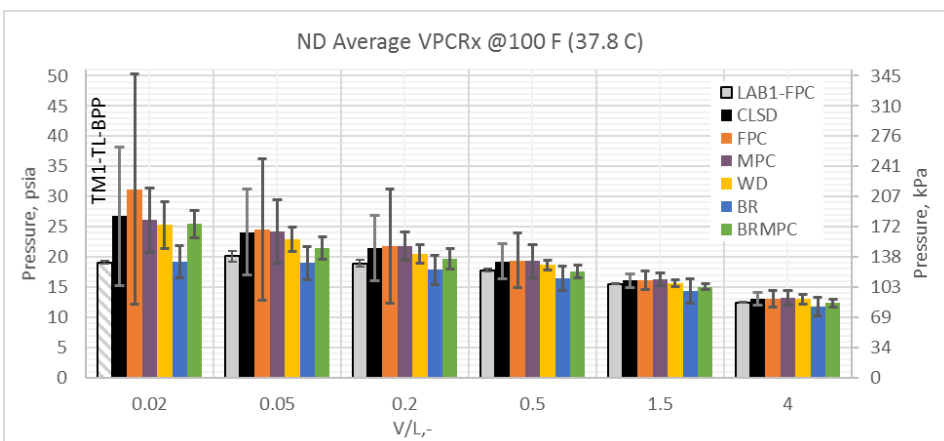

Figure 6-1. Bar chart showing average and 2σ VPCRx (100°F) for the ND Bakken oil sorted by V/L and sampling type. (This figure is a repeat of Figure 5-2).

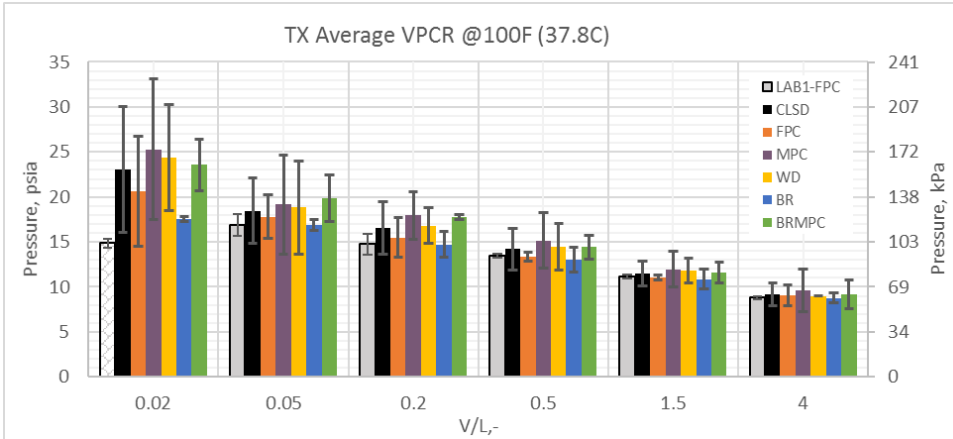

Figure 6-2. Bar chart showing average and 2σ VPCRx (100°F) for the TX Eagle Ford oil sorted by V/L and sampling type. (This figure is a repeat of Figure 5-20).

Sampling in colder weather provides a greater opportunity for retention of light ends in a produced fluid as it progresses through a supply chain that is exposed to ambient conditions. This could, in turn, lead to greater potential for a difference in performance between open and closed sampling for VPCR. In order to explore this potential, sampling teams returned to the same ND and TX terminals visited before, but this time in March, to collect open and closed samples for VPCR analysis. The samples collected in the colder seasonal conditions exhibited similar behavior to those collected during warmer conditions, showing no significant differences in performance in VPCRx(100°F) for open vs. closed sampling. However, the process temperatures for the TX summer and winter samples were both above lab ambient conditions and very close to one another (around 96°F). Therefore, the TX summer and winter samples ended up being very similar. On the other hand, the process temperatures for the ND winter and summer samples were lower, and further from one another (48°F and 70°F, respectively). This is illustrated in Figure 6-3 (ND) and Figure 6-4 (TX), where summer and winter open (BRMPC) and closed (CLSD, MPC) average VPCRx are compared on a single figure for each sampling location. While differences in individual bar heights (avg. VPCRx) at a given V/L may vary by several psi, they all fall inside the 2σ error bars for summer closed sampling and are therefore effectively the same within the resolution of the methods observed here.

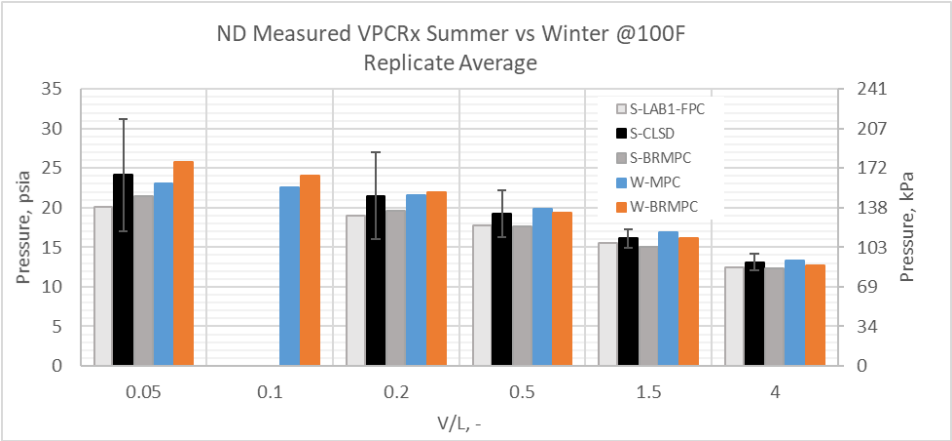

Figure 6-3. Bar chart showing average ASTM D6377 VPCRx(100F) at V/L = 0.02 to 4.0 for average summer and winter open and closed sampling events at the ND Bakken sampling site (This figure is a repeat of Figure 5-44).

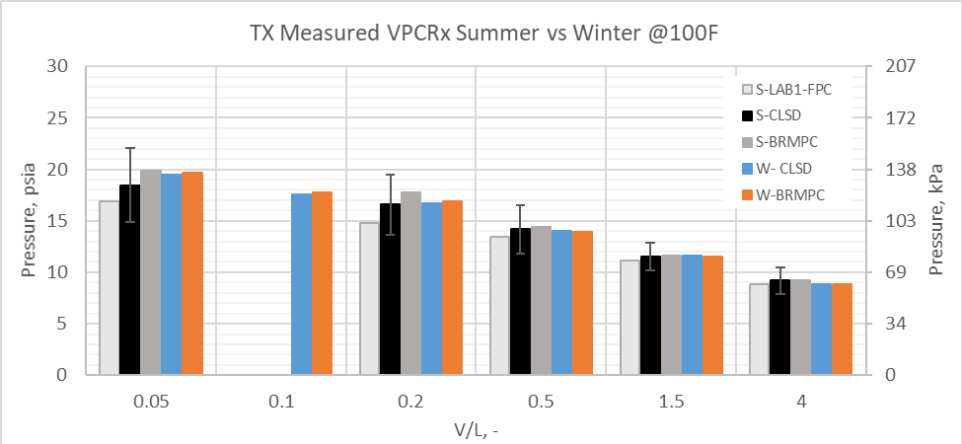

Figure 6-4. Bar chart showing average ASTM D6377 VPCRx(100°F) at V/L = 0.02 to 4.0 for average summer and winter open and closed sampling events at the TX Eagle Ford sampling site (This figure is a repeat of Figure 5-45).

6.1.2 Effects of Open vs. Closed Sampling on Composition

Switching focus to oil compositions, all sampling methods returned generally equivalent results for hydrocarbon content, though there was variation in nitrogen and oxygen and methane. The tight-line TVP-95 (TM1) system consistently returned the lowest nitrogen/oxygen concentrations, as illustrated in Figure 6-5 (ND) and Figure 6-6 (TX). In contrast, the spot samples (FPC, MPC, WD, BR, BRMPC) showed wide variation in nitrogen and oxygen, but there was no specific trending with sampling type or analysis type. This suggests that the nitrogen/oxygen was present only in low concentration in the parent material and may have been introduced inadvertently and sporadically during the spot sample acquisition process in the field or possibly during handling in the analysis laboratory during processes that are common to all spot sampling types, especially where high-pressure nitrogen is used to maintain backpressure on closed sample cylinders and/or

push samples into analytical instrument systems. Sampling cylinders and manifolds may also have dead volumes containing air or inert gas that could be inadvertently dissolved into the hydrocarbon sample when contained in a closed system under pressure. The reader is reminded that even the open BR samples must be transferred to closed, pressurized systems in the laboratory in order to run certain analyses such as pressurized gas chromatography in TM2, TM3, TM4 and TM4a. Reviewing the hydrocarbon concentrations, C1 mole fraction measured a little lower in the BRMPC samples than for other methods, but no systematic differences were seen for the remainder of the carbon numbers tested. The three compositional analysis methods (TM1, TM3, TM4) generally gave the same results across most carbon numbers.

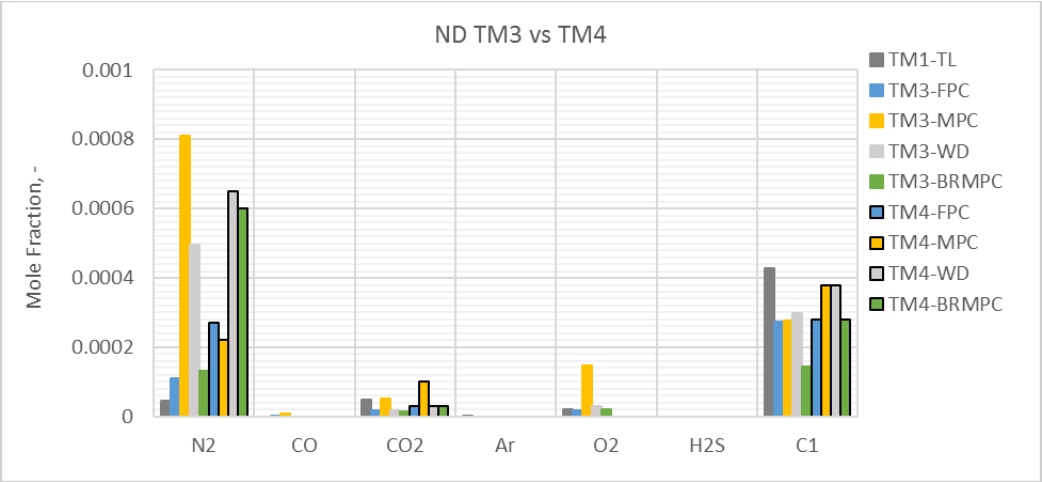

Note: N2 for TM4 is N2+O2.

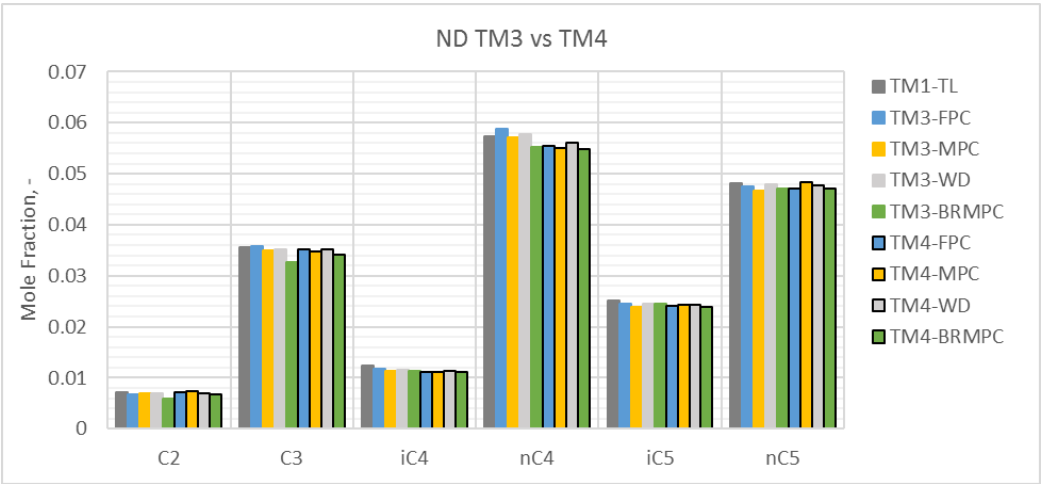

Note: TM4 data outlined in black. Only replicate 1 for TM3 is shown

Figure 6-5. Bar chart comparison of composition from TM3 and TM4 for ND Bakken. Components N2 – C1 in upper figure and C2 – nC5 in lower figure (This figure is a repeat of Figure 5-16).

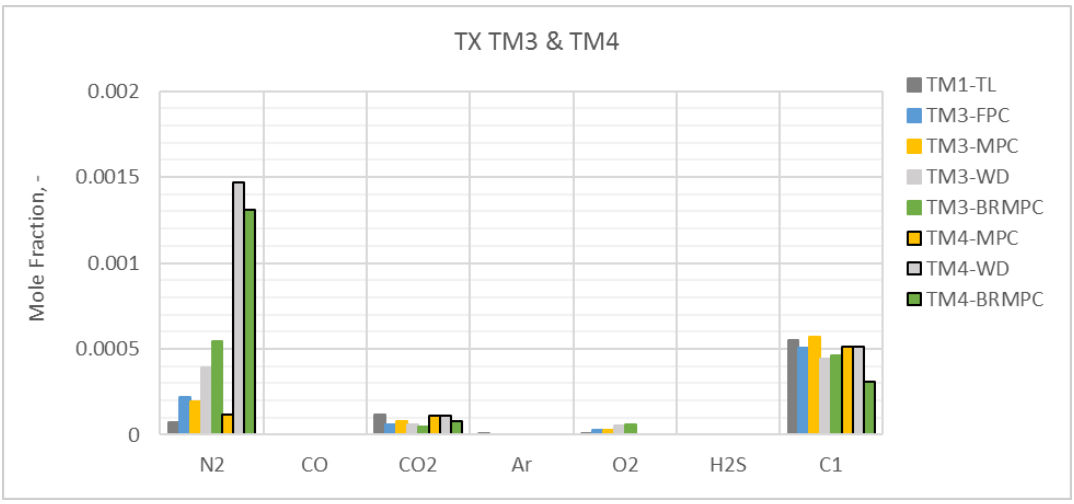

Note: N2 for TM4 is N2+O2.

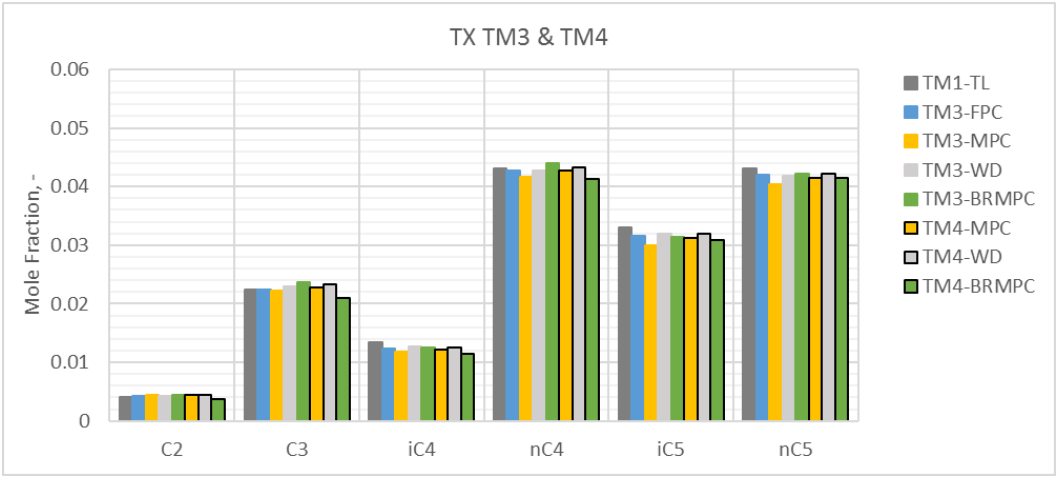

Figure 6-6. Bar chart comparison of composition for TX Eagle Ford TM3 and TM4 samples. Components N2-C1 in upper chart and C2-nC5 in lower (This figure is a repeat of Figure 5-32).

Compositional data resulting from the winter sampling generally showed some slight sensitivity to sampling method, with light ends trending slightly higher from C1-C6 for closed versus open methods (see Figure 6-7). The same was observed in summer, though to a lesser degree.

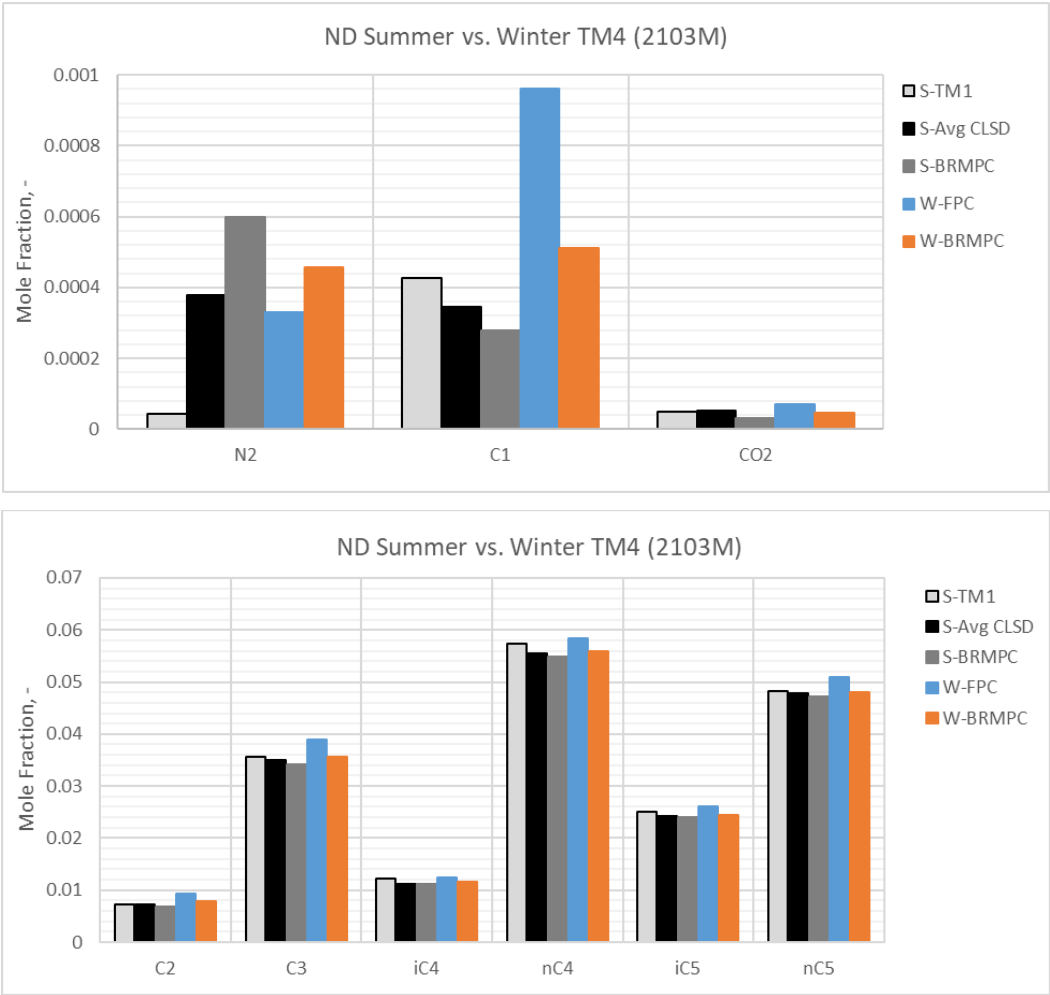

Figure 6-7. Bar chart comparison of composition for ND Bakken TM4 samples. Components N2 – C1 in upper figure and C2 – nC5 in lower (This figure is a repeat of Figure 5-46).

A closer look at the relationship between crude oil light ends and fixed gas composition and VPCRx(T) can help clarify how composition can directly affect vapor pressure of crude oils. A specific case is selected here for illustration. Note the relatively high nitrogen concentrations reported by TM4 for WD and BRMPC samples as shown in Figure 6-6. These whole oil concentration values for TM4 were passed through an equation of state model (EOS) to simulate VPCRx(100°F), and the simulated values were plotted in Figure 6-8. Note that the magnitude of the VPCRx(T) in Figure 6-8, especially at low V/L, correlate strongly with the nitrogen concentrations shown in Figure 6-6 by sampling type. The WD and BRMPC both show much higher in nitrogen relative to others in Figure 6-6 and as a result, return higher simulated VPCRx(T) in Figure 6-8.

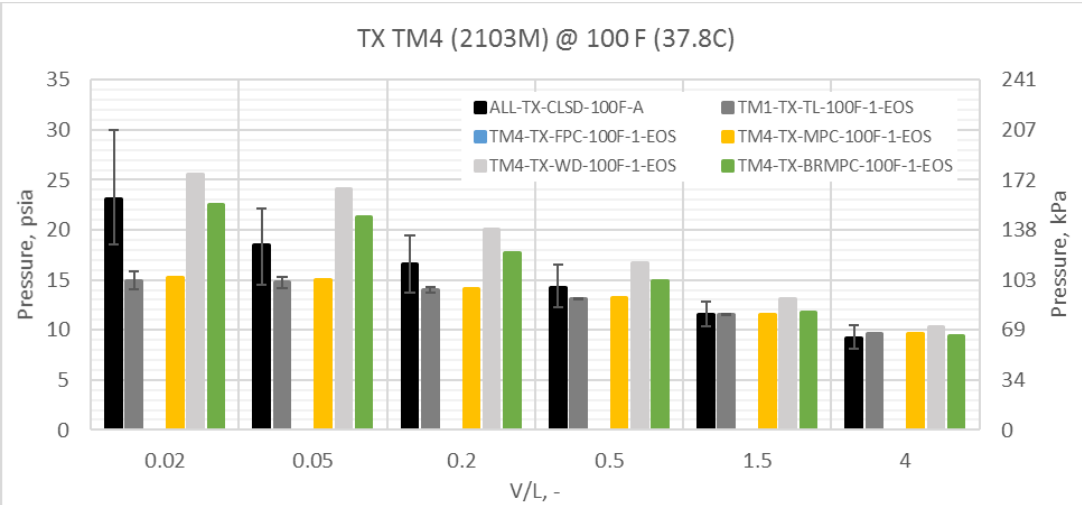

Note: TM4-FPC data not available.

Figure 6-8. Bar chart comparison of VPCRx(100°F) generated by EOS model from TM4, TM1, and D6377 instrument for TX Eagle Ford samples (This figure is a repeat of Figure 5-29).

The above findings relative to open vs. closed sampling may then be summarized as follows:

- Vapor Pressure of Crude Oil ($VPCR_4$) at vapor-liquid ratio 4:1 and 1.5:1 (V/L = 4 and 1.5) showed low sensitivity to sample collection method for the two oils analyzed in this study. This finding is only valid for oils that have been stored in atmospheric storage tanks with bulk storage temperature equal to or greater than the sample collection and analysis temperatures.
- Low measured VPCRx(T) associated with D6377 sample draw from the open bottle method at atmospheric pressure was observed relative to closed methods. This effect was most evident at low V/L (0.02. 0.05) and was likely a function of ambient pressure in the laboratory combined with the vacuum draw method into the 6377 instrument, and not a material property of the original sample. This observation supports a requirement in the new ASTM D6377-16 standard stipulating that sample shall be contained in a floating piston cylinder for V/L < 1.
- Tight line sampling consistently yielded the lowest nitrogen concentrations observed here.
- Nitrogen appears to be common to samples that show higher vapor pressure, particularly at low V/L. The source of this nitrogen is unclear and may come from the sampling system (e.g. dead volumes in sample lines, valves) and/or from handling in the field or lab.
- Closed sampling methods appear to retain slightly higher concentration of C1 than open sampling, though the implications in measured and modeled VPCR are minimal due to the complicating effect of highly variable sample-to-sample fixed gas concentrations and generally small differences between open and closed sample concentrations.

6.1.3 Comparison of Pressurized Compositional Methods

This report describes the results of four pressurized compositional methods (TM2, 3, 4, 4a) as compared to the baseline TM1 compositional data generated for a ND Bakken and a TX Eagle Ford crude in Task 2 of the Crude Oil Characterization Research Study. The four methods evaluated here include

- TM2: GPA 2177 + ASTM D7900 + ASTM D7169 data merge
- TM3: ASTM D8003 + GOR + ASTM D7169 data merge
- TM4: GPA 2103M + physical shrink + ASTM D2887 data merge
- TM4a: GPA 2103M + physical shrink + $C30^{+}$ GC data merge.

Summarized compositional results delineated by analytical method (TM1, 2, etc) and open/closed (BR/CLSD) are shown in Figure 6-9 and Figure 6-10. Generally speaking the methods all return whole oil compositions that are comparable to the baseline TM1. TM2 is distinct, however, in that it shows a uniquely high C1 for the closed sample and then low C2-C5 relative to all of the other methods, CLSD and BR.

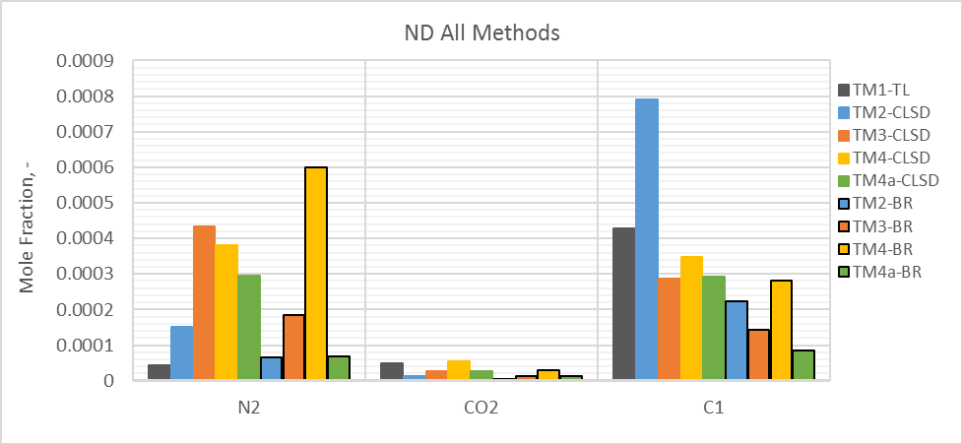

Note: N2 for TM4 is N2+O2

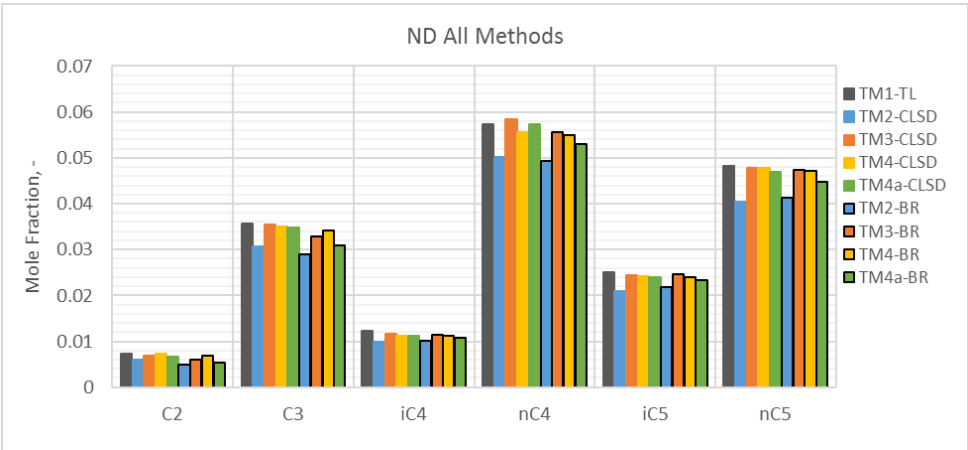

Figure 6-9. Comparison of averaged measured light ends and fixed gases for each test method - ND Bakken samples. Results for Boston Round samples are outlined in black.

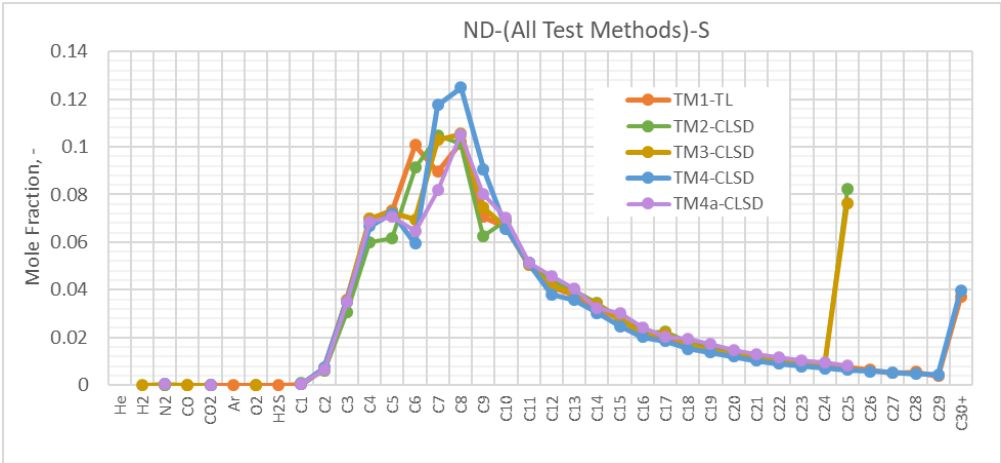

Figure 6-10. Aggregate plot of mole fraction versus carbon number for average ND Bakken summer closed samples for all test methods.

While the above observations indicate that TM2 performance is slightly less desirable than the others relative to the baseline TM1, the authors understand that this is the newest methodology among the group, and it has the distinction of requiring no physical property measurements--only gas chromatography. Every other compositional method examined here entails a physical flash separation step coupled with sensitive material balance measurements that require additional resources (laboratory space, equipment, skilled labor, time) to obtain. The physical property measurements add robustness to the overall measurement set, but come with additional cost. TM2 therefore has the potential for a cost advantage over the others (TM1, 3, 4, 4a). This GC-only data merge is just at a beginning stage, and could prove to be a viable alternative to flash separator-based options as the methods, instrumentation, user skills, and data merge processes are improved with time.

The lowest measured C1 mole fractions tend to appear in the BR samples, independent of compositional analysis method. This likely indicates small losses of C1 in open bottle handling and transfers. The net effects of spurious air/nitrogen intrusion appear to swamp these small losses in C1 in BR samples when considering resultant VPCRx, calculated or measured.

The above findings relative to compositional methods may then be summarized as follows:

- Commercially available compositional Test Methods TM3 (GOR+ASTM D8003+ASTM D7169 Merge), TM4 (GPA 2103M+physical shrink+ASTM D2887M Merge), and TM4a (GPA 2103M+physical shrink+C30+ GC Merge) provided whole oil compositions consistent with TM1 (Separator flash gas analysis and C30+ with numerical merge), particularly for hydrocarbons.
- While TM2 performance is slightly less desirable than the others relative to the baseline, it has a potential cost advantage over the others (TM1, 3, 4, 4a) as it requires no physical shrink/GOR step. The authors encourage the industry to look closely at ways to improve performance of this method.

6.1.4 Issues with Reproducibility in VPCR at V/L = 0.02 and 0.05

Current analytical methods applied to the two oils in this study do not provide a reproducible measure of VPCR at V/L = 0.02 or 0.05. These observations are drawn from the large standard deviations for VPCR at V/L = 0.02 and 0.05 apparent in all of the associated bar charts in this report. This is further supported by comparing the calculated reproducibility intervals (2.8σ) with published values of R_{std} (Table 6-1) specified in the ASTM D6377-16 standard. The fact that reproducibility intervals regularly exceed R_{std} implies that simple random chance is not the likely driver for the magnitude of standard deviation that is observed, and differences in execution of test method are a more likely explanation. The authors are assuming that the parent crude oil sample material was reasonably homogeneous coming out of a given sampling location, as supported by the stable performance of the TVP-95 on-site at each sampling event. Test method from sample acquisition forward includes all the details of sample cylinder purge process and potential entrapment of gases that could affect the sample, any and all connections and disconnections to equipment in the field or in the lab, and details of sample introduction into the test equipment at the laboratory.

Table 6-1. Reproducibility Interval (2.8σ) for measured VPCRx(100°F) for the ND Bakken oil samples, grouped by V/L and sampling method, compared with R_{std} from ASTM D637 (This table is a repeat of Table 5-10).

ND Sample	V/L					
	0.02	0.05	0.2	0.5	1.5	4.0
LAB1-FPC*	0.40	1.27	0.83	0.42	0.08	0.08
Closed**	16.06	9.96	7.64	4.11	1.62	1.50
FPC	26.71	16.51	13.16	6.40	2.15	1.93
MPC	7.38	7.38	3.27	3.82	1.53	1.67
WD	5.45	2.93	2.22	1.22	0.74	1.18
BR	3.70	3.88	3.35	2.89	2.79	2.15
BRMPC	3.16	2.61	2.38	1.41	0.64	0.92
R_{std} FPC	2.94	–	–	–	–	0.62
R_{std} Nonpress.	–	–	–	–	–	0.76

*Day-to-day variability for LAB1-FPC.
**Reproducibility across FPC, MPC, and WD closed sampling methods.

The above findings relative to VPCR at V/L = 0.02 and 0.05 may then be summarized as follows:

- Current analytical methods applied to the two oils in this study do not provide a reproducible measure of VPCR at V/L = 0.02 and 0.05. The large standard deviation of the current dataset may indicate sample-to-sample variances in the test method related to handling in the field or at the lab rather than true variances in the properties of the source oil.

6.1.5 Performance of Commercial Process Simulator Model for Predicting Vapor-Liquid Equilibrium of Test Crudes

The commercially available process simulator model (PSM) employed in this study performed well against measured pressure-volume-temperature (PVT) data collected for the Bakken and Eagle Ford oils analyzed here. The PSM utilized a Soave-Redlich-Kwong (SRK) cubic equation of state (EOS) with default binary interaction coefficients and was populated with oil compositions imported from all three compositional test methods TM1, TM3, and TM4.

Two scenarios were simulated successfully:

1. Equilibrium vapor pressure (VPCRx(T)) for the ambient temperature range (68-122°F; 20-50°C) and V/L range 0.02 to 4.0. Resulting pressures were in the range ~5-35 psia (35-240 kPa).
2. Pressure-volume temperature for fixed crude oil mass at starting V/L = 1.5 in a test cell heated from ~122-572°F (50-300°C). Resulting pressures were in the range ~15-500 psia (100-3450 kPa).

Simulated pressure visually compared well with PVT data from ~122-392°F (50-200°C) and then diverted high by about 20% from measured from through 392-572°F (200-300°C). The cause for the diversion is not clear, but could be related to the presence of water in the system that is not fully addressed in the simulation. These conditions are relevant to initial conditions for combustion tests that will be addressed in a subsequent report.

Two figures are reproduced here to illustrate the basis for stating that the PSM (with embedded EOS) model performance is adequate. The first, Figure 6-11, compares measured TVP-95 baseline (TM1), D6377-measured VPCRx(T) (ALL), and modeled vapor pressure results for the Bakken oil (EOS suffix). The figure shows that the D6377 measurements generally form an upper bound, the TVP-95 baseline generally forms a lower bound the lower bound, and the EOS model results fall in between. The margins between methods fall within the 2σ error bars shown and can effectively be considered to yield the same results. The second, Figure 6-12, compares PSM/EOS model pressure-temperature to that from a laboratory-measured system, with starting V/L= 1.5, through a heating process from 50-300°C. Overlay is generally favorable though there is some deviation above 200°C.

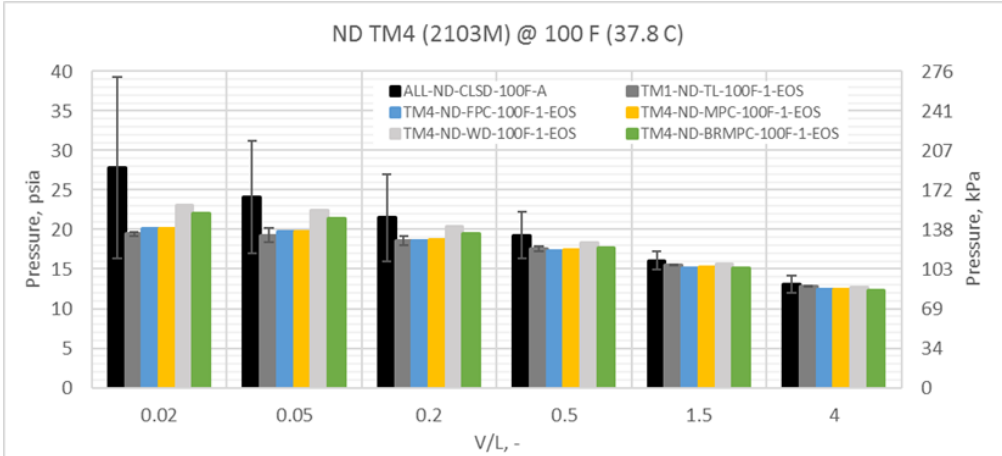

Figure 6-11. Bar chart comparison of VPCRx(100°F) generated by EOS model from TM4, TM1, and D6377 instrument for ND Bakken samples. (This figure is a repeat of Figure 5-13).

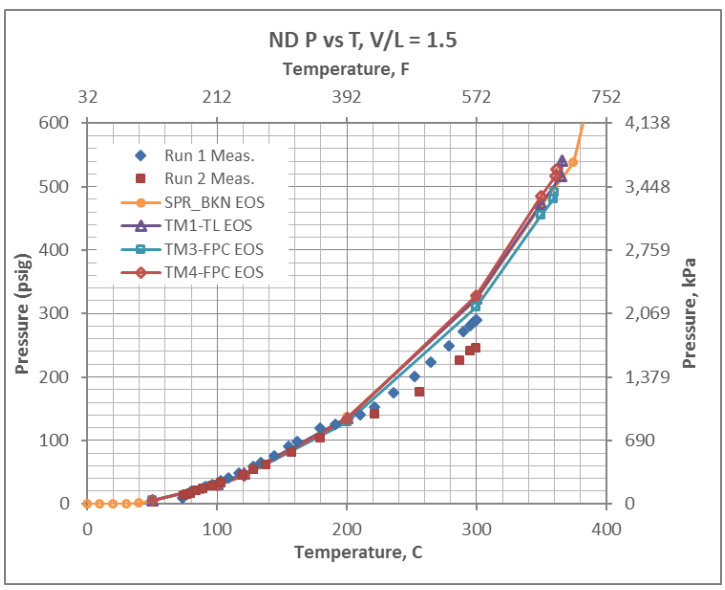

Figure 6-12. Overlay of measured and EOS-simulated PVT for ND Bakken crude at starting V/L = 1.5 for T = 50 - 300°C (This figure is a repeat of Figure 5-51).

The reader is reminded that the adequacy of any model must be judged against the needs in a given application. While a model will rarely predict an absolute match to the physical world, some models produce results close enough to be useful in a given situation. The above PSM performance with the compositional data provided by TM1, 3, or 4 was adequate for the current work.

A key finding from the above discussion may be summarized as follows:

- Application of a commercially available process simulation model (PSM) with a cubic equation of state (EOS) using data from TM1, TM3, and TM4 yielded favorable performance against measured pressure-volume-temperature (PVT) data for process environments relevant to this study.

The value in confirming adequate model performance has several benefits:

- Provides a quality assurance check on the VPCR versus compositional data acquired
- Confirms the model's ability to predict fluid behavior (vapor pressure, flash gas volume, vapor composition) in circumstances that are too expensive or difficult to measure directly.
- Provides the ability to design fluid handling and treatment processes that have a strong quantitative basis.

6.1.6 Conditionally Live Oils

The two oils tested in this study, one Bakken and one Eagle Ford, exhibited conditional stability and are not easily characterized as "dead" versus "live" as defined in industry literature (CCQTA 2014; ASTM 2016c). The industry definition is written with specific application to handling and measurement at laboratory conditions, stating that an oil is "live" if it would boil if exposed to normal atmospheric pressure at room temperature. While this may be a useful characterization for anticipating and controlling volatility losses in samples destined for the lab, there are many circumstances along the crude oil supply chain where the oils that were examined here could be considered "live" at one point and alternatively "dead" at another. For example, the ND Bakken sample taken in September exhibited VPCR at V/L = 0.2 at ambient sampling conditions (nominally 70°F (21°C)) of about 15 psia (103 kPa) (see Figure 5-1). This corresponds well with the ambient pressure that was reported at 14 psia (97 kPa). When heated to 100°F (37.8 °C), VPCR for the same V/L increased by about 5 psi (34 kPa), and GOR as measured by the TVP-95 at T = 100°F was around 12 scf/bbl. This implies that the source oil would either flash significantly in an open container subjected to 100°F or apply additional pressure of around 5 psi (35 kPa) in a closed container at V/L near 0.2. This same oil would be defined as "dead" in the lab context. If we alternatively consider subjecting the same oil to a pressure reduction in an ambient storage tank, the slope of the pressure-expansion curve in Figure 5-4 illustrates how V/L (or GOR) will increase with each incremental pressure step downward. Weather events such as low-pressure storms or handling events like opening a sealed transport vessel at a lower exterior pressure than was loaded will incur the vapor volume expansion as indicated.

A key finding relative to labeling the selected oils as "live" vs. "dead" is:

- The two oil samples collected in this study, one Bakken and one Eagle Ford, showed levels of equilibrium vapor pressure and relative vapor-liquid volume (V/L) that were clearly dependent upon process conditions (temperature, pressure) relevant to measurement, handling, and storage, and did not fit neatly into the common definition of "live" or "dead" crude that is often used to categorize oils for tendency to volatilize at laboratory conditions.

6.2 Elaboration on Selected Key Findings

6.2.1 VPCRx Discussion

The low sensitivity of VPCR at V/L = 4 and V/L = 1.5 to sample collection method appears to differ at face value from the findings in prior studies reviewed in Background Section 3 above, though a closer look reveals consistency when considering possible temperature effects during the sampling event. Warm sampling conditions have the potential to lower dependence of vapor pressure to open versus closed sampling methods, whereas cold sampling can amplify it. The two oils collected here appeared to have been equilibrated with ambient conditions (70-96°F) consistent with summer and early fall weather upstream of the sample collection point, as indicated by the fact that their vapor pressures at V/L = 0.05 and 0.20 reflected local atmospheric pressure at sampling temperature.

Note the work by Konecnik (2014) measured consistently higher $VPCR_4$(100°F) for 12 FPC vs. open samples, while the work by Bagawandoss (2015a) measured consistently higher $VPCR_4$(100°F) for 7 WD vs. bottle samples. Line temperature for the Konecnik samples was reported (by personal communication) at ~77°F (25°C), so there was likely no meaningful temperature change in those samples from the field to the lab. Line temperature for the Bagawandoss samples ranged from 55-62°F, which presents the potential for vapor losses during BR handling when bringing the BR samples to lab (room) temperature and then opening the bottle to insert the sample draw tube or during the VPCR sample draw itself. Alternatively, line temperature for the Sandia samples was ~70°F in ND and ~96°F in TX. If the crude oil in each case for the Sandia work was already equilibrated to atmospheric pressure at atmospheric storage tank/line temperature prior to sampling, then no measurable light ends and fixed gas losses would be expected during open sample capture, and no additional losses would be expected for the bottle samples as they were either maintained or cooled to room temperature for vapor pressure testing. The fact that the Sandia samples showed low sensitivity of V/L = 4 to sample collection method is conceptually consistent with collecting samples that were equilibrated with ambient conditions upstream of the sampling point.

For broader application of these results to the crude oil supply chain, Sandia believes that it will be important going forward to investigate the effects of open vs. closed sampling where two critical conditions are addressed that should conceptually lead to the most visible differentiation between performance of open and closed sampling for retention of light ends, fixed gas, and vapor pressure of the parent material:

(i) Temperature effects – When oil is both equilibrated to atmospheric pressure in a stock tank and sampled at a bulk liquid temperature below lab ambient (68°F, 20°C), it is expected that the temperature gain experienced by the sample up to lab ambient will liberate gases from the open sample that are prone to escape the instant the bottle is opened to facilitate analytical testing. Such a condition becomes more likely in the winter when unpressurized stock tanks are subject to low seasonal temperatures and samples are collected at nominally the same temperature. The primary risk in this situation is that VPCRx(T) will be underreported for bottle samples because gases escaped when the bottle was opened on the benchtop or and/or a two-phase sample was drawn into the 6377 instrument. A winter sampling effort within this report evaluated performance of open versus closed sampling for winter samples, and found that overall pressurized composition were not sensitive to sampling method (with caveats for low

V/L), though methane concentration measured for open sampling was generally lower than for closed methods. This effect was slightly more evident in winter than summer. Note that only one of the four samples across oils and sampling seasons, ND Bakken winter, was acquired from a process temperature (48°F) below typical lab ambient (70°F), so the significance of the results is limited. Additional data at low temperatures would be beneficial to providing more clarity and robustness of findings around seasonal temperature effects.

(ii) Pressure effects – When local atmospheric pressure at the sample collection point differs from the atmospheric pressure inside the analytical laboratory, an open bottle sample is subject to loss or gain of gases depending on the direction of the pressure differential. The magnitude of the VPCRx(T) measurement will be influenced in a manner proportional to the loss or gain of atmospheric pressure between the collection point and the analysis point. Therefore, it would be advantageous to use closed sampling techniques when possible.

The authors caution that there is no basis from the Sandia data collected in this study that would justify extending the finding that $VPCR_4$ has low sensitivity to sampling methods to "live" oils that visibly boil when handled in open containers.

6.2.2 Issues around Closed Sampling and Air/Nitrogen

Closed sampling has the benefit of reducing the probability of loss of volatiles from the parent material relative to open sampling, but the results shown above indicate an inverse problem: potential for inadvertent gas addition or "contamination" of the samples. Review of the vapor pressure and compositional data above indicate that generally speaking, the hydrocarbon contents returned for all of the sampling types and analysis methods compare very well. Where they differ is in nitrogen/air content. The tight line samples run through the TVP-95 all show the lowest nitrogen levels in this study. All of the other sampling methods that involve spot samples show occasional high values of nitrogen, and a similar frequency of high VPCR at the lowest V/L (0.02, 0.05) where nitrogen at the measured levels would have an effect. The BR is not immune to this either because the sample must be transferred to a closed cylinder (BRMPC) to allow for pressurized injection into laboratory equipment, and these BRMPC are subject to the same spurious high values for nitrogen and similarly high VPCR at low V/L as the closed samples.

Selected results from section 5.3 above are reproduced in Figure 6-13 to illustrate the magnitude of impact that a known amount of nitrogen has on the EOS-calculated pressure-expansion curve for the Bakken oil. Figure 6-13 shows three cases for the ND Bakken oil: (i) FPC with N2 = 1e-4 mole fraction, (ii) WD with N2 = 5e-4 mole fraction, and (iii) MPC with N2 = 8e-4 mole fraction. The oils are otherwise nearly identical in composition. The greatest impact of the nitrogen is seen at V/L = 0 (calculated bubblepoint pressure) where the BPP(100°F) ranges from 25 psia to 19 psia depending on N2 content. VPCR at V/L = 1.5 collapse to a much tighter band between 15-16 psia, and are all effectively the same at V/L = 4.0.

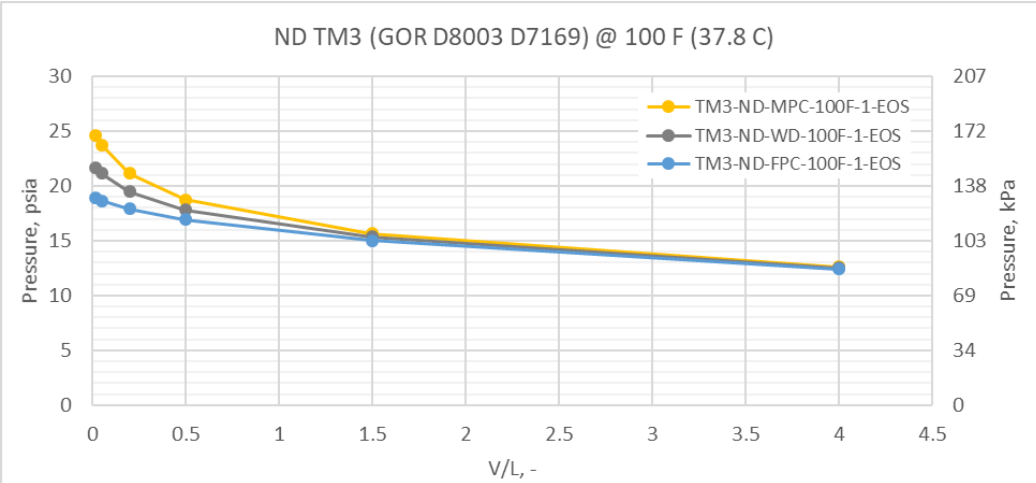

Figure 6-13. Pressure-expansion curves for ND Bakken oil generated by EOS for samples containing 1e-4 (FPC), 5e-4 (WD), and 8 e-4(MPC) mole fraction nitrogen.

The implications of small amounts of nitrogen, air, or similar inert gas dissolved into a hydrocarbon liquid include: (i) Observed vapor pressure at low V/L can be visibly higher than the vapor pressure of the hydrocarbon liquid alone; (ii) the V/L range where inert gases can increase crude oil vapor pressure is going to be a function of overall concentration level, but for cases observed in this study where incidental contact with air or dead space volume was likely a driving factor, inert gases appear to have virtually no visible effect on VPCR above V/L = 1.5.

Sandia discussion with sampling experts about this issue has brought forward an idea that a more rigorous approach to closed cylinder preparation, purge steps, and handling will be necessary to reduce the incidence of air/nitrogen contamination for closed cylinder sampling. Some initial conceptual plans have been drafted that Sandia will be using in subsequent testing that give new, explicit instructions on means to minimize air entrapment in closed sample cylinders.

6.2.3 Open vs. Closed Sampling for Follow-on Tasks in Current Research Study

The current Sandia position moving forward in this research is to employ closed methods for sample capture for sourcing all vapor pressure, light ends, and fixed gas measurements. Both piston cylinder (floating piston "FPC" or manual "MPC" depending on source line pressure) and water displacement "WD" will be utilized and analyzed in parallel. While the possibility for nitrogen contamination has been observed in closed sampling, its presence can be detected and documented. Also, a revised closed cylinder purge technique to minimize nitrogen contamination from dead volume was developed by the technical team as a result of this work and will be employed moving forward (see section 6.3.3). Regarding compositional analysis, TM1 (separator flash gas analysis with C30+ and numerical merge), TM3 (GOR+ASTMD8003+D7169 Merge), TM4 (GPA 2103M+ASTMD2887M Merge), and TM4a (GPA 2103M+C30+ GC Merge) appear equally suitable from a technical perspective for measuring pressurized composition. TM4 is currently available to Sandia through contract agreements.

6.3 Additional Topics

6.3.1 Sweep vs. Single Point Injection

Some issues with VPCR measurement repeatability were observed with a particular VPCR instrument depending on whether it was operated in "sweep" mode or "single point" mode. Sweep mode allows a single aliquot of sample fluid to be exposed to up three expansion points before it is ejected, which is useful when multiple V/L points are desired. This conserves sample material and analysis time. Single point mode, a more common configuration in benchtop applications, exposes the sample aliquot to only one expansion point before it is ejected. Some small differences in VPCRx were noted by Sandia depending on whether the data were collected in sweep vs. single point mode. Some examples are given below.

The D6377 instrument uses a fixed volume reservoir (L+V), so for a V/L sweep (one crude oil injection for a series of V/Ls), the largest V/L determines the initial volume of liquid, L_0, which is small (1/5 total volume) so relative errors at large V/ L are larger. For single point injections, L_0 is optimized for the specific V/L so a larger L_0 can be used for small V/L minimizing relative errors. Thus, single point injections should be more accurate, particularly at small V/L. At large V/L, pressure is much less sensitive to small variations in V/L due to L_0 issues.

Initial data received from Lab 3 contained a mixture of sweep results and single injection results. Upon review and clarification of test procedure, Lab 3 was asked to repeat the sweep measurements using the single point injection procedure for pressurized samples. Note: All VPCR results shown in prior sections of this report are for single point mode only. The results from the two test procedures are compared in Figure 6-14, where sample type is differentiated by color, the first bar of each pair is sweep result and the 2nd bar is single point injection result. All bars represent an average of two replicates. In most cases, particularly for WD samples the single point results showed lower VP at a given V/L and the differences were greater for smaller V/L. The one exception was for FPC samples, for which the single point result was larger (The following note was included in the lab notes: *Pressure for 0.02 originally decreased. Was run again next day and the pressure increased*). Similar results, but without the FPC exception, were seen at 68 and 122°F (20 and 50°C).

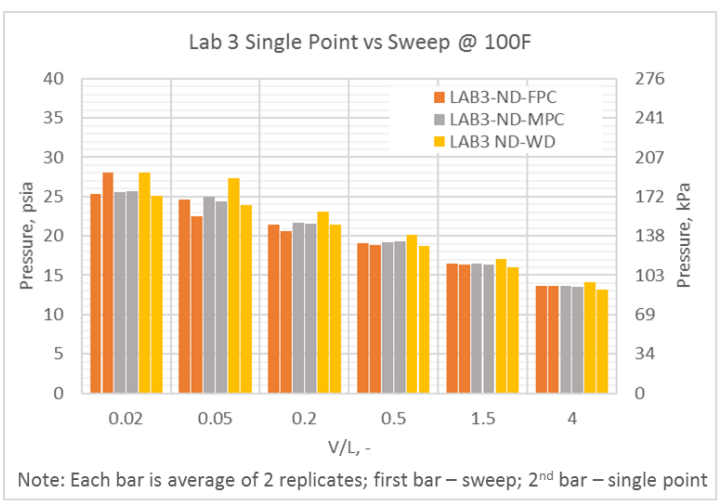

Figure 6-14. Single point injection vs. V/L sweep for D6377 VPCRx at 100°F by LAB3 with ND Bakken oil.

6.3.2 Issues with Standard Compositional Methods

Individual labs' ability to run a specific compositional method to include light ends and fixed gas analysis varied significantly. Each lab appeared to have their own specialty. This was observed in spite of the fact that all the compositional methods utilized were referenced back to industry standards.

6.3.3 New Purge Method for Manual or Floating Piston Cylinders

As discussed above in section 6.2.3 it appears that inadvertent introduction of N2/air into the closed sampling cylinders, either due to trapped N2/air in cylinders, fittings, valves, etc. can contribute significantly to measured VPCR's at low V/L's. Additionally, observing the manual VPCR-F results for V/L=0.24, it appears that the multiple purges of the sample cylinder with the source liquid to be sampled reduced the likelihood of inadvertent introduction of N2/air into the virgin sample. Based upon these observations the project team developed new sampling procedures to utilize a MPC and perform multiple purges of the sample through the sample lines, valves, and cylinder to attempt to fully purge any potential dead spaces in the system of any gases. This new procedure was incorporated into the Task 2A sampling plan for sampling with a MPC which was used in the 1st quarter 2017 ND Bakken winter sampling efforts.

6.3.4 Shortcomings in Current Standards

The peer review panel that convened in November 2016 came to consensus that current shortcomings in sampling and analysis standards associated with crude oil vapor pressure determination has some role in the variations that were observed in the VPCR data presented in this report. The team concluded that there would be value in revising the standards based on the collective work within the industry as well as findings from this study. Outcomes from this peer review panel will be taken to industry standards drafting committees as revision points moving forward.

Some of the key areas for improvement include:

1. Sampling methodology issues:
    a. BR method
        i. Atmospheric capture of sample can be sensitive to differences in sample source temperature and ambient temperature at time of sampling. (e.g. sample source temperature lower than ambient capture temperature potential light end loss at time of sampling.)
        ii. Atmospheric transfer to analyzer can be sensitive to differences in sample source temperature and lab (room) temperature. (e.g. ambient lab temperature higher than sample source temperature potential for light ends and fixed gas loss when sample bottle opened at lab conditions.)
        iii. Bottle not stoppered with analyzer withdrawal tube can allow light ends and fixed gas losses as sample sits exposed to open atmosphere.
        iv. Atmospheric draw into D6377 analyzer can produce non-zero initial/fill V/L condition (V/L > 0) in measurement cell, resulting in reporting VPCRx at V/L's less than actual conditions in measurement cell.

v. Lab barometric pressure can impact atmospheric draw in two ways:

1. Lab barometric pressure lower than sample location barometric pressure, can increase potential for light ends and fixed gas losses in lab.
2. Lower lab barometric pressure can tend to increase probability of initial/fill V/L > 0.

b. WD method

i. Water used as displacement fluid that contains dissolved gas can contaminate the hydrocarbon sample. May need specifications/controls for dissolved gas content in the displacement water.

c. MPC/FPC method

i. Medium used for back-pressure may contaminate sample with dissolved gases. Means of preventing contamination may include specifications/controls on piston seals and pressure differential across piston seals for vapor pressure samples.

2. Testing standards issues:

a. Atmospheric draw with stoppered bottle at 68°F fill—address vulnerability of method to create a two-phase vapor-liquid in test cell

b. ASTM subcommittee is considering changes to standard to stipulate that the sample be drawn into analyzer under pressure, and after filling of measurement cell, allow measurement cell temperature to come to measurement temperature prior to closure of the measurement cell sample inlet valve. This is to allow for thermal expansion of the sample to measurement temperature and eliminate need for temperature pre-conditioning of the sample cylinder to measurement temperature.

Page intentionally blank.

7 References

Alapati, R. R., B. H. Sonnier and H. M. Shammai (1997). System for Continuous Analysis and Modification of Characteristics of a Liquid Hydrocarbon Stream. United States Patent and Trademark Office. United States.

ANSI/API 2014 (Sep-2014) "Classifying and Loading of Crude Oil into Rail Tank Cars." Recommended Practice 3000. American Petroleum Institute, Washington, DC.

API (2011). "Crude Oil Category Assessment Document." High Production Volume Testing Group. American Petroleum Institute, Washington, DC 14-Jan-2011.

ASTM 2011 "Standard Test Method for Boiling Point Distribution of Samples with Residues Such as Crude oils and Atmospheric and Vacuum Residues by High Temperature Gas Chromatography." ASTM D7169-11. ASTM International, West Conshohocken, PA 19429-2959.

ASTM 2012 "Standard Practice for Manual Sampling of Petroleum and Petroleum Products." ASTM D4057-12. ASTM International, West Conshohocken, PA 19428-2959.

ASTM 2013a "Standard Test Method for Density and Relative Density of Crude Oils by Digital Density Analyzer." ASTM D5002-13. ASTM International, West Conshohocken, PA 19428-2959.

ASTM 2013b "Standard Test Method for Detailed Analysis of Petroleum Napthas through n-Nonane by Capillary Gas Chromatography." ASTM D5134-13. ASTM International, West Conshohocken, PA 19429-2959.

ASTM 2013c "Standard Test Method for Determination of Light Hydrocarbons in Stabilized Crude Oils by Gas Chromatography." ASTM D7900-13E1. ASTM International,

ASTM 2014a "Standard Practice for Obtaining LPG Samples Using a Floating Piston Cylinder." ASTM D3700-14. ASTM International, West Conshohocken, PA 19428.

ASTM 2014b "Standard Practice for Sampling and Handling of Fuels for Volatility Measurement." ASTM D5842-14. ASTM International, West Conshohocken, PA 19428-2959.

ASTM 2014c "Standard Test Method for Determination of Vapor Pressure of Crude Oil: VPCRx-F(TmC) (Manual Expansion Method)." ASTM D7975-14. ASTM International, West Conshohocken, PA 19428-2959.

ASTM 2014d "Standard Test Method for Determination of Vapor Pressure of Crude Oil: VPCRx(Expansion Method)." ASTM D6377-14. ASTM International, West Conshohocken, PA 14928-2959.

ASTM 2014e "Standard Test Method for Dynamic Viscosity and Density of Liquids by Stabinger Viscometer (and the Calculation of Kinematic Viscosity)." ASTM D7042-14. ASTM International, West Conshohocken, PA 19428-2959.

ASTM 2015a "Standard Practice for Manual Piston Cylinder Sampling for Volatile Crude Oils, Condensates, and Liquid Petroleum Products." ASTM D8009-15. ASTM International, West Conshohocken, PA 19428-2959.

ASTM 2015b "Standard Test Method for Determination of Light Hydrocarbons and Cut Point Intervals in Live Crudes and Condenates by Gas Chromatography." ASTM D8003-15. ASTM International, West Conshohocken, PA 19428-2959.

ASTM 2016a "Standard Test Method for Boiling Point Distribution of Samples with Residues Such as Crude Oils and Atmospheric and Vacuum Residues by High Temperature Gas Chromatography." ASTM D7169-16. ASTM International, West Conshohocken, PA 19429-2959.

ASTM 2016b "Standard Test Method for Boiling Range Distrbution of Petroleum Fractions by Gas Chromatography." ASTM D2887-16a. ASTM International, West Conshohocken, PA 19428-2959.

ASTM 2016c "Standard Test Method for Determination of Vapor Pressure of Crude Oil: VPCRx(Expansion Method)." ASTM D6377-16. ASTM International, West Conshohocken, PA 14928-2959.

ASTM 2016d "Standard Test Method for Distillation of Petroleum Products and Liquid Fuels at Atmospheric Pressure." ASTM D86-16a. ASTM International, West Conshohocken, PA 19428-2959.

ASTM 2016e "Standard Test Method for Flash Point by Tag Closed Cup Tester." ASTM D56-16a. ASTM International, West Conshohocken, PA 19429-2959.

ASTM 2016f "Standard Test Method for Sulfur in Petroleum and Petroleum products by Energy Dispersive X-Ray Fluorescence Spectrometry." ASTM D4294-16. ASTM International, West Conshohocken, PA 14928-2959.

Auers, J. R., R. M. Couture and D. L. Sutton (2014). "The North Dakota Petroleum Council Study on Bakken Crude Properties." Bakken Crude Characterization Task Force. North Dakota Petroleum Council, Bismarck, ND 58501. 4-Aug-2014.

Bagawandoss, K. (2015a). "Sampling and Analysis - Vapor Pressure Measurements in light of the new NDIC rule and RP3000." *presented at* Crude Oil Quality Association Meeting, Houston, TX, 19-Feb-2015, Crude Oil Quality Association.

Bagawandoss, K. (2015b). "Sampling and Analysis in Light of the PHMSA/DOT Final Rule." *presented at* COQA Meeting, New Orleans, LA, 22-Oct-2015, Crude Oil Quality Association.

CCQTA (2014). "CCQTA Information Regarding the Measurment and Reporting of Light Ends and Vapor Pressure of Live Crude." Canadian Crude Quality Technical Association, Edmonton, Alberta, Canada TR6 2V4.

CCQTA (2016). "Temperature Correction of Field Vapor Pressure Measurement." Canadian Crude Quality Technical Association, Edmonton, Alberta, Canada TR6 2V4.

CCQTA (2017). "Vapor Pressure Measurement Best Practice." Canadian Crude Technical Quality Association, Edmonton, Alberta, Canada T6R 2V4. Jun-2017.

GPA 2003 "Tentative Method for the Analysis of Natural Gas Condensate Mixtures Containing Nitrogen and Carbon Dioxide by Gas Chromatography." GPA Standard 2103-03. Gas Processors Association, Tulsa, OK 74145.

GPA 2013 "Analysis of Natural Gas Liquid Mixtures Containing Nitrogen and Carbon Dioxide by Gas Chromatography." GPA Standard 2177-13. Gas Processors Association, Tulsa, OK 74145.

GPA 2014 "Obtaining Liquid Hydrocarbons Samples for Analysis by Gas Chromatography." GPA 2174-14. Gas Processors Association, Tulsa, OK 74145.

Grabner-Instruments (V2.00). APPLICATION NOTE - Crude Oil Measurement with MINIVAP according to D6377-10, AMETEK, Inc.

Hinkebein, T. (2003). "Compilation of Gas Intrusion Measurements, Variations, and Consequence Modeling for SPR Caverns." *Unlimited Release SAND2003-0330*. Sandia National Laboratories, Albuquerque, NM.

Howe, K. (2016). "Sample Point Temp-Pressures," memo to D. Lord, 22-Nov-2016, Intertek, Bismarck, ND.

Konecnik, C. (2014). "HPLIS/Gas Chromatography vs. ASTM D6377 VPCR Results." *presented at* Crude Oil Quality Association San Francisco, CA, 30-Oct-2014, TransCanada.

Lord, D., A. Luketa, C. Wocken, S. Schlasner, R. Allen and D. Rudeen (2015). "Literature Survey of Crude Properties Relevant to Handling and Fire Safety in Transport." *Unlimited Release SAND2015-1823*. Sandia National Laboratories, Albuquerque, NM 87185.

Lord, D. L. and D. K. Rudeen (2010). "Strategic Petroleum Reserve Crude Oil Equation of State Model Development--Current Performance Against Measured Data." *SAND2010-4526*. Geotechnology & Engineering Department, Sandia National Laboratories, Albuquerque, NM. August, 2010.

Lott, S. E. (1996). "Analysis of Strategic Petroleum Reserve Bubble Point Pressure Data." *SAND96-1172*. Sandia National Laboratories, Albuquerque, NM.

Murray, D. (2014). "Canadian Crude Oil Quality--Handle with Care!" *presented at* Canadian Heavy Oil Association Meeting, Edmonton, Alberta, Canada, 27-Jan-2014, Canadian Crude Oil Quality Technical Association.

NDIC (2014). "Industrial Commission Adopts New Standards to Improve Oil Transportation Safety." Industrial Commision of North Dakota. North Dakota Oil & Gas Division. Bismarck, ND 58505-0840.

Prefontaine, A. (2015). "Final Report: Crude Oil Sampling and Analysis." Transport Dangerous Goods Directorate. Transport Canada. 10-Aug-2015.

Ullman, N. (2009). "What are Repeatability and Reproducibility?" ASTM Standardization News(May/June 2009).

Wispinski, D., A. Prefontaine and D. Seth (2016). "Latest Developments in Light Hydrocarbon Testing in Crude Oils." *presented at* CCQTA/COQA Joint Meeting, Edmonton, Alberta, Canada, 9-Jun-2016, Crude Oil Quality Association.

Wybenga, F. (2014). "A Survey of Bakken Crude Oil Characteristics Assembled for the U.S. Department of Transportation." Dangerous Goods Transport Consulting Inc., American Fuel & Petrochemical Manufacturers. 14-May-2014.

Page intentionally blank.

8 Appendix: Measured D6377 VPCRx and Whole Oil Composition Data

ND Summer VPCRx	V/L					
	0.02	0.05	0.2	0.5	1.5	4
LAB1-ND-FPC-68F-1	–	16.28	13.88	12.27	10.32	8.28
LAB1-ND-FPC-68F-2	–	16.15	13.06	11.96	10.35	8.31
LAB1-ND-FPC3-68F-3	–	16.08	13.05	11.51	9.57	7.44
LAB1-ND-TL-100F-1	18.99	–	–	–	–	–
LAB1-ND-TL-100F-2	19.19	–	–	–	–	–
LAB1-ND-TL3-100F-3	19.24	–	–	–	–	–
LAB1-ND-FPC-100F-1	–	19.79	18.72	17.70	15.54	12.44
LAB1-ND-FPC-100F-2	–	20.43	19.14	17.91	15.50	12.48
LAB1-ND-FPC3-100F-3	–	19.18	17.98	16.78	14.37	11.54
LAB1-ND-FPC-122F-1	–	25.70	24.35	22.90	19.75	15.91
LAB1-ND-FPC-122F-2	–	24.58	24.33	22.97	19.94	16.01
LAB1-ND-FPC3-122F-3	–	24.03	22.64	21.19	18.18	14.80
LAB2-ND-FPC-68F-1	32.69	18.26	14.48	12.05	10.18	8.16
LAB2-ND-FPC-68F-2	27.70	18.75	14.22	11.70	10.16	8.12
LAB2-ND-MPC-68F-1	25.68	16.53	13.96	12.03	10.37	8.04
LAB2-ND-MPC-68F-2	25.77	16.53	13.57	11.99	10.32	8.12
LAB2-ND-WD-68F-1	23.13	16.83	15.93	13.09	10.42	8.83
LAB2-ND-WD-68F-2	24.71	16.43	15.95	12.82	10.51	8.44
LAB2-ND-BR-68F-1	14.70	14.02	12.79	11.47	9.80	7.91
LAB2-ND-BR-68F-2	14.53	13.99	12.70	11.44	9.80	7.83
LAB2-ND-BRMPC-68F-1	17.14	17.08	13.60	11.67	9.90	7.93
LAB2-ND-BRMPC-68F-2	17.81	16.88	13.61	11.70	9.93	8.13
LAB2-ND-FPC-100F-1	23.43	21.94	18.99	18.28	15.59	12.48
LAB2-ND-FPC-100F-2	23.80	22.59	18.84	18.33	15.53	12.37
LAB2-ND-MPC-100F-1	25.26	21.78	21.33	18.57	15.82	12.48
LAB2-ND-MPC-100F-2	24.99	22.04	20.98	18.57	15.75	12.40
LAB2-ND-WD-100F-1	23.40	21.87	20.05	18.14	15.37	12.42
LAB2-ND-WD-100F-2	23.43	21.77	20.00	18.24	15.46	12.67
LAB2-ND-BR-100F-1	20.24	19.95	18.70	17.28	15.11	12.42
LAB2-ND-BR-100F-2	20.11	19.97	18.65	17.11	15.06	12.32
LAB2-ND-BRMPC-100F-1	25.80	21.13	19.52	17.53	14.93	11.98
LAB2-ND-BRMPC-100F-2	26.04	21.74	19.33	17.49	14.92	11.95
LAB2-ND-FPC-122F-1	30.53	29.61	26.46	23.84	20.17	15.99
LAB2-ND-FPC-122F-2	30.86	29.80	26.23	23.65	20.34	15.86
LAB2-ND-MPC-122F-1	34.11	33.31	28.74	25.35	21.13	16.51
LAB2-ND-MPC-122F-2	34.83	32.76	28.63	25.38	21.00	16.54
LAB2-ND-WD-122F-1	30.25	27.84	25.00	22.98	19.69	15.88
LAB2-ND-WD-122F-2	30.57	27.36	24.74	22.75	19.72	15.86
LAB2-ND-BR-122F-1	25.19	25.10	23.51	21.69	19.04	15.66
LAB2-ND-BR-122F-2	25.74	25.04	23.40	21.68	19.01	15.53
LAB2-ND-BRMPC-122F-1	33.09	27.03	24.77	22.42	19.21	15.46
LAB2-ND-BRMPC-122F-2	32.72	26.74	24.68	22.48	19.18	15.41
LAB3-ND-FPC-68F-3	18.48	15.74	14.90	13.31	11.12	9.41
LAB3-ND-FPC-68F-4	18.58	15.77	14.87	13.31	11.12	9.43
LAB3-ND-MPC-68F-3	19.55	19.14	15.74	13.78	11.31	9.54
LAB3-ND-MPC-68F-4	19.58	19.13	15.71	13.76	11.36	9.56
LAB3-ND-WD-68F-3	17.71	16.91	15.36	14.23	11.20	9.14
LAB3-ND-WD-68F-4	17.65	16.90	15.32	14.17	11.20	9.14
LAB3-ND-BR-68F-3	12.44	12.18	11.47	10.63	9.22	7.69
LAB3-ND-BR-68F-4	12.49	12.20	11.49	10.63	9.22	7.67
LAB3-ND-BRMPC-68F-3	15.90	15.36	14.16	12.89	10.44	8.47
LAB3-ND-BRMPC-68F-4	15.95	15.30	14.21	12.85	10.44	8.51
LAB3-ND-FPC-100F-3	27.95	22.52	20.57	18.81	16.35	13.65
LAB3-ND-FPC-100F-4	28.08	22.54	20.62	18.77	16.35	13.65
LAB3-ND-MPC-100F-3	25.67	24.41	21.54	19.25	16.36	13.56

ND Summer VPCRx	V/L					
	0.02	0.05	0.2	0.5	1.5	4
LAB3-ND-MPC-100F-4	25.67	24.47	21.54	19.26	16.33	13.59
LAB3-ND-WD-100F-3	25.08	23.92	21.42	18.65	15.94	13.10
LAB3-ND-WD-100F-4	25.14	23.89	21.42	18.70	15.95	13.14
LAB3-ND-BRMPC-100F-3	24.16	20.61	18.90	17.13	14.92	12.44
LAB3-ND-BRMPC-100F-4	24.22	20.61	18.87	17.11	14.92	12.47
LAB3-ND-FPC-122F-3	30.05	28.69	25.40	23.66	20.51	17.16
LAB3-ND-FPC-122F-4	30.07	28.67	25.40	23.63	20.55	17.16
LAB3-ND-MPC-122F-3	32.46	30.05	26.35	23.95	20.58	17.01
LAB3-ND-MPC-122F-4	32.42	30.02	26.41	23.95	20.57	16.97
LAB3-ND-WD-122F-3	30.88	29.25	27.11	23.95	20.60	16.69
LAB3-ND-WD-122F-4	30.91	29.27	27.02	23.92	20.62	16.72
LAB3-ND-BRMPC-122F-3	27.60	26.09	23.19	21.06	18.67	15.77
LAB3-ND-BRMPC-122F-4	27.73	25.93	23.15	21.07	18.65	15.77
LAB4-ND-FPC-68F-1	33.26	19.23	17.69	13.42	10.50	8.62
LAB4-ND-MPC-68F-1	33.84	24.48	18.45	14.05	10.67	8.57
LAB4-ND-WD-68F-1	17.77	17.36	13.56	12.01	10.05	8.28
LAB4-ND-BRMPC-68F-1	21.60	18.39	14.47	12.31	9.83	7.99
LAB4-ND-FPC-100F-1	41.89	33.23	28.75	22.80	17.14	13.63
LAB4-ND-MPC-100F-1	29.94	27.18	23.34	21.20	16.88	13.33
LAB4-ND-WD-100F-1	27.30	23.03	20.07	19.06	15.69	13.37
LAB4-ND-BRMPC-100F-1	26.31	22.47	20.55	18.12	15.32	12.59
LAB4-ND-FPC-122F-1	44.70	36.93	28.24	23.38	20.02	16.65
LAB4-ND-MPC-122F-1	37.77	32.46	25.87	23.22	19.74	16.24
LAB4-ND-WD-122F-1	101.92	39.75	28.24	24.63	20.58	16.48
LAB4-ND-BRMPC-122F-1	32.74	29.85	26.98	23.64	20.00	16.62

ND Winter VPCRx	V/L					
	0.05	0.1	0.2	0.5	1.5	4
LAB2-NDw-BR2-68F-1	17.91	16.99	15.78	13.34	10.87	8.58
LAB2-NDw-BR2-68F-2	17.39	16.73	15.91	13.34	10.83	8.58
LAB2-NDw-BR3-68F-1	16.94	16.40	15.76	13.44	10.60	8.42
LAB2-NDw-BR3-68F-2	16.89	16.86	15.76	13.44	10.55	8.36
LAB2-NDw-MPC-68F-1	20.23	18.78	17.52	14.14	11.50	9.38
LAB2-NDw-MPC-68F-2	20.40	18.14	17.39	14.09	11.50	9.36
LAB2-NDw-BR2-100F-1	23.75	23.33	22.13	19.63	16.33	12.96
LAB2-NDw-BR2-100F-2	23.68	23.58	22.14	19.55	16.27	12.90
LAB2-NDw-BR3-100F-1	28.41	24.97	22.17	19.56	16.12	12.63
LAB2-NDw-BR3-100F-2	26.81	23.96	22.49	19.34	16.21	12.83
LAB2-NDw-MPC-100F-1	22.94	22.55	21.53	19.78	16.88	13.41
LAB2-NDw-MPC-100F-2	23.24	22.59	21.53	19.81	16.83	13.32
LAB2-NDw-BR1-100F-1	26.30	24.49	21.62	19.13	15.91	12.61
LAB2-NDw-BR1-100F-2	25.93	24.00	21.42	19.11	15.99	12.57
LAB2-NDw-BR2-122F-1	32.79	29.37	27.49	24.52	20.40	16.37
LAB2-NDw-BR2-122F-2	33.11	29.12	27.32	24.48	20.46	16.38
LAB2-NDw-BR3-122F-1	30.92	29.21	27.87	24.67	20.21	15.90
LAB2-NDw-BR3-122F-2	31.77	29.54	27.55	24.30	20.14	16.01
LAB2-NDw-MPC-122F-1	28.89	27.74	26.88	25.03	21.21	16.92
LAB2-NDw-MPC-122F-2	28.23	27.97	26.80	24.88	21.48	16.89

TX Summer VPCRx	V/L					
	0.02	0.05	0.2	0.5	1.5	4
LAB1-TX-FPC-68F-1	–	16.99	11.05	9.26	7.22	5.74
LAB1-TX-FPC-68F-2	–	16.83	10.18	9.15	7.36	5.62
LAB1-TX-FPC-68F-3	–	16.46	9.93	9.03	7.26	5.67
LAB1-TX-TL-100F-1	14.6	–	–	–	–	–
LAB1-TX-TL-100F-2	15.11	–	–	–	–	–
LAB1-TX-TL-100F-3	14.89	–	–	–	–	–
LAB1-TX-FPC-100F-1	–	17.41	15.41	13.56	11.03	8.76
LAB1-TX-FPC-100F-2	–	16.2	14.57	13.38	11.16	8.78
LAB1-TX-FPC-100F-3	17.85	16.99	14.31	13.38	11.24	8.91
LAB1-TX-FPC-122F-1	–	20.49	19.08	17.3	14.5	11.61
LAB1-TX-FPC-122F-2	–	18.75	18.46	17.09	14.63	11.54
LAB1-TX-FPC-122F-3	20.05	18.6	18.5	17.09	14.7	11.66
LAB2-TX-FPC-68F-1	18.66	16.25	11.86	9.49	7.17	5.65
LAB2-TX-FPC-68F-2	18.47	16.31	11.83	9.16	7.16	5.64
LAB2-TX-MPC-68F-1	19.75	16.89	10.8	8.67	7.12	5.72
LAB2-TX-MPC-68F-2	19.5	16.83	10.35	8.61	7.07	5.64
LAB2-TX-WD-68F-1	18.3	16.83	11.95	9.63	7.49	5.81
LAB2-TX-WD-68F-2	17.82	17.11	11.95	10.25	7.55	5.77
LAB2-TX-BR-68F-1	12.77	11.96	10.39	8.62	7.03	5.56
LAB2-TX-BR-68F-2	12.03	11.51	10.22	8.9	6.9	5.54
LAB2-TX-BRMPC-68F-1	22.78	17.75	12.85	8.94	7.3	5.62
LAB2-TX-BRMPC-68F-2	22.08	18.52	12.38	9.29	7.22	5.64
LAB2-TX-FPC-100F-1	24.35	17.28	14.89	13.12	10.96	8.62
LAB2-TX-FPC-100F-2	23.49	17.41	14.95	13.09	11.18	8.65
LAB2-TX-MPC-100F-1	27.15	17.17	16.89	14.25	11.31	8.78
LAB2-TX-MPC-100F-2	28.92	17.24	17.11	13.92	11.21	8.77
LAB2-TX-WD-100F-1	27.1	16.95	15.92	13.43	11.26	9.00
LAB2-TX-WD-100F-2	25.77	17.01	16.28	13.6	11.35	9.00
LAB2-TX-BR-100F-1	17.81	17.12	15.21	13.45	11.25	8.99
LAB2-TX-BR-100F-2	17.5	16.96	15.21	13.54	11.26	8.97
LAB2-TX-BRMPC-100F-1	25.12	18.4	17.78	13.88	11.16	8.61
LAB2-TX-BRMPC-100F-2	23.98	19.55	17.94	14.05	11.24	8.65
LAB2-TX-FPC-122F-1	32.98	22.98	20.26	17.44	14.25	11.05
LAB2-TX-FPC-122F-2	33.57	23.55	20.01	17.01	14.12	11.21
LAB2-TX-MPC-122F-1	33.51	24.84	20.66	18.18	14.96	11.6
LAB2-TX-MPC-122F-2	32.76	24.81	20.72	18.34	15.12	11.63
LAB2-TX-WD-122F-1	36.31	21.34	19.01	17.33	14.48	11.45
LAB2-TX-WD-122F-2	35.4	20.6	19.08	17.36	14.56	11.54
LAB2-TX-BR-122F-1	20.55	20.16	18.52	17.24	14.82	11.92
LAB2-TX-BR-122F-2	20.1	20.1	18.55	17.24	14.82	12
LAB2-TX-BRMPC-122F-1	29.83	23.84	20.47	17.89	14.35	11.32
LAB2-TX-BRMPC-122F-2	28.74	24.27	20.56	18.05	14.41	11.39
LAB3-TX-FPC-68F-1	14.40	13.74	12.18	10.98	8.47	6.51
LAB3-TX-FPC-68F-2	14.39	13.78	12.24	10.98	8.43	6.50
LAB3-TX-MPC-68F-1	17.19	16.19	14.52	11.40	8.14	6.50
LAB3-TX-MPC-68F-2	17.16	16.17	14.50	11.36	8.14	6.53
LAB3-TX-WD-68F-1	18.80	17.46	12.53	10.92	8.60	6.70
LAB3-TX-WD-68F-2	18.77	17.43	12.52	10.91	8.59	6.72
LAB3-TX-BR-68F-1	11.23	10.44	9.73	8.46	6.87	5.66
LAB3-TX-BR-68F-2	11.23	10.50	9.76	8.47	6.87	5.66
LAB3-TX-BRMPC-68F-1	16.95	16.58	14.63	11.70	8.25	6.21
LAB3-TX-BRMPC-68F-2	16.94	16.55	14.61	11.75	8.27	6.25
LAB3-TX-FPC-100F-1	20.22	19.14	16.75	13.53	10.86	9.69
LAB3-TX-FPC-100F-2	20.23	19.17	16.75	13.53	10.86	9.72
LAB3-TX-MPC-100F-1	22.51	21.10	18.88	16.26	12.68	10.41

TX Summer VPCRx	V/L					
	0.02	0.05	0.2	0.5	1.5	4
LAB3-TX-MPC-100F-2	22.54	21.12	18.87	16.24	12.66	10.44
LAB3-TX-WD-100F-1	22.26	20.62	17.55	15.36	12.26	8.99
LAB3-TX-WD-100F-2	22.29	20.64	17.52	15.36	12.27	8.96
LAB3-TX-BR-100F-1	17.45	16.62	14.21	12.53	10.47	8.57
LAB3-TX-BR-100F-2	17.46	16.61	14.21	12.53	10.47	8.57
LAB3-TX-BRMPC-100F-1	22.52	20.78	17.65	14.88	11.99	9.75
LAB3-TX-BRMPC-100F-2	22.57	20.84	17.62	14.92	12.01	9.78
LAB3-TX-FPC-122F-1	22.79	21.90	19.97	17.61	14.78	12.20
LAB3-TX-FPC-122F-2	22.76	21.89	19.91	17.61	14.78	12.20
LAB3-TX-MPC-122F-1	28.75	26.45	23.32	19.62	15.88	12.91
LAB3-TX-MPC-122F-2	28.80	26.50	23.32	19.61	15.90	12.86
LAB3-TX-WD-122F-1	27.75	26.03	22.45	18.75	15.55	12.44
LAB3-TX-WD-122F-2	27.76	26.02	22.47	18.77	15.55	12.43
LAB3-TX-BR-122F-1	19.64	19.84	17.93	16.16	13.81	11.34
LAB3-TX-BR-122F-2	19.68	19.88	17.93	16.16	13.81	11.34
LAB3-TX-BRMPC-122F-1	26.48	24.12	20.77	18.16	15.24	12.39
LAB3-TX-BRMPC-122F-2	26.51	24.15	20.74	18.16	15.29	12.43

TX Winter VPCRx	V/L					
	0.05	0.1	0.2	0.5	1.5	4
LAB2-TXw-WD-100F-1	19.4	17.5	16.49	13.8	11.39	8.74
LAB2-TXw-WD-100F-2	19.05	17.62	16.12	13.8	11.41	8.71
LAB2-TXw-MPC-100F-1	19.65	17.73	17.2	14.47	11.82	8.96
LAB2-TXw-MPC-100F-2	19.78	17.34	16.86	14.17	11.71	8.96
LAB2-TXw-BR2-100F-1	20.07	17.82	16.96	13.8	11.38	8.93
LAB2-TXw-BR2-100F-2	19.97	17.7	16.86	13.77	11.5	8.87
LAB2-TXw-BR3-100F-1	21.36	18.53	17.27	14.19	11.6	8.89
LAB2-TXw-BR3-100F-2	21.49	18.7	17.27	14.21	11.83	8.86
LAB2-TXw-BR1-100F-1	17.66	17.01	16.49	13.63	11.41	8.81
LAB2-TXw-BR1-100F-2	17.66	16.96	16.49	13.67	11.39	8.76

ND-TVP-95-BPP							
	BPP 1-1	BPP 1-2	BPP 2-1	BPP 2-2	BPP 3-1	BPP 3-2	Avg Day1&2 Used in EOS
Date	8/31/2016	8/31/2016	9/1/2016	9/1/2016	9/2/2016	9/2/2016	–
T(°F)	99.7	99.7	99.8	99.8	100.4	100.4	–
P, psia	18.99	18.99	19.19	19.19	19.24	19.24	–
GOR	0	0	0	0	0	0	–
Measured Off-Gas (mole%)							
N2	1.9040	1.6512	3.2877	3.3299	6.3432	7.4418	–
CO2	0.2860	0.2928	0.2962	0.3083	0.2850	0.2850	–
Ar	0.0246	0.0213	0.0357	0.0215	0.0650	0.0814	–
O2	0.3308	0.2791	0.5094	0.4851	1.0727	1.3879	–
H2S	0	0	0	0	0	0	–
C1	6.0811	5.5348	6.2442	6.6021	8.2771	7.8481	–
C2	22.400	22.672	22.354	22.342	20.028	19.911	–
C3	35.130	35.377	34.075	33.742	31.313	30.559	–
iC4	4.9799	5.0031	4.8905	4.8681	4.8168	4.7672	–
nC4	16.994	17.128	16.529	16.426	15.877	15.712	–
iC5	3.0037	3.0340	2.9668	2.9715	3.0042	3.0274	–
NC5	4.4334	4.4832	4.3935	4.4162	4.3338	4.3889	–
iC6	1.3558	1.3810	1.3443	1.3589	1.3787	1.3954	–
NC6	1.0144	1.0288	1.0053	1.0211	1.0196	1.0372	–
MCP	0.4239	0.4394	0.4220	0.4247	0.4502	0.4432	–
BEN	0.0797	0.0806	0.0833	0.0852	0.0832	0.0857	–
CC6	0.1522	0.1550	0.1532	0.1554	0.1594	0.1625	–
C7	0.6352	0.6509	0.6360	0.6489	0.6743	0.6670	–
MCH	0.1851	0.1883	0.1873	0.1912	0.2003	0.1983	–
TOL	0.0396	0.0398	0.0426	0.0432	0.0440	0.0440	–
iC8	0.1642	0.1709	0.1663	0.1678	0.1838	0.1775	–
C8s	0.2848	0.2911	0.2859	0.2935	0.2945	0.2865	–
ETB	0.0089	0.0087	0.0087	0.0088	0.0084	0.0085	–
XYL	0.0290	0.0296	0.0287	0.0295	0.0297	0.0288	–
C9	0.0519	0.0523	0.0489	0.0515	0.0506	0.0491	–
C10+	0.0064	0.0066	0.0056	0.0073	0.0072	0.0073	–
EOS Calculated Whole Oil (mole%)							
N2	4.055E-03	3.517E-03	7.068E-03	7.156E-03	1.364E-02	0.015996	4.418E-03
CO2	4.529E-03	4.639E-03	4.737E-03	4.929E-03	4.547E-03	0.004547	4.856E-03
Argon	1.023E-04	8.833E-05	1.495E-04	9.012E-05	2.723E-04	0.000341	1.159E-04
O2	1.383E-03	1.167E-03	2.149E-03	2.046E-03	4.525E-03	0.005853	1.926E-03
C1	0.0367	0.0334	0.0380	0.0402	0.0503	0.0477	0.0428
C2	0.6836	0.6927	0.6884	0.6883	0.6150	0.6112	0.7256
C3	3.6141	3.6440	3.5367	3.5040	3.2354	3.1569	3.5639
iC4	1.2545	1.2618	1.2428	1.2378	1.2172	1.2046	1.2300
nC4	5.9157	5.9696	5.8036	5.7711	5.5409	5.4826	5.7341
iC5	2.5831	2.6119	2.5730	2.5787	2.5867	2.6068	2.5128
NC5	4.9858	5.0472	4.9824	5.0114	4.8773	4.9394	4.8241
C6	10.362	10.575	10.370	10.502	10.568	10.677	10.0811
C7	8.8412	9.0508	8.9438	9.1321	9.4001	9.3026	8.6650
BEN	0.2890	0.2925	0.3045	0.3119	0.3019	0.3106	0.2846
TOL	0.4766	0.4788	0.5169	0.5248	0.5288	0.5289	0.4616
ETB	0.3157	0.3103	0.3116	0.3150	0.2977	0.2999	0.2888
XYL	1.2390	1.2646	1.2369	1.2733	1.2651	1.2248	1.1303
C8+	59.394	58.758	59.437	59.095	59.493	59.581	60.444

GOR 1-2 as received from lab appears to be a duplicate of GOR 1-1

ND-TVP-95- GOR						
	GOR 1-1	**GOR 1-2**	**GOR 2-1**	**GOR 2-2**	**GOR 3-1**	**GOR 3-2**
Date	8/31/2016	8/31/2016	9/1/2016	9/1/2016	9/2/2016	9/2/2016
T(°F)	100	100	100.1	100.1	100	100
P, psia	13.96	13.96	14.06	14.06	13.72	13.72
GOR	12.4	12.4	12.8	12.8	9.7	9.7
Measured Off-Gas (mole%)						
N2	0.0773	0.0773	0.2496	0.2138	0.6068	0.3411
CO2	0.1381	0.1381	0.1714	0.1834	0.1623	0.1546
Ar	0.0000	0.0000	0.0107	0.0104	0.0165	0.0131
O2	0.0413	0.0413	0.1519	0.1353	0.2548	0.1644
H2S	0	0	0	0	0	0
C1	1.4786	1.4786	2.1784	2.7394	2.1916	2.2210
C2	16.954	16.954	18.717	19.729	17.759	17.788
C3	38.476	38.476	37.432	36.522	36.688	36.771
iC4	6.1015	6.1015	6.0132	5.8079	6.0650	6.0135
nC4	21.435	21.435	20.286	19.616	20.702	20.685
iC5	3.8691	3.8691	3.7853	3.7173	3.9617	3.9574
NC5	5.6670	5.6670	5.5175	5.4909	5.7472	5.7952
iC6	1.7630	1.7630	1.7234	1.7454	1.8063	1.8428
NC6	1.2915	1.2915	1.2726	1.3199	1.3391	1.3761
MCP	0.5692	0.5692	0.5376	0.5461	0.5605	0.5777
BEN	0.0999	0.0999	0.0970	0.1120	0.1066	0.1138
CC6	0.1929	0.1929	0.1886	0.2042	0.2094	0.2180
C7	0.8292	0.8292	0.7889	0.8607	0.8443	0.8874
MCH	0.2378	0.2378	0.2240	0.2563	0.2510	0.2683
TOL	0.0501	0.0501	0.0411	0.0530	0.0525	0.0707
iC8	0.2275	0.2275	0.2119	0.2242	0.2179	0.2266
C8s	0.3811	0.3811	0.3181	0.3892	0.3539	0.3841
ETB	0.0110	0.0110	0.0077	0.0113	0.0094	0.0119
XYL	0.0351	0.0351	0.0235	0.0365	0.0309	0.0402
C9	0.0664	0.0664	0.0472	0.0666	0.0564	0.0695
C10+	0.0074	0.0074	0.0053	0.0085	0.0072	0.0095
EOS Calculated Whole Oil (mole%)						
N2	1.657E-03	1.657E-03	5.515E-03	4.722E-03	1.036E-02	5.825E-03
CO2	4.325E-03	4.325E-03	5.489E-03	5.871E-03	4.354E-03	4.147E-03
Argon	0	0	2.515E-04	2.457E-04	3.055E-04	2.420E-04
O2	9.466E-04	9.466E-04	3.581E-03	3.189E-03	4.722E-03	3.046E-03
C1	0.0358	0.0358	0.0542	0.0682	0.0435	0.0440
C2	0.7085	0.7085	0.7956	0.8390	0.6598	0.6613
C3	3.6068	3.6068	3.5402	3.4588	3.2434	3.2557
iC4	1.2262	1.2262	1.2150	1.1755	1.1780	1.1699
nC4	5.7893	5.7893	5.5019	5.3321	5.4324	5.4395
iC5	2.4719	2.4719	2.4250	2.3872	2.4818	2.4846
NC5	4.7009	4.7009	4.5873	4.5772	4.6816	4.7319
C6	9.7565	9.7565	9.5302	9.7971	9.8655	10.1402
C7	8.3338	8.3338	7.9227	8.7614	8.4450	8.9297
BEN	0.2632	0.2632	0.2555	0.2967	0.2766	0.2968
TOL	0.4369	0.4369	0.3583	0.4638	0.4515	0.6108
ETB	0.2838	0.2838	0.1987	0.2913	0.2373	0.3021
XYL	1.0844	1.0844	0.7255	1.1341	0.9414	1.2317
C8+	61.295	61.295	62.875	61.404	62.043	60.688

ND-TM1-C30+ (mole%)					
	Test 1	Test 2	Test 3	Test 3 - GOR	Renormalized Avg Used in EOS
C1	0.074	0.077	0.076	0.085	–
C2	0.180	0.169	0.142	0.158	–
C3	1.966	1.858	1.591	1.603	–
iC4	0.900	0.859	0.818	0.807	–
nC4	4.583	4.518	4.114	3.900	–
iC5	2.304	2.277	2.263	2.188	–
nC5	4.900	4.927	4.854	4.607	–
iC6	3.447	3.438	3.514	3.441	–
nC6	3.612	3.602	3.819	3.681	–
MCP	2.000	1.989	1.905	1.923	–
Ben	0.354	0.354	0.398	0.368	–
cC6	1.017	1.009	1.136	1.109	–
iC8	0.114	0.113	0.113	0.113	–
C7	7.392	7.419	7.742	7.693	–
McC6	2.056	2.049	2.364	2.333	–
Tol	0.732	0.732	0.831	0.774	–
C8	8.278	8.316	8.696	8.654	9.748
Etb	0.605	0.608	0.586	0.584	–
M&P-Xyl	0.809	0.799	0.991	0.933	–
o-Xyl	0.365	0.366	0.417	0.396	–
C9	6.041	6.061	6.308	6.258	5.637
C10	7.057	7.114	7.280	7.253	6.601
C11	5.465	5.513	5.527	5.550	5.114
C12	4.400	4.449	4.381	4.426	4.122
C13	4.085	4.042	4.059	4.106	3.786
C14	3.441	3.483	3.412	3.465	3.225
C15	2.990	3.026	2.954	2.840	2.802
C16	2.401	2.439	2.359	2.407	2.255
C17	2.131	2.033	2.068	2.066	1.940
C18	1.853	1.878	1.801	1.908	1.738
C19	1.694	1.692	1.635	1.680	1.577
C20	1.439	1.487	1.326	1.451	1.363
C21	1.294	1.289	1.246	1.280	1.203
C22	1.097	1.107	1.006	1.110	1.027
C23	0.993	1.029	0.941	0.999	0.942
C24	0.887	0.903	0.844	0.868	0.834
C25	0.808	0.788	0.685	0.790	0.743
C26	0.666	0.709	0.617	0.702	0.641
C27	0.474	0.616	0.510	0.537	0.508
C28	0.583	0.608	0.530	0.572	0.555
C29	0.412	0.417	0.449	0.437	0.386
C30+	4.101	3.838	3.692	3.945	3.698

ND-TM2: 2177+D7900+D7169 Merge (mole%)								
	FPC-1	**FPC-2**	**MPC-1**	**MPC-2**	**WD-1**	**WD-2**	**BRFPC-1**	**BRFPC-2**
N2	1.601E-04	1.723E-04	1.617E-04	1.506E-04	1.176E-04	1.531E-04	6.869E-05	6.470E-05
CO2	1.233E-05	1.301E-05	1.096E-05	1.120E-05	1.233E-05	1.170E-05	6.293E-06	5.264E-06
C1	0.0973	0.0927	0.0598	0.0600	0.0828	0.0815	0.0232	0.0217
C2	0.6406	0.6080	0.5484	0.5676	0.6256	0.6309	0.5017	0.4965
C3	3.2548	3.1788	2.8361	2.9162	3.0925	3.1409	2.8905	2.8993
iC4	1.0316	1.0150	0.9136	0.9345	1.0336	1.0277	1.0001	1.0169
nC4	5.3013	5.1892	4.6235	4.7198	5.1040	5.1234	4.9291	4.9446
neo C5	0	0	0	0	0	0	0	0
iC5	2.2047	2.1682	1.9444	1.9860	2.1160	2.1794	2.1826	2.1803
nC5	4.2442	4.1484	3.7233	3.8271	4.1151	4.2219	4.1240	4.1397
C6	9.3606	8.9664	11.1470	10.3182	7.9252	7.1268	8.2428	8.3741
C7	10.2618	10.5936	10.2195	10.4936	10.5663	10.7806	10.8733	10.9195
C8	9.8922	10.1887	9.9905	9.8614	10.1754	10.5588	10.4924	10.5701
C9	6.0788	6.1456	6.5418	5.9710	6.2517	6.4000	6.2478	6.2967
C10	7.0122	6.7825	6.8415	6.8294	7.0357	6.9307	7.1171	6.8185
C11	4.7877	4.9506	5.2054	5.2105	5.3098	5.2260	5.0818	4.9923
C12	4.5747	4.2119	4.3482	4.3437	4.4354	4.2529	4.5368	4.5582
C13	3.6475	3.8750	4.0004	3.9962	4.0806	4.1036	3.8892	3.8123
C14	3.3596	3.4820	3.4275	3.4178	3.4962	3.5159	3.4074	3.4236
C15	2.6219	2.8101	2.8452	2.8291	2.9022	2.8375	2.7399	2.6719
C16	2.2118	2.2351	2.2001	2.1751	2.2442	2.2568	2.2433	2.1788
C17	2.3480	2.1634	2.2669	2.2482	2.3124	2.2549	2.3114	2.3224
C18	1.9562	1.7792	1.7513	1.7911	1.7864	1.7965	1.8518	1.7942
C19	1.4936	1.4464	1.4857	1.4562	1.4523	1.4605	1.4517	1.4586
C20	1.3689	1.3232	1.3616	1.3926	1.4493	1.3968	1.3884	1.3343
C21	1.2936	1.2504	1.2868	1.2016	1.2555	1.2626	1.2550	1.2036
C22	1.0733	1.0303	1.0142	1.0919	1.0890	1.0404	1.0341	1.0390
C23	1.0294	0.9362	0.9727	0.9425	0.9400	0.9978	0.9918	0.9965
C24	0.8901	0.8495	0.8853	0.8552	0.9031	0.8577	0.8526	0.8566
C25+	7.9466	8.5344	7.5868	8.5919	8.2703	8.5841	8.3334	8.6731

ND-TM3: GOR+D8003+D7169 Merge (mole%)								
	FPC-1	FPC-2	MPC-1	MPC-2	WD-1	WD-2	BRFPC-1	BRFPC-2
CO2	1.914E-03	1.835E-03	5.209E-03	3.137E-03	1.634E-03	1.650E-03	1.331E-03	1.300E-03
CO	1.647E-05	6.250E-05	8.540E-04	1.453E-03	0	2.271E-04	0	0
H2S	0	0	0	0	0	0	0	0
He	0	0	0	0	0	0	1.497E-04	1.623E-04
H2	2.697E-04	2.593E-04	1.345E-03	6.855E-04	7.359E-05	2.947E-04	0	1.926E-04
O2	1.846E-03	1.758E-03	1.459E-02	9.890E-03	2.894E-03	1.785E-03	2.197E-03	4.474E-03
N2	1.116E-02	1.038E-02	8.091E-02	5.657E-02	4.948E-02	5.163E-02	1.330E-02	2.386E-02
C1	0.0273	0.0282	0.0277	0.0285	0.0299	0.0302	0.0143	0.0144
C2	0.6739	0.6834	0.6886	0.7026	0.6868	0.6888	0.5981	0.6055
C3	3.5718	3.6227	3.4983	3.5715	3.5148	3.5343	3.2598	3.3021
iC4	1.1714	1.1892	1.1329	1.1565	1.1634	1.1708	1.1448	1.1589
nC4	5.8714	5.9622	5.7188	5.8390	5.7784	5.8187	5.5178	5.5882
neo C5	0	0	0	0	0	0	0	0
iC5	2.4595	2.5023	2.3872	2.4367	2.4482	2.4685	2.4459	2.4777
nC5	4.7602	4.8443	4.6724	4.7709	4.7926	4.8333	4.7077	4.7750
C6	6.9194	7.0560	6.7788	6.9179	6.9712	7.0606	7.0831	7.1951
Benzene	0.3703	0.3809	0.3582	0.3678	0.3943	0.4018	0.3851	0.3950
C7	9.8688	10.0846	9.6371	9.8254	9.9774	10.1372	10.4606	10.6409
C8	10.4329	10.7124	10.1341	10.3776	10.7141	10.8673	11.1001	11.2966
C9	7.3513	7.5513	7.2172	7.2842	7.5751	7.7625	7.6971	7.8370
C10	6.6476	6.4646	6.8018	6.6667	6.6696	6.4429	6.7135	6.4822
C11	4.9776	4.8938	5.2038	5.0726	5.0132	5.0188	4.8314	4.7272
C12	4.1496	3.9718	4.3469	4.2288	4.1877	3.9974	4.3133	4.3161
C13	3.9085	3.8368	3.9062	3.7978	3.8527	3.7673	3.6976	3.6098
C14	3.4325	3.3656	3.5121	3.4127	3.3009	3.3873	3.2396	3.2417
C15	2.8570	2.7162	2.8443	2.7542	2.7401	2.6670	2.6049	2.5300
C16	2.1496	2.0883	2.1994	2.1176	2.1188	2.1212	2.1328	2.0631
C17	2.2149	2.1585	2.2662	2.1887	2.1832	2.1194	2.1976	2.1990
C18	1.7111	1.7197	1.7508	1.7437	1.6866	1.6885	1.7606	1.6989
C19	1.4516	1.3981	1.4852	1.4176	1.3712	1.3728	1.4402	1.3811
C20	1.3304	1.2789	1.3612	1.3558	1.3684	1.3129	1.2626	1.2634
C21	1.2026	1.2086	1.2305	1.1698	1.1854	1.1867	1.1932	1.1397
C22	1.0431	0.9959	1.0673	1.0630	1.0282	0.9779	0.9832	0.9838
C23	0.9504	0.9049	0.9725	0.9176	0.8875	0.9379	0.9430	0.9436
C24	0.8170	0.8211	0.8851	0.8326	0.8527	0.8062	0.8106	0.8111
C25+	7.6630	7.5456	7.8123	7.9106	7.4535	7.3662	7.4446	7.2927

Summer ND-TM4: GPA2103M+ASTMD2887 Merge (mole%)				
	BR	WD	MPC	FPC
N2	0.060	0.065	0.022	0.027
C1	0.028	0.038	0.038	0.028
CO2	0.003	0.003	0.010	0.003
C2	0.678	0.701	0.732	0.727
C3	3.414	3.508	3.476	3.509
iC4	1.122	1.127	1.120	1.110
nC4	5.489	5.602	5.499	5.549
iC5	2.396	2.440	2.434	2.414
nC5	4.715	4.775	4.844	4.700
iC6	2.666	2.653	2.657	2.662
nC6	3.289	3.275	3.279	3.285
iC8	0.101	0.101	0.101	0.101
Ben	0.399	0.400	0.400	0.400
C7	11.386	11.337	11.345	11.362
Tol	0.939	0.936	0.937	0.939
C8	11.487	11.433	11.449	11.467
ETB	0.447	0.447	0.447	0.446
Xyl	1.481	1.477	1.478	1.480
C9	7.159	7.129	7.134	7.142
C10	6.580	6.553	6.558	6.569
C11	5.138	5.115	5.121	5.127
C12	3.815	3.798	3.802	3.806
C13	3.586	3.570	3.574	3.578
C14	3.035	3.022	3.025	3.028
C 15	2.484	2.473	2.476	2.479
C16	2.020	2.011	2.013	2.016
C 17	1.859	1.851	1.853	1.855
C18	1.531	1.524	1.526	1.528
C19	1.372	1.366	1.367	1.369
C20	1.201	1.195	1.197	1.198
C21	1.030	1.025	1.026	1.027
C22	0.911	0.907	0.908	0.909
C23	0.799	0.795	0.796	0.797
C24	0.698	0.695	0.696	0.696
C25	0.641	0.639	0.639	0.640
C26	0.578	0.575	0.576	0.576
C27	0.538	0.535	0.536	0.536
C28	0.480	0.478	0.479	0.479
C29	0.452	0.450	0.450	0.451
C30+	3.993	3.976	3.980	3.985

ND-TM4a: GPA 2103M Final Report (mole%)								
	FPC-1	FPC-2	MPC-1	MPC-2	WD-1	WD-2	BRFPC-1	BRFPC-2
N2	1.187E-02	1.408E-02	6.468E-02	4.650E-02	1.301E-02	2.717E-02	7.149E-03	6.564E-03
CO2	2.580E-03	1.996E-03	3.824E-03	4.245E-03	1.565E-03	1.479E-03	1.403E-03	1.144E-03
C1	0.0273	0.0292	0.0436	0.0243	0.0248	0.0267	0.0088	0.0081
C2	0.6901	0.6644	0.7072	0.6411	0.6425	0.6516	0.5309	0.5315
C3	3.5269	3.4891	3.5539	3.5229	3.3686	3.4736	3.0830	3.0806
iC4	1.1384	1.1335	1.1439	1.1595	1.0727	1.1289	1.0758	1.0801
nC4	5.7171	5.7424	5.8231	5.9248	5.5099	5.7080	5.3005	5.2790
neoC5	0.0000	0.0000	0.0000	0.0000	0.0000	0.0000	0.0000	0.0000
iC5	2.4029	2.4039	2.4726	2.4832	2.2730	2.3733	2.3364	2.3147
nC5	4.6513	4.6725	4.8560	4.8542	4.4409	4.6269	4.4815	4.4614
neoC6	0.0483	0.0478	0.0440	0.0385	0.0603	0.0457	0.0379	0.0317
2,3-dimethylC4, 2-methylC5	2.0143	2.0249	2.1023	2.0945	1.8974	1.9777	1.9954	1.9744
3-methylC5, cycloC5	1.1757	1.1970	1.2302	1.2532	1.1109	1.1371	1.1748	1.1905
nC6	3.2224	3.2940	3.3920	3.3932	2.9741	3.1358	3.1924	3.1922
C7+	75.3719	75.2854	74.5809	74.5857	76.6102	75.6860	76.7742	76.8474

ND-TM4a: GPA 2103M C30+ by GC (mole%)								
	FPC-1	FPC-2	MPC-1	MPC-2	WD-1	WD-2	BRFPC-1	BRFPC-2
C2	0.00320	0.00205	0.00123	0.00377	0.00608	0.00144	0.00141	0.00393
C3	0.03528	0.01775	0.00657	0.02300	0.07374	0.00414	0.02270	0.08193
iC4	0.02227	0.01774	0.00877	0.01007	0.05280	0.01420	0.02641	0.05558
nC4	0.16819	0.14803	0.08404	0.08955	0.37593	0.13818	0.21355	0.36931
iC5	0.21978	0.21739	0.19368	0.22269	0.42774	0.26310	0.32501	0.39630
nC5	0.58969	0.59116	0.58614	0.73280	1.11243	0.74452	0.89646	1.03982
nC6	3.27033	3.20146	3.39078	4.19879	4.31892	3.64565	3.97572	4.12292
Mcyclo-C5	1.19799	1.11238	1.17578	1.34444	1.32938	1.15891	1.19443	1.25245
Benzene	0.26780	0.24388	0.27853	0.31285	0.32559	0.29042	0.31414	0.29539
Cyclo-C6	0.79567	0.78675	0.79695	0.83640	0.83748	0.78658	0.84350	0.85167
nC7	8.02077	7.94608	7.76782	8.22367	8.23010	7.88283	8.20503	8.24142
Mcyclo-C6	2.10940	2.01292	2.07473	1.84804	1.86041	1.96135	2.03033	2.09320
Toluene	0.92910	0.94893	0.96079	0.97292	0.98635	0.99028	0.97202	0.94095
nC8	10.25764	10.36322	10.16251	10.38783	10.38379	10.44812	10.49872	10.55407
C2-Benzene	0.93381	0.92908	0.92734	0.95883	0.95116	0.94948	0.92229	0.89780
P&M-Xylene	1.33810	1.37141	1.56200	1.54573	1.42128	1.54254	1.51515	1.47489
O-Xylene	0.50817	0.52585	0.52147	0.52624	0.53455	0.54112	0.53336	0.52377
nC9	7.20410	7.19062	7.07346	7.24202	7.26446	7.32843	7.23235	7.26324
nC10	8.75025	8.91710	8.86181	8.86760	8.82855	9.02957	8.81967	8.84554
nC11	6.48561	6.56204	6.55724	6.45892	6.37745	6.58709	6.36619	6.37637
nC12	5.75314	5.82015	5.82782	5.73068	5.63915	5.82450	5.61089	5.62047
nC13	5.09905	5.17832	5.18798	5.06814	4.98079	5.09527	4.96881	4.96374
nC14	4.12254	4.08593	4.09273	3.99730	3.93370	4.12625	3.93428	3.92472
nC15	3.86456	3.87869	3.89599	3.79246	3.73308	3.85602	3.75020	3.74235
nC16	3.08373	3.06688	3.11261	3.00964	2.95646	3.06615	2.98732	2.95584
nC17	2.59188	2.58994	2.59019	2.51800	2.46049	2.54611	2.49754	2.47071
nC18	2.51065	2.45274	2.50637	2.40581	2.34609	2.42730	2.38722	2.35215

ND-TM4a: GPA 2103M C30+ by GC (mole%)								
	FPC-1	**FPC-2**	**MPC-1**	**MPC-2**	**WD-1**	**WD-2**	**BRFPC-1**	**BRFPC-2**
nC19	2.26000	2.19417	2.24552	2.14176	2.09853	2.16996	2.15284	2.10173
nC20	1.93772	1.88136	1.92597	1.84672	1.79337	1.87300	1.86798	1.82274
nC21	1.69146	1.65097	1.70481	1.60345	1.56751	1.61262	1.63226	1.57742
nC22	1.53472	1.46410	1.51667	1.44741	1.41769	1.45899	1.45161	1.42565
nC23	1.38308	1.28786	1.33580	1.23752	1.22771	1.26434	1.27890	1.23567
nC24	1.18919	1.19588	1.24833	1.19267	1.14406	1.18900	1.20154	1.15915
nC25	1.05614	1.04705	1.03821	1.01240	0.97175	1.01353	1.00432	0.99150
nC26	0.99858	0.90532	0.93929	0.91354	0.86398	0.92608	0.91009	0.92184
nC27	0.79982	0.78020	0.86708	0.73781	0.77867	0.73637	0.79625	0.71547
nC28	0.79830	0.83530	0.77624	0.75925	0.72129	0.76715	0.77572	0.76865
nC29	0.70903	0.62456	0.64991	0.66845	0.65488	0.67163	0.66703	0.62483
C30+	5.50926	5.95472	5.54683	5.11088	5.01260	5.06778	5.21675	4.94484

Winter ND-TM4: GPA2103M+ASTMD2887 Merge (mole%)				
	W-FPC	W-BR1MPC	W-BR2MPC	W-BR3MPC
N2	0.033	0.038	0.038	0.061
C1	0.096	0.057	0.048	0.048
CO2	0.007	0.007	0.003	0.004
C2	0.925	0.837	0.797	0.729
C3	3.903	3.744	3.601	3.357
iC4	1.237	1.217	1.179	1.108
nC4	5.846	5.763	5.634	5.365
iC5	2.614	2.505	2.48	2.375
nC5	5.104	4.881	4.854	4.686
iC6	2.757	2.94	2.872	2.774
nC6	3.344	3.552	3.541	3.165
iC8	0.098	0.114	0.114	0.107
Ben	0.415	0.43	0.433	0.368
C7	11.319	12.106	12.18	11.34
Tol	0.909	0.924	0.935	0.829
C8	11.494	11.529	11.917	11.563
ETB	0.407	0.448	0.472	0.473
Xyl	1.583	1.585	1.641	1.439
C9	6.526	6.823	7.009	7.522
C10	6.384	5.889	5.932	6.35
C11	5.299	4.509	4.513	4.873
C12	3.719	3.672	3.655	3.943
C13	3.494	3.365	3.369	3.553
C14	2.945	2.802	2.812	2.98
C 15	2.373	2.396	2.363	2.475
C16	1.976	2.028	2.017	2.136
C 17	1.8	1.755	1.743	1.817
C18	1.476	1.535	1.53	1.608
C19	1.305	1.386	1.362	1.423
C20	1.146	1.199	1.198	1.24
C21	0.984	1.047	1.023	1.076
C22	0.866	0.926	0.921	0.961
C23	0.757	0.812	0.8	0.833
C24	0.664	0.717	0.716	0.728
C25	0.602	0.649	0.631	0.664
C26	0.549	0.578	0.575	0.592
C27	0.504	0.524	0.513	0.536
C28	0.451	0.478	0.461	0.483
C29	0.407	0.415	0.423	0.436
C30+	3.682	3.818	3.695	3.98

TX-TVP-95-BPP							
	BPP 1-1	**BPP 1-2**	**BPP 2-1**	**BPP 2-2**	**BPP 3-1**	**BPP 3-2**	**Avg used in EOS**
Date	10/12/16	10/12/16	10/13/16	10/13/16	10/14/16	10/14/16	–
T(°F)	100	100	99.7	99.7	100.1	100.1	–
P, psia	14.6	14.6	15.11	15.11	14.89	14.89	–
GOR	0	0	0	0	0	0	–
Measured Off-Gas (mole%)							
N2	4.324	4.185	4.589	4.468	4.230	3.968	–
CO2	0.870	0.859	0.968	0.976	0.962	0.946	–
Ar	0.051	0.048	0.050	0.049	0.047	0.044	–
O2	0.243	0.262	0.086	0.084	0.060	0.054	–
H2S	0	0	0	0	0	0	–
C1	11.271	10.621	12.041	11.903	12.587	12.385	–
C2	16.917	16.949	17.174	17.314	16.629	16.522	–
C3	28.011	28.440	27.962	28.136	27.162	27.555	–
iC4	6.972	7.001	6.688	6.707	6.902	6.939	–
nC4	16.068	16.084	15.526	15.613	15.838	15.918	–
iC5	4.974	4.979	4.726	4.721	5.015	5.006	–
NC5	4.951	4.965	4.763	4.754	4.989	4.988	–
iC6	1.963	1.993	1.905	1.869	2.017	2.029	–
NC6	1.312	1.346	1.292	1.265	1.348	1.365	–
MCP	0.344	0.355	0.342	0.332	0.348	0.355	–
BEN	0.123	0.130	0.128	0.122	0.127	0.130	–
CC6	0.220	0.231	0.226	0.218	0.226	0.231	–
C7	0.791	0.814	0.830	0.795	0.842	0.862	–
MCH	0.188	0.207	0.203	0.192	0.201	0.206	–
TOL	0.092	0.107	0.110	0.101	0.103	0.106	–
iC8	0.029	0.064	0.030	0.030	0.031	0.032	–
C8s	0.230	0.274	0.280	0.266	0.265	0.276	–
ETB	0.003	0.005	0.004	0.004	0.004	0.004	–
XYL	0.020	0.033	0.031	0.034	0.026	0.032	–
C9	0.028	0.045	0.041	0.041	0.037	0.043	–
C10+	0.003	0.004	0.004	0.004	0.003	0.004	–
EOS Calculated Whole Oil (mole%)							
N2	7.022E-03	6.776E-03	7.687E-03	7.484E-03	6.995E-03	6.554E-03	7.086E-03
CO2	1.057E-02	1.043E-02	1.219E-02	1.228E-02	1.190E-02	1.171E-02	1.151E-02
Argon	1.621E-04	1.511E-04	1.627E-04	1.601E-04	1.512E-04	1.417E-04	1.548E-04
O2	7.773E-04	8.357E-04	2.852E-04	2.772E-04	1.962E-04	1.752E-04	4.245E-04
C1	5.174E-02	4.874E-02	5.723E-02	5.654E-02	5.898E-02	5.804E-02	0.055
C2	0.393	0.394	0.415	0.418	0.395	0.393	0.401
C3	2.199	2.236	2.283	2.295	2.178	2.211	2.234
iC4	1.343	1.351	1.341	1.343	1.357	1.366	1.350
nC4	4.276	4.289	4.305	4.324	4.304	4.331	4.305
iC5	3.277	3.288	3.246	3.239	3.373	3.371	3.299
NC5	4.267	4.288	4.281	4.268	4.389	4.393	4.314
C6	10.375	10.633	10.620	10.386	10.862	10.988	10.644
C7	8.133	8.498	8.963	8.559	8.834	9.052	8.673
BEN	0.344	0.365	0.373	0.357	0.363	0.372	0.362
TOL	0.858	0.998	1.070	0.981	0.974	1.009	0.982
ETB	0.084	0.126	0.123	0.124	0.106	0.117	0.113
XYL	0.669	1.105	1.077	1.190	0.868	1.071	0.997
C8+	63.712	62.361	61.825	62.439	61.919	61.250	62.251

TX-TVP-95-GOR						
	GOR 1-1	**GOR 1-2**	**GOR 2-1**	**GOR 2-2**	**GOR 3-1**	**GOR 3-2**
Date	10/12/16	10/12/16	10/13/16	10/13/16	10/14/16	10/14/16
T(^{o}F)	99.7	99.7	100.2	100.2	100.1	100.1
P, psia	14.61	14.61	14.66	14.66	14.68	14.68
GOR	0.22	0.22	0.2	0.2	0.14	0.14
Measured Off-Gas (mole%)						
N2	4.023	4.150	4.338	4.326	3.064	2.596
CO2	0.847	0.814	0.996	0.994	0.928	0.925
Ar	0.047	0.048	0.050	0.050	0.034	0.030
O2	0.214	0.224	0.075	0.068	0.058	0.049
H2S	0	0	0	0	0	0
C1	10.977	10.782	12.253	12.019	12.046	12.314
C2	17.028	16.686	16.955	17.073	16.919	16.641
C3	27.989	28.167	27.456	27.899	28.135	28.533
iC4	7.204	7.179	6.655	6.685	7.028	7.019
nC4	16.037	16.085	15.741	15.835	16.257	16.396
iC5	5.097	5.104	4.841	4.799	5.035	5.000
NC5	4.985	5.013	4.929	4.880	5.023	5.008
iC6	2.027	2.064	1.989	1.920	1.991	1.973
NC6	1.348	1.379	1.355	1.299	1.333	1.324
MCP	0.344	0.355	0.365	0.346	0.342	0.342
BEN	0.115	0.130	0.135	0.123	0.122	0.124
CC6	0.218	0.228	0.239	0.223	0.221	0.222
C7	0.842	0.878	0.875	0.802	0.813	0.816
MCH	0.196	0.209	0.214	0.192	0.192	0.197
TOL	0.100	0.110	0.113	0.089	0.096	0.102
iC8	0.029	0.029	0.034	0.031	0.029	0.030
C8s	0.256	0.277	0.297	0.266	0.255	0.269
ETB	0.004	0.004	0.005	0.004	0.004	0.004
XYL	0.030	0.035	0.037	0.033	0.030	0.037
C9	0.040	0.045	0.049	0.040	0.040	0.043
C10+	0.004	0.004	0.005	0.005	0.004	0.005
EOS Calculated Whole Oil (mole%)						
N2	8.044E-05	8.287E-05	8.529E-05	8.521E-05	5.732E-05	4.850E-05
CO2	1.063E-04	1.022E-04	1.246E-04	1.243E-04	1.155E-04	1.150E-04
Argon	1.65E-06	1.7E-06	1.763E-06	1.769E-06	1.167E-06	1.039E-06
O2	7.657E-06	7.979E-06	2.639E-06	2.410E-06	1.992E-06	1.680E-06
C1	0.0005	0.0005	0.0006	0.0006	0.0006	0.0006
C2	0.0040	0.0040	0.0040	0.0040	0.0040	0.0039
C3	0.0222	0.0224	0.0217	0.0220	0.0223	0.0226
iC4	0.0140	0.0140	0.0129	0.0129	0.0136	0.0136
nC4	0.0431	0.0433	0.0421	0.0422	0.0435	0.0439
iC5	0.0339	0.0340	0.0320	0.0316	0.0334	0.0331
NC5	0.0434	0.0437	0.0426	0.0421	0.0435	0.0434
C6	0.1075	0.1101	0.1070	0.1024	0.1056	0.1050
C7	0.0871	0.0914	0.0906	0.0825	0.0838	0.0845
BEN	0.0032	0.0037	0.0038	0.0034	0.0034	0.0035
TOL	0.0094	0.0104	0.0105	0.0082	0.0089	0.0096
ETB	0.0011	0.0012	0.0013	0.0011	0.0010	0.0012
XYL	0.0101	0.0117	0.0122	0.0109	0.0098	0.0124
C8+	0.620	0.610	0.618	0.636	0.626	0.623

TX-TM1-C30+ (mole%)				
	Test 1	Test 2	Test 3	Renormalized Avg Used in EOS
C1	0.171	0.147	0.154	–
C2	0.089	0.100	0.094	–
C3	1.094	1.148	1.069	–
iC4	0.829	0.836	0.820	–
nC4	3.123	3.166	3.124	–
iC5	2.748	2.726	2.716	–
nC5	4.177	4.168	4.143	–
iC6	3.751	3.724	3.697	–
nC6	3.652	3.653	3.624	–
MCP	1.246	1.247	1.235	–
Ben	0.495	0.500	0.487	–
cC6	1.210	1.226	1.204	–
iC8	0.080	0.080	0.078	–
C7	6.244	6.276	6.142	–
McC6	2.002	2.025	1.973	–
Tol	1.787	1.806	1.764	–
C8	6.862	6.982	6.785	8.358
Etb	0.419	0.405	0.409	–
M&P-Xyl	1.793	1.795	1.814	–
o-Xyl	0.547	0.553	0.547	–
C9	6.143	6.145	6.176	5.744
C10	7.152	7.170	7.143	6.678
C11	5.459	5.462	5.506	5.110
C12	4.245	4.238	4.246	3.960
C13	4.138	4.133	4.145	3.863
C14	3.525	3.521	3.534	3.291
C15	3.095	3.095	3.114	2.894
C16	2.414	2.406	2.482	2.272
C17	2.194	2.061	2.209	2.011
C18	2.078	2.081	2.094	1.945
C19	1.926	1.903	1.955	1.799
C20	1.576	1.570	1.581	1.471
C21	1.349	1.343	1.298	1.241
C22	1.208	1.216	1.223	1.135
C23	1.081	1.091	1.098	1.017
C24	0.969	0.978	0.985	0.912
C25	0.881	0.887	0.890	0.827
C26	0.732	0.804	0.740	0.708
C27	0.717	0.736	0.737	0.681
C28	0.637	0.646	0.647	0.600
C29	0.598	0.574	0.571	0.542
C30+	5.564	5.377	5.747	5.191

TX-TM3: GOR+D8003+D7169 Merge (mole%)								
	FPC-1	FPC-2	MPC-1	MPC-2	WD-1	WD-2	BRMPC-1	BRMPC-2
CO2	5.753E-03	5.971E-03	7.873E-03	8.086E-03	5.960E-03	6.413E-03	4.785E-03	4.598E-03
CO	0	0	0	0	0	0	0	0
H2S	0	0	0	0	0	0	0	0
He	0	0	0	0	0	0	0	0
H2	4.036E-04	3.073E-04	3.838E-04	4.132E-04	2.909E-04	2.181E-04	2.276E-04	2.379E-04
O2	2.827E-03	2.640E-03	3.159E-03	2.678E-03	5.242E-03	4.287E-03	6.158E-03	8.041E-03
N2	0.0221	0.0220	0.0193	0.0202	0.0395	0.0311	0.0545	0.0621
C1	0.0507	0.0511	0.0570	0.0569	0.0443	0.0448	0.0461	0.0406
C2	0.4293	0.4345	0.4345	0.4345	0.4280	0.4329	0.4459	0.4284
C3	2.2405	2.2681	2.2239	2.2321	2.2908	2.3175	2.3746	2.3313
iC4	1.2387	1.2541	1.1724	1.1783	1.2684	1.2776	1.2516	1.2382
nC4	4.2721	4.3266	4.1619	4.1832	4.2789	4.2983	4.3910	4.3481
neo C5	0	0	0	0	0	0	0	0
iC5	3.1582	3.1948	2.9902	3.0062	3.1901	3.1842	3.1458	3.1232
nC5	4.1933	4.2419	4.0449	4.0682	4.1781	4.1693	4.2264	4.1952
C6	7.5356	7.6044	7.2209	7.2621	7.6096	7.5938	7.5528	7.4974
Benzene	0.5065	0.5095	0.4979	0.5005	0.5079	0.5054	0.5130	0.5099
C7	8.5035	8.5523	8.2054	8.2536	8.5664	8.5635	8.5826	8.5023
C8	10.3324	10.3664	10.0055	10.0709	10.4671	10.4886	10.6111	10.5189
C9	8.7057	8.7032	8.3909	8.4372	8.8007	8.8420	8.8159	8.7093
C10	6.9538	6.9510	7.1152	7.2114	7.0901	6.9300	6.6249	7.0952
C11	4.9282	4.8063	4.9470	4.9591	4.8650	4.8818	4.8199	4.8792
C12	4.6043	4.5974	4.3018	4.3173	4.6486	4.6646	4.1912	4.2477
C13	3.7546	3.6528	4.0566	4.0688	3.7065	3.6239	3.7595	3.8126
C14	3.3695	3.3644	3.5540	3.5691	3.4138	3.3378	3.3739	3.4238
C15	2.6989	2.6948	2.7737	2.7981	2.6643	2.7545	2.7024	2.6720
C16	2.2008	2.1217	2.2618	2.2910	2.1726	2.1801	2.1277	2.1789
C17	2.4170	2.4133	2.4839	2.4321	2.4561	2.3942	2.3490	2.3929
C18	2.0137	2.0106	2.0695	2.0938	1.9878	1.9947	1.9491	1.9936
C19	1.5374	1.5351	1.5800	1.5471	1.5177	1.5229	1.5394	1.5221
C20	1.4091	1.4069	1.3852	1.4179	1.3910	1.3958	1.4109	1.4557
C21	1.2737	1.2718	1.4280	1.3982	1.3145	1.2617	1.2754	1.2037
C22	1.1600	1.1031	1.1922	1.2229	1.0906	1.1491	1.1062	1.1485
C23	1.0066	1.0051	1.0890	1.0662	1.0460	0.9971	1.0079	0.9966
C24	0.9162	0.9148	0.9416	0.9219	0.9044	0.9076	0.8664	0.9071
C25+	8.5586	8.6129	9.3845	8.9699	8.0497	8.2443	8.8735	8.5525

Summer TX-TM4: GPA2103M+ASTMD2887 Merge (mole%)			
	MPC	WD	BRMPC
N2	0.012	0.147	0.131
C1	0.051	0.051	0.031
CO2	0.011	0.011	0.008
C2	0.436	0.438	0.372
C3	2.285	2.327	2.090
iC4	1.212	1.248	1.149
nC4	4.271	4.321	4.120
iC5	3.118	3.189	3.090
nC5	4.152	4.210	4.152
iC6	3.898	3.781	3.052
nC6	3.702	3.670	3.362
iC8	0.027	0.027	0.028
Ben	0.545	0.539	0.509
C7	9.948	10.027	9.949
Tol	2.036	2.087	2.093
C8	10.089	10.257	10.345
ETB	0.377	0.376	0.387
Xyl	2.891	3.082	3.024
C9	6.839	7.491	7.229
C10	6.203	5.995	6.32
C11	4.672	4.520	4.751
C12	3.666	3.544	3.736
C13	3.528	3.429	3.587
C14	2.972	2.891	3.019
C 15	2.631	2.558	2.655
C16	2.133	2.093	2.190
C 17	1.899	1.856	1.929
C18	1.779	1.732	1.804
C19	1.641	1.592	1.665
C20	1.364	1.321	1.383
C21	1.180	1.146	1.199
C22	1.042	1.014	1.065
C23	0.929	0.901	0.947
C24	0.817	0.792	0.831
C25	0.742	0.719	0.756
C26	0.671	0.649	0.682
C27	0.616	0.596	0.629
C28	0.539	0.521	0.549
C29	0.483	0.467	0.494
C30+	4.593	4.385	4.688

Note: FPC data not available

TX-TM4a: GPA 2103M Final Report (mole%)								
	FPC-1	FPC-2	MPC-1	MPC-2	WD-1	WD-2	BRFPC-1	BRFPC-2
N2	1.033E-02	1.851E-02	1.001E-01	9.516E-02	8.426E-03	7.634E-03	2.817E-02	2.794E-02
CO2	5.745E-03	1.076E-02	6.245E-03	5.652E-03	6.806E-03	5.733E-03	4.442E-03	5.024E-03
C1	0.0081	0.0467	0.0719	0.0504	0.0529	0.0413	0.0422	0.0285
C2	0.5315	0.4201	0.4313	0.4407	0.4382	0.4304	0.4343	0.3829
C3	3.0806	2.2103	2.2826	2.3256	2.3527	2.3395	2.3655	2.1665
iC4	1.0801	1.1800	1.2098	1.2085	1.2222	1.2610	1.2685	1.1451
nC4	5.2790	4.2429	4.2955	4.2466	4.2850	4.2654	4.3136	4.0482
neoC5	0	0	0	0	0	0	0	0
iC5	2.3147	3.0420	3.0533	3.0403	3.0494	3.1208	3.0986	2.8885
nC5	4.4614	4.0552	4.0623	4.0482	4.0526	4.0719	4.0252	3.8597
neoC6	0.0317	0.1310	0.1224	0.2057	0.1987	0.0950	0.0947	0.1355
2,3-dimethylC4, 2-methylC5	1.9744	2.2317	2.2373	2.2078	2.1872	2.2498	2.1806	2.0771
3-methylC5, cycloC5	1.1905	1.3233	1.3298	1.2966	1.2666	1.3516	1.2935	1.2279
nC6	3.1922	3.2337	3.2946	3.2781	3.2689	3.3203	3.1555	3.0563
C7+	76.8474	77.8671	77.5770	77.5398	77.5210	77.4378	77.7147	78.9433

TX-TM4a: GPA 2103M C30+ by GC (mole%)								
	FPC-1	FPC-2	MPC-1	MPC-2	WD-1	WD-2	BRFPC-1	BRFPC-2
C2	0.00947	0.00687	0.00216	0.00214	0.00382	0.00179	0.00424	0.00268
C3	0.23659	0.07669	0.04449	0.03967	0.05499	0.03004	0.10119	0.04310
iC4	0.16042	0.04790	0.03974	0.03390	0.05070	0.03517	0.07362	0.03914
nC4	0.56042	0.21629	0.16504	0.15548	0.23703	0.17416	0.28231	0.18107
iC5	0.54450	0.44229	0.26166	0.33810	0.48017	0.42575	0.39139	0.37257
nC5	0.92020	0.82048	0.48780	0.67155	0.85384	0.79019	0.74666	0.71994
nC6	4.20779	4.20943	8.56233	4.03983	4.27920	4.34636	4.18305	4.01523
Mcyclo-C5	0.64372	0.63848	0.55995	0.64326	0.61820	0.62811	0.64814	0.62861
Benzene	0.37996	0.37379	0.32999	0.37093	0.36666	0.37114	0.37305	0.36684
Cyclo-C6	0.94543	0.91847	0.88198	0.94181	0.89452	0.91475	0.93619	0.92195
nC7	6.77671	6.71202	6.44936	6.70065	6.87508	7.01210	6.80083	6.69524
Mcyclo-C6	1.93214	1.81580	1.92422	1.94354	1.86808	1.89151	1.86100	1.88706
Toluene	2.08037	2.02818	2.00354	2.05851	2.10241	2.12862	2.05922	2.06708
nC8	8.39622	8.47819	8.07799	8.47465	8.66856	8.73503	8.73156	8.70023
C2-Benzene	0.58857	0.61242	0.56157	0.61277	0.58680	0.57975	0.62583	0.62464
P&M-Xylene	2.59815	2.60779	2.57984	2.62830	2.72446	2.75121	2.60382	2.65064
O-Xylene	0.78379	0.79299	0.74311	0.75119	0.78996	0.78965	0.75241	0.77243
nC9	7.27143	7.42882	6.90610	7.38004	7.53351	7.46392	7.51900	7.50503
nC10	8.33972	8.45466	7.95335	8.44020	8.53787	8.68701	8.52266	8.55707
nC11	6.32667	6.39918	6.04384	6.39475	6.45429	6.47410	6.43439	6.47425
nC12	5.17057	5.25596	4.94358	5.23352	5.29306	5.27911	5.26891	5.30143
nC13	4.90241	4.93474	4.69266	4.95553	4.95453	4.93082	4.95528	4.95530
nC14	4.05982	4.10396	3.88591	4.11300	4.10797	4.13917	4.09935	4.17417
nC15	3.72391	3.76575	3.57489	3.79095	3.74784	3.73449	3.75677	3.78591
nC16	3.44178	3.48414	3.09346	3.28253	3.45938	3.24186	3.24637	3.50107
nC17	2.30229	2.32317	2.41186	2.55653	2.30497	2.49921	2.50356	2.31182
nC18	2.59296	2.62061	2.49683	2.64885	2.58660	2.57650	2.59112	2.62127
nC19	2.42357	2.47219	2.34399	2.48590	2.40776	2.39151	2.42109	2.45170

TX-TM4a: GPA 2103M C30+ by GC (mole%)								
	FPC-1	**FPC-2**	**MPC-1**	**MPC-2**	**WD-1**	**WD-2**	**BRFPC-1**	**BRFPC-2**
nC20	1.96842	1.98465	1.88781	2.01281	2.01610	1.92731	1.95568	1.96899
nC21	1.69760	1.72088	1.63849	1.74657	1.59481	1.65446	1.67507	1.69002
nC22	1.54503	1.57811	1.49157	1.59610	1.51221	1.50642	1.53017	1.55239
nC23	1.38773	1.39782	1.33236	1.42224	1.35747	1.33955	1.36916	1.37932
nC24	1.23495	1.25787	1.19413	1.27172	1.21214	1.19881	1.21799	1.23614
nC25	1.11113	1.12230	1.07098	1.14158	1.07930	1.07177	1.09312	1.09232
nC26	0.99037	0.99229	0.96215	1.01598	0.96782	0.95233	0.97842	0.99555
nC27	0.87916	0.92252	0.84642	0.93182	0.85941	0.84735	0.86619	0.88704
nC28	0.81045	0.80621	0.78351	0.81657	0.77584	0.75359	0.81090	0.79495
nC29	0.68411	0.70560	0.67573	0.72070	0.66434	0.66091	0.67138	0.70164
C30+	5.37147	5.47050	6.09562	5.63584	5.11830	5.06444	5.33891	5.37417

Winter TX TM4: GPA2103M+ASTMD2887 Merge (mole%)				
	W-FPC	**W-BR1MPC**	**W-BR2MPC**	**W-BR3MPC**
N2	0.012	0.048	0.067	0.072
C1	0.062	0.031	0.032	0.031
CO2	0.019	0.011	0.008	0.008
C2	0.482	0.44	0.443	0.448
C3	2.422	2.326	2.319	2.33
iC4	1.267	1.215	1.239	1.2
nC4	4.457	4.278	4.341	4.242
iC5	3.159	3.017	3.104	2.988
nC5	4.173	4.11	4.219	4.08
iC6	3.369	2.794	2.548	2.895
nC6	3.468	3.233	3.17	3.266
iC8	0.028	0.028	0.027	0.027
Ben	0.525	0.506	0.457	0.5
C7	9.916	9.588	9.348	9.402
Tol	2.081	1.983	1.879	2.007
C8	10.118	9.631	9.696	9.754
ETB	0.377	0.377	0.363	0.378
Xyl	2.954	2.744	2.517	2.763
C9	7.027	6.705	7.324	6.788
C10	6.084	6.371	6.412	6.355
C11	4.679	4.783	4.869	4.943
C12	3.668	3.854	3.844	3.815
C13	3.55	3.745	3.786	3.799
C14	3.033	3.187	3.168	3.146
C 15	2.67	2.803	2.799	2.806
C16	2.179	2.306	2.3	2.283
C 17	1.936	2.055	2.034	2.058
C18	1.805	1.892	1.913	1.875
C19	1.692	1.793	1.764	1.768
C20	1.386	1.476	1.451	1.452
C21	1.191	1.269	1.27	1.259
C22	1.054	1.139	1.119	1.114
C23	0.955	1.007	0.99	0.998
C24	0.835	0.897	0.892	0.881
C25	0.761	0.818	0.804	0.793
C26	0.686	0.735	0.72	0.72
C27	0.632	0.67	0.661	0.661
C28	0.552	0.593	0.584	0.588
C29	0.491	0.533	0.528	0.525
C30+	4.245	5.009	4.991	4.982

Page intentionally blank.

Glossary

API gravity: Common oil industry unit of measure for liquid density of a crude oil.

ASTM D3700 Standard Practice for Obtaining LPG Samples Using a Floating Piston Cylinder.

ASTM D6377-16 Standard Test Method for Determination of Vapor Pressure of Crude Oil: VPCRx (Expansion Method)

ASTM D4057 Ambient Pressure Bottle Sampling – Ambient-pressure sample collected using bottom-fill tube to minimize splashing and resultant vapor generation.

ASTM D8009 Manual Piston Cylinder – Pressurized sample collected using manually operated piston cylinder.

Bubble Point Pressure (BPP): The BPP of a pure substance or mixture is a special case of TVP where the V/L = 0. Also defined as the pressure at which the first incipient vapor bubble is formed at a temperature of interest.

Conventional oil and natural gas production: Crude oil and natural gas that is produced by a well drilled into a geologic formation in which the reservoir and fluid characteristics permit the oil and natural gas to readily flow to the wellbore.

Crude oil: A mixture of hydrocarbons that exists in liquid phase in natural underground reservoirs and remains liquid at atmospheric pressure after passing through surface separating facilities. Depending upon the characteristics of the crude stream, it may also include 1. Small amounts of hydrocarbons that exist in gaseous phase in natural underground reservoirs but are liquid at atmospheric pressure after being recovered from oil well (casing head) gas in lease separators and are subsequently comingled with the crude stream without being separately measured. Lease condensate recovered as a liquid from natural gas wells in lease or field separation facilities and later mixed into the crude stream is also included; 2. Small amounts of nonhydrocarbons produced with the oil, such as sulfur and various metals; 3. Drip gases, and liquid hydrocarbons produced from tar sands, oil sands, gilsonite, and oil shale.

C30+: Laboratory analysis based on unpressurized gas chromatography yielding a carbon number report showing relative compositions of carbon numbers in mass% (or mol%, vol%) from C1, C2,...up to an aggregate C30+ group.

Dead or Weathered Crude: oil that when exposed to normal atmospheric pressure at room temperature, will not result in boiling of the sample

Gas-oil ratio (GOR): The volume ratio of gas to liquid evolved from an oil that is depressurized to known P, T conditions. In this study, P = 1 atm, and T = 100°F unless otherwise noted. Volume units are in standard cubic feet of gas per standard barrel of liquid (scf/bbl). (Note that standard conditions for reported gas standard cubic feet per industry standards are P = 1 atm and T= 60°F.)

GPA 2174 Obtaining Liquid Hydrocarbons Samples for Analysis by Gas Chromatography, describes how to obtain pressurized sample obtained via displacement of water.

Hydrocarbon: An organic chemical compound of hydrogen and carbon in the gaseous, liquid, or solid phase. The molecular structure of hydrocarbon compounds varies from the simplest (methane, a constituent of natural gas) to the very heavy and very complex.

Fixed gases: Fixed gases in the current work refer to inorganic gases such as nitrogen, carbon dioxide, and oxygen that may have only minor contribution to overall mass% in a crude oil, but can exert significant effects on vapor pressure.

Light ends: In the context of the current work, refer to components of a crude oil with low molecular weight that will readily vaporize at typical ambient pressure and temperature conditions where crude oils may be handled in open containers. Light ends would include the familiar short-chain hydrocarbons such as methane, ethane, etc., through pentane, that may have only minor contribution to overall mass% but can exert significant effects on crude oil vapor pressure.

Live Crude: an oil contained in a pressurized system that, when brought to normal atmospheric pressure at room temperature, will result in boiling of the sample

Pipeline (petroleum): Crude oil and product pipelines used to transport crude oil and petroleum products, respectively (including interstate, intrastate, and intracompany pipelines), within the 50 states and the District of Columbia.

Pool fires: Fires resulting from the burning of liquid fuel pools.

Refinery: An installation that manufactures finished petroleum products from crude oil, unfinished oils, natural gas liquids, other hydrocarbons, and oxygenates.

Terminal location: The physical location of one end of a transmission line segment.

Tight-line to mobile laboratory: Minimum achievable sample handling at or above original process line pressure in order to convey sample to analytical instruments.

Tight oil: Oil produced from petroleum-bearing formations with low permeability such as the Eagle Ford, the Bakken, and other formations that must be hydraulically fractured to produce oil at commercial rates. Shale oil is a subset of tight oil.

True Vapor Pressure: The TVP of a pure substance is easily defined as the total pressure exerted by a gas in equilibrium with a liquid at a temperature of interest. The measurement of TVP for a pure substance is constant provided there are distinct vapor and liquid phases in the measurement cell.

The TVP of a mixture is still the total pressure of gas in equilibrium with a liquid, but the TVP of a mixture, unlike a pure substance, is also dependent upon the molar vapor and liquid volumes (V/L) at a temperature of interest. The addition of the V/L term is required due to the differing volatilities of the components in the mixture.

Vapor Pressure: The term vapor pressure for crude oils is confusing upon review of the literature. The term vapor pressure as used in the literature can mean True Vapor Pressure (TVP), BPP, RVP or now, with variable volume expansion vapor pressure analyzers, we can have vapor pressures determined at various expansion ratios.

VPCRx(T)*:* Equilibrium vapor pressure over a liquid at vapor/liquid volume ratio = x, and a temperature = T. Measurements should be compliant with ASTM D6377.

Wellhead: The point at which the crude (and/or natural gas) exits the ground. Following historical precedent, the volume and price for crude oil production are labeled as "wellhead, "even though the cost and volume are now generally measured at the lease boundary. In the context of domestic crude price data, the term "wellhead" is the generic term used to reference the production site or lease property.

DISTRIBUTION

External Distribution

Electronic Copies to:

Evan Frye (evan.frye@hq.doe.gov) Office of Oil & Natural Gas, U.S. Department of Energy, 1000 Independence Avenue, S.W., Washington D.C. 20585

Joseph Nicklous (joseph.nicklous@dot.gov) Office of Hazardous Materials Safety, Pipeline and Hazardous Materials Safety Administration, U.S. Department of Transportation, 1200 New Jersey Avenue, SE, Washington, D.C. 20590

Mark Raney (mark.raney@dot.gov) Volpe National Transportation Systems Center, U.S. Department of Transportation, 55 Broadway, Cambridge, MA 02142

Barbara Di Bacco (barbara.dibacco@tc.gc.gov) Transport Canada Dangerous Goods Directorate, Ottawa, Ontario, Canada K1A0N5

Sandia Distribution

8	MS0706	David Lord	8865
1	MS0899	Technical Library	9536 (electronic copy)

Sandia National Laboratories